



THESIS / THÈSE

DOCTOR OF SCIENCES

Study of cell cycle regulators and DNA repair following alkylating stress in *Brucella abortus*

Poncin, Katy

Award date:
2018

Awarding institution:
University of Namur

[Link to publication](#)

General rights

Copyright and moral rights for the publications made accessible in the public portal are retained by the authors and/or other copyright owners and it is a condition of accessing publications that users recognise and abide by the legal requirements associated with these rights.

- Users may download and print one copy of any publication from the public portal for the purpose of private study or research.
- You may not further distribute the material or use it for any profit-making activity or commercial gain
- You may freely distribute the URL identifying the publication in the public portal ?

Take down policy

If you believe that this document breaches copyright please contact us providing details, and we will remove access to the work immediately and investigate your claim.



Study of cell cycle regulators and DNA repair following alkylating stress in *Brucella abortus*

Katy Poncin

Dissertation presented in preparation
of the degree of PhD in Sciences

Jury members:

Pr. Patrick Viollier, University of Geneva, Switzerland

Pr. Ivan Matic, Université Paris Descartes, France

Pr. Bernard Hallet, UCL, Belgium

Dr. Régis Hallez, University of Namur, Belgium

Pr. Xavier De Bolle, University of Namur, Belgium

Acknowledgments/Remerciements

I would like to start by thanking the jury members, Pr. Patrick Viollier, Pr. Ivan Matic, Pr. Bernard Hallet and Dr. Régis Hallez, for the time that you have spent reading this thesis. More than that, most of you have also contributed to the improvement of my thesis over the last few years, either as my colleague, official advisor or even non-official advisor. For this, I will never say thank you enough. It was a real pleasure to meet you and share a part of my research adventure with you.

Je remercie bien évidemment aussi mon promoteur, le Pr. Xavier De Bolle. Tes qualités humaines et ton aptitude à voir le côté positif des choses, même avec les manip foireuses et/ou foirées, auront vraiment contribué à la réussite de cette thèse. Essaie juste de garder cette attitude positive avec mon papier, stp... Autant viser la lune, au pire on atteindra les étoiles ! ;D

Un merci tout particulier aussi à JJJ, qui a toujours su montrer de l'enthousiasme et de l'intérêt pour mes recherches. Un grand merci à la Xa team, également. Pierre, Agnès et Caro, je vous souhaite tout le bonheur du monde pour la suite de votre thèse. Mathilde, courage pour la dernière ligne droite ! Crois-moi, la pente est raide mais ça en vaut la peine. Angy, merci pour cette année passée en ta compagnie. Et vraiment, essaie de penser un peu plus à toi-même au lieu d'aider tout le temps les autres (je dis ça mais je ne crache quand même pas sur un peu d'aide pour le reviewing de mon papier ☺). Vicky, good luck with your long holidays and your post-doc ! Aux anciens, JF, Nayla et Kévin, je voudrais aussi vous dire merci pour tous ces moments passés ensemble. Seb, merci pour tes conseils sur les arbres phylogénétiques et les « T'en es où toi ? Ha, tu n'as pas commencé non plus ? Cool, je me sens moi seul(e) tout d'un coup ». Evidemment, je n'oublie pas tous les autres URBMiens (anciens et présents, chanteurs ou pas), ni les GEMO ! Les GEMO, parlons-en ! Carlo et Oli, je vous dis : « eggplant ». Na ! J'ai gagné le jeu. Wouhou ! Bon d'accord, je triche, c'est vrai. Mais mes neurones sont en bouillie à ce stade-ci de ma thèse, donc j'ai une vraie excuse.

Merci aussi à mes amis: Lauren, Céline, Stéphanie, Sophie, Olivier, Adeline, Marie, Manhattan, Céline et Pauline. Vous savez pourquoi.

Last but not least, je voudrais remercier ma famille, sans qui rien de tout cela n'aurait été possible. Depuis le début, vous avez été les témoins de mes réussites et de mes larmes et vous avez toujours été là pour moi. Merci aussi pour votre confiance et pour m'avoir aidé à m'envoler. Laurent, merci de me rejoindre dans cette aventure. Tu ne sais pas à quel point je suis heureuse de t'avoir dans ma vie. A vous tous, mille fois merci ! Je vous aime.

Table of content

List of abbreviations.....	4
Summary	5
Introduction.....	6
I. Alkylating stress	6
I.1. What is alkylating stress?.....	6
I.1.1. What are the effects of alkylating stress?.....	6
I.1.2. What are the natural sources of alkylating agents?.....	7
I.2. DNA repair pathways involved in alkylated DNA repair	9
I.2.1. The adaptive response	9
I.2.2. The SOS response	10
I.2.3. Homologous recombination	12
I.2.4. Nucleotide excision repair	13
I.2.5. Mismatch repair	13
I.2.6. The MutM DNA glycosylase.....	14
I.3. Is alkylating stress relevant for intracellular bacteria?.....	15
II. <i>Brucella abortus</i>	16
II.1. <i>Brucella</i> is an α -proteobacterium.....	16
II.2. Brucellosis	17
II.3. <i>Brucella</i> inside host cells	18
II.3.1. <i>Brucella</i> intracellular trafficking	18
II.3.2. Growth and replication of <i>Brucella</i>	20
II.3.3. Brief summary of the immune response	21
II.3.4. Intracellular stresses	22
II.3.5. DNA repair capacities of <i>Brucella</i>	25
II.4. <i>Brucella</i> as a model for alkylating stress studies.....	27
III. Cell cycle transcription factors.....	28
III.1. Why work on cell cycle regulators?	28
III.2. Roles and regulation of CtrA	29
III.2.1. <i>B. abortus</i> CtrA regulation is similar to that of <i>C. crescentus</i>	29
III.2.2. The expression of ctrA is not crucial for <i>B. abortus</i> trafficking to the rBCV	31
III.2.3. The regulon of CtrA	32
III.3. Roles and regulation of GcrA	33
Objectives.....	36
Results.....	37
I. Detection and sources of alkylating stress in <i>B. abortus</i>	37
I.1 Intracellular bacteria possess genes to face alkylating stress	37
I.2. Alkylating stress is encountered by <i>B. abortus</i> inside host cells	37
I.3. N-nitrosation events occur inside the eBCV	38
II. Defenses of <i>B. abortus</i> against alkylating stress	39
II.1. Ogt is a key actor against alkylating stress in <i>B. abortus</i>	39
II.2. The expression of <i>ogt</i> is dependent on the transcription factor GcrA	41
II.3. Individual DNA repair pathways are not essential for <i>B. abortus</i> infection.....	42

II.4. Unpublished data.....	42
II.4.1. DNA repair deletion strains in other infection models	42
II.4.2. GcrA depletion strain is also attenuated in BMDM... but recovers.....	43
II.4.3. GcrA depletion strain is impaired for normal DNA content	43
II.4.4. The SOS system could be required for intracellular survival	44
II.4.5. We could not determine if CtrA was involved in DNA repair after alkylating stress ..	45
II.4.6. Genes coding for alkylated DNA repair are not required against H ₂ O ₂	46
II.4.7. Set up of a probe to detect oxidative stress on <i>B. abortus</i>	46
Material and methods.....	48
I. Bacterial strains and media.....	48
I.1. Growth conditions	48
I.2. Deletion, depletion and overexpression strains construction	48
I.3. Cloning of the reporter system for alkylating stress	52
II. Synthesis and binding of the probes to bacteria.....	53
II.1. N-nitrosation sensitive probe	53
II.2. Texas Red succinimidyl ester (TRSE)	53
II.3. OxyBURST.....	54
III. Cell cultures and infections	54
III.1. RAW 264.7 macrophages	54
III.2. HeLa cells.....	54
III.3. Bone marrow-derived macrophages (BMDM).....	55
IV. Immunolabeling of infected cells.....	55
V. Microscopy and analyses of fluorescence.....	55
VI. Growth curves and colony forming units counts.....	56
VI.1. Growth curves	56
VI.2. CFU after infection	56
VI.3. CFU after liquid culture (survival assay)	56
VI.4. CFU on plates supplemented with alkylating agents (plating assay).....	56
VII. Chromatin immunoprecipitation with anti-GcrA antibodies	56
VII.1. ChIP-seq.....	56
VII.2. Analyses	57
VIII. Whole genome sequencing after infection and liquid cultures	58
IX. Reverse transcription followed by quantitative PCR.....	58
X. Western blot	59
XI. Flow cytometry.....	60
XII. Disk assays	60
Discussion and perspectives	61
I. On the existence of intracellular alkylating stress	61
I.1. What are the sources of the detected alkylating stress?.....	61
I.2. Could <i>B. abortus</i> actively avoid alkylating stress?	63
I.2.1. What we can expect.....	63
I.2.2. The case of oxidative stress.....	64
I.2.2. Are RNS produced against <i>B. abortus</i> ?	65
II. On the genes that are required to face alkylating stress <i>in vitro</i>.....	66
II.1. Inducible genes.....	66
II.2. Non-inducible genes.....	68

III. On the absence of attenuation of the mutant strains inside host cells	69
III.1. Alkylating agents induce a non-linear dose response	69
III.2. Did we look at the right phenotype?.....	70
III.3. On the role of the SOS response inside host cells	71
III.3.1. What part does the SOS system play in <i>Brucella</i> infectious process?.....	71
III.3.2. Why would a BER deficient mutant help when the SOS system is repressed?	72
III.3.3. What about phages?	72
IV. On the role of cell cycle transcription factors to regulate DNA repair	72
IV.1. GcrA and CtrA as regulators of DNA repair	72
IV.2. What would be the advantage of regulating DNA repair along the cell cycle?.....	74
V. Model for <i>Brucella</i> resistance to alkylating stress.....	75
VI. What about other intracellular bacteria?	77
Conclusion	79
Bibliography	80
Appendix	94

List of abbreviations

aBCV	Autophagy-derived <i>Brucella</i> -containing vacuole
AP sites	Apurinic/aprimidic/abasic sites
BCV	<i>Brucella</i> -containing vacuole
BER	Base excision repair
BMDM	Bone marrow-derived macrophages
CFU	Colony forming unit
ChIP-seq	Chromatin immunoprecipitation followed by deep sequencing
DMS	Dimethyl sulfate
DR	Direct repair
dsDNA	Double stranded DNA
eBCV	Endocytic <i>Brucella</i> -containing vacuole
EMS	Ethyl methane sulfonate
ER	Endoplasmic reticulum
HNE	4-hydroxy-2-nonenal
iNOS	Inducible nitric oxide synthase
LAMP1	Lysosomal membrane-associated protein-1
LOGEL	Lowest observed genotoxic effect level
MDA	Malondialdehyde
mePtriester	Methylphosphotriester
MMS	Methyl methane sulfonate
MNNG	<i>N</i> -methyl- <i>N'</i> -nitro- <i>N</i> -nitrosoguanidine/methylnitronitrosoguanidine
MNU	<i>N</i> -methyl- <i>N</i> -nitroso- <i>N</i> -nitroso- <i>N</i> -methylurea
MOI	Multiplicity of infection
MR	Mismatch repair
NER	Nucleotide excision repair
OMP	Outer membrane protein
<i>ori</i>	Origin of replication
PAMPs	Pathogen associated molecular patterns
PI	Post infection
PRRs	Pattern-recognition receptors
PUFA	Polyunsaturated fatty acids
rBCV	Replicative <i>Brucella</i> -containing vacuole
RNS	Reactive nitrogen species
ROS	Reactive oxygen species
RT-qPCR	Quantitative reverse transcription PCR
SAM	S-adenosylmethionine
S _N 1	Type 1 nucleophilic substitution
S _N 2	Type 2 nucleophilic substitution
ssDNA	Single stranded DNA
<i>ter</i>	Terminator
TLR	Toll-like receptors
TRSE	Texas Red Succinimidyl Ester

Summary

All living organisms must ensure that their DNA will remain protected against stresses. Intracellular bacteria are no exception, as they have developed strategies to face DNA damaging stresses inside their host cells. One well-known example is oxidative stress, which can result from the oxidative burst of macrophages. Another DNA damaging stress that is predicted to be encountered by intracellular bacteria is alkylating stress, resulting from the peroxidation of lipids, the N-nitrosation of metabolites or the presence of weak endogenous alkylating agents, such as S-adenosyl-methionine. Despite previous attempts, to our knowledge, the occurrence of alkylating stress inside host cells still needs to be experimentally demonstrated.

Here, we studied the response of the class III pathogen *Brucella abortus* inside host cells, and we showed, for the first time, that an intracellular bacterium is meeting alkylating stress inside its host. Indeed, the construction of a fluorescence-based reporter system detecting alkylation events on DNA allowed us to find out that *B. abortus* is mainly subjected to alkylation stress during the first stage of its infection, while it is still residing inside its endosomal *Brucella*-containing vacuole (eBCV) and before to reach its replicative niche, the endoplasmic reticulum (rBCV). To go further, and in order to better assess the environment in which *Brucella* is residing inside its host cell, a probe was designed so it could be covalently attached at the bacterial surface and report, based on fluorescence emission, the level of N-nitrosation events occurring inside the eBCV. This technique revealed that N-nitrosation events do take place inside this compartment in host cells. However, this reaction was innocuous to *Brucella*. Instead, we found that the alkylating stress felt by the bacterium was mainly due to the endogenous formation of N-nitroso compounds, which were produced by bacterial metabolism.

Without surprise, the deletion of DNA repair genes was inconclusive in showing an attenuation of the bacterium inside host cells, as it was the case for previous reports on other intracellular pathogens, such as *Mycobacterium tuberculosis*. It is thus likely that DNA is protected by numerous and redundant DNA repair pathways that ensure that it is protected at all times. Most bacteria possess a DNA repair pathway that is specialized in coping with alkylated DNA. It is the so-called adaptive system. Interestingly, *B. abortus* does not possess a functional adaptive system. Instead, we found that this bacterium is relying on its SOS system, as well as on the essential and well-conserved transcription factor GcrA to regulate a series of genes involved in DNA repair.

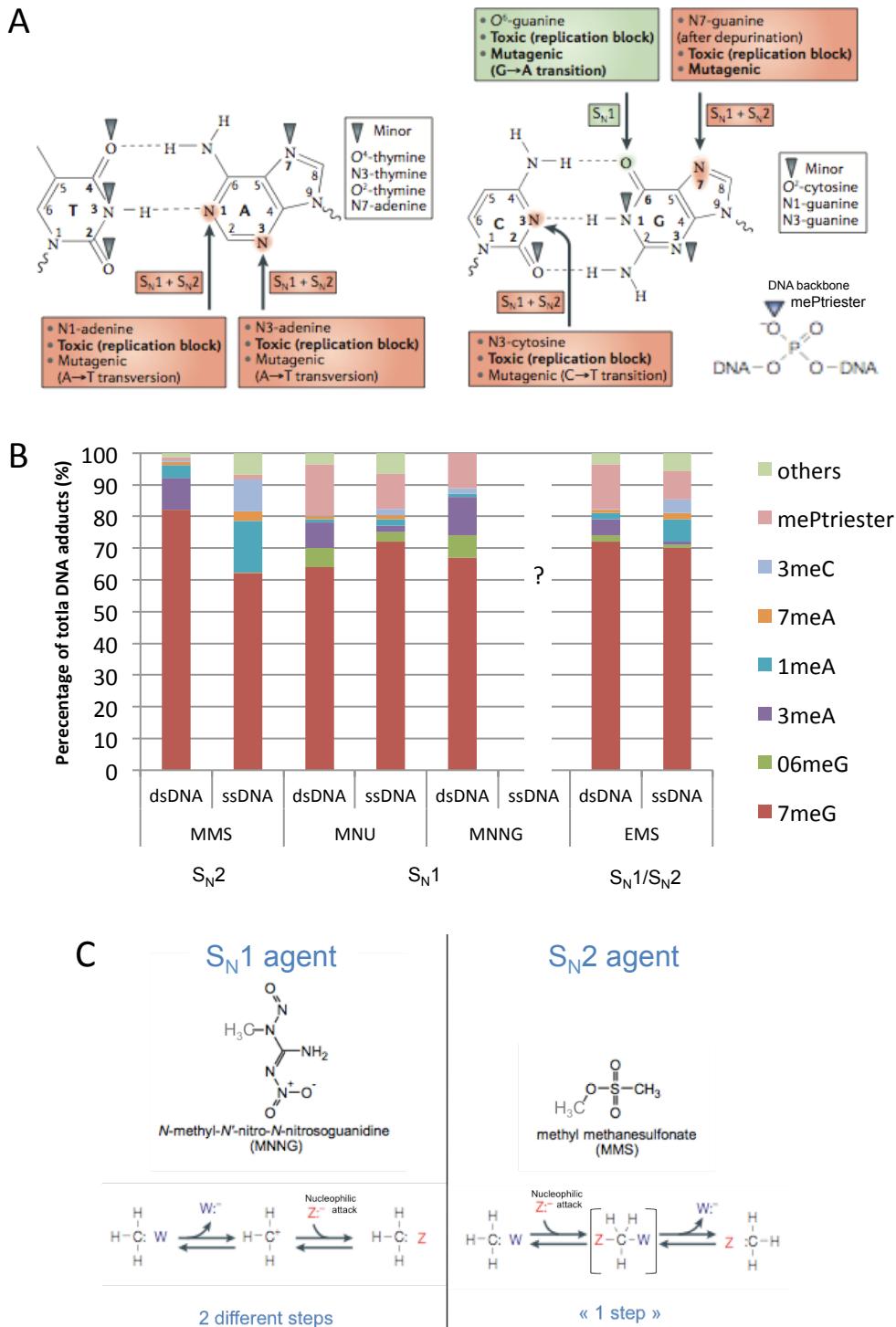


Fig 1. Effects of alkylating agents on DNA. **A)** Effects of the main positions of DNA that are modified by alkylating agents (adapted from Fu *et al.*, 2012). mePTriester stands for methylphosphotriester. **B)** Main DNA adducts generated *in vitro* by four different alkylating agents on single stranded or double stranded DNA (based on Beranek, 1990 and Mielecki *et al.*, 2015). MMS stands for methyl methane sulfonate; MNU for *N*-methyl-*N*-nitrosourea; MNNG for methylnitronitrosoguanidine and EMS for ethyl methane sulfonate. Note that we could not find data about the adducts formed by MNNG on ssDNA. **C)** Mechanism of action of the two types (S_N1 and S_N2) of alkylating agents. W represents the leaving group and Z represents a nucleophile (*i.e.* DNA in this case).

Introduction

I. Alkylating stress

I.1. What is alkylating stress?

I.1.1. What are the effects of alkylating stress?

Alkylation is a chemical reaction that consists on the transfer of an alkyl group from one molecule to another. As alkyl groups are characterized by the formula C_nH_{2n+1} , their simplest form is a CH_3 methyl group, with $n = 1$. Therefore, on DNA, alkylating stress typically results in aberrant methylation patterns, even if more complicated adducts do exist. Any atomic positions of DNA can be targeted and the consequences of the modifications range from innocuous to mutagenic or cytotoxic (**Fig 1A**) (Beranek, 1990; Fu *et al.*, 2012; Mielecki *et al.*, 2015). Alkylating stress is therefore very different from epigenetic methylation, which targets specific position on DNA. In that regard, there exists a report of alkylating stress leading to modification in gene expression, probably via the recognition of the alkyl adducts as epigenetic markers (Di Pasquale *et al.*, 2016). The effects of alkylating agents on other biomolecules, such as proteins, is less studied but they are known to occur (Boffa & Bolognesi, 1985). Importantly, in humans, alkylating agents can eventually lead to cancer but they are also used to treat cancer (Fu *et al.*, 2012).

Any base of DNA can be affected by alkylating agents and even the ribose-phosphodiester backbone is also susceptible to modification and breakage (**Fig 1A**) (Wyatt & Pittman, 2006). Note that guanine is disproportionately damaged (**Fig 1B**). This is because of its lower reduction potential, compared to other bases (Candeias & Steenken, 1993). Chemical alkylating agents have been extensively used to study the effect of alkylating stress on DNA. The most common agents are methyl methane sulfonate (MMS), dimethyl sulfate (DMS), *N*-methyl-*N*-nitrosourea (MNU) and *N*-methyl-*N'*-nitro-*N*-nitrosoguanidine (MNNG) (Wyatt & Pittman, 2006). Alkylating agents are usually classified into two categories, depending on their reaction mechanism. S_N1 agents react with biomolecule in two main steps via a unimolecular nucleophilic substitution, while S_N2 agents react in one step with the rate-limiting step involving two reactive species (Smith & March, 2007) (**Fig 1C**). MMS and DMS are S_N2 -type agents, while MNNG and MNU are considered as S_N1 -type agents. Incidentally, there have been discussions about the real classification of MNNG, which could belong to a third category termed “oxyphilic”, as it does not generate a methyl carbocation ($^+CH_3$) but instead a methyl-diazonium cation ($CH_3-^+N\equiv N$) (Loechler, 1994). There also exist alkylating agents that belong to both S_N1 and S_N2 categories, such as ethyl methane sulfonate (EMS) (Hoffmann, 1980).

According to their category, alkylating agents will react differentially with nitrogen and oxygen adducts. O-methyl adducts (O^6meG in particular) have been pointed as more toxic and

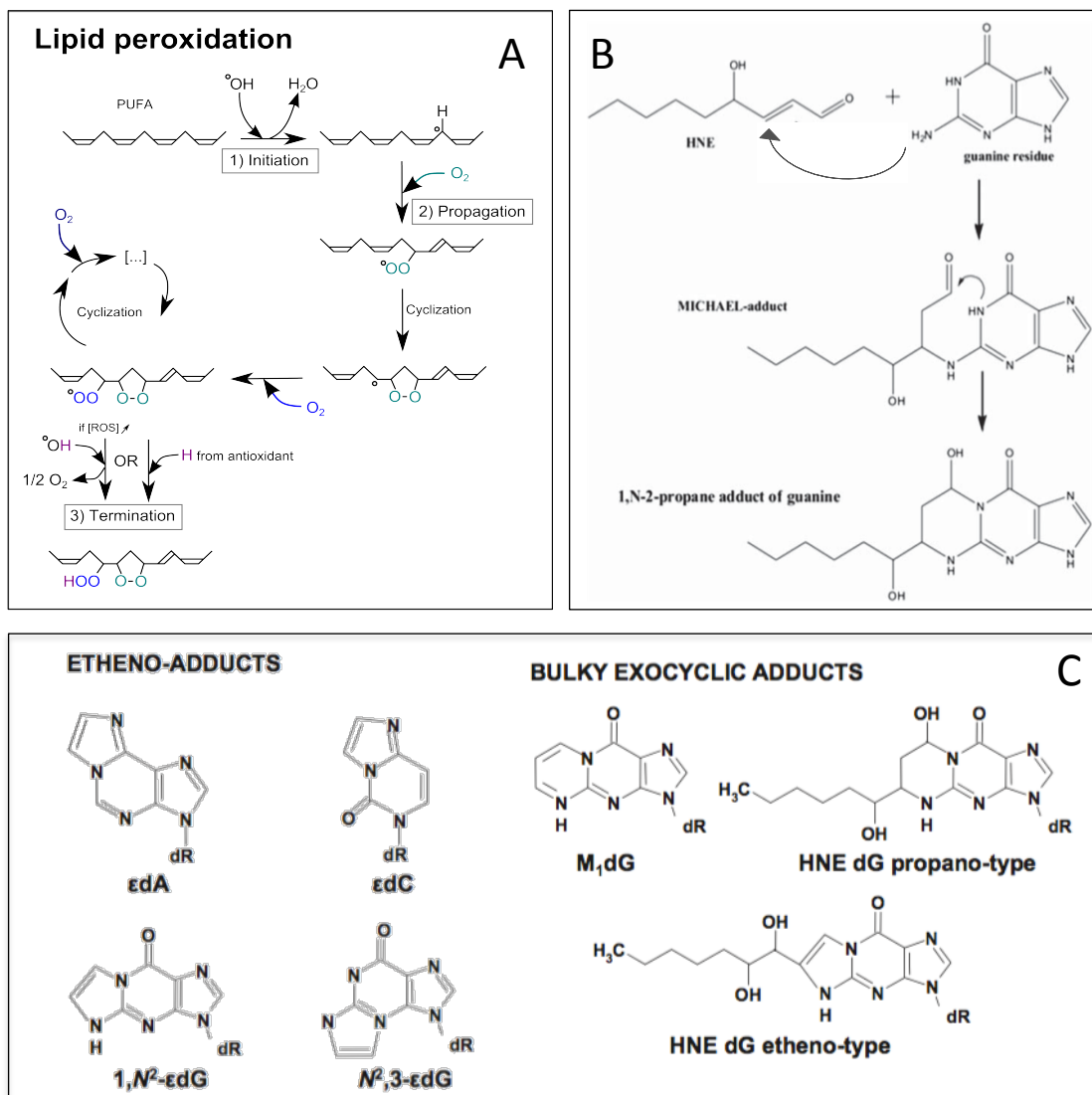


Fig 2. Products of lipid peroxidation. **A)** Polyunsaturated fatty acids (PUFA) get peroxidated when ROS or RNS are present in the cells. The initiation step starts when an oxidant abstract an H atom from the lipid. The reactive lipid that is formed by this reaction then reacts with oxygen during the propagation stage, leading to the cyclization of the molecule. More cyclization steps can arise, depending on the number of double bonds of the PUFA. Eventually, the termination of the process happens through the reaction of the molecule with another radical, or via the action of an antioxidant. Once stabilized, the terminal lipid can actually undergo further rearrangements to get reduced to an alcohol or to be sliced in several small other molecules, such as HNE, which can react with other biomolecules. **B)** Chemical reaction between HNE and guanine (Winczura *et al.*, 2012). **C)** Examples of exocyclic DNA adducts generated by lipid peroxidation (Tudek *et al.*, 2017).

mutagenic than N-methyl adducts (Wyatt & Pittman, 2006). One thing to take into account is the state of DNA, *i.e.* if it is in its double stranded form (dsDNA) or in its single stranded form (ssDNA) when it gets alkylated. Indeed, some positions of DNA are protected by hydrogen bonding in dsDNA. It is the case of N1-adenine (1meA) and N3-cytosine (3meC), which are much more present in ssDNA (**Fig 1B**) (Mielecki *et al.*, 2015). As they possess an extra pair of electron, the occurrence of O-methyl adducts that also participate in the hydrogen bonding (O⁶meG, O²meC and O⁴meT) is not particularly affected by the state of DNA (Bodell & Singer, 1979). As for the N3 or N7 positions of purines, they destabilize the N-glycosidic bond, so they make the modified bases more susceptible to being hydrolyzed into an abasic site (Osborne & Phillips, 2000). Lastly, note that methylphosphotriesters (mePtriesters), which arise after alkylating stress on DNA sugar-phosphate backbone, are much more present with S_N1 agents than with S_N2 agents (**Fig 1B**) (Maxam & Gilbert, 1980). These adducts have long been considered as innocuous, but they have recently been demonstrated to be mutagenic and slightly cytotoxic, depending on their diastereomer conformation (Wu *et al.*, 2018).

1.1.2. What are the natural sources of alkylating agents?

Alkylating agents are ubiquitous, due to their presence in the environment via tobacco smoke and fuel combustion products, for example (Hecht, 1999). They also have endogenous and dietary sources (Catsburg *et al.*, 2014; Zhu *et al.*, 2014). Inside an organism, there exist three sources of generation of alkylating agents. The first one is the intracellular S-adenosylmethionine (SAM). This coenzyme is found in all living organisms and it is involved in three key metabolic pathways: transmethylation, transsulfuration, and polyamine synthesis (Lu, 2000). In bacteria, it is also a precursor of two quorum sensing molecules that are involved in the virulence of several gram-negative pathogens (Zano *et al.*, 2013). As a methyl donor, SAM can target DNA, RNA, proteins, phospholipids and even neurotransmitters (Fontecave *et al.*, 2004). One protein that is dependent on SAM and that is very important in α -proteobacteria is the methyltransferase CcrM, itself involved in epigenetic methylation (Berdis *et al.*, 1998). Since one of the functions of SAM is to give methyl groups to other molecules, it is logical that it is also an alkylating agent. Its mechanism of action as such is similar to MMS, with a S_N2 type of reaction (Naslund *et al.*, 1983). Nevertheless, compared to MMS, it is 100 times less reactive with cysteine (Naslund *et al.*, 1983) and 1000-3000 times less reactive with DNA (Rydberg & Lindahl, 1982). Its concentration inside eukaryotic cells has been evaluated to correspond to the continuous exposure of cells to 20 nM of MMS, which could cause weak endogenous alkylating damage (Rydberg & Lindahl, 1982). However, in some bacteria, SAM could be innocuous. Indeed, a 100-fold range of SAM levels was achieved experimentally without causing any change in the mutation rate of *E. coli* (Posnick & Samson, 1999).

The second source of alkylating agents are the reactive alkyls that are created by the peroxidation of lipids. Lipid peroxidation occurs when the cells encounter oxidative or nitrosative stress (**Fig 2A**). Importantly, lipid peroxidation occurs on polyunsaturated fatty

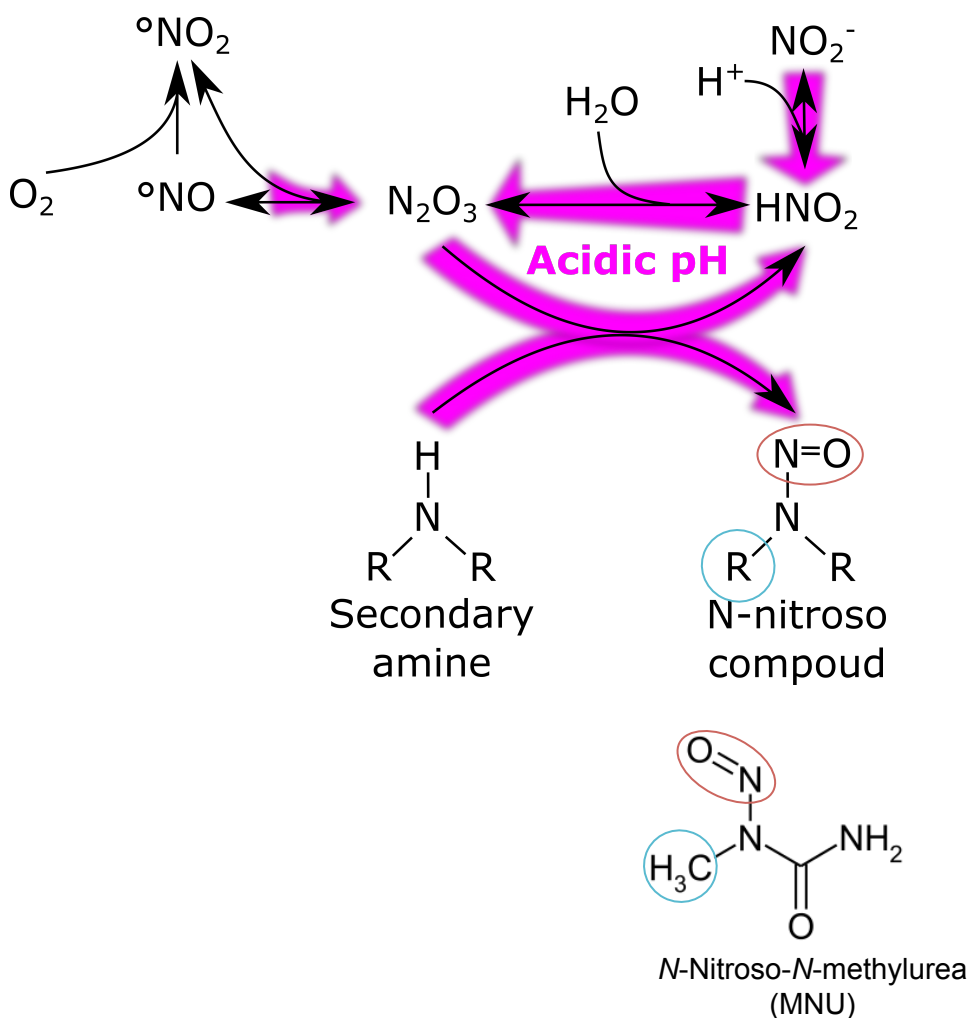


Fig 3. Generation of N-nitroso compounds. In presence of N_2O_3 , secondary amines or amides (such as the precursor of MNU) can get nitrosated. This reaction is greatly favored in acidic conditions. If the N-nitroso compound possesses an alkyl group, as with MNU, it can act as a direct alkylating agent. If not, the N-nitroso compound will become an alkylating agents only after metabolic activation (see main text for details).

acids (PUFA) only, as they possess several double bonds (Bielski *et al.*, 1983; Winczura *et al.*, 2012) (**Fig 2A**). These particular alkylating agents can generate exocyclic etheno- or propano-adducts on DNA, but the formation of these adducts *in vivo* is not completely clear yet (Tudek *et al.*, 2017). Two major lipid peroxidation products are malondialdehyde (MDA) and 4-hydroxy-2-nonenal (HNE). MDA forms mainly M₁dG, which are the equivalent of 3-(2-deoxy-β-D-*erythro*-pentofuranosyl)pyrimido-[1,2α]purine-10(3H)-one DNA adducts (**Fig 2C**) (Tudek *et al.*, 2017). As for HNE, it can generate bulky adducts (**Fig 2B, C**) or, in its epoxide form, simple etheno adducts such as 1,*N*²-εdG (**Fig 2C**). Some exocyclic adducts can undergo spontaneous rearrangements into a ring-opened conformation, which can lead to the formation of abasic sites (AP sites) on DNA (Tudek *et al.*, 2017). Exocyclic adducts can also generate inter- and intra-strand DNA-DNA crosslinks, as well as DNA-protein crosslinks (Tudek *et al.*, 2017). Typically, simple unsubstituted etheno-adducts are slightly mutagenic and cytotoxic in bacteria thanks to efficient DNA repair, whereas large substituted adducts are a strong barrier for replication (Pandya *et al.*, 2000; Winczura *et al.*, 2012; Tudek *et al.*, 2017). Considering that bacteria are very poor in such fatty acids, and contain mainly mono-unsaturated and saturated fatty acids, it is considered that they face marginal lipid-derived alkylating stress (Bielski *et al.*, 1983; Nichols & McMeekin, 2002). *Borrelia burgdorferi* is the exception that proves the rule as it acquires PUFA from its eukaryotic host, which makes the bacterium vulnerable to lipid peroxidation (Boylan *et al.*, 2008).

The third source of alkylating agents is the generation of N-nitroso compounds. These compounds are produced when metabolites containing a secondary amine or an amide group meet N₂O₃, following oxidative and nitrosative stress. Importantly, this reaction mainly takes place under acidic pH (**Fig 3**). One example of N-nitroso compound generation is the formation of MNU by the nitrosation of methylurea, itself the result of the condensation between the catabolite methylamine and carbamyl phosphate, a precursor of pyrimidines. MNNG could apparently also be produced naturally (Vaughan *et al.*, 1993). Interestingly, amino acids can also undergo N-nitrosation (Shephard *et al.*, 1987; Ulusoy *et al.*, 2016). Tryptophan is the most reactive amino acids and it is a potent alkylating agent (Shephard *et al.*, 1987; Ulusoy *et al.*, 2016). As for the non-mutagenic N-nitrosoproline, it can transfer its nitroso group to thiourea under acidic conditions and transform it into MNU (Inami *et al.*, 2015). Polyamines, such as spermidine, can also be N-nitrosated into alkylating agents (Sedgwick, 1997). Note that many N-nitroso compounds are not direct alkylating agents and require metabolic activation. The cytochrome P450 proteins have been found to play a major role in their biotransformation (Guttenplan, 1987), but alternative pathways of activation also exist, such as through the action of the alcohol dehydrogenase enzyme (Eisenbrand *et al.*, 1984). Oxidation of the N-nitroso compounds by hydroxyl radicals can also activate the mutagenic potential of some compounds (Mestankova *et al.*, 2014). Note that it is also the case of photo-activation in presence of phosphate or carboxylate, such as citrate or succinate (Arimoto-Kobayashi & Hayatsu, 1998).

In *E. coli*, the majority of the spontaneous mutations are generated via the endogenous formation of N-nitroso compounds (Mackay *et al.*, 1994; Taverna & Sedgwick, 1996).

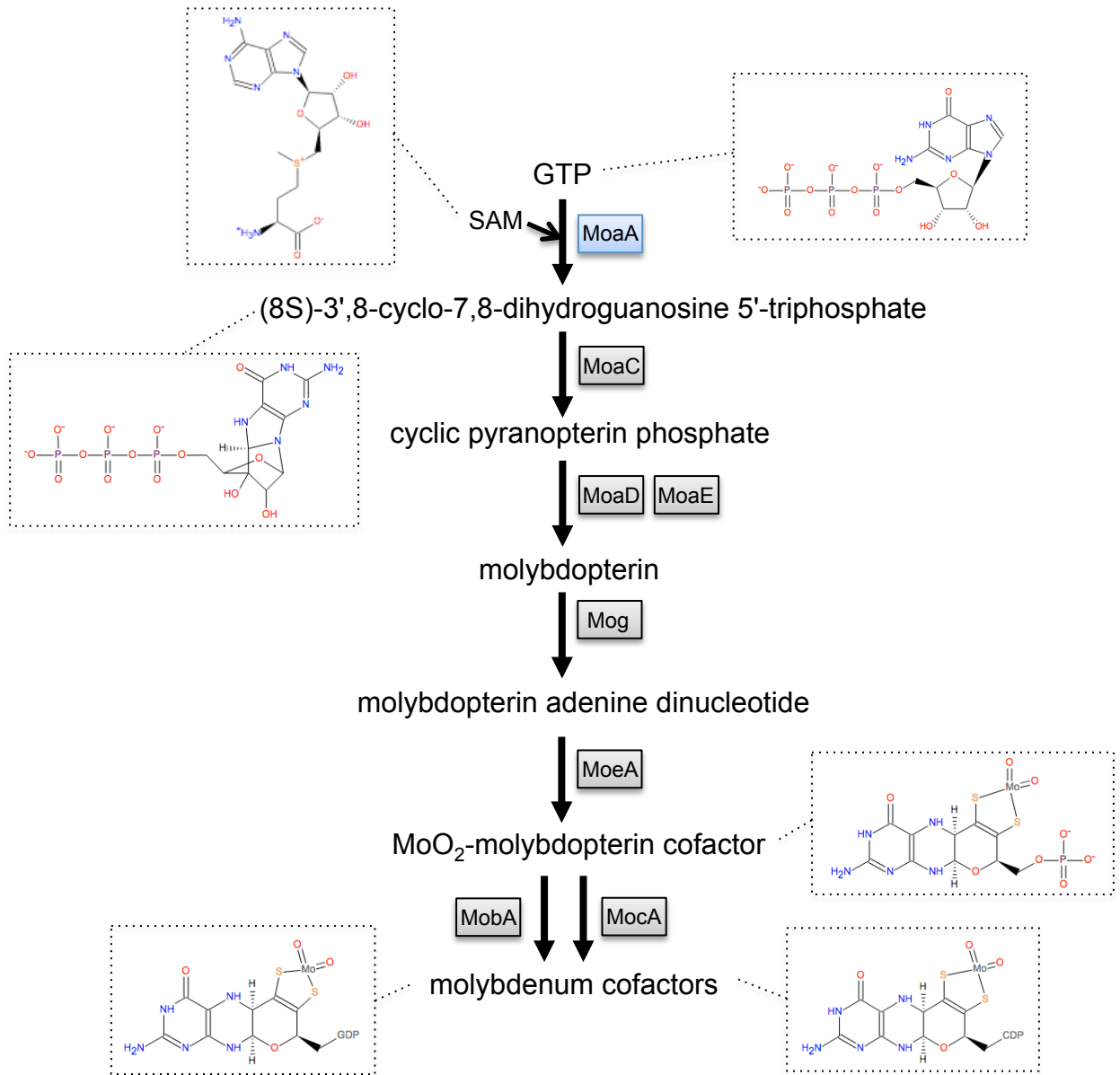


Fig 4. Pathway for molybdenum cofactors biosynthesis in *E. coli*. MoeA is the first enzyme of this pathway and its role is to catalyze the insertion of a purine carbon into the ribose of GTP. Note that this purine comes from a S-adenosylmethionine (SAM) molecule. *In fine*, three types of cofactors can be formed: the MoO₂-molybdopterin cofactor, the guanylyl molybdenum cofactor (on the left) and the cytidylyl molybdenum cofactor (on the right). Those three cofactors are required by diverse enzymes, among which nitrate reductases and periplasmic methionine sulfoxide reductase (involved in the protection of periplasmic proteins from oxidative damage) (Leimkühler, 2017).

Bacteria are particular in the sense that they can perform N-nitrosation at physiological pH (Calmels *et al.*, 1985). Indeed, it has been reported that under anaerobic conditions, even at neutral pH, the catalysis of amine nitrosation by *E. coli* is happening through a side reaction of nitrate reductase enzymes (Taverna & Sedgwick, 1996). Three *E. coli* mutants have been shown to be deficient in nitrosation: (1) *narG* encoding the catalytic subunit of nitrate reductase A, (2) *fnr* encoding a pleiotropic activator that influences the expression of the *narGHJ* operon, and (3) *moa* genes, involved in the synthesis of the molybdenum cofactor (**Fig 4**), which is required by nitrate reductase enzymes (Calmels *et al.*, 1988; Ralt *et al.*, 1988; Taverna & Sedgwick, 1996; Leimkühler, 2017). Note that in the case of *Pseudomonas aeruginosa*, nitrite reductase activity seems to be the key to N-nitrosation reaction (Calmels *et al.*, 1988). *Pseudomonas denitrificans* has an even more complex mechanism of generation of N-nitroso compounds, as it is apparently dependent on nitrate reductase activity, but modulated negatively by high nitrite concentrations (Calmels *et al.*, 1988). In conclusion, the study of N-nitrosation in bacteria is very complex, as results differ even among the same genera. One common finding is that N-nitrosation reactions typically occur under anaerobic conditions, not because this reaction is inhibited by oxygen, but most probably because the enzymes responsible for N-nitrosation reactions are induced upon oxygen deprivation (Ralt *et al.*, 1988).

Key information

Alkylating agents can damage DNA, resulting in innocuous, mutagenic or cytotoxic modifications. The three sources of natural alkylating agents are (1) SAM, (2) lipid peroxidation and (3) N-nitrosation of metabolites. In eukaryotic cells, N-nitrosation reactions occur in the presence of acidic pH and N₂O₃. Bacteria can also perform N-nitrosation reactions at physiological pH, typically via a side activity of nitrate reductase enzymes.

1.2. DNA repair pathways involved in alkylated DNA repair

1.2.1. The adaptive response

In the late 70's, a specific response to alkylating stress was described *in vitro* for *E. coli* (Samson & Cairns, 1977). This system was called “adaptive response” and it is based on the detection, by the Ada protein, of a meP3ester modification on DNA (McCarthy *et al.*, 1983). If meP3esters are the triggering adducts for the activation of this system, it is probably because they are not very frequent, hence their presence denotes the presence of a persisting alkylating stress (Friedberg *et al.*, 1995). In *E. coli*, *ada* is stochastically expressed to produce on average only one Ada protein per generation (Uphoff *et al.*, 2016). The detected meP3ester group is captured on the cysteine 38 (C38) residue of Ada, which becomes active as a transcription factor, upregulating the expression of a series of genes coding for proteins dedicated to the repair of alkylated DNA. These proteins comprise Ada itself, AlkB, AlkA and AidB (**Fig 5A**).

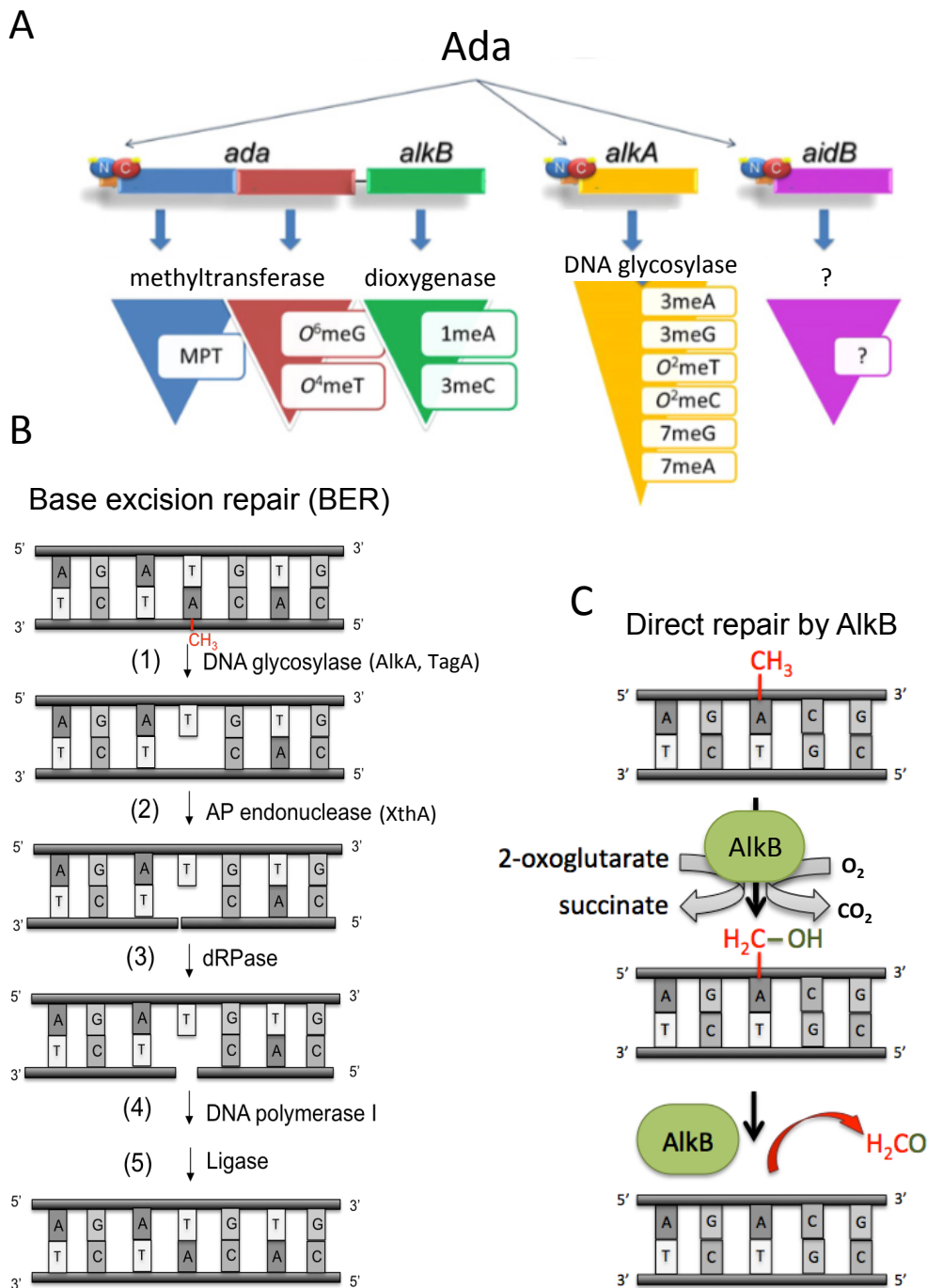


Fig 5. DNA repair pathways activated by the adaptive response in *E. coli*. **A)** Regulon of *E. coli* Ada proteins and targeted DNA adducts. MPT stands for methylphosphotriester (adapted from Mielecki *et al.*, 2014). **B)** Base excision repair pathway: (1) a DNA glycosylase, such as TagA or AlkA, removes the damaged base but leaves the ribose in place, creating an AP site; (2) an AP endonuclease cuts DNA on its 5' side; (3) a DNA deoxyribose phosphodiesterase (dRPase) free the sugar on its 3' side; (4) the single strand break is repaired by the DNA polymerase I and by (5) a DNA ligase. **C)** Direct repair by AlkB. In presence of Fe^{2+} , the dioxygenase AlkB can catalyze the hydroxylation of the methyl group, which leads to the restoration of the native base.

In addition to its role as a transcription factor, Ada can also directly repair O⁶meG and O⁴meT via the capture of the methyl group on its C321 residue. As for the dioxygenase AlkB, it is involved in the direct repair of the mutagenic lesions 1meA and 3meC (**Fig 5C**), as well as several etheno adducts repair (Zdzalik *et al.*, 2015). The DNA glycosylase AlkA removes the most cytotoxic lesion 3meA via the base excision repair (BER) pathway (see **Fig 5B** for details on the pathway) (Lindahl *et al.*, 1988). Regarding the *aidB* gene, it is known that it is also overexpressed by the adaptive response, but its function still remains elusive. The current hypothesis is that AidB is involved in protecting specific sequences of DNA and destroying alkylating agents before they reach DNA (Bowles *et al.*, 2008; Rippa *et al.*, 2011). Note that the expression of *ada* is also upregulated by 20-fold via RpoS (σ^S) during the transition from the exponential to the stationary phases of growth (Taverna & Sedgwick, 1996). In contrast, the Ada protein can be induced *in vitro* by as much as 1000-fold upon exposure of *E. coli* to alkylating agents (Taverna & Sedgwick, 1996). At all times, there are also two proteins constitutively produced and independent of the adaptive system, which assure the protection of DNA from endogenous alkylating agents. These are the direct repair protein Ogt, which has a C139 residue with similar function than the C321 of Ada, and the BER glycosylase TagA, which is functionally similar to AlkA (**Fig 5B**) (Lindahl *et al.*, 1988).

Importantly, the Adaptive response is well conserved in the prokaryotic world, but the regulon of Ada can be different following the bacterial genera and species (Mielecki *et al.*, 2015). For example, in *Pseudomonas putida*, the expression of *alkB* is not regulated by the Ada response but constitutively (Mielecki *et al.*, 2013). As for *Mycobacterium tuberculosis*, its *ada* gene has been split into two, with one gene (*adaA*) that is fused to *alkA* (Yang *et al.*, 2011). In this bacterium, both *ada* genes are inducible by more than 15 fold, but *alkB* and *aidB* can be only moderately upregulated by 2.6 and 1.6 times, respectively (Yang *et al.*, 2011). In the case of *Salmonella enterica* serovar Typhimurium, the Ada regulon is organized as in *E. coli*, but the bacterium is unable to adapt to challenging doses of MNNG (Hakura *et al.*, 1991).

1.2.2. The SOS response

Other DNA repair pathways can be involved in repairing alkylated DNA. For example, it is known that the SOS pathway, mediated by LexA, is activated early following alkylating stress, before the adaptive response is activated to limit mutagenesis (Uphoff, 2018). If the BER pathway is impaired or insufficient, the SOS response is even more important. Indeed, in this case, at the population level, the activation of the SOS response occurs at even lower doses of alkylating agent because of the accumulation of cytotoxic lesions that are taken care of by homologous recombination (Costa de Oliveira *et al.*, 1987).

Under non-stressing conditions, *E. coli* contains about 1300 molecules of LexA (Sassanfar & Roberts, 1990). LexA is a dimeric repressor for the expression of about 50 genes, which are recognized by the transcription factor at the so-called “SOS-box sequences”

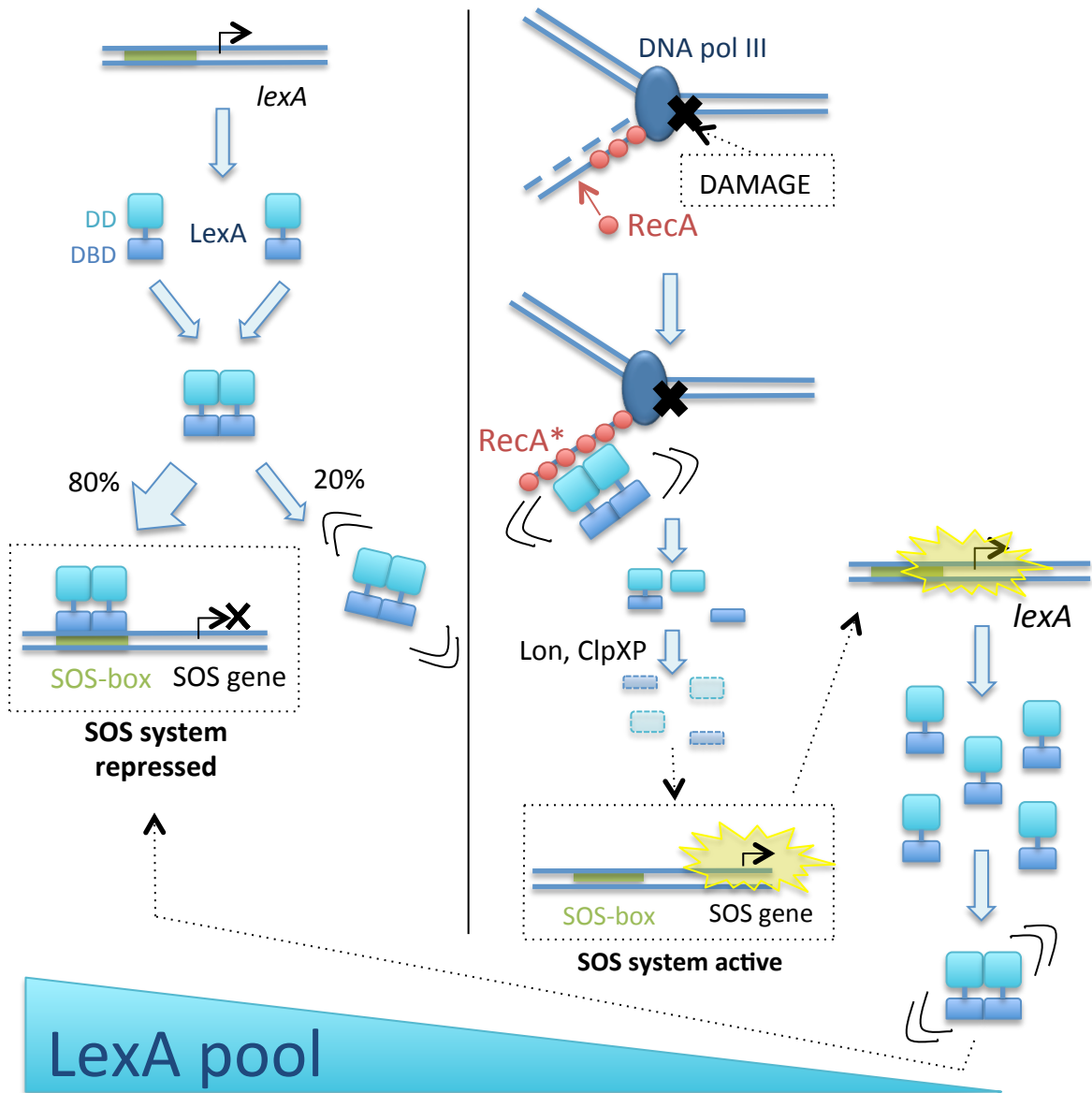


Fig 6. Activation of the SOS system in *E. coli*. In absence of genotoxic stress, most dimers of LexA bind to SOS-boxes on DNA in promoter regions, which prevents the recruitment of RNA polymerase and thus transcription of the target genes. Upon genotoxic stress, RecA accumulates on ssDNA and becomes competent for its co-protease activity (*) on unbound LexA. Cleaved LexA products are rapidly degraded by the ClpXP and Lon proteases, leading to the decrease of the LexA pool. This results in the active transcription of SOS genes, amongst which there are many genes involved in DNA repair (*recA*, *uvrA*, *ruvA*, *dnaE*, *dinB*, *umuD*, etc). One of the first promoters to be free from LexA is the promoter of *lexA* itself. This leads to the production of LexA proteins, which are rapidly degraded. Nevertheless, when the SOS response needs to be shut off, the production of sufficient LexA proteins is swift. DD stands for dimerization domain and DBD stands for DNA binding domain (based on Butala *et al.*, 2011).

in their promoter (Courcelle *et al.*, 2001; Wade *et al.*, 2005). Most LexA proteins are bound to DNA, but they can dissociate and reassociate to DNA, so that 20 % of the proteins are also found free (Mohana-Borges *et al.*, 2000). When the bacteria encounter genotoxic stresses, RecA proteins are recruited on single stranded DNA (ssDNA) and change their conformation to acquire a RecA* activity, which promotes the auto-cleavage of LexA (Little, 1991; Butala *et al.*, 2011). Eventually, the pool of LexA proteins decreases and gene expression gets derepressed (**Fig 6**) (Courcelle *et al.*, 2001). Promoters are not equal in the timing of LexA unbinding. Indeed, two criteria are involved in LexA affinity for a given promoter: (1) the number of mismatches away from a perfect palindromic TACTG(TA)₅CAGTA SOS-box and (2) the pattern of mismatches (Janion, 2008; Zhang *et al.*, 2010). This results in the temporal ordering of gene expression, with genes separated into subsets of early, middle and late categories.

Interestingly, the early accumulation of LexA is a sign of SOS response activation, because *lexA* itself is part of its early regulon, so that the response can be stopped eventually (Little & Mount, 1982). Apart from the constitutively expressed DNA replicating polymerase III, three other DNA polymerases are regulated by the SOS response. Actually, the expression of *polB*, coding for the proofreading DNA polymerase II and of *dinB*, coding for the error-prone DNA polymerase IV are increased relatively early upon LexA cleavage as they belong to the middle category (Little & Mount, 1982; Iwasaki *et al.*, 1990; Janion, 2008). Conversely, the expression of *umuDC*, coding for the most error-prone DNA polymerase V occurs in late SOS-induced cells (Little & Mount, 1982; Fernandez De Henestrosa *et al.*, 2000; Janion, 2008). It is believed that this sequential timing of gene induction allows the bacterium to first facilitate a non-mutagenic response, before to eventually use a more extreme survival strategy (Simmons *et al.*, 2008).

Very recently, this model of SOS genes activation has been improved by taking into account the fact that the dose of DNA damage is also strongly impacting the response. Actually, the activation pattern of the SOS network changes according to the relative gene induction, but also in terms of the relative timing of peak activation for each gene, which changes with damage importance (Culyba *et al.*, 2018). One typical example is the gene *sulA*, coding for a cell division inhibitor, and belonging to the category of late stage genes, like *umuDC*. Under highly stressing conditions, the promoter of *sulA* is strongly activated, but late, with a maximum activity after 90 minutes. At the opposite, under lower stressing conditions, such as UV doses 100 times less aggressive, the maximal activity of the promoter is about 10 times weaker, but it is reached much faster as it takes about 25 minutes (Culyba *et al.*, 2018). This dual response to stress is probably part of the explanation for how *E. coli* induces the expression of *dinB* and *umuDC*, coding for the translesion DNA polymerases, very early against exogenous DNA alkylation damage (Uphoff, 2018). This way, bacteria prioritize the continuation of DNA replication over the potential harmful effects of mutagenesis (Uphoff, 2018). Note that this response is viable because the constitutively produced TagA is present to cope with the most cytotoxic lesions at the same time (Uphoff, 2018).

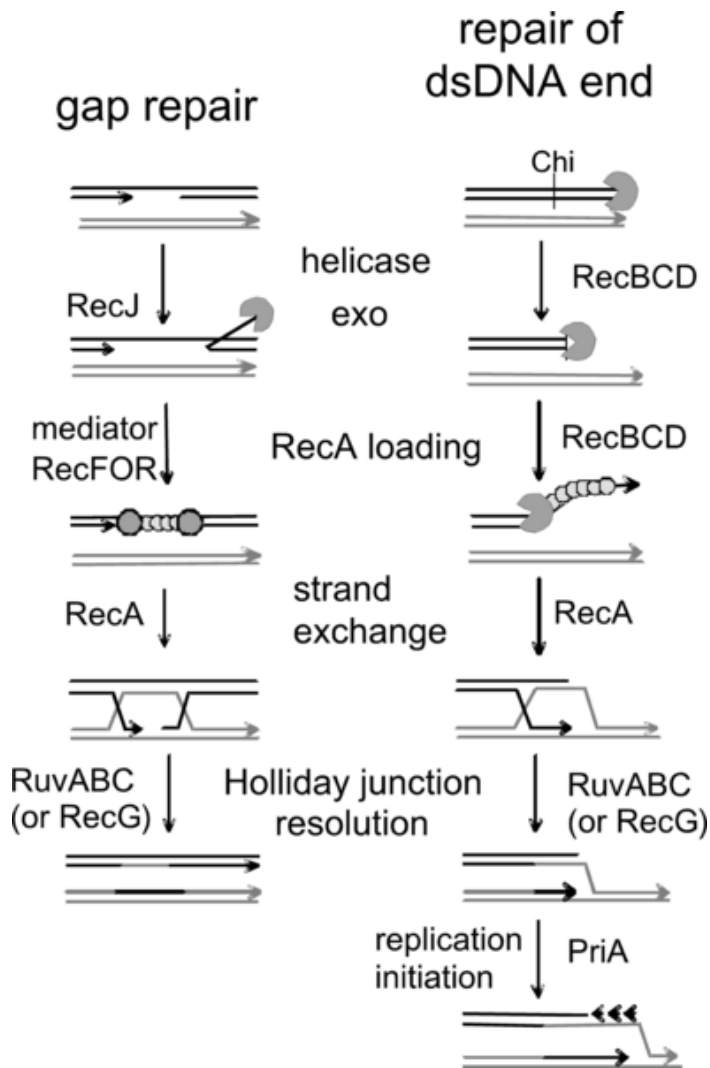


Fig 7. Models for homologous recombination in *E. coli*. At gaps, the 5' single-stranded (ssDNA) exonuclease RecJ increases the size of the ssDNA region, then RecF, RecO and RecR promote the binding of RecA on ssDNA, which is covered by single strand binding proteins. In the case of double strand breaks, the RecBCD complex (replaced by AddAB in some bacteria, such as in *B. abortus*) degrades DNA until it finds a *Chi* site. It then forms 3'-ended ssDNA where RecA can be recruited. The homology search and strand exchange steps are then performed by RecA, which forms a Holliday junction (*i.e* a "X" structure). The resolution of the Holliday junctions are possible through the action of RuvC, which first requires a branch migration performed by RuvAB or RecG. Note that the RecBCD-mediated recombination is always coupled with PriA-dependent replication restart (Rocha *et al.*, 2005)

Interestingly, in α -proteobacteria, the SOS boxes are not palindromic, but composed of direct repeats: GTTC-N₇-GTTC and its reverse and complementary sequence GAAC-N₇-GAAC (Fernandez de Henestrosa *et al.*, 1998; Tapias & Barbe, 1998; Erill *et al.*, 2004). In addition, a few genes have been found to be downregulated upon the activation of the SOS system in α -proteobacteria (Tapias *et al.*, 2002; da Rocha *et al.*, 2008). Therefore, the mode of action of LexA in α -proteobacteria could be quite different than what is observed in *E. coli*. One hypothesis is that, instead of blocking the access of the RNA polymerase to the promoter region, LexA can recruit the polymerase, but represses transcription by interfering with its clearance process. Indeed, under high LexA concentrations only, the RNA polymerase is stalled at the + 5 region in *Rhodobacter sphaeroides* *recA* promoter (Tapias *et al.*, 2002).

The regulon of LexA in α -proteobacteria has been determined for the model bacterium *Caulobacter crescentus* only (da Rocha *et al.*, 2008), but an earlier study proposed that the core SOS regulon of α -proteobacteria is composed of *lexA*, *recA*, *ssb*, *uvrA*, *ruvC*, *dnaE*, *dinB* (coding for the error-prone DNA polymerase IV), *imuA* (previously known as *sulAI*, and coding for a subunit of another error-prone DNA polymerase (Galhardo *et al.*, 2005)), *parE*, *ispE* (but it seems to be wrongly annotated in the paper, as the given ORF correspond to another gene coding for a transporter), *comM* (absent in *Brucella* species) and *rmuC* (previously known as *yigN*) (Erill *et al.*, 2004). Note that in *C. crescentus*, the promoter of *tagA*, coding for an enzyme performing alkylated DNA repair, is regulated by LexA (da Rocha *et al.*, 2008), whereas it is proposed to be regulated by CtrA in *Brucella abortus* (Francis *et al.*, 2017).

1.2.3. Homologous recombination

The adaptive response typically regulates the BER and direct repair pathways (Lindahl *et al.*, 1988), whereas the SOS system is in charge of homologous recombination, nucleotide excision repair (NER) and translesion synthesis (TLS) (Baharoglu & Mazel, 2014). RecA itself is involved in homologous recombination and in the SOS response, but also in stimulating the activity of AlkB by physically interacting with the dioxygenase (Shivange *et al.*, 2016).

In the case of alkylating stress, homologous recombination has been shown to be very important (Nowosielska *et al.*, 2006). Homologous recombination is a process that exists in all forms of life and that allows high-fidelity repair of DNA damage in a template-dependent way (Rocha *et al.*, 2005). In bacteria, the two major homologous recombination pathways are RecBCD, which processes double-strand breaks (Kuzminov & Stahl, 1999), and RecFOR, which processes single-strand gaps (Morimatsu & Kowalczykowski, 2003) (**Fig 7**). Both pathways have been found to be required during alkylating stress (Nowosielska *et al.*, 2006). Indeed, single-strand gaps are produced by the AP endonuclease of the BER pathway, as well as by DNA replication at blocking lesions. Then, if replication occurs before successful

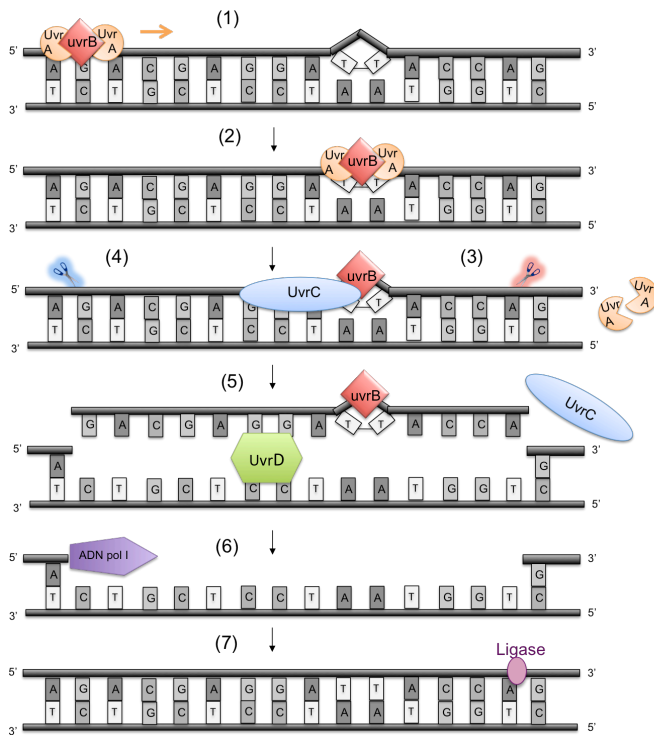
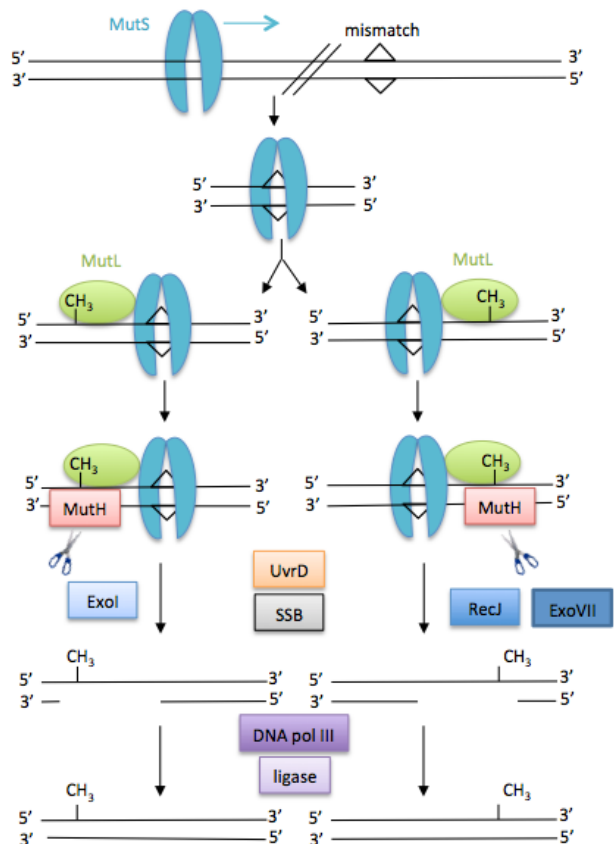


Fig 8. Model for nucleotide excision repair in *E. coli*. (1-2) Bulky lesions (such as pyrimidine dimers) are recognized by UvrA, which is in complex with UvrB. (3-4) UvrA is then replaced by UvrC, which cleaves a phosphodiester bond 8 nucleotides upstream of the damage, while UvrB cleaves a phosphodiester bond 4 nucleotides downstream of the damage. (5) A fragment of 12 nucleotide is thus removed with the help of the UvrD helicase. (6-7) The gap is eventually filled with the action of the DNA polymerase I and a DNA ligase.

Fig 9. Model for mismatch repair in *E. coli*. The MutS proteins are in charge of scanning the genome until they detect mismatched bases. In *E. coli*, mismatch repair is methyl-directed. Indeed, MutH is able to discern the methylated parental DNA strand from the non-methylated newly synthesized DNA strand. Therefore, when MutH is recruited by MutL, it nicks specifically the non-methylated strand. The UvrD helicase is then recruited to separate the two strands and push the MutSLH complex toward the mismatch. Depending on the localization of the mismatch, different exonucleases can digest the ssDNA trail. Note that the leftover ssDNA gets coated with single strand binding (SSB) proteins until the gap is repaired by the DNA polymerase III and a DNA ligase.



repair, single-strand gaps get converted into double strands breaks (Nowosielska *et al.*, 2006). Note that some bacteria, such as *B. abortus* and *C. crescentus*, do not possess a RecBCD complex, but instead use an AddAB system, which is considered as functionally equivalent (Martins-Pinheiro *et al.*, 2007; Wigley, 2013).

As homologous recombination requires the presence of a template, this DNA repair pathway only works during the S phase (characterized by ongoing replication) and G2 phase (with fully replicated DNA) of the cell cycle. At the opposite, the non-homologous end joining pathway can work at all stages of the cell cycle (Mao *et al.*, 2008). However, this pathway is absent in most bacterial species, including *E. coli*, *C. crescentus* and *B. abortus* (Weller *et al.*, 2002; Martins-Pinheiro *et al.*, 2007). Nevertheless, it exists in *M. tuberculosis* and *Bacillus subtilis* (Weller *et al.*, 2002; Gong *et al.*, 2005), but the relevance of this pathway against alkylating stress on these bacteria has not been investigated.

1.2.4. Nucleotide excision repair

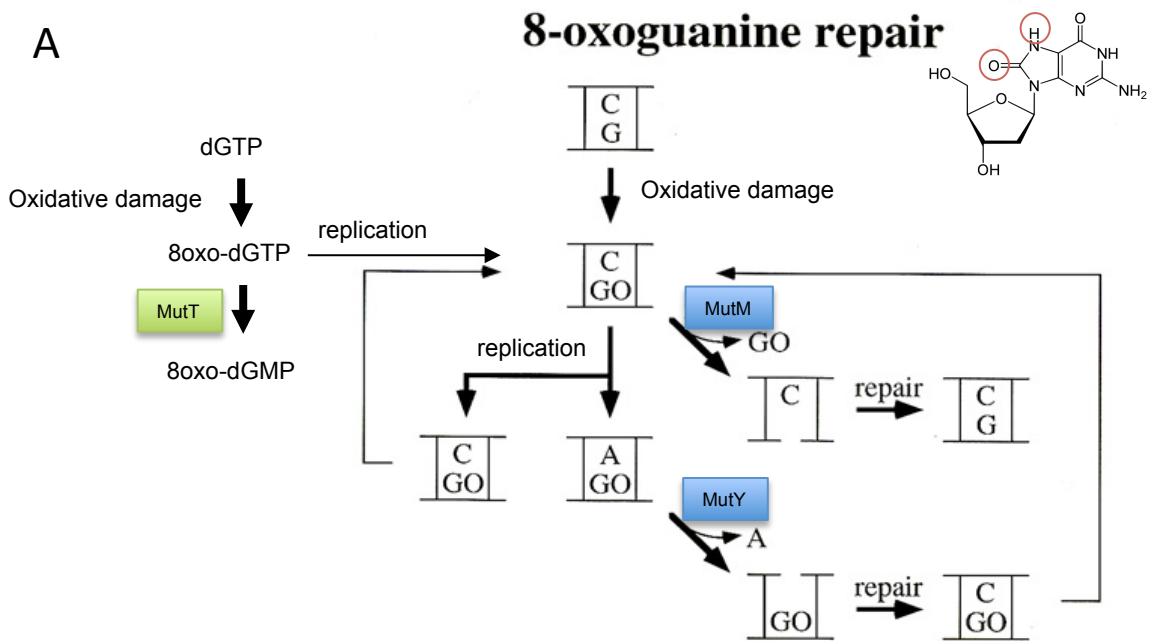
NER relies on the four Uvr proteins: UvrA, UvrB, UvrC, and UvrD (also known as DNA helicase II). This pathway is taking care of bulky lesion on DNA. Briefly, UvrA and UvrB are charged of scanning the genome until UvrA detects a distortion in DNA, such as pyrimidine dimers. UvrA is then replaced by UvrC and the UvrBC dimer cleaves DNA on phosphodiester bonds of both sides of the damage. UvrD then breaks the hydrogen bonds between the complementary bases and a segment of 12 nucleotides is removed. New DNA is synthesized by DNA polymerase I to fill the gap and the repair process finishes with a DNA ligase (Truglio *et al.*, 2006) (**Fig 8**). Importantly, NER can be coupled to transcription via the ATPase TRCF (also called Mfd), which removes the stalled RNA polymerase and also recruits UvrA (Deaconescu *et al.*, 2006).

Regarding alkylating stress, NER is necessary when adducts are large and distort DNA. It is for example the case of ethyl adducts (Nakano *et al.*, 2017) or interstrand cross-links, which are caused by bi-functional alkylating agents or following lipid peroxidation (Kondo *et al.*, 2010; Tudek *et al.*, 2017). Interestingly, the NER pathway also contributes to the cytotoxic and mutagenic O⁶meG lesion repair during the first hours after alkylating stress in *E. coli*, before the adaptive response can be fully induced (Samson *et al.*, 1988).

1.2.5. Mismatch repair

Mismatch repair (MR) is charged of editing replication errors. The MR system, composed of MutH, MutL and MutS proteins, is dependent on the Dam-related methylation status of *E. coli* DNA. Indeed, in this γ -proteobacterium, MutH is able to discern the parental DNA strand (that serves as template) from the newly synthesized one by recognizing the non-methylated state of the new DNA (Yamaguchi *et al.*, 1998; Kunkel & Erie, 2005). Thus, after MutS has detected the distortion in the helix caused by a base mismatch, MutL is recruited to allow the interaction between MutS and MutH. MutH then nicks the mutated and non-methylated strand, and the UvrD helicase is recruited by MutL to separate the two strands and

A



B

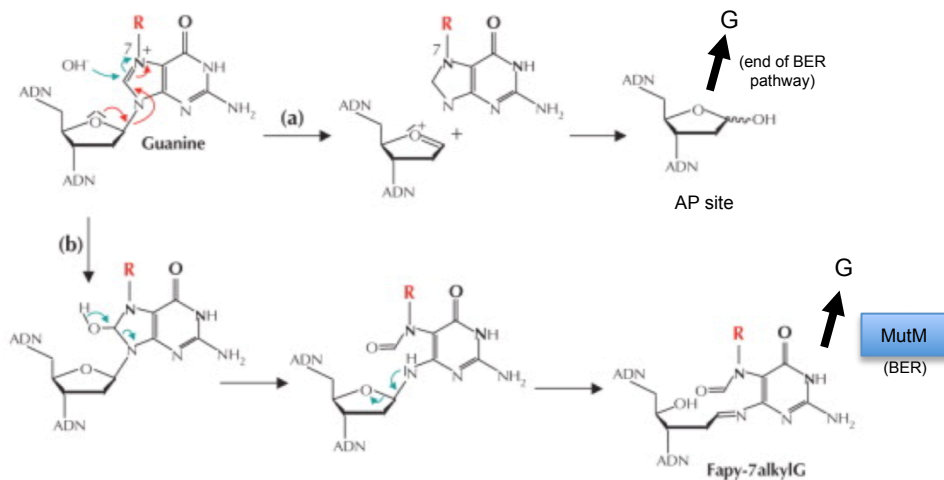


Fig 10. Models for MutM functions. **A)** repair of 8-oxoguanine, a highly mutagenic base analog, either as a constituent of DNA (8-oxodG/GO) or when present as a deoxynucleoside triphosphate (8-oxodGTP). The MutM protein is a DNA glycosylase that can initiate base excision repair (BER) of 8-oxodG when it is paired with a C. If left unrepaired, 8-oxodG can be mispaired with a A by replication events. In this case, the MutY DNA glycosylase can remove the A. There also exists a MutT protein, which hydrolyzes 8-oxodGTP to 8-oxodGMP and pyrophosphate in order to prevent its incorporation into DNA (image adapted from <http://cmgm.stanford.edu/biochem201/Slides/DNA%20Repair/>). **B)** MutM can also repair Fapy-7meG adducts. Upon alkylating stress, 7meG adducts can be formed. They are considered as innocuous. Nevertheless, they can (a) destabilize the N-glycosidic bond, which leads to spontaneous depurination of this lesion and the resulting toxic AP sites, or (b) manifest toxicity by converting into their toxic and slightly mutagenic imidazole ring-opened form, which are the Fapy-7meG adducts. Note that MutM is also known under the name of Fpg (formamidopyrimidine-DNA glycosylase). R stands for methyl in this example (image adapted from <https://ars.els-cdn.com/content/image/1-s2.0-S0007455115305518-gr4.jpg>).

push the MutSLH complex toward the mismatch. An exonuclease digests the resulting ssDNA trail and the leftover ssDNA gets coated with single strand binding (SSB) proteins. The gap is later repaired by the DNA polymerase III and a ligase (Kunkel & Erie, 2005) (**Fig 9**). In *B. abortus* and other α -proteobacteria, a gene homologous to *mutH* is missing (Martins-Pinheiro *et al.*, 2007; Guarne, 2012). However, it has been proposed that in such a case, MutL is able to also perform the MutH function (Kadyrov *et al.*, 2006; Pillon *et al.*, 2010).

In eukaryotic cells, O⁶meG:T mispairs have been demonstrated to be recognized by the MR system, but this results in futile cycles of repair, as the alkyl adducts remain in the template (Lips & Kaina, 2001). This leads to the formation of single strand breaks, and then double strand breaks and apoptosis (Kondo *et al.*, 2010; Li *et al.*, 2016). MR proteins have also been found to be recruited in the presence of alkylation DNA damage in bacteria (Taira *et al.*, 2008; Nakano *et al.*, 2017; Uphoff, 2018). In *E. coli*, O⁶meG:T mispairs are efficiently repaired by the MR system (Taira *et al.*, 2008). However, *E. coli* MR pathway can generate futile cycles of repair following O⁴meT:A detection, by either re-pairing the modified T with a A, or with a G (Nakano *et al.*, 2017). In addition, during replication, O⁴meT is mistaken for a C, which leads to the incorporation of a G. Considering that *E. coli* MR MutS protein is less able to recognize O⁴meT:G than O⁴meT:A, AT-to-GC mutagenesis is enhanced (Nakano *et al.*, 2017).

1.2.6. The MutM DNA glycosylase

The MutM enzyme, also known as Fpg, is best known for its role in 8-Oxo-2'-deoxyguanosine (8-oxodG) repair. The 8-oxodG adducts are the major products of DNA oxidation and they have ambiguous base-pairing properties, as they get paired with either A or C during DNA synthesis. There exist three enzymes dedicated to protect the cells against those adducts: (1) the MutM enzyme, which is a DNA glycosylase of the BER pathway; (2) MutY, which is also a DNA glycosylase; and (3) MutT, which is necessary if the oxidized base is present as a deoxynucleoside triphosphate (8-oxodGTP). Indeed, MutT can hydrolyze 8-oxodGTP, thus preventing its incorporation into DNA (**Fig 10A**) (Fowler *et al.*, 2003).

What is less known about MutM is that it is also involved in alkylated DNA repair. First, it has been found to be able to remove Fapy-7meG, which are 7meG with alkali-opened imidazole rings (formamidopyrimidines) (**Fig 10B**) (Chetsanga *et al.*, 1981). It is also able to remove the ring-opened derivative of the etheno adduct 1,N⁶-ethenoadenine (ϵ dA), which is called “product B” (Speina *et al.*, 2001).

Key information

Most DNA repair pathways can be used by cells to cope with alkylating stress. In addition to housekeeping DNA repair pathways, there also exist two inducible pathways in bacteria: (1) the alkylation-specific adaptive response, which regulates the expression of genes of the base excision and direct repair pathways, and (2) the SOS response, which plays on homologous recombination, nucleotide excision repair and translesion synthesis.

1.3. Is alkylating stress relevant for intracellular bacteria?

One question that remains about alkylating stress is whether it is occurring on bacteria that infected host cells. Macrophages and neutrophils are known to produce N-nitroso compounds, some of which are direct alkylating agents (Iyengar *et al.*, 1987; Miwa *et al.*, 1987; Grisham *et al.*, 1992; Vermeer *et al.*, 2004). However, the occurrence of this stress on intracellular bacteria has never been proven. The production of N-nitroso compounds by eukaryotic cells is dependent on acidic pH and high intracellular RNS concentration, as they lead to N_2O_3 formation (Fig 3) (Iyengar *et al.*, 1987; Ohshima *et al.*, 1991). Moreover, it is also known that bacterial membranes have a higher permeability for some alkylating agents when they are in an acidic environment (Guttenplan & Milstein, 1982). It has been hypothesized that N-nitroso compounds could be differentially produced in subcellular compartments (Espey *et al.*, 2001), so one could wonder if vacuoles containing bacteria are also prone to accumulating such compounds. Indeed, many intracellular bacteria first transit through an endosomal-derived vacuole, before reaching their replicative compartment (Kumar & Valdivia, 2009).

Importantly, the endogenous production of N-nitroso compounds is known to be more important in anaerobic and resting *E. coli* (Kunisaki & Hayashi, 1979). It has been shown that Ogt plays a major role in coping with alkylating stress under such conditions (Rebeck & Samson, 1991; Mackay *et al.*, 1994). As a reminder, the catalysis of amine and amides nitrosation by *E. coli* is happening through a side reaction of nitrate reductase enzymes (Taverna & Sedgwick, 1996).

There exist a very few papers on the potential detection of alkylating stress on bacteria during infection. Importantly, those studies were all based on DNA repair deletant mutants and were inconclusive as for the existence of the stress inside host cells. It is for example the case of *Mycobacterium tuberculosis*, as an *ogt* deletion mutant was not attenuated in mice (Durbach *et al.*, 2003). It has been proposed that the absence of attenuation could be due to a functional redundancy in diverse DNA repair pathways (Puri *et al.*, 2014). Actually, *in vitro*, bacteria are faced with stresses without warning. On the contrary, *in vivo*, there is a preexisting response of the bacteria stemming from their interactions with their host, which could explain why the absence of one DNA repair pathway is not detrimental in this case. The study performed on *Salmonella enterica* serovar Typhimurium is a good argument in favor of

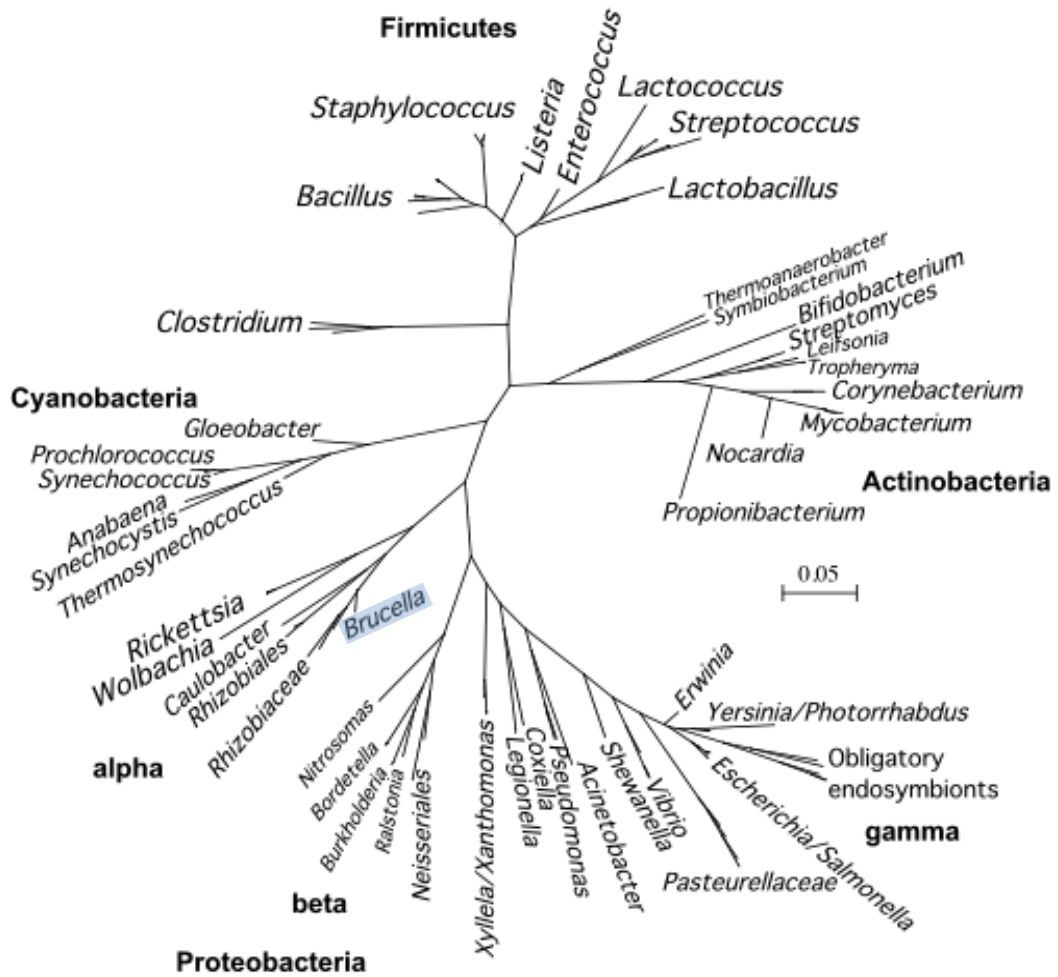


Fig 11. Phylogenetic tree of several bacteria. *Brucella* belongs to the alpha-proteobacteria class (image taken from <http://wwwabi.snv.jussieu.fr/erocha/research/ordersvdisorder.html>). Note that a more detailed phylogenetic tree (of alpha-proteobacteria only) can be found in the appendix 4.

this hypothesis. Indeed, the authors had to create a quintuple deletion mutant ($\Delta ada \Delta ogt \Delta tagA \Delta uvrA \Delta mfd$) before they could observe an attenuation in orally-infected mice (Alvarez *et al.*, 2010). Amazingly, this attenuation was of approximately 200-fold compared to the wild type (WT) strain, but was completely absent in intraperitoneally-infected mice (Alvarez *et al.*, 2010).

The following section will focus on *B. abortus*, as we used this bacterium as a model for the study of alkylating stress on an intracellular bacterial pathogen.

Key information

In theory, it is possible that intracellular bacteria encounter alkylating stress inside host cells, both endogenously, because of their metabolism, and exogenously, via the host cell defense. Nevertheless, it still needs to be demonstrated experimentally.

II. *Brucella abortus*

II.1. *Brucella* is an α -proteobacterium

Brucella belongs to the proteobacteria phylum (**Fig 11**). This phylum was named after Proteus, a Greek god of the sea who could change shape at will (Stackebrandt, 1988). Nowadays, the adjective "protean" is used to refer to versatility and adaptability. As their name suggests it, the α -proteobacteria class consists of very diverse organisms. They are Gram-negative bacteria and this class includes pathogens for animals (*Brucella*, *Rickettsia*) and plants (*Agrobacterium*), symbionts of arthropods (*Wolbachia*) and plants roots (Rhizobiales which fix nitrogen) as well as free living and opportunistic bacteria like *Caulobacter* and *Ochrobactrum*, respectively (Moreno & Moriyon, 2006). The α -proteobacteria class also seems to represent the most abundant marine cellular organisms (Giovannoni *et al.*, 2005), yet what they are most famous for is the fact that they are considered as the ancestors of mitochondria (Esser *et al.*, 2004).

Without surprise, α -proteobacteria also display very different morphologies. The best known are stalked bacteria. They include bacteria such as *C. crescentus*, *Asticacaulis biprosthicum* and *Hyphomonas neptunium*. These three bacteria are characterized by a dimorphic life cycle resulting from the production of two functionally and morphologically different cells at every cell division: a motile swarmer cell and a sessile stalked cell. Stalks are thin tubular extensions of the cell body and seem to be involved in nutrient uptake (Wagner & Brun, 2007). Even the other α -proteobacteria that appear to have a more classical rod-shaped phenotype can be regarded as having very different phenotypes. For example, *Ochrobactrum* and *Agrobacterium* possess peritrichous flagellae, while *Brucella* is a non-motile coccobacillus. There also exist spiral-shaped bacteria such as *Rhodospirillum* or the mono-flagellated *Kiloniella laminariae* (Wiese *et al.*, 2009).

Despite their obvious heterogeneity, α -proteobacteria seem to share common features. One of them is that they divide asymmetrically, or at least it is the case for *C. crescentus*, *B. abortus*, *Sinorhizobium meliloti*, *Agrobacterium tumefaciens* and *Methylobacterium extorquens* (Hallez *et al.*, 2004; Bergmiller & Ackermann, 2011). This characteristic is very clear in *C. crescentus* but it is less obvious in the other bacteria since they do not display polar organelles. However, the two daughter cells have different sizes and an asymmetric subcellular localization of a signal transduction protein called DivK can be observed in *S. meliloti* and *B. abortus*, for example (Lam *et al.*, 2003; Hallez *et al.*, 2007). It has also been shown that a magnetotactic bacterium (*i.e.* able to orient itself in function of a magnetic field) called *Magnetospirillum gryphiswaldense* had to divide asymmetrically in order to overcome its intrinsic magnetic force (Katzmann *et al.*, 2011).

Key information

Brucella belong to the α -proteobacteria, the same phylogenetic group than *Caulobacter crescentus*, *Agrobacterium tumefaciens*, *Sinorhizobium meliloti* and Rickettsiales, such as *Wolbachia*.

II.2. Brucellosis

Brucella species are responsible for Brucellosis, a major and worldwide zoonosis. They have been divided into six classical species: *B. melitensis*, *B. abortus*, *B. suis*, *B. canis*, *B. ovis* and *B. neotomae*. Since the improvement of detection methods, several new species have been discovered. For instance, *B. ceti*, *B. pinnipedialis* and *B. microti*. Even though their genomes share more than 94% of sequence identity, these species have very different host preferences amongst mammals. Indeed, they infect preferentially goats, cattle, pigs, dogs, sheep, desert wood rats, cetaceans, seals and common voles, respectively (Godfroid, 2018). In animals, Brucellosis occurs as a chronic infection that is characterized by epididymitis in males or placentitis and abortion in pregnant females (Carvalho Neta *et al.*, 2010). The placenta is reported to be a relatively suppressed immune zone, as it is linking the mother and her genetically different offspring. Its physical and hormonal characteristics thus make it a privileged tissue in which *Brucella* and other pathogens, such as *Coxiella burnettii*, can proliferate in large numbers (Alexander *et al.*, 1981; Hansen *et al.*, 2011). This particular tropism of *Brucella* for the placenta could also be explained by the high concentration of the sugar alcohol erythritol in ruminant placental trophoblasts during the third trimester of pregnancy (Smith *et al.*, 1962; Samartino & Enright, 1993). Indeed, erythritol is one of the favorite carbon sources for *Brucella* (Sperry & Robertson, 1975). The excessive proliferation of the bacteria in the reproductive tract of its host eventually leads to the disruption of the placenta, which can cause abortion or the birth of an infected and weak offspring (Roop *et al.*, 2009). The bacteria can then spread from one animal to another, as they are present in high numbers in the aborted fetus, the discharged reproductive tract and milk (Moreno & Moriyon, 2006).

Humans are accidental hosts of *B. melitensis*, *B. abortus* and *B. suis*, in which they are responsible for a debilitating disease known as undulant fever or Malta fever (Moreno & Moriyon, 2006). Usually, human infections happen through the ingestion of contaminated dairy products or by exposure to infected animals. A major way of infection is through the aerosol route, which is why *Brucella* strains are subjected to strict regulations in laboratories (Yagupsky & Baron, 2005). There are currently no vaccines available for humans and the only treatment is the use of a combination of antibiotics (Moreno & Moriyon, 2006). Clinical manifestations commonly appear within 5 to 60 days after exposure to the bacteria. According to a systematic review of 33 databases, the main symptoms are weakness and fever, followed by joint, muscle, and back pain (Dean *et al.*, 2012). Testicular infection concerns one man over ten and severe complications such as endocarditis and neurological cases occur respectively with 1 and 4 cases per 100 patients (Dean *et al.*, 2012). Because the symptoms of Brucellosis are not specific but instead present themselves as an acute febrile illness, it is believed that cases of Brucellosis are largely underestimated. Despite this, in 2006, Brucellosis was still considered as the commonest zoonotic disease worldwide and had been estimated to affect more than 500 000 new cases annually (Pappas *et al.*, 2006). Thanks to massive eradication programs in the 70's and 80's, Brucellosis has disappeared from many countries including the USA, as well as Northern and Western Europe (Pappas *et al.*, 2006). However, it is still a major health problem in many parts of the world, and especially in Mediterranean countries of Europe, the Middle East, south and central Asia, north and east Africa, as well as Central and South America (WHO, 2006 report on Brucellosis).

Key information

Brucella are responsible for one of the biggest zoonosis worldwide. These bacteria are facultative intracellular pathogens that target species-specific mammalian hosts, with humans being accidental hosts of *B. abortus*, *B. suis* and *B. melitensis*.

II.3. *Brucella* inside host cells

This part of the manuscript has been published in a review (Poncin *et al.*, FEMS Microbiology Reviews, 2018) (see appendix 4).

II.3.1. *Brucella* intracellular trafficking

A whole genome-based phylogeny study revealed that Brucellosis probably appeared in wildlife populations in the past 86,000 to 296,000 years (Foster *et al.*, 2009). It thus happened before livestock domestication, even though this crucial step in history probably played a role in allowing the worldwide spreading of *Brucella* species (Foster *et al.*, 2009). Even though they can be cultivated on artificial media, it is established that *Brucella* need to enter inside their host cells in order to complete a successful infection process (Moreno & Moriyon, 2006). This is why they are now considered as facultatively extracellular intracellular pathogens (Moreno & Moriyon, 2002).

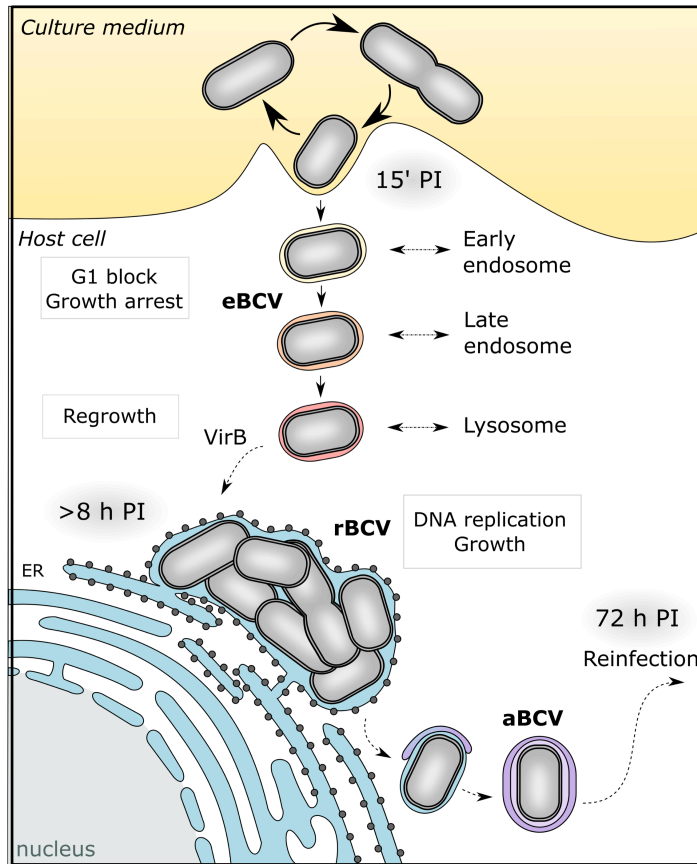


Fig 12. Schematic representation of *B. abortus* trafficking inside host cells. Once inside its host cell, *B. abortus* extensively interacts with the endocytic pathway. The compartment in which it resides at that stage can be referred to as the endocytic *Brucella*-containing vacuole (eBCV). In HeLa cells and RAW 264.7, during this first step of the infection, the bacterium is blocked in G1 and its growth is arrested. After a transient interaction with the lysosomes and thanks to its type IV secretion system VirB, the bacterium reaches its replicative niche (rBCV), which is part of the endoplasmic reticulum (ER) in most cell types. Later on, bacteria are found in autophagy-dependent vacuoles (aBCV) and are proposed to reinfect neighbor cells.

The mechanism by which *Brucella* manage to invade their host organism is not very clear but they seem to cross the mucosal barrier, which could imply an interaction with epithelial cells (Roop *et al.*, 2009). The role of these cells has not been deciphered yet but epithelial HeLa cells have been effectively used as models for *Brucella* infection in non-professional phagocytes (Pizarro-Cerda *et al.*, 1998; Castaneda-Roldan *et al.*, 2004; Starr *et al.*, 2008). Once inside its host, *Brucella* can also get internalized by professional phagocytes such as macrophages or dendritic cells. There, the bacterium can survive and multiply before disseminating in the organism (Archambaud *et al.*, 2010). Surprisingly, *B. melitensis* has also been reported to be able to invade murine erythrocytes during infection, which suggests that other cellular and *in vivo* models of infection should be developed to fully understand *Brucella* pathogenesis (Vitry *et al.*, 2014).

The entry of *Brucella* into epithelial or phagocytic cells occurs within minutes after cell-to-cell contact (Pizarro-Cerda *et al.*, 1998). Once internalized, the bacterium stays in a membrane-bound *Brucella*-containing vacuole (BCV) that interacts with the endocytic pathway (therefore termed eBCV) (**Fig 12**). Early endosomal markers, such as Rab5, are rapidly followed by the acquisition of late endosomal markers, typically lysosomal membrane-associated protein-1 (LAMP1) (Pizarro-Cerda *et al.*, 1998). Transient interactions with lysosomes have also been reported (Starr *et al.*, 2008). This eventually leads to eBCV acidification, which is deleterious to many bacteria, but nonetheless necessary for *Brucella* to reach their replicative niche and survive in the long-term (Porte *et al.*, 1999; Boschioli *et al.*, 2002; Celli *et al.*, 2003; Starr *et al.*, 2008). Indeed, the acidic pH of the eBCV has been linked to the capacity of the pathogen to induce the expression of the *virB* operon (Boschioli *et al.*, 2002). These genes code for a type IV secretion system that is essential for the bacteria to reach their proliferation niche (Boschioli *et al.*, 2002).

The *Brucella* replicative niche (rBCV) has been known for years to be somehow associated with the endoplasmic reticulum (ER), in both HeLa cells and macrophages (Pizarro-Cerda *et al.*, 1998; Celli *et al.*, 2003). It is only recently that the rBCV was shown to actually be part of the endoplasmic reticulum (Sedzicki *et al.*, 2018) (**Fig 12**). The transition from eBCV to rBCV is not clearly understood yet, but it has been suggested that its maturation could occur at the ER exit sites (Celli *et al.*, 2005; Celli, 2015). Several ER-associated functions have been linked to *Brucella* infection, such as the unfolded protein response IRE1a signaling pathway (Qin *et al.*, 2008; Smith *et al.*, 2013; Taguchi *et al.*, 2015), some autophagy-associated factors such as ATG9 and WIPI (Taguchi *et al.*, 2015) and the early secretory trafficking depending on the Sar1/coat protein complex II (Celli *et al.*, 2005; Taguchi *et al.*, 2015). Since the type IV secretion system is essential for *Brucella* to reach the rBCV, it is expected that the maturation of the BCV would be mediated by the delivery of bacterial effectors inside the host cell. One such effector is BspB, shown to target the Golgi apparatus by interacting with the oligomeric Golgi tethering complex (Miller *et al.*, 2017). This leads to the redirecting of Golgi-derived vesicles to the BCV by remodeling the ER-Golgi secretory trafficking (Miller *et al.*, 2017). It is important to note that there exist alternatives to the ER-derived replicative niche since opsonized *B. abortus* proliferate in a

non-acidic LAMP1-positive compartment in the human monocytic cell line THP-1 (Bellaire *et al.*, 2005) and in endosomal inclusions in extravillous trophoblasts (Salcedo *et al.*, 2013).

Once the number of bacteria within a cell reaches a critical level, destruction of this host cell can be observed (Moreno & Moriyon, 2006). Another means for *Brucella* to spread from one cell to its neighbors has been shown by Starr *et al.* (2012). The formation of a compartment with autophagic features (aBCV) could be the key to this important step of the infection (Fig 12). Indeed, autophagy-deficient *Brucella* are not able to perform cell-to-cell spreading when cellular infections are prolonged for long periods, typically 72 h (Starr *et al.*, 2012). Interestingly, only the initiation complex of autophagy seems to be needed by *Brucella* to promote reinfection (Starr *et al.*, 2012). Indeed, markers of the elongation phase of autophagy such as ATG5 and LC3 were not found to be associated with the aBCV (Starr *et al.*, 2012). It should be noted that autophagy is particularly important at birth. At that time, the transplacental nutrient supply is no longer available, which suggests that autophagy is strongly activated in the neonate in order to adapt to the early starvation period (Kuma *et al.*, 2004). The use of this process by the bacteria could therefore be relevant for their spreading inside newborn calves.

II.3.2. Growth and replication of *Brucella*

B. abortus possesses two distinct chromosomes (Chain *et al.*, 2005). Surprisingly, bacteria with multipartite genomes are not uncommon, as they represent about 10% of the sequenced species (Val *et al.*, 2014). Contrarily to most plasmids that are known to initiate replication several times during the bacterial cell cycle, chromids (also known as megaplasmids) encode essential genes and initiate their replication only once per cell cycle, like chromosomes (Pinto *et al.*, 2012; Val *et al.*, 2014). In *B. abortus*, the large and circular chromosome (I) is 2.1 Mb long and possesses a ParAB segregation system with three centromere-like *parS* sites, while the small chromosome (II) of 1.2 Mb is a chromid, with its segregation being controlled by a RepABC system (see Pinto *et al.*, 2012 for a review on this segregation system). The *repABC* operon also contains two centromere-like sequences called *repS* (Livny *et al.*, 2007; Deghelt *et al.*, 2014). The chromosomal replication status of *B. abortus*, and thus the stage of its cell cycle, can be followed with fluorescent reporters of the segregation markers ParB and RepB, as well as with fluorescent reporters allowing the localization of the replication origins (*ori*) and terminators (*ter*). Both chromosomes are oriented along the cell length, with *oriI* and *terI* associated with the poles, whereas *oriII* and *terII* are usually found closer to the midcell (Deghelt *et al.*, 2014). This is in agreement with what has been found in *S. meliloti*, another α -proteobacterium. Indeed, this bacterium possesses a tripartite genome with one primary chromosome (3.65 Mb) and two chromids (1.35 Mb for pSymA and 1.68 Mb for pSymB) (Galibert *et al.*, 2001). Both chromids are segregated by a RepABC system and their *ori* are not anchored to the poles (Kahng & Shapiro, 2003; Frage *et al.*, 2016). *S. meliloti* is capable of colonizing the soil rhizosphere as a free-living bacterium, but also of invading the roots of leguminous plants as an intracellular symbiotic nitrogen-fixing bacterium, involving complex interactions between the bacterium

and its host (Gibson *et al.*, 2006). Similarly to the model bacterium *C. crescentus* and *B. abortus*, free-living *S. meliloti* regulate their cell cycle so that replication of their genome occurs once-and-only-once per cell division (Mergaert *et al.*, 2006). In both *B. abortus* and *S. meliloti*, a temporal coordination of replication and segregation was found, as the initiation of replication of their chromids is always delayed compared to the main chromosome (Deghelt *et al.*, 2014; Frage *et al.*, 2016). In *Brucella*, the replication of *oriI* starts before *oriII* and both chromosomes would finish their replication at approximately the same time (Deghelt *et al.*, 2014). Note that the size of the chromids do not seem to be the determining factor for the temporal regulation of their replication initiation. Indeed, in *S. meliloti*, it has been proposed that the smaller pSymA initiates its replication when the *ori* of the main chromosome has reached the new pole and that it is followed by the bigger pSymB, which behaves in a similar manner after the pSymA *ori* has been replicated (Frage *et al.*, 2016).

Two main phases can be observed during HeLa cells infection by *B. abortus*. Indeed, when the bacterium is transiting within the eBCV, it is unable to proliferate, which reflects the fact that the number of colony forming unit (CFU) is stable during this non-proliferative stage (Comerci *et al.*, 2001; Starr *et al.*, 2008; Deghelt *et al.*, 2014). The second phase occurs when *Brucella* reaches its ER-derived proliferative niche, with the number of CFU increasing drastically (Pizarro-Cerda *et al.*, 1998; Celli *et al.*, 2003; Starr *et al.*, 2008).

Thanks to fluorescent reporter systems that can track the *ori*, it has been possible to follow *B. abortus* cell cycle inside host cells. One interesting observation was that during the non-proliferative stage of the trafficking in HeLa cells and RAW 264.7 macrophages, the bacteria are blocked in G1 (only one focus of *oriI*), similarly to what happens in the carbon-starved swarmer cells of *C. crescentus*, a free living α -proteobacterium (Lesley & Shapiro, 2008; Deghelt *et al.*, 2014). As *Brucella* exhibits asymmetric growth like other Rhizobiales (Brown *et al.*, 2012), it is also possible to use Texas Red Succinimidyl Ester (TRSE) – a fluorescent compound that covalently binds amine groups on the bacterial surface – as a mean to follow the bacterium unipolar growth (Brown *et al.*, 2012) inside host cells (Deghelt *et al.*, 2014). These techniques brought to light the fact that the bacteria found within the eBCV at early times after infection are predominantly non-growing newborn cell types. This term refers to bacteria that recently divided but did not initiate chromosome replication yet (Deghelt *et al.*, 2014). They stay in this state for up to eight hours before resuming their growth and chromosome replication when they still reside within an eBCV (Deghelt *et al.*, 2014). Importantly, even if they do not divide in the eBCV, *B. abortus* still seem to be able to restart their growth just before they reach the rBCV (Deghelt *et al.*, 2014) (**Fig 12**).

II.3.3. Brief summary of the immune response

The innate immune system generally recognizes the presence of a pathogen through the detection of pathogen associated molecular patterns (PAMPs). This recognition is mediated by pattern-recognition receptors (PRRs). The response of the host cells is not specific to one pathogen and will lead to the three major actions: (1) the phagocytosis of the intruder, (2) an

inflammatory reaction that recruits more phagocytic cells and (3) cytotoxicity via apoptosis of the infected cells (Topham & Hewitt, 2009; Moser & Leo, 2010).

Brucella is known for its exquisite ability to hide from its host immune system. One typical example is the lipopolysaccharide (LPS) of *Brucella* that is very weakly immunogenic, as it is poorly recognized by toll-like receptors (TLR) 4, which are PRR for LPS (Barquero-Calvo *et al.*, 2007). The host cells are thus less prone to generate reactive nitrogen species (RNS) via the expression of the inducible nitric oxide synthase (iNOS), to undergo a respiratory burst, or to release pro-inflammatory cytokines (Lapaque *et al.*, 2006). *Brucella* can also directly interfere with the signalization pathways of TLR2 and TLR4 (Cirl *et al.*, 2008; Salcedo *et al.*, 2008). In addition, *Brucella* does not possess any *pili* or capsule that could be recognized by PRR (Martirosyan *et al.*, 2011). Nevertheless, some TLR can recognize *B. abortus*. It is for example the case of TLR9, which detects the DNA of *Brucella* and helps to induce IFN γ and iNOS protein production (Copin *et al.*, 2007). Of course, bacterial DNA is only accessible if bacterial lysis occurs, thus the ability of the bacteria to escape a quick release of such PAMPs seems to have been selected along evolution.

If the innate immune response is not sufficient to get rid of a pathogen, the adaptive immune response takes over. This response takes more time, but it is also more specific and therefore more efficient. The adaptive response is based on the activation of T and B lymphocytes. T cells recognize their targets by binding to antigen-associated major histocompatibility complexes (MHC) on antigen presenting cells. Here again, the LPS of *Brucella* is able to sequester the class I and class II MHC so that they are less able to display peptide fragments of non-self proteins to cytotoxic T cells (Forestier *et al.*, 2000; Barrionuevo *et al.*, 2013). The host is still able to generate an immune response, mainly a Th1 response that is specialized with intracellular pathogens, but also a Th17 response that plays mainly on extracellular bacteria (Hanot Mambres *et al.*, 2016), and even a memory response (Vitry *et al.*, 2014). However, *Brucella* generally manages to stay hidden and Brucellosis becomes chronic (Hanot Mambres *et al.*, 2015).

II.3.4. Intracellular stresses

The ability of *Brucella* to survive and replicate inside host macrophages and dendritic cells is a key aspect of its ability to produce chronic infections (Köhler *et al.*, 2003; Billard *et al.*, 2005). Indeed, in addition to its poor recognition by the immune system, *Brucella* can also prevent the apoptosis of its host macrophage (Gross *et al.*, 2000) and interfere with the maturation of dendritic cells (Salcedo *et al.*, 2008). The fact that it can stay for prolonged periods inside the spleen and the liver also help in maintaining the chronicity of the infection (Roop *et al.*, 2009).

The intracellular stresses that *Brucella* could encounter inside its host cells are multiples, even though it is clear that the bacterium seems to work upstream of the formation of these stresses to decrease their impact. Nevertheless, macrophages still rely on a weak

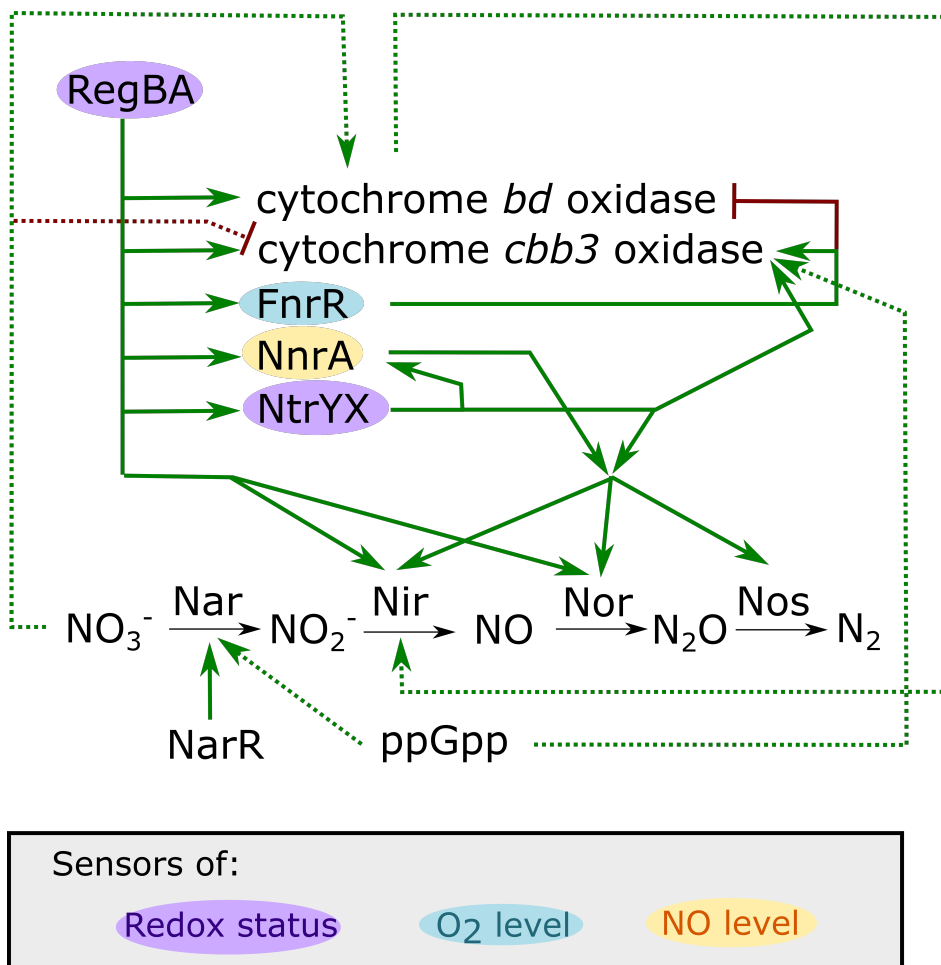


Fig 13. The two-component regulatory system RegBA is a key player in the response of *Brucella* to low oxygen tension. RegB is a membrane-bound histidine kinase, with an auto-kinase activity in response to redox changes. After auto-phosphorylation, its phosphate group is transferred from its conserved histidine residue to the response regulator RegA, a transcription factor. RegA positively regulates the expression of three other transcription factors: (1) FnrR, further activated by oxygen depletion; (2) NnrA, a sensor of NO; and (3) NtrY, another redox-sensing response regulator belonging to the NtrYX two-component system (Abdou *et al.*, 2013; Carrica Mdel *et al.*, 2013). The expression of both the cytochrome *bd* oxidase and the cytochrome *cbb3* oxidase genes is also upregulated by the RegBA system (Abdou *et al.*, 2013; Carrica Mdel *et al.*, 2013). Importantly, the overexpression of the genes coding for the cytochrome *bd* oxidase requires the presence of nitrate, too (Abdou *et al.*, 2013). Since RegA, NnrA and NtrY participate in the upregulation of the denitrification genes *nir*, *nor* and *nos*, nitrate consumption eventually increases, leading to a further overexpression of the genes coding for the cytochrome *cbb3* oxidase (Abdou *et al.*, 2013; Carrica Mdel *et al.*, 2013). This regulation is reinforced by the parallel actions of NtrYX and FnrR, which also represses the expression of the genes coding for the cytochrome *bd* oxidase (Abdou *et al.*, 2013; Carrica Mdel *et al.*, 2013). Note that *nar* are the only genes that are not upregulated by these proteins, but instead by an independent NarR transcription factor (Haine *et al.*, 2006) and by the stringent response molecule ppGpp, which also upregulates genes coding for the cytochrome *cbb3* oxidase (Hanna *et al.*, 2013). Solid lines indicate proposed direct interactions and dashed lines represent interactions demonstrated by gene expression experiments only.

oxidative burst via the activity of NADPH oxidases in order to produce bactericidal and bacteriostatic reactive oxygen species (ROS) (Jiang *et al.*, 1993). *Brucella* is particularly well equipped to face ROS. Indeed, its first line of defense against incoming ROS are the periplasmic Cu/Zn superoxide dismutase SodC and the catalase KatE, detoxifying O₂⁻ and H₂O₂, respectively (Gee *et al.*, 2005; Steele *et al.*, 2010). A Δ sodC strain is attenuated in mice and in macrophages (Gee *et al.*, 2005). This phenotype of attenuation can be compensated by the addition of an inhibitor of NADPH oxidase, so it seems clear that *Brucella* does encounter oxidative stress to a certain degree (Gee *et al.*, 2005). On the other hand, the bacterium also possesses cytoplasmic enzymes such as the Fe superoxide dismutase SodA and the peroxidase AhpC (Steele *et al.*, 2010; Martin *et al.*, 2012). Since O₂⁻ is charged, it cannot cross the membranes, so SodA has logically been reported to deal with endogenous oxidative stress only (Martin *et al.*, 2012). KatE and AhpC are partially redundant in function, as only a double mutant is severely attenuated in macrophages and in the mice (Steele *et al.*, 2010). Note that contrarily to what is most commonly believed, the main source of endogenous ROS is not aerobic respiration, but the autoxidation of non-respiratory flavoproteins (reviewed in Imlay, 2013). The respiratory cytochrome oxidases of *Brucella* are actually a help for the bacterium, as they scavenge O₂ to prevent ROS toxicity (Endley *et al.*, 2001; Jimenez de Bagues *et al.*, 2007).

These respiratory cytochrome oxidases are actually very important for *Brucella* inside host cells. Indeed, inside the phagosomes of macrophages, the oxygen concentration is lower than in the extracellular environment (James *et al.*, 1995). Being obligate aerobe bacteria, *Brucella* thus need to adapt to low intracellular oxygen tension (Al Dahouk *et al.*, 2009). One way to do this is by upregulating the expression of their two high-oxygen-affinity terminal oxidases, the cytochrome *cbb3* oxidase and the cytochrome *bd* ubiquinol oxidase, upon microaerobiosis. In these conditions, *Brucella* are thus still able to grow (Jimenez de Bagues *et al.*, 2007) and they can even survive under strong oxygen-limited conditions such as inside granulomas (Loisel-Meyer *et al.*, 2006). In addition to the upregulation of the cytochrome oxidases, when oxygen becomes scarce, *Brucella* also use nitrogen oxides as electron acceptors in order to get enough energy to keep their basic metabolic activities (Al Dahouk *et al.*, 2009). Actually, the denitrification pathway and these cytochrome oxidases are co-regulated. Indeed, the two-component regulatory system RegB/RegA (also known as PrrB/PrrA) regulates both directly and indirectly the expression of those two types of targets (see **Fig 13** for details) (Abdou *et al.*, 2013; Carrica Mdel *et al.*, 2013). As a matter of fact, the double deletion of the two genes coding for the redox-sensors RegB and NtrY (also involved in the co-regulation of denitrification genes and the cytochrome *cbb3* oxidase; see **Fig 13**) is very deleterious to *Brucella* inside host macrophages, even at 2h post infection (Carrica Mdel *et al.*, 2013).

RNS are produced by macrophages via the expression of the iNOS. *Brucella* possesses a nitric oxide reductase (Nor), which probably helps the bacterium to detoxify exogenous NO, in addition to its role in denitrification (**Fig 13**) (Haine *et al.*, 2006; Loisel-Meyer *et al.*, 2006). *Brucella* also possesses a DacF D-alanyl-D-alanine carboxypeptidase, which is known

to help the bacterium to resist NO *in vitro* and inside macrophages, but in a still unknown way (Kikuchi *et al.*, 2006). Peroxynitrite (ONOO⁻) is a molecule that exists at the crossroad of ROS and RNS. It is a potent antimicrobial agent, but recent findings indicate that in some cases, it is produced very rarely by host cells. Indeed, during *Salmonella* infection, NADPH oxidases and iNOS are temporally separated (Vazquez-Torres *et al.*, 2000; Craig & Schlauch, 2009; Burton *et al.*, 2014). Typically, NADPH oxidases play a role only during the first few hours after phagocytosis, then iNOS levels increase slowly but stays present longer (Vazquez-Torres *et al.*, 2000). Therefore, it is unknown if *Brucella* has to face peroxynitrite inside host cells.

Acidic pH is also a stress that *Brucella* was selected to cope with. More than that, it is actually a signal used by the bacterium to trigger the expression of the genes encoding its type IV secretion system, which is essential for *Brucella* to proceed to its replicative niche (Boschioli *et al.*, 2002). Most *Brucella* species produce a functional urease, which seems to be very important for the survival of the bacterium inside the gastrointestinal tract. However, it is not involved in intracellular survival (Bandara *et al.*, 2007; Sangari *et al.*, 2007). Currently, the key factor(s) necessary for *Brucella* to survive against acidic pH are still unknown.

Several studies point out the fact that *Brucella* probably encounters starvation inside the eBCV (Kohler *et al.*, 2002; Lamontagne *et al.*, 2009; Rossetti *et al.*, 2011). Very recently, our team confirmed that genes involved in purine biosynthesis, pyrimidine biosynthesis and transport are required very early during macrophages infection by *B. abortus* (Sternon *et al.*, 2018). As iron is an essential nutrient for most bacteria, host cells have developed ways to restrict iron accessibility to pathogens (Appelberg, 2006). To get access to sufficient iron levels, *B. abortus* is able to produce two siderophores, the 2,3-dihydroxybenzoic acid (Lopez-Goni *et al.*, 1992) and brucebactin (Gonzalez Carrero *et al.*, 2002). These two siderophores seem to be important inside pregnant cows, but apparently not inside macrophages (Roop, 2012). The reason of their inefficiency inside macrophages is that the host cells can develop a lipocalin 2-dependent response in order to capture *Brucella* siderophores (Hop *et al.*, 2018). Therefore, instead, *Brucella* seems to be relying on heme transport to get iron (Paulley *et al.*, 2007). Access to manganese seems to also be required by *Brucella* to proliferate, as the manganese-specific transporter MntH has been found to be essential during macrophages and mice infection (Anderson *et al.*, 2009; Sternon *et al.*, 2018). Incidentally, one important enzyme that requires manganese is the pyruvate kinase PykM, which is required for glucose utilization in mice (Pitzer *et al.*, 2018). Another indication that *Brucella* species encounter starvation inside host cells is that the stringent response regulator Rsh, which synthesizes 3',5'-bis-pyrophosphate (ppGpp) under nutrient deprivation, is necessary during infection (Dozot *et al.*, 2006). The role of ppGpp is to help the bacterium to adapt to its poor environment by inducing large-scale transcriptional changes after binding to the RNA polymerase (Boutte & Crosson, 2013). Interestingly, ppGpp also upregulates genes coding for *Brucella* nitrate reductase (Nar) and the cytochrome *cbb3* oxidase (**Fig 13**) (Hanna *et al.*, 2013), indicating that starvation and low oxygen tension can probably occur simultaneously. Importantly,

ppGpp accumulation is known to extend the G1 phase of *C. crescentus* (Ronneau *et al.*, 2016). The link between ppGpp and the cell cycle of *B. abortus* is currently under investigation in our lab.

II.3.5. DNA repair capacities of *Brucella*

There exist only three papers that directly focus on the topic of *Brucella* DNA repair capacities. The first one is about *B. abortus* XthA1 exonuclease (III), which is involved in the BER pathway (Hornback & Roop, 2006). As such, its role is to cut the phosphate backbone 5' of the AP site to produce a free 3' hydroxyl group on the neighboring nucleotide (**Fig 5B**). In *E. coli*, XthA is the main AP endonuclease but there exists a second enzyme accounting for 10% of the activity: the endonuclease IV, coded by the *nfo* gene (Ljungquist *et al.*, 1976; Cunningham *et al.*, 1986). In *B. abortus*, there is no gene homologous to *nfo*, but there exist two copies of *xthA*, thus named *xthA1* and *xthA2* (Hornback & Roop, 2006). A *B. abortus* $\Delta xthA1$ deletion strain was found to be more sensitive to MMS, H₂O₂ and peroxyntirite than the WT strain, suggesting that it is an authentic AP endonuclease (Hornback & Roop, 2006). Infection experiments have also been performed with the $\Delta xthA1$ deletion strain, but it was attenuated neither in murine macrophages nor in BALB/c mice, possibly because of the presence of the XthA2 enzyme, which was not studied (Hornback & Roop, 2006).

The two other research articles focus on the RecA protein, DNA repair, and SOS regulation in *B. abortus* (Tatum *et al.*, 1993; Roux *et al.*, 2006). As a reminder, in *E. coli*, the SOS system is triggered by the auto-cleavage of the repressor LexA following the activation of RecA into RecA* after its polymerization on ssDNA (Butala *et al.*, 2011). A *B. abortus* $\Delta recA$ deletion mutant was found to be sensitive to MMS, contrarily to a $\Delta uvrA$ mutant (Tatum *et al.*, 1993; Roux *et al.*, 2006). Interestingly, the $\Delta recA$ strain was also slightly attenuated in non-activated and activated macrophages (Tatum *et al.*, 1993; Roux *et al.*, 2006). In addition, this strain was strongly attenuated in mice, but it was found to be able to persist in this *in vivo* model for as long as the WT strain (Tatum *et al.*, 1993). Contrarily to most bacteria, the *B. abortus* $\Delta recA$ mutant exhibited a modest sensitivity to UV radiation (Roux *et al.*, 2006). The authors suspected that *B. abortus* *radA* gene could code for a functional homologue to RecA, which would account for the UV resistance of the $\Delta recA$ mutant. However, a $\Delta recA \Delta radA$ double mutant was as sensitive to UV as the $\Delta recA$ single mutant, indicating that RadA does not have the same activity as RecA (Roux *et al.*, 2006). The activity of the promoters of *B. abortus* *recA* (p_{recA}) and *uvrA* (p_{uvrA}) were followed by fusing them with a *lacZ* gene on a plasmid. This allowed the authors to find a high basal activity for both promoters (Roux *et al.*, 2006). Interestingly, the addition of an SOS-inducer, mitomycin C, led to a small 2-fold increase of p_{recA} activity (Roux *et al.*, 2006), which is weak compared to the 6 to 10-fold induction of *E. coli* p_{recA} in a similar experiment (Kim & Oh, 2000; Roux *et al.*, 2006). More surprising, the expression of the p_{recA} -*lacZ* reporter system was greatly reduced in a *B. abortus* $\Delta recA$ strain, independently of mitomycin C addition (Roux *et al.*, 2006). The authors concluded that *B. abortus* RecA is involved in its own high basal activation without a requirement for high DNA damage (Roux *et al.*, 2006). They thus

inferred that *B. abortus* RecA could possess a natural RecA* activity for SOS induction, independently of its polymerization on ssDNA (Roux *et al.*, 2006). To further investigate this hypothesis, they heterocomplemented an *E. coli* $\Delta recA$ strain carrying a $p_{recA-E.coli}-lacZ$ reporter system with *B. abortus* *recA* gene (Roux *et al.*, 2006). They observed that *B. abortus* RecA led to a high constitutive expression of the reporter system in *E. coli*, with a 2-fold induction achieved after mitomycin C treatment (Roux *et al.*, 2006). Their conclusion from these surprising results was that “the high basal *recA-lacZ* expression was the result of constitutive RecA activation (RecA*), leading to the cleavage of LexA without the normal requirements for an inducing treatment” (Roux *et al.*, 2006).

A few other papers bring indirect information about DNA repair capacities of *Brucella*. It is for example the case of the proteomic study of Lamontagne *et al.* (2009), which showed that *B. abortus* XseA (a subunit of the exonuclease VII), involved in MR, and UvrB, involved in NER, were both more abundant at 3 h post infection inside RAW 264.7 macrophages compared to pre-infection conditions. Both proteins levels then dropped back to basal levels at later time points (44 and 20 h post infection, respectively) (Lamontagne *et al.*, 2009). In the same model of infection, it was also found that *B. abortus* *mutM*, coding for a DNA glycosylase, was overexpressed at 4 h post infection (Eskra *et al.*, 2001). Still in the same model and more recently, our group showed that transposon mutants of *recF*, impaired for homologous recombination, are attenuated at 24 h post infection (Sternon *et al.*, 2018) (see **appendix 3**).

As mentioned earlier, *B. abortus* appears to be devoid of a few genes that code for DNA repair enzymes. Indeed, we could not find homologues for *polB*, coding for the DNA polymerase II; *umuDC*, coding for the DNA polymerase V; *recBCD*, involved in double strand break repair; *nfo*, coding for an AP endonuclease; *phr* photolyase genes, which repair damage caused by exposure to ultraviolet light; and genes coding for the non-homologous end-joining pathway. Still, it seems that other genes are present to compensate for their absence, such as the *addAB* genes instead of *recBCD*; a second copy of the *xthA* gene instead of *nfo*; or *imuABC* instead of *umuDC*.

As for genes that code for alkylated DNA repair enzymes, such as *ada*, *alkA*, *tagA*, *alkB*, *ogt*, and *aidB*, we found that they were all present in the genome of *B. abortus* (see **results section I.1.** for more details).

Key information

Inside host cells such as RAW 264.7 macrophages and HeLa cells, *B. abortus* has a globally biphasic trafficking: (1) the bacterium first resides inside an endosomal *Brucella*-containing vacuole (BCV), where it is blocked in a G1-like phase for several hours. At that time, *Brucella* is thought to encounter many stresses, among which starvation, ROS, RNS and acidic pH. (2) In the second phase, the bacterium reaches its replicative niche, the rBCV, which is part of the endoplasmic reticulum. The DNA repair capacities of *Brucella* are largely uncharacterized. Nevertheless, there is a report on the fact that *B. abortus* could possess a constitutively active RecA* activity, which could trigger the basal induction of some SOS-dependent genes.

II.4. *Brucella* as a model for alkylating stress studies

As explained earlier, intracellular bacteria could meet alkylating stress, either because the host cells are defending themselves against their intrusion, or because of their own metabolism. Let us analyze those two possibilities on a theoretical point of view for the case of *Brucella*.

Firstly, *Brucella* is known to thrive inside macrophages (Celli *et al.*, 2003; Archambaud *et al.*, 2010). As a matter of fact, macrophages were shown to be able to produce N-nitroso compounds, one source of alkylating stress (Miwa *et al.*, 1987; Kosaka *et al.*, 1989). It has also been shown that the production of such compounds is directly dependent on NO level and thus on the induction of iNOS (Iyengar *et al.*, 1987; Ohshima *et al.*, 1991). It is true that *Brucella* LPS is much less immunogenic than *E. coli* LPS (Lopez-Urrutia *et al.*, 2000), but it is nevertheless expected that *Brucella* would meet some level of nitrosative stress inside host cells (Roop *et al.*, 2009). Interestingly, iNOS proteins are known to localize to phagosomal membranes of activated macrophages (Vodovotz *et al.*, 1995; Miller *et al.*, 2004), which is where *Brucella* would reside for several hours before to reach its replicative niche (Celli, 2015). In addition, the eBCV is known to get acidified to pH 4.0 – 4.5 (Porte *et al.*, 1999; Starr *et al.*, 2008). Acidic pH is known to contribute to the formation of N-nitroso compounds (Fig 3), but also to their permeability through membranes (Guttenplan & Milstein, 1982). All the ingredients for the generation of N-nitroso compounds inside the eBCV thus seem to be present. As for host cell lipid peroxidation as a source of alkylating stress on *Brucella*, it is unclear. There is a report on the fact that *B. melitensis* can trigger lipid peroxidation in the liver and the spleen of mice after a week, but earlier time points have not been studied and it is unknown if those molecules would reach the bacteria themselves (Melek *et al.*, 2006).

Secondly, it seems likely that *Brucella* would generate endogenous N-nitroso compounds when it is residing inside host cells. Indeed, the production of those compounds is known to be more important in anaerobic and resting *E. coli* (Kunisaki & Hayashi, 1979) and *B. abortus* was shown to be blocked in the G1 stage of its cell cycle (characterized by a non-growing and non-replicating state) during the first hours of infection, when it is still inside the

eBCV (Deghelt *et al.*, 2014). In addition, for most bacteria, the production of N-nitroso compounds has been linked to nitrate reductase activity, which can be abolished by molybdenum cofactor deprivation (Calmels *et al.*, 1985; Taverna & Sedgwick, 1996). Contrarily to *E. coli* that possesses three nitrate reductase enzymes (Sparacino-Watkins *et al.*, 2014), *Brucella* only possesses one. *Brucella* would thus be a good model for endogenous alkylating stress studies, as it will be easier to investigate the role of a single enzyme in this process. Moreover, *Brucella* was found to upregulate the expression of *narG* (coding for the catalytic subunit of the nitrate reductase) at 4 hours post infection, possibly via ppGpp accumulation (Rossetti *et al.*, 2011; Hanna *et al.*, 2013). If the nitrate reductase of *Brucella* is indeed involved in the formation of N-nitroso compounds, it would suggest that these alkylating agents are generated when the bacterium is still in the eBCV, which also corresponds to the theoretically most stressing period of *Brucella* trafficking (Roop *et al.*, 2009). As for *Brucella* lipid peroxidation, it is expected to be minor if not nonexistent. Indeed, the amount of PUFA in the cellular fatty acid composition of *Brucella* is virtually null (Dees *et al.*, 1980). However, a paper reported that if looking at the cell wall only, *B. abortus* does possess octadecadienoic acids (C18:2) (Bobo & Eagon, 1968). It is thus difficult to evaluate the real impact of the peroxidation of those fatty acids on the bacterium. Note that *Brucella* also possesses a SAM synthase, which could also contribute to endogenous alkylating stress.

Key information

We expect that *Brucella* would be a good model for studies on alkylating stress. Indeed, all the requirements for the exogenous and the endogenous formations of this stress are present.

III. Cell cycle transcription factors

III.1. Why work on cell cycle regulators?

Since the invasive *B. abortus* are mainly in the G1 phase of their cell cycle (Deghelt *et al.*, 2014), it is possible that transcription factors involved in cell cycle regulation could be also important for *Brucella* virulence. Considering that the block in G1 phase correlates with the time when *Brucella* is supposed to meet the most stressing conditions inside host cells, *i.e.* inside the eBCV, the two phenomenon could be linked. Indeed, the G1 phase is characterized by stable dsDNA, with no replication fork going on. It could thus be a way for *Brucella* to protect its DNA from genotoxic stresses.

There exist two major cell cycle regulators in α -proteobacteria: CtrA and GcrA. Both of them are highly conserved in this phylum (Brilli *et al.*, 2010). Besides, these two transcription factors have been found to regulate the expression of genes coding for DNA repair enzymes in several α -proteobacteria (Laub *et al.*, 2002; Haakonsen *et al.*, 2015; Poncin *et al.*, 2018). They were thus obvious candidates for this study.

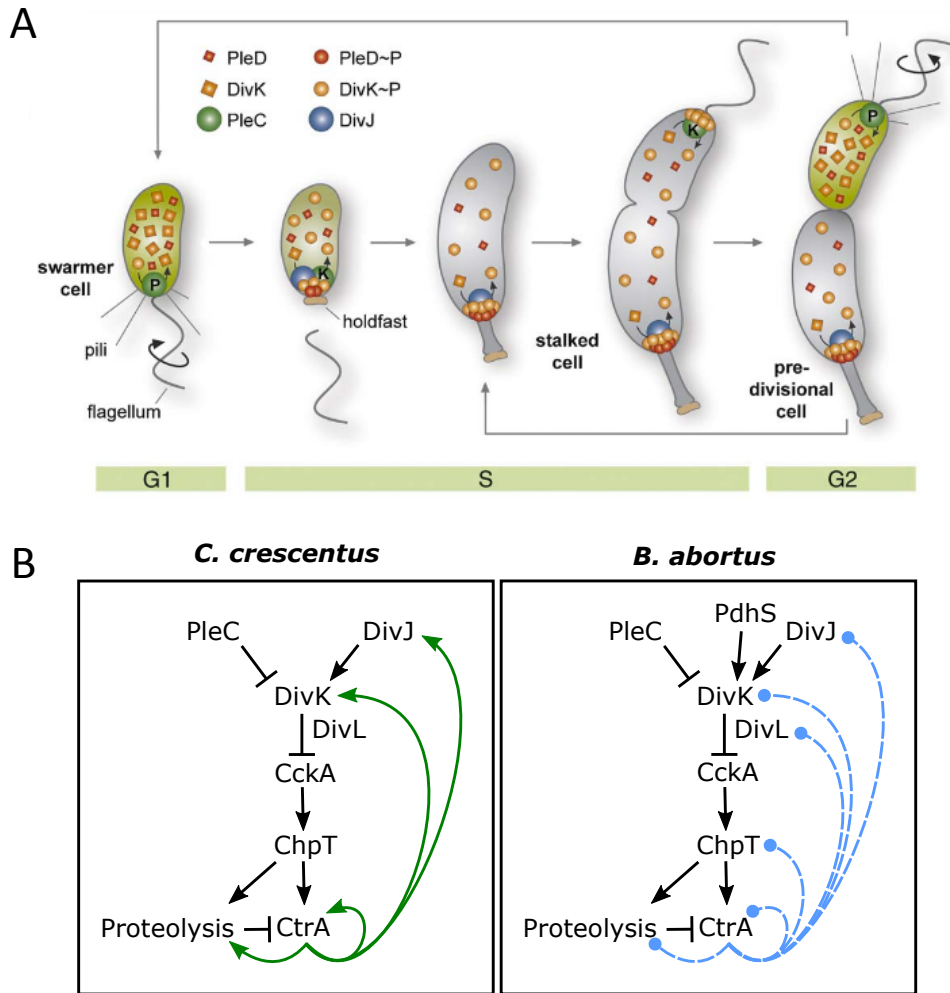


Fig 14. Models for CtrA regulation. **A)** The PleC-DivJ-DivK signaling network in *C. crescentus*. The non-phosphorylated form of the response regulator DivK is evenly distributed within the cell, at the opposite of its phosphorylated form that interacts with the cell poles. Its phosphorylation state is dependent on both PleC, a bifunctional enzyme (kinase/phosphatase) and DivJ, a histidine kinase. In the swarmer cell, PleC works in its phosphatase mode. It leads to an accumulation of non-phosphorylated DivK and, eventually, to CtrA phosphorylation (green background). The differentiation process from a swarmer to a stalked cell occurs, among others, through the phosphorylation of the response regulator PleD by PleC. In the stalked cell, DivJ is present and, in this model, the switch of activity of PleC from the phosphatase to the kinase mode triggers the phosphorylation of DivK. This induces the elimination of CtrA~P. CtrA stays present in the pre-divisional cell and in the swarmer cell in order to block the initiation of replication. As for the stalked cell, it has to be free of CtrA to initiate a new cell division (Thanbichler, 2009). **B)** Comparison of CtrA regulation in two α -proteobacteria. The schemes represented here are mainly based on *C. crescentus* CtrA regulation (Laub *et al.*, 2000; Laub *et al.*, 2002; Fumeaux *et al.*, 2014), therefore it is important to take into consideration the fact that the phosphorylation cascade events might not happen exactly as depicted. In the case of *B. abortus*, data were obtained from Willet *et al.* (2015) and Francis *et al.* (2017). Green arrows correspond to confirmed CtrA targets that are positively regulated by the transcription factor. Blue rounded arrows correspond to targets that are bound by CtrA on their promoter, but for which the effect of this binding still remains unknown.

III.2. Roles and regulation of CtrA

This part of the manuscript has been published in a review (Poncin *et al.*, FEMS Microbiology Reviews, 2018) (see appendix 4).

III.2.1. *B. abortus* CtrA regulation is similar to that of *C. crescentus*

CtrA has been best studied in the model organism *C. crescentus*. As a reminder, this remarkable bacterium possesses two distinct life forms. One is a sessile stalked form, which allows the bacterium to adhere to surfaces when it is in a nutrient-rich environment. The other form is a motile swarmer cell that is used for scouting and colonizing new favorable environments but that is not competent for replication (Ausmees & Jacobs-Wagner, 2003; Quardokus & Brun, 2003). Importantly, *C. crescentus* divides asymmetrically into its two phenotypically different daughter cells after each cell division. This is why this bacterium is considered as an excellent model for bacterial cell cycle studies. In this context, the transcription factor CtrA has been found to be of utmost importance as it is a master regulator of *C. crescentus* cell cycle (Quon *et al.*, 1996).

In *C. crescentus*, CtrA is responsible for the direct regulation of about 100 genes that are involved in many different processes (Laub *et al.*, 2002). In general, CtrA is considered as an activator of gene expression, but that is not true for all of its targets. Indeed, *C. crescentus* CtrA was shown to repress the expression of *moaA*, involved in the synthesis of molybdenum, and *lexA*, involved in the regulation of the SOS response (Laub *et al.*, 2002). Another one of CtrA many targets is the *ori*, thus sterically preventing the DnaA protein from initiating the replication of *C. crescentus* chromosome as long as CtrA is present (Quon *et al.*, 1998; Siam & Marczyński, 2000). As CtrA needs to be phosphorylated to be active, a tight regulatory network based on two-component regulators is in charge of its synthesis, phosphorylation and degradation (**Fig 14**) (Quon *et al.*, 1996; Domian *et al.*, 1997; Wu *et al.*, 1998; Biondi *et al.*, 2006; Thanbichler, 2009; Tsokos *et al.*, 2011).

In *C. crescentus*, the dual CckA enzyme that possesses both kinase and phosphatase activities regulates the phosphorylation level of CtrA and CpdR, a response regulator stimulating CtrA proteolysis when dephosphorylated (Jenal & Fuchs, 1998; Jacobs *et al.*, 2003; Biondi *et al.*, 2006). CckA does so by interacting with the phosphotransferase ChpT (Biondi *et al.*, 2006). The kinase activity of CckA is inhibited by the phosphorylated form of the response regulator DivK, which is stabilized by the atypical histidine kinase DivL (Tsokos *et al.*, 2011; Childers *et al.*, 2014). DivK phosphorylation is itself regulated by the histidine kinase DivJ and by the phosphatase PleC (Wu *et al.*, 1998; Wheeler & Shapiro, 1999) (**Fig 14**). PleC is also able to phosphorylate the diguanylate cyclase PleD, which in turn will synthesize cyclic di-GMP (Paul *et al.*, 2008). The binding of this secondary messenger to CckA will force CckA to switch from its kinase to its phosphatase mode, thus preventing the phosphorylation of CtrA (Lori *et al.*, 2015). Cyclic di-GMP also binds to PopA, which interacts with RcdA, another protein involved in CtrA proteolysis at the stalked cell pole (Ozaki *et al.*, 2014; Smith *et al.*, 2014). Interestingly, several genes coding for proteins

regulating CtrA are also part of its regulon, including *divK* (Laub *et al.*, 2000) and *divJ* (Fumeaux *et al.*, 2014) in *C. crescentus* (**Fig 14B**).

At the transcription level, *ctrA* is regulated by two proteins in *C. crescentus*. One of them is CtrA itself (Domian *et al.*, 1999). The other one is GcrA, an unconventional transcription factor that binds to the housekeeping σ^{70} factor (see **introduction section III.3.**) (Haakonsen *et al.*, 2015). Since *gcrA* transcription is repressed by CtrA and *ctrA* transcription is activated by GcrA, the two transcription factors are present temporally and spatially out-of-phase during the cell cycle of *C. crescentus* (Holtzendorff *et al.*, 2004).

The spatio-temporal regulation of CtrA is particularly well adapted to *C. crescentus* aquatic free-living lifestyle, but it appears to be surprisingly conserved in other α -proteobacteria with very different ways of life (Brilli *et al.*, 2010; Pini *et al.*, 2015; Schallies *et al.*, 2015; Willett *et al.*, 2015). In *B. abortus*, the core actors involved in the CtrA regulatory network, defined here as the PleC/DivJ/DivK and CckA/ChpT/CtrA two-component systems, are conserved (Hallez *et al.*, 2004; Brilli *et al.*, 2010) (**Fig 14B**). Another gene, called *pdhS* for PleC/DivJ homologue sensor, has also been found to be part of this network (Hallez *et al.*, 2004). Both *pleC* and *divK* from *B. abortus* are able to heterocomplement the corresponding deletion mutants in *C. crescentus*, which suggests that their function is conserved between both organisms (Hallez *et al.*, 2007). In addition, in *B. abortus*, DivK has been found by yeast two-hybrid experiment to bind to DivJ, PleC, DivL and PdhS (Hallez *et al.*, 2007). Nevertheless, the localization of PleC is different between *B. abortus* and *C. crescentus* and DivJ was not found to be crucially involved in DivK phosphorylation (Hallez *et al.*, 2007). Indeed, in a $\Delta divJ$ background, DivK did not lose its phosphorylation-dependent polar localization (Hallez *et al.*, 2007), while a loss-of-function of *pdhS* generates delocalization of DivK-YFP (Van der Henst *et al.*, 2012). As *pdhS* is an essential gene and depletion strain techniques were not available at that time, its involvement in DivK phosphorylation could only be suggested through indirect experiments. PdhS was also shown to accumulate at the old pole of the large cells, which is the same localization as the phosphorylated form of DivK (Hallez *et al.*, 2007). Of note, this localization is similar to the one of DivJ in *C. crescentus*, which suggests a common function between *B. abortus* PdhS and *C. crescentus* DivJ (Hallez *et al.*, 2007). As PdhS is cytoplasmic in *B. abortus*, it is possible that its function is shared with DivJ depending on the time and/or space of DivK phosphorylation (Hallez *et al.*, 2007). The polar localization of PdhS is conserved at 48 hours post infection in bovine macrophages (Hallez *et al.*, 2007), but nothing is known about the role of DivJ in this context and at later times of the infection. As for the phosphorelay going from CckA to CtrA and CpdR via ChpT, it has been confirmed to be functional in *B. abortus* (Willett *et al.*, 2015). As it was the case for *C. crescentus* (Laub *et al.*, 2000; Fumeaux *et al.*, 2014), several genes predicted to be involved in CtrA regulation have been found by chromatin immunoprecipitation followed by deep sequencing (ChIP-seq) to be potentially part of CtrA regulon in *B. abortus*, including *ctrA* itself, *divK*, *divJ*, *divL*, *chpT*, *cpdR* and *rcdA* (Francis *et al.*, 2017). If all of these genes are indeed regulated by *B. abortus* CtrA, it would mean that the control of this transcription factor is more complex in this bacterium than

in *C. crescentus* (Fig 14B). One tempting hypothesis is that the regulation of *B. abortus* CtrA could reflect a need for the bacterium to precisely regulate its cell cycle depending on its intracellular environment.

III.2.2. The expression of *ctrA* is not crucial for *B. abortus* trafficking to the rBCV

The regulation of genes according to the stage of *B. abortus* cell cycle can be observed through the use of a fluorescent-based reporter system. Such genes are *ccrM* and the *repABC* operon, and both are probably regulated by CtrA as the activities of their promoters were abolished when their respective CtrA-binding boxes were mutated (Francis *et al.*, 2017). As the activity of the promoter of the *repABC* operon seems to be inverted compared to the one of *ctrA*, it is expected that CtrA acts as a negative regulator of chromosome II replication (Francis *et al.*, 2017). Knowing that *B. abortus* first has to go through a non-replicative phase inside the eBCV, one can expect that CtrA would be important during this specific stage of the infection. However, CtrA was not found to be essential for the ability of *B. abortus* to infect cells in the models of infection tested thus far. Indeed, a study performed with a thermo-sensitive allele of *B. abortus ctrA* concluded that the transcription factor is not required for the entry of the bacterium inside THP-1 macrophages (Willett *et al.*, 2015). Inside HeLa cells, the CtrA depletion phenotypes of *B. abortus* were also visible around or after 10 h post infection (Francis *et al.*, 2017). Furthermore, a *B. abortus* CtrA depletion strain was able to reach its rBCV replicative niche in the same proportion as the wild type strain (Francis *et al.*, 2017). This supports the view that CtrA function is dispensable for *B. abortus* trafficking inside these host cells.

Nevertheless, at 48 h post infection, CtrA depletion strains underwent a clear drop of CFU in both cellular infection models (Willett *et al.*, 2015; Francis *et al.*, 2017). The defects leading to bacterial cell death are unclear but could be explored by the analysis of suppressor mutants. The fact that CtrA might only be necessary at late time points during *Brucella* infection does make sense, though, as its level needs to be regulated more particularly during late phases of other intracellular α -proteobacteria life cycle. For example, in the obligate intracellular pathogen *Ehrlichia chaffeensis*, CtrA is important during the late stage of intracellular growth (Cheng *et al.*, 2011). In this bacterium, it has been observed that the *ctrA* gene is up-regulated at 72 h post infection, which corresponds to the time when the bacteria differentiate back from large reticulate cells to small infectious dense-cored cells in order to prepare to spread from the present to the next host cells (Zhang *et al.*, 2007; Cheng *et al.*, 2011). Similarly, in *S. meliloti*, CtrA levels are high before infection, then a decrease of *ctrA* transcription coincides with bacteroid differentiation within the nodule (Roux *et al.*, 2014) and the CtrA protein is absent in mature bacteroids (Pini *et al.*, 2013).

It is also possible that CtrA is only required when *Brucella* find themselves in a particular situation. For instance, *C. crescentus* is known to regulate CtrA levels in response to stresses affecting its envelope, and this in a CckA-dependent manner, but independently of DivK and cyclic-di-GMP (Heinrich *et al.*, 2016). In *E. chaffeensis*, *surE* has been proposed to

code for a protein involved in bacterial growth under stress and it is thought to be part of CtrA regulon (Cheng *et al.*, 2011). It is therefore possible that the *in vitro* models of infection tested thus far for *B. abortus* CtrA function do not reflect the environment and the stresses that the bacteria would have to face inside a living animal. In this respect, an *in vivo* model of infection might prove to be much more relevant for deciphering the potential impact of CtrA depletion in *B. abortus*.

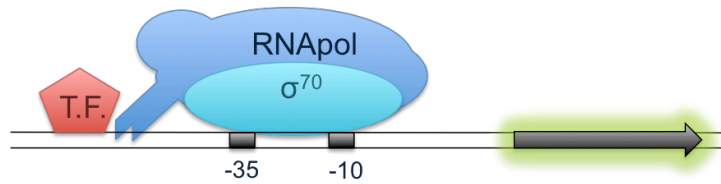
III.2.3. The regulon of CtrA

We believe that DNA repair regulation could be an ancestral function of CtrA. Indeed, all α -proteobacteria studied in the context of CtrA regulation have at least one DNA repair gene predicted or effectively shown to be part of CtrA regulon (Poncin *et al.*, 2018). Some DNA repair pathways seem to be regulated by CtrA for whole clusters of bacteria, such as mismatch repair for Rhizobiales, Caulobacteriales and Rickettsiales (Poncin *et al.*, 2018) (see **appendix 4**). Interestingly, each α -proteobacterium also seems to possess its own specific CtrA-dependent DNA repair targets. For example, *Dinoroseobacter shibae* CtrA could regulate *recA* expression (Wang *et al.*, 2014), while it seems to be *uvrB* in the case of *Rhodobacter capsulatus* (Mercer *et al.*, 2010). As for *E. chaffeensis*, it has a perfect 8-mer CtrA binding box in the promoter of its *mfd* gene, which codes for the Transcription Repair Coupling Factor that affects nucleotide excision repair (Selby & Sancar, 1993). Thus, each bacterium probably optimized the different cellular functions regulated by CtrA through evolution according to its specific lifestyle.

In *B. abortus*, the promoter of *tagA*, which codes for a DNA glycosylase specifically involved in repairing alkylated DNA (Mielecki & Grzesiuk, 2014), is directly bound by CtrA (Francis *et al.*, 2017). It is also the case of the promoters of *mutM*, another DNA glycosylase, and *uvrC*, involved in NER (Francis *et al.*, 2017). Nevertheless, the absence of attenuation of the CtrA depletion strain inside host cells suggests that the potential regulation of these genes by CtrA inside these cells is not primordial, at least during the first 48 h.

Incidentally, one other striking feature of *B. abortus* CtrA regulon is the high number of genes involved in envelope biogenesis (Francis *et al.*, 2017). Indeed, in addition to revealing the direct interaction between CtrA and the promoters of genes involved in the regulation of LPS and peptidoglycan synthesis, a ChIP-seq experiment also showed that promoters of genes coding for abundant outer membrane proteins (OMP) are also bound by CtrA (Francis *et al.*, 2017). Note that the regulation of genes involved in the structure of the bacterial envelope by CtrA is probably not exclusive to *B. abortus* as many other α -proteobacteria do seem to regulate such genes via CtrA (Laub *et al.*, 2000; Brilli *et al.*, 2010). Nevertheless, it could have a more important impact on intracellular bacteria, as their envelope will be presented at the interface with their host cell and could therefore impact the host immune response and the survival of the bacteria inside them.

Classical model of transcription :



Model for GcrA :

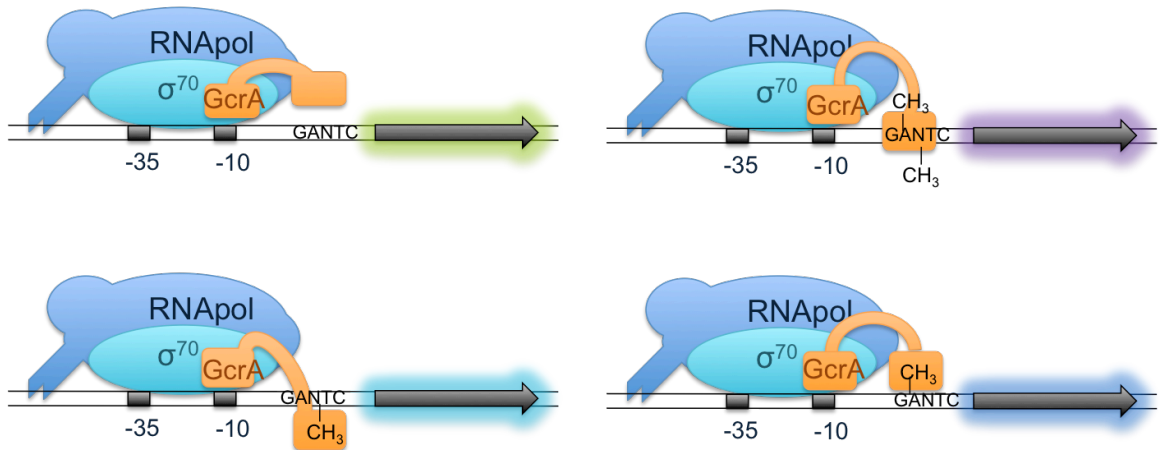


Fig 15. Model for GcrA regulation in *C. crescentus*. Contrarily to most transcription factors, GcrA binds first to the RNA polymerase on the second domain of the σ^{70} factor via its C-terminal domain, then the whole complex binds to DNA with a preference for GANTC-rich sequences, which are recognized by the N-terminal domain of GcrA. *In vitro*, GcrA can even distinguish the full-, hemi-, or non-methylated state of GANTC sites (based on Fioravanti *et al.*, 2013; Haakonsen *et al.*, 2015; Wu *et al.*, 2018).

Key information

CtrA is a master regulator of the cell cycle of *C. crescentus*. It is extremely well conserved in other α -proteobacteria, and it is very probable that it is also involved in the regulation of the cell cycle in *B. abortus*. A ChIP-seq experiment revealed that in *B. abortus*, CtrA could directly regulate the expression of genes involved in DNA repair. It is for example the case of *tagA*, which codes for a DNA glycosylase specifically involved in repairing alkylated DNA.

III.3. Roles and regulation of GcrA

As mentioned earlier, GcrA and CtrA participate in the regulation of the expression of each other in *C. crescentus* (Domian *et al.*, 1999; Holtzendorff *et al.*, 2004). Of note, DnaA also participates to *gcrA* transcription (Collier, 2012). As CtrA and GcrA are out of phase in this bacterium, GcrA is known to accumulate in the stalked cell early during S phase, throughout the transition from stalked to swarmer cell (Holtzendorff *et al.*, 2004). However, the regulon and mode of action of *C. crescentus* GcrA remained very obscure for many years. Eventually, these two points have been elucidated.

First, it was shown that GcrA can bind to GANTC sequences on DNA (Fioravanti *et al.*, 2013). These sequences are methylated on the 6th position of the adenine nucleic acid (N⁶meA) by the methyltransferase CcrM in late predivisive cells and serve as epigenetic markers (Stephens *et al.*, 1996; Reisenauer *et al.*, 1999). Actually, *C. crescentus* GcrA can even distinguish the full-, hemi-, or non-methylated state of GANTC sites, with a higher affinity for full methylation (**Fig 15**) (Fioravanti *et al.*, 2013). *In vitro*, GcrA proteins coming from *C. crescentus*, *B. abortus* and *S. meliloti* have also been shown to have an affinity for hemi-methylated sequences that depends on the strand that is methylated (Fioravanti *et al.*, 2013). In *C. crescentus*, *gcrA* is not essential in minimal medium but its depletion strain exhibits a filamentous morphology with an accumulation of chromosomes (Fioravanti *et al.*, 2013; Murray *et al.*, 2013; Haakonsen *et al.*, 2015). Interestingly, the hetero-complementation of *C. crescentus* $\Delta gcrA$ by either *B. abortus gcrA* or *S. meliloti gcrA* can support viability in rich medium (Fioravanti *et al.*, 2013), suggesting that they have similar functions. However, bacterial morphology is altered, with the formation of long filaments with the gene of *B. abortus*, and thicker bacteria with the one of *S. meliloti* (Fioravanti *et al.*, 2013). The migration profiles of GcrA in electrophoretic mobility shift assays were also different, depending on their bacterial origin (Fioravanti *et al.*, 2013). In theory, GcrA could form dimers (Fioravanti *et al.*, 2013) but structural analyses suggest that the protein is totally functional as a monomer in *C. crescentus* (Wu *et al.*, 2018). The disparity of phenotypes between the three different GcrA could thus be explained by a difference of abundance, activity, conformation or targets.

The regulon of *C. crescentus* GcrA has finally been determined in 2015, with the paper of Haakonsen *et al.* It had previously been shown by ChIP-seq that GcrA binding sites were

three times more likely to possess a GANTC site than other regions of *C. crescentus* chromosome (Fioravanti *et al.*, 2013). However, many *in vivo* targets that are devoid of GANTC sequence were also bound by GcrA (Fioravanti *et al.*, 2013). This observation could be explained by the fact that GcrA preferentially binds to the housekeeping σ^{70} and not to DNA like many other transcription factors (Haakonsen *et al.*, 2015). Actually, ChIP-seq experiments revealed that *C. crescentus* GcrA was virtually binding to all σ^{70} targets, at least in the tested conditions (Haakonsen *et al.*, 2015). GcrA can also bind to GANTC sequences on DNA, but it seems that the adjacent nucleic acids also strongly impact GcrA binding. An extended consensus sequence as been proposed as being YGAKTCK, where Y = C or T and K = G or T (Haakonsen *et al.*, 2015). In the end, the regulon of *C. crescentus* GcrA was determined with these three criteria: (1) a change of minimum 1.75 fold between RNA levels in GcrA depletion strain, compared to the WT strain, after 30 or 45 minutes of cell cycle synchronization; (2) a high ratio of ChIP-seq peak intensities between GcrA and σ^{70} ; (3) GANTC sites in the promoters of the targets (Haakonsen *et al.*, 2015). These criteria led to the establishment of a list of 204 targets, amongst which many are involved in motility, nucleotide synthesis, DNA organization and repair, cell biogenesis and cell division (Haakonsen *et al.*, 2015). Many of these targets were also cell cycle-regulated, but not all of them (Haakonsen *et al.*, 2015). Interestingly, it also appeared that the expression of genes of the replisome was not regulated directly via GcrA, with the exception of *dnaE*, coding for the α subunit of DNA polymerase III (Haakonsen *et al.*, 2015). Nevertheless, since the promoter of *ctrA* is a target of *C. crescentus* GcrA, the expression of many genes that are required later than GcrA in the cell cycle was also shown to be influenced by GcrA (Haakonsen *et al.*, 2015).

GcrA is clearly an atypical transcription factor, as its mechanism of action is different from any other transcription activator characterized to date (Wu *et al.*, 2018). Most transcription factors bind to DNA, and then recruit the RNA polymerase holoenzyme (*i.e.* the polymerase core composed of the $\alpha_2\beta\beta'\omega$ subunits, plus a σ factor), either through an α subunit, or through the fourth domain of the σ factor, the one that recognizes the -35 box on DNA (Lee *et al.*, 2012). Only a handful of transcription factors directly bind to the RNA polymerase, amongst which *E. coli* DksA that can decrease the open complex stability at specific promoters and thus decrease the rate of transcription of its target genes (Paul *et al.*, 2004; Lennon *et al.*, 2012). In the case of *C. crescentus* GcrA, the transcription factor C-terminal domain first binds to the RNA polymerase on the second domain of the σ^{70} factor (the one that recognizes the -10 box on DNA), then the whole complex binds to DNA with a preference for GANTC-rich sequences, which are recognized by the N-terminal domain of GcrA (**Fig 15**) (Haakonsen *et al.*, 2015; Wu *et al.*, 2018). This results in the facilitation of the DNA strands separation by the formation of an open complex and in the overexpression of the target genes (Haakonsen *et al.*, 2015; Wu *et al.*, 2018). As the other typical binding sites of transcription factors are still available in this conformation, promoters can be co-regulated by several proteins. It is for example the case of the *ftsZ* promoter, which is directly regulated by GcrA (Haakonsen *et al.*, 2015), but also by DnaA (Hottes *et al.*, 2005). Importantly, the regulon and operating mode of GcrA is still completely unknown in other bacteria.

Key information

GcrA is another well-conserved transcription factor of the α -proteobacteria class. Its regulon in *C. crescentus* corresponds to genes involved in motility, nucleotide synthesis, DNA organization and repair, cell biogenesis and cell division. In *C. crescentus*, it was found to follow the σ^{70} factor in an atypical way. We suspect that it works in a similar way in other α -proteobacteria, such as *Brucella*, but it still needs to be confirmed.

Objectives

The aim of this thesis was double: firstly, continue previous work on cell cycle regulators in *B. abortus* and secondly, investigate the stresses that *B. abortus* meets inside host cells. As cell cycle and infection are coordinated in *B. abortus* (De Bolle *et al.*, 2015), we assumed that there could be a functional link between cell cycle regulators and the ability of the bacterium to survive against genotoxic stresses.

The responses of bacteria to alkylating stress have been studied over the last forty years, but almost never in a natural environment. Indeed, there are only a handful of articles that tried to investigate the natural occurrence of this stress on bacteria. Considering that all the ingredients (RNS, acidic pH, nitrate reductase activity) of the generation of alkylating stress are present inside host cells, and that we found many genes predicted to code for alkylated DNA repair proteins in the genome of *B. abortus*, we decided to examine the potential occurrence of this stress on our model bacterium during infection.

Another area of research that has been very poorly investigated is the DNA repair capacity of *B. abortus*. We therefore also attempted to draw a picture of the DNA repair pathways that are required by *B. abortus* during infection and against *in vitro* alkylating stress. In this context, we wanted to investigate the potential role played by the transcription factors CtrA and GcrA. This part of the work follows my master thesis project, which was about elucidating the regulon of *B. abortus* CtrA in culture and in infection (Poncin K., Master thesis 2014). As for the role of GcrA, another well-conserved transcription factor that is linked to the regulation of the cell cycle in *C. crescentus* (Brilli *et al.*, 2010), its role had never been investigated in *B. abortus*. We thus worked on the characterization of *B. abortus* GcrA regulon, and more particularly on its function as a regulator of genes involved in DNA repair.

Results

I. Detection and sources of alkylating stress in *B. abortus*

The data presented here are part of a research article, which is currently under revision for Nature Communication.

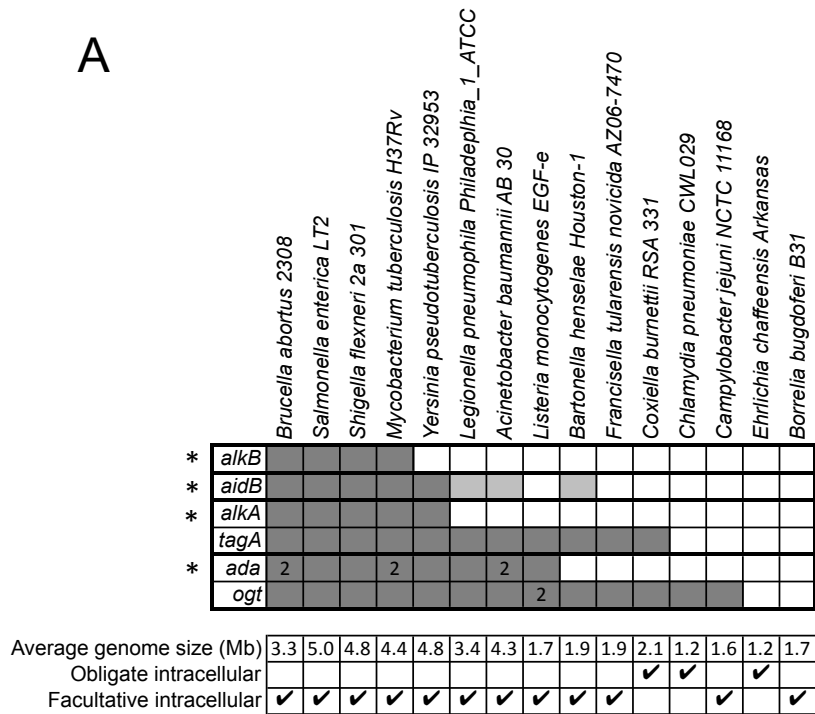
I.1 Intracellular bacteria possess genes to face alkylating stress

The response to alkylating stress by bacteria has been best studied in *E. coli*, with the discovery of genes of the adaptive system, as well as other non-inducible genes that code for proteins specialized in repairing alkylated DNA (Mielecki & Grzesiuk, 2014). These genes include *ada*, *alkA*, *alkB*, *aidB*, *ogt* and *tagA*. We found that many intracellular bacteria, including obligate ones such as *Chlamidia pneumonia* and *Coxiella burnettii*, retained some of the alkylated DNA repair genes (**Fig 16A**), supporting the hypothesis that alkylating stress could be met by these intracellular bacteria. Note that *Brucella abortus* and other *Brucella* species are predicted to be particularly well equipped against such a stress, as they possess genes homologous to all of the genes listed here, except *B. ovis* that does not have a *tagA* gene (**Fig 16B**). Most *Brucella* strains also have a second copy of *ada* (**Fig 16B**). Incidentally, the two genes that are most often conserved in the bacteria reported in **Fig 16A** are *tagA* (coding for a DNA glycosylase) and *ogt* (coding for a dioxygenase), both reported to be independent of an adaptive system.

I.2. Alkylating stress is encountered by *B. abortus* inside host cells

Until now, strategies to detect the presence of alkylating stress inside host cells have been based on the survival of mutant strains attenuated for alkylated DNA repair. These studies were unsuccessful, maybe because of the likely redundancy between the repair systems (Durbach *et al.*, 2003; Alvarez *et al.*, 2010). Here, we took advantage of the ability of the auto-regulated protein Ada from *E. coli* (Ada_{*E. coli*}) to detect meP3ester groups on DNA (Sedgwick, 1987), using a transcription-based fluorescent reporter system. The *ada* gene being in operon with *alkB* in *E. coli* (Kondo *et al.*, 1986), we cloned *ada* and replaced *alkB* by a superfolder *gfp* in a medium-copy plasmid (**Fig 17A**). A mutated version of the reporter system was also constructed to be used as negative control, in which a C38A mutation was introduced in Ada_{*E. coli*}, in order to prevent the protein to capture meP3ester groups.

The system was first tested *in vitro* in *E. coli*, with the use of MMS, as alkylating agent (**Fig 17B**). The plasmids carrying either version of the reporter system (pBBRMCS1-*pada-ada-gfp* or pBBRMCS1-*pada-ada*^{C38A}-*gfp*) were also transferred to *Salmonella enterica* biovar Typhimurium, which does not possess a functional adaptive system (Hakura *et al.*, 1991). In both *E. coli* and *S. enterica*, the reporter system was switched on in the presence of MMS and only with the wild type Ada_{*E. coli*} (**Fig 17B**). The reporter system was also functional in *B.*



Legend

- 2 Two genes with high homology to *E. coli* K12
- Gene with high homology to *E. coli* K12
- Gene with low homology to *E. coli* K12
- No homologous gene found

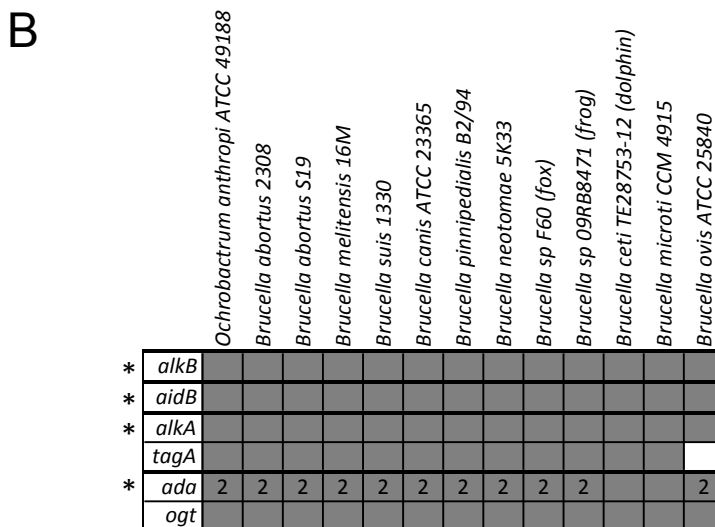


Fig 16. Conservation of genes coding for alkylated DNA repair proteins in **A)** different bacteria and in **B)** different *Brucella* species and a close relative, *Ochrobactrum anthropi*. Genes were grouped by function. Homology was calculated based on *E. coli* K12 genome (www.patricbrc.org/). In the case of *aidB*, genes annotated as acyl-coA dehydrogenase with e-value between 10^{-29} and 10^{-44} were considered as genes with low homolog and genes with e-value lower than 10^{-133} were considered as genes with high homology. In the case of *B. ceti* and *B. microti*, two distinct homologues of *ada* and *ogt* were also found but not included in the figure. Asterisks indicate genes that are regulated by Ada in *E. coli*.

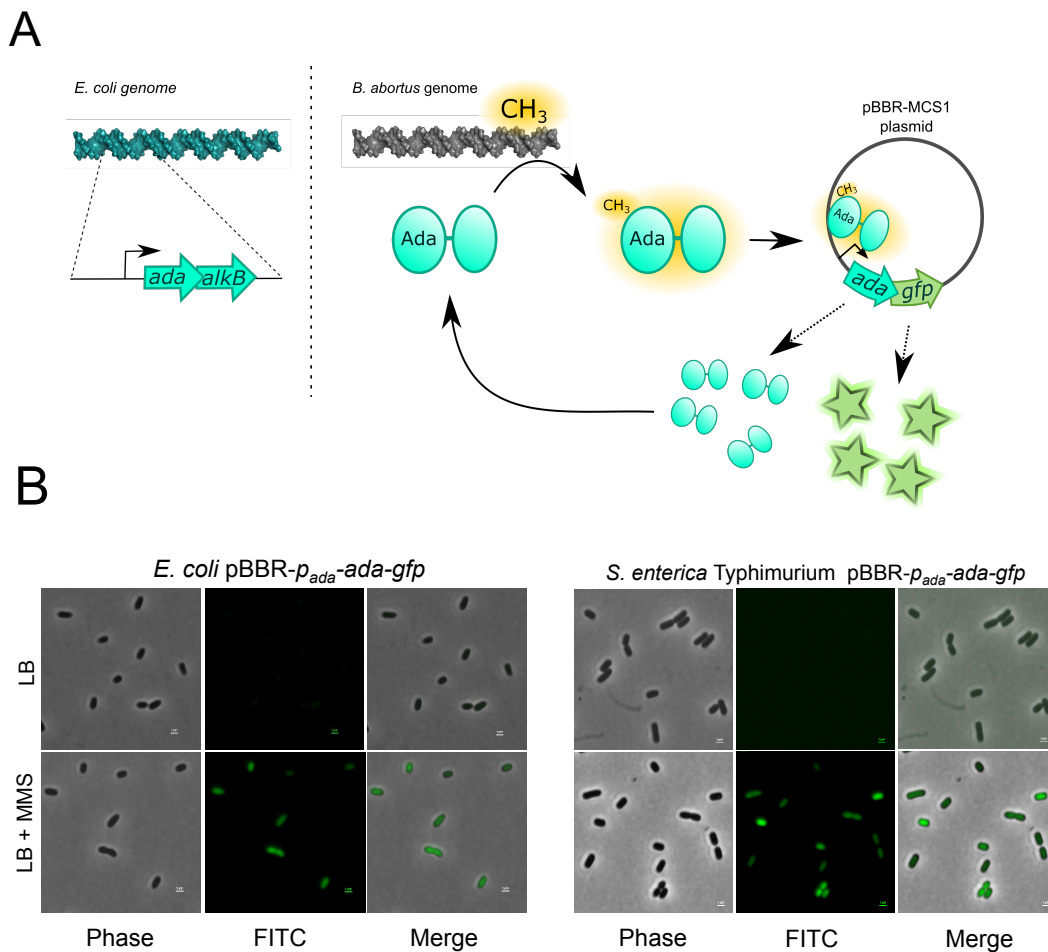


Fig 17. Reporter system for alkylation stress. **A.** Schematic representation of the reporter system. The sequence corresponding to $ada_{E. coli}$ and its promoter were cloned into a pBBR-MCS1 plasmid and a superfolder gfp was inserted downstream $ada_{E. coli}$. This plasmid (pBBR- p_{ada} - ada - gfp) was transferred to *B. abortus*. When $Ada_{E. coli}$ detects a methylphosphotriester group on *B. abortus* DNA, it activates the expression of its own promoter, which leads to an accumulation of $Ada_{E. coli}$ and GFP. Note that a mutation in $ada_{E. coli}$ (C38A) leads to the abrogation of its ability to bind methylphosphotriester. **B.** The reporter system to detect alkylating stress was used in *E. coli* and *S. enterica* Typhimurium cultured for 1h45 in the absence of stress (LB only) or in the presence of an alkylating agent (LB supplemented with 0.5 and 1 mM of MMS, respectively). Scale bars represent 1 μ m.

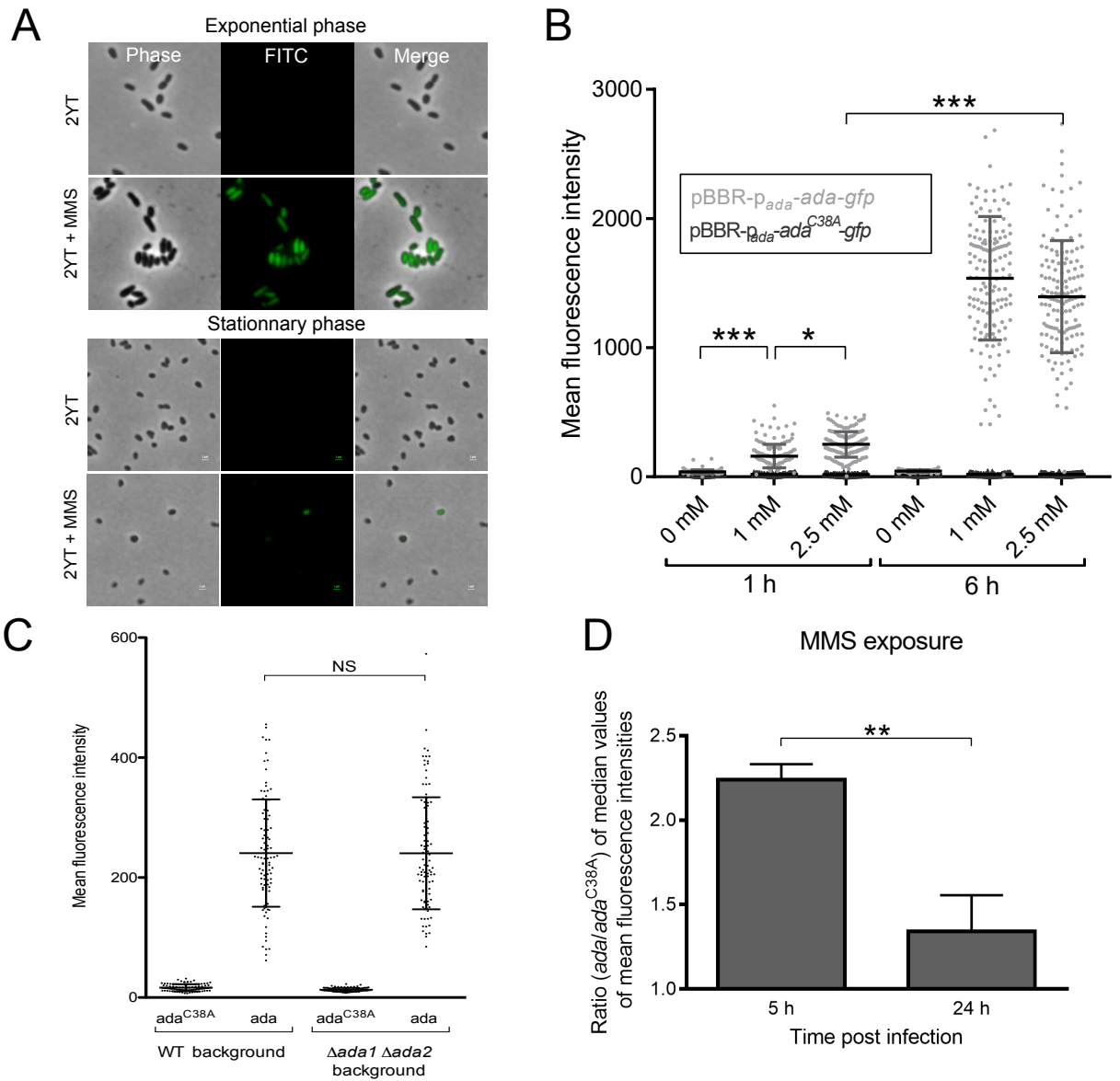


Fig 18. Reporter system for alkylation stress in *B. abortus*. **A)** *B. abortus* carrying the pBBR- p_{ada} - ada - gfp reporter system was cultured to reach either exponential phase (OD₆₀₀ 0.6) or stationary phase (OD₆₀₀ 1.2) in rich liquid medium (2YT), then it was exposed to 5 mM of MMS for 1h45. Scale bars represent 1 μ m. **B)** Exponential phase *B. abortus* carrying either the pBBR- p_{ada} - ada - gfp reporter system or its mutated version (ada^{C38A}) were cultured in rich medium (TSB) and exposed to various doses of MMS for 1 or 6 h. Mean fluorescence intensities were calculated for n = 150 bacteria in each condition. Scheffe statistical analyses were performed with $p < 0.05$ (*) and $p < 0.001$ (***), clearly showing that both time of exposure and dose of alkylating agent impact the response of the reporter system. **C)** The two versions of the reporter system were also tested in the WT and $\Delta ada1 \Delta ada2$ *B. abortus* backgrounds exposed to 2.5 mM MMS for 1 h. Student's t test revealed that there is no statistical difference in the responses between the two genetic backgrounds ($p > 0.05$, NS). Error bars represent standard deviation from the mean. **D)** Bacteria carrying either the pBBR- p_{ada} - ada - gfp reporter system or its mutated version (ada^{C38A}) were used to infect RAW 264.7 macrophages and mean fluorescence intensities (FITC channel) were calculated at 5 h or 24 h post infection (n = 60). Ratio of median values (ada/ada^{C38A}) were plotted for biological triplicates. Error bars correspond to standard deviation. Student's t test was performed with $p < 0.01$ (**).

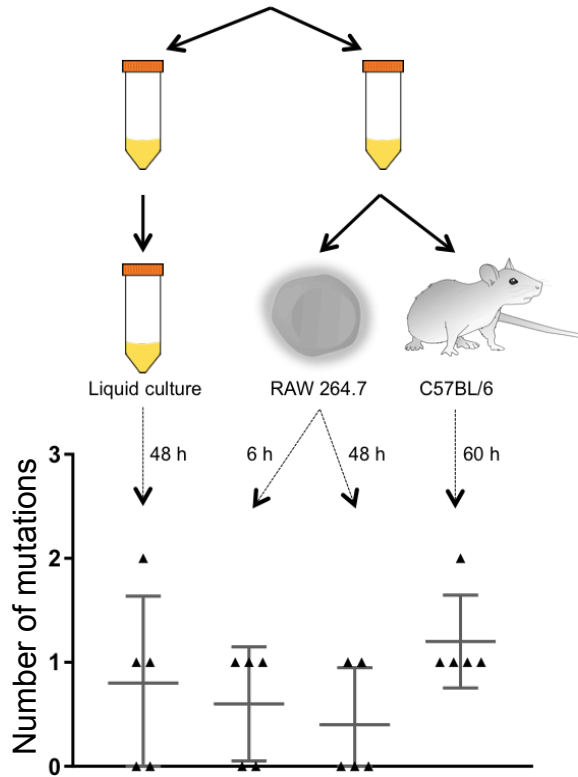


Fig 19. Number of mutations occurring after infection and liquid cultures of *B. abortus* 544. Whole genome sequencings were performed on liquid cultures resulting from colonies originating from (1) liquid cultures diluted twice in the course of 48 h, (2) bacteria recovered after 6 and 48 h post infection in RAW 264.7 macrophages and (3) bacteria recovered from mice spleen after 60 h of infection (n = 5 for each condition). Each triangle correspond to the number of mutations for one individual colony from one individual experiment. Microsatellites and positions with less than 10 reads were excluded. All mutations occurred in the *btaE* gene (BAB1_0069) at different positions, except one in the *cls* gene (BAB2_1021, cardiolipin synthase-like gene) after mice infection. A one-way ANOVA followed by a Tukey's statistical analysis was performed with $p > 0.05$ (NS).

abortus, and we observed that it was more reactive with exponential phase cultures compared to stationary phase cultures (**Fig 18A**). The emitted fluorescence was also dependent on the time of exposure and concentration of MMS (**Fig 18B**). In order to ensure that the reporter system was not affected by *B. abortus* endogenous Ada production ($Ada_{B. abortus}$), the mean fluorescence intensities of the system in a *B. abortus* $\Delta ada1 \Delta ada2$ background were compared to the results in the WT background (**Fig 18C**). No statistical difference could be observed between the two experiments, supporting the idea that $Ada_{B. abortus}$ is not affecting the level of activation of the reporter system.

The reporter system was then tested at the single cell level in a RAW 264.7 macrophages infection model for two time points. The first time point was 5 h PI, which corresponds to the end of the first phase of the infection, when *B. abortus* is non growing and blocked in a G1-like phase inside the eBCV (Deghelt *et al.*, 2014). The second time point was chosen at 24 h PI, when the bacteria are actively dividing inside the rBCV (Deghelt *et al.*, 2014). The ratio between mean fluorescence intensities of the functional reporter system and its mutated version (Ada^{C38A}) were calculated for the two time points. The level of fluorescence was much higher at 5h PI than at 24h PI (**Fig 18D**), suggesting that the bacterium is indeed meeting alkylating stress inside host cells, but mainly during the first phase of the infection.

The occurrence of alkylating stress on *B. abortus* during the first phase of the trafficking could result in mutagenesis of the bacterium during infection. To investigate the mutagenic properties of the intracellular environment, compared to other conditions, we sequenced the genome of several individual clones of *B. abortus* before and after infection in RAW 264.7 macrophages (6 and 48 h) and after mice infection (60 h), as well as after a similar number of generations in liquid culture (48 h). The genomes of 5 individual clones resulting from these different conditions were sequenced and subsequent analyses indicated that the number of mutations was not increased in the infection conditions compared to the culture. Indeed, *B. abortus* accumulated a very few mutations in all conditions, and no statistical difference could be detected between them (**Fig 19**).

I.3. N-nitrosation events occur inside the eBCV

Alkylating agents can arise from different sources, such as the peroxidation of lipids and the N-nitrosation of metabolites; or, to a lesser extent, they could be already present as weak endogenous alkylating agents, such as SAM (Rydberg & Lindahl, 1982; Posnick & Samson, 1999). Since the content of the eBCV is unclear regarding the sources of the stress *B. abortus* encounters, we developed a new tool to investigate the presence of N-nitrosation in the eBCV. The use of succinimidyl ester groups to label the outer membrane of bacteria with fluorescent molecules has been successfully applied over the last years (Brown *et al.*, 2012; Deghelt *et al.*, 2014). Besides, Miao *et al* (2016) set up a highly specific probe relying on its N-nitrosation in order to emit fluorescence. The two techniques were combined in order to

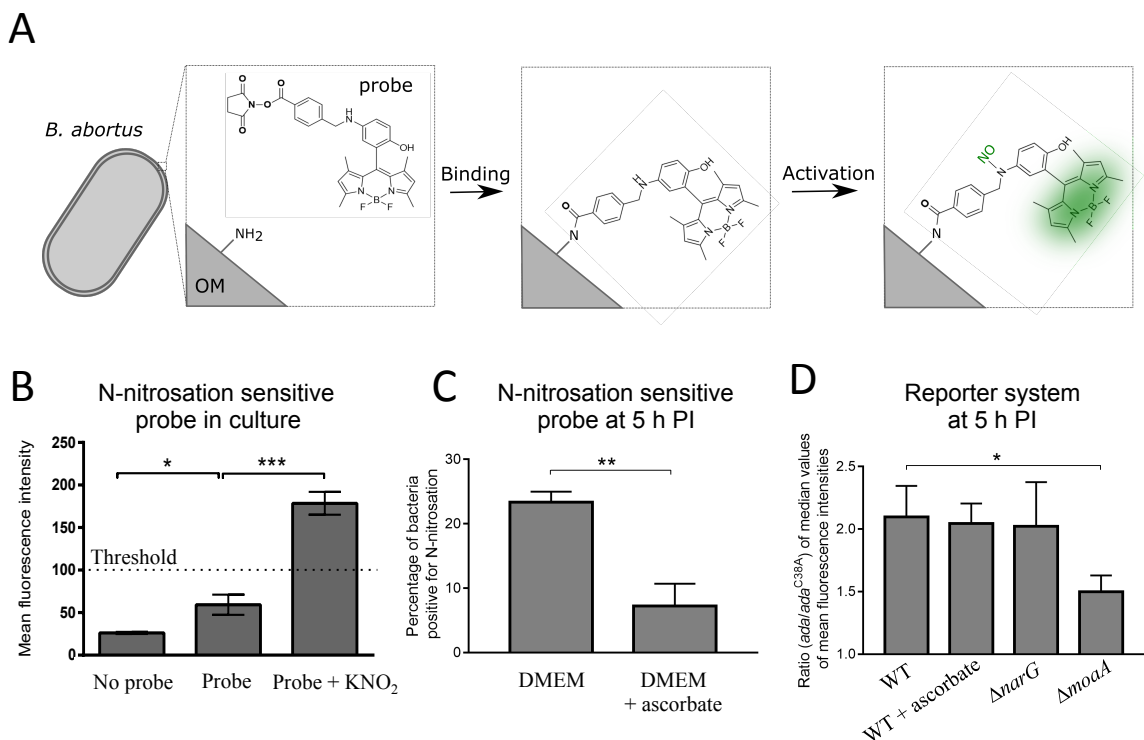


Fig 20. Production of N-nitroso compounds. **A)** Schematic representation of the N-nitrosation sensitive probe reacting with primary amine from *B. abortus* outer membrane (OM), and subsequently being activated by NO. **B)** The mean fluorescence intensities (MFI) of bacteria (FITC channel) were measured after 1 hour of incubation in PBS supplemented or not with KNO₂, a N-nitrosating agent. MFI were also measured for non-labeled bacteria in order to evaluate *B. abortus* autofluorescence (No probe). Experiments were done in biological triplicates and median values of MFI were plotted. Error bars represent standard deviations. The number of bacteria analyzed in this study were 152, 333, 556 for non-labeled bacteria; 155, 260, 246 for labeled bacteria; and 430, 402, 496 for labeled bacteria subjected to KNO₂. A one-way ANOVA followed by a Tukey's statistical analyzes were performed with $p < 0.05$ (*) and $p < 0.001$ (***). **C)** Evaluation of exogenous N-nitrosation by calculating the percentage of positive labeled-bacteria. Bacteria were labeled with the N-nitrosation-sensitive probe and used to infect RAW 264.7 macrophages. Mean fluorescence intensities were calculated at 5 h post infection ($n = 60$) and values above 100 (set up base on *in vitro* experiments, see figure 20C) were considered as positive. The addition of 163 μ M of ascorbate to the cell culture medium at time 0 was used to inhibit N-nitrosation. Experiments were done in biological triplicates. Error bars correspond to standard deviation. Student's t test was performed with $p < 0.01$ (**). **D)** Evaluation of endogenous N-nitroso compounds formation via the alkylation-sensitive reporter system. The Ada_{*E. coli*}-based reporter system was used in three genetic backgrounds (WT, $\Delta narG$ and $\Delta moaA$) and in the presence of ascorbate (for the WT background only). Bacteria carrying either the pBBR-p_{ada}-ada-gfp reporter system or its mutated version (ada^{C38A}) were used to infect RAW 264.7 macrophages and mean fluorescence intensities were calculated at 5 h post infection ($n = 60$). Ratio of median values (ada/ada^{C38A}) were plotted for biological triplicates. Error bars correspond to standard deviation. A Student's t test was performed with a $p < 0.05$ (*). PI stands for post infection.

create a N-nitrosation sensitive probe that could be attached to the surface of *B. abortus* and thus follow whether N-nitrosation could take place inside the eBCV (**Fig 20A**).

Labeled bacteria were first tested for their fluorescence *in vitro*, in the presence of KNO_2 , which generates the NO donor N_2O_3 in aqueous solution (**Fig 20B**). The autofluorescence of non-labeled *B. abortus* was also compared to the fluorescence of the labeled bacteria in the absence of KNO_2 (**Fig 20B**). It could thus be concluded that the probe is, as expected, emitting fluorescence when N-nitrosated. RAW 264.7 macrophages were then infected with labeled bacteria and mean fluorescence intensities were calculated at 5 h PI at the single cell level (**Fig 20C**). The negative control consisted in the cell culture medium supplemented with 163 μM of ascorbate, as this concentration of antioxidant is known to inhibit N-nitrosation reactions in RAW 264.7 macrophages (Kosaka *et al.*, 1989). We observed that about a quarter (23.3 %) of the bacterial population was subjected to N-nitrosation inside the eBCV (**Fig 20C**). The addition of ascorbate strongly decreased the mean fluorescence intensity of labeled bacteria (**Fig 20C**).

We also investigated the endogenous production of N-nitroso compounds. To do so, the *adaE. coli*-based reporter system was tested in different genetic backgrounds (WT, $\Delta narG$ and $\Delta moaA$) at 5 h PI. We found out that the deletion of *narG* alone is not sufficient to reduce the stress, whereas it is the case with the $\Delta moaA$ strain (**Fig 20D**). Importantly, the addition of 163 μM of ascorbate to the cell culture medium did not statistically reduce the detected alkylating stress (**Fig 20D**). Overall, this suggests that alkylating stress is mainly produced endogenously by *B. abortus* metabolism.

II. Defenses of *B. abortus* against alkylating stress

II.1. Ogt is a key actor against alkylating stress in *B. abortus*

In order to evaluate which DNA repair genes are required by *B. abortus* to face alkylating stress, deletion strains were constructed and plated on rich medium supplemented with alkylating agents. Mutants were constructed for genes predicted to code for proteins involved in direct repair ($\Delta ada1$, $\Delta ada2$, Δogt and $\Delta alkB$), BER (the glycosylases *tagA*, *alkA* and the endonucleases *xthA1* and *xthA2*), as well as other DNA repair pathways, including $\Delta recA$, involved in HR, $\Delta uvrA$, involved in NER, and the double mutant $\Delta mutS \Delta mutL$ involved in MR. Two strains were also used as negative controls: the triple mutant $\Delta mutM \Delta mutY \Delta mutT$, required for DNA repair following oxidative stress, and the $\Delta virB$ strain, coding for *B. abortus* type IV secretion system. All these mutant strains were tested for their survival against the $\text{S}_\text{N}1$ agent MNNG that reacts directly with DNA, and the $\text{S}_\text{N}2$ agent MMS that reacts in two steps via an intermediate product (Beranek, 1990) (**Fig 1**). Interestingly, some genes seem to be required against one type of alkylating agent only, such as *alkB* and the BER mutants that are attenuated only on plates supplemented with MMS. A $\Delta xthA1$ mutant had been previously reported to be sensitive to MMS (Hornback & Roop, 2006), but the question remained as to the function of XthA2. Here, we show that XthA1 is the major

		TSB	MNNG	MMS
Function	WT	1,95E+08	2,12E+08	1,80E+08
	<i>Δada1</i>	1,43E+08	1,48E+08	1,30E+08
DR	<i>Δada2</i>	1,77E+08	1,73E+08	1,33E+08
	<i>Δada1 Δada2</i>	1,52E+08	9,56E+07	8,68E+07
	<i>Δada1 Δada2 Δogt</i>	1,87E+08	7,93E+05	4,99E+04
	<i>Δogt</i>	1,90E+08	9,26E+06	7,48E+04
	<i>ΔalkB</i>	1,52E+08	1,30E+08	2,07E+07
	<i>ΔtagA</i>	1,72E+08	1,57E+08	4,95E+06
BER	<i>ΔtagA ΔalkA</i>	1,70E+08	1,23E+08	2,03E+03
	<i>ΔalkA</i>	1,75E+08	1,25E+08	1,40E+08
	<i>ΔxthA1</i>	1,72E+08	1,63E+08	1,22E+07
	<i>ΔxthA2</i>	2,15E+08	1,65E+08	1,43E+08
	<i>ΔxthA1 ΔxthA2</i>	1,58E+08	1,60E+08	1,08E+05
HR	<i>ΔrecA</i>	1,40E+08	2,13E+07	9,90E+04
NER	<i>ΔuvrA</i>	2,13E+08	2,17E+08	1,32E+08
MR	<i>ΔmutS ΔmutL</i>	2,57E+08	2,19E+08	1,91E+08
Others	<i>ΔmutM ΔmutY ΔmutT</i>	2,18E+08	1,70E+08	1,40E+08
	<i>ΔvirB</i>	2,32E+08	2,53E+08	1,38E+08

Survival

Fig 21. Survival of DNA repair mutants against alkylating agents *in vitro*. Deletion strains were plated on rich medium (TSB) supplemented or not with alkylating agents (35 μ M of MNNG or 2.5 mM of MMS). Data shown here are the mean values of colony forming units for biological triplicates. DR stands for direct repair, BER for base excision repair, HR for homologous recombination, NER for nucleotide excision repair and MR for mismatch repair. The category “others” comprises 8-oxo-dG repair (*mutM mutY mutT*) and the type IV secretion system (*virB*) as negative controls.

A

```

E_coli_Ogt          MLRLLEEKIATPLGLPWVICDEQFRLRAVWEEYSERM-VQLLDIHYRKEGYERISATNP 59
B_abortus_2308_Ogt_BAB1_0185 MESFGITVFETPIGPGCIARWRGS-KIVGVEVGEADEKETRHLRERFAGGEYAEPPAF-I 58
* : : **:* : . : : .** * . : : * : : * . *

E_coli_Ogt          GGLSDKLERFAGNLSIIDTLPTA-TGGTFPQREVKTLRTIPCGQVMHYGQLAELGRP 118
B_abortus_2308_Ogt_BAB1_0185 RQTIEKVRALLDGSADPSDTPLALDSVPDLNRRVYEIILELKPGETTTYGAIRRLLGDV 118
: : * : * : * : : . * * . : : * : : : : * : . * * : * : * *

E_coli_Ogt          GAARAVGAANGSNPISIVVFCRHRVIGRNGTMTGYAGGV--QRKEWLLRHEGYLLL----- 171
B_abortus_2308_Ogt_BAB1_0185 SLSQAVGYALGKNPEPIIVFCRHRVLSNGKVGGSAAAGGTATKRLRLNIERARTTSEPDL 178
. : : * * * * * : : * * * * * * * * * * * * * * * * * * * * * * *

E_coli_Ogt          -----171
B_abortus_2308_Ogt_BAB1_0185 FGGLPLQERPQTGW 192
S134 C139

```

B

```

B_abortus_Ada2_BAB2_0347 ----MLFTLPNQDKLYDALVARDASIEGRAYVGVLTSTGIFCRRLTCPARKPKPENCRFFAS 56
E_coli_Ada          ---MKKATCLTDDQRWQSVLARDPNADGEFVFAVRTTGIFCRPSCRARHALRENVSPYAN 57
B_abortus_Ada1_BAB1_0398 MNLMIPKTHDPDESRWQVLDLRKASDGFVYAVRTTGIVCRPSCPSRRGKRENVQPFNG 60
* : : : : * : * . * * * : * : * : * : * : * : * : * : * : * : * : * : *

B_abortus_Ada2_BAB2_0347 VAECMADGFRPCCKRCHSLQPAABEILV-----KLLNALETDPERRWSEEDVVR 106
E_coli_Ada          ASEALAAAGFRPCCKRQPEKANAQQ-----HRLDKITHACRLLEQ-ETPVT---LEALDQ 108
B_abortus_Ada1_BAB1_0398 CEDAERAGFRPCCLRCKPLSDTLATQNNARHAEMVASACRFIETAETQPS---LEEIANV 117
: . * * * * * : : : : * * * * * * * * * * * * * * * * * * * * * * *
D107

B_abortus_Ada2_BAB2_0347 MGFDPSTVRRSFRRHFGMTFLEMARQERLRHGFQVL-AGGGCVIDAQVDAGFESPEAFRS 165
E_coli_Ada          VAMSPFHLHRLFKATGMPKAWQQAWRARRLRESLAKG-ESVTTSLNAGFPDSSSYR 167
B_abortus_Ada1_BAB1_0398 VKASPAHFHRVFKAFPTGLTPKAHADHRAGRMRAALDMPQIRVTDTIYDAGYNSSRFYE 177
: . * . * * * : * * * * * * * * * * * * * * * * * : : * * : . :

B_abortus_Ada2_BAB2_0347 AFVRIVGLPPAKLRKEGLLRADWFK---TPLGTMIAICDVRSLHLEF-ADRKALPAELK 221
E_coli_Ada          KADETLGMTAKQFRHGGENLAVRYALADCELGRCLVAESERGIICAILGDDDATLISELQ 227
B_abortus_Ada1_BAB1_0398 ASDRILGMTPKAYRAGGKDADIRFAIGQSTLGAVLVAASGKSVCAIFMGDDPQGLIHDL 237
. : * : * * * * : : * * : . . : : : : * * * : * :

B_abortus_Ada2_BAB2_0347 KLHAACRGDIGIGRFETHDLVERQLNAFFEGRSVAVFDLPLVMHGSPTQDVWRELQNIRA 281
E_coli_Ada          QMPFAADN---APADLMFQQHVRVIEASLNQRDTPLTLPLDIRGTAFQQQVWQALRTIPC 284
B_abortus_Ada1_BAB1_0398 KRFPKANL---IGADRNFNELVAEVVGFVEAPGIGLDLPLDLRGTAFQQRVWRALCEIPA 294
: . . : : : : : : : * * * : * * * * * * * * * * * * *

B_abortus_Ada2_BAB2_0347 GETRSYSEIARAIEKPLAVRAVARANGANQIAIVICRHRVIGADGALFGYGGGLWRKQKL 341
E_coli_Ada          GETVSYQQLANAIGKPKAVRAVASACAANKLAIIIIHRVVRGDTLSGYSYRWGVSRAKQQL 344
B_abortus_Ada1_BAB1_0398 GETVSYTDIAERISAPRAVRAVAQACAANKIYAVVICRHRVVRNDGGISGYSYRWGVERKRD 354
* * * * * : * * * * * * * * * * * * * * * * * * * * * * * * * * * * *

B_abortus_Ada2_BAB2_0347 IEIEAQYRR- 350
E_coli_Ada          LRREAENEER 354
B_abortus_Ada1_BAB1_0398 LERERKA--- 361
: . * :
C321

```

Fig 22. Alignments of sequences for **A)** *ogt* and **B)** *ada* in *E. coli* K12 and *B. abortus* 2308. Clustal Omega (<https://www.ebi.ac.uk/Tools/msa/clustalo/>) was used to align amino acid sequences. Black boxes indicate catalytic sites in *E. coli* (C39 and C321 for O⁶-methylguanine and O⁴-methylthymine repair and C38 for methylphosphotriester capture). The blue box correspond to a position that confers broader substrate specificity to Ogt, if mutated into a proline, as in *B. abortus*. The red box indicates a position which could be responsible for the absence of a functional adaptive response in *B. abortus*.

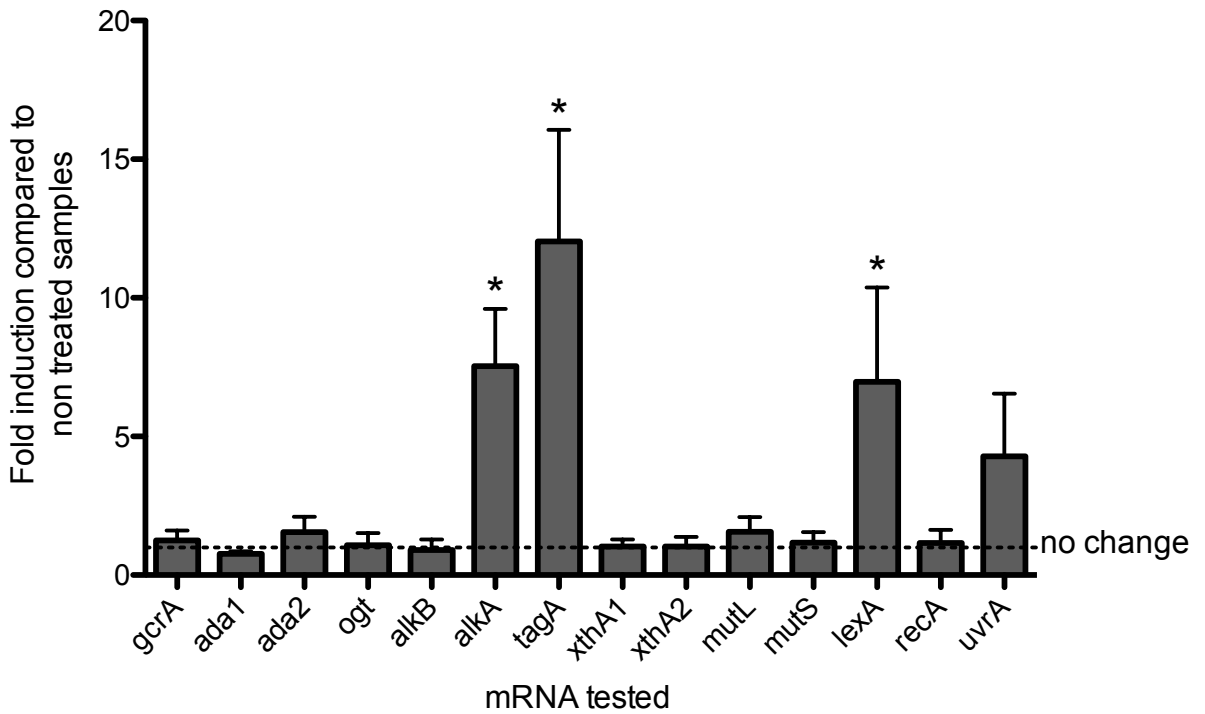


Fig 23. Gene expression following MMS treatment. RT-qPCR was performed on exponential phase *B. abortus* cultured in rich medium for 5 hours in the presence or absence of 2.5 mM MMS. Experiments were performed three times and mean values were compared between the stressed and non-stressed conditions. Error bars represent standard deviation. Student's t test was performed on data with minimum 1.5 fold induction ($p < 0.05$, *).

endonuclease, since its sole deletion is enough to confer sensitivity to MMS whereas it is not the case for the deletion of *xthA2*. However, the double mutant is about 105 times more attenuated than the single $\Delta xthA1$ (**Fig 21**), so it is clear that both genes have (partially) redundant functions. Similarly, it appears that $\Delta tagA$ and $\Delta alkA$ have also a synergetic effect, as the $\Delta alkA$ mutant is not affected by MMS whereas the $\Delta tagA$ mutant displays a 35-fold decrease in the number of CFU. The $\Delta tagA \Delta alkA$ mutant is even more strongly affected with a decrease in CFU of 5 orders of magnitude compared to the control condition (**Fig 21**). This result strongly suggests that AlkA and TagA share a common DNA glycosylase function, which is crucial for survival in the presence of MMS in *B. abortus*, as it is the case in *E. coli* (Kaasen *et al.*, 1986). The $\Delta recA$ mutant is also strongly affected by MMS, and slightly by MNNG (**Fig 21**). The Δogt mutant is particularly noteworthy, as it appears to be very sensitive to MMS exposure. Moreover, the triple methyltransferase mutant $\Delta ada1 \Delta ada2 \Delta ogt$ is only marginally more attenuated than the single Δogt mutant against MMS, and slightly more against MNNG (**Fig 21**). This clearly indicates that the presence of Ogt is a key factor for *B. abortus* survival against alkylating agents, unexpectedly more than the two Ada proteins compared to the *E. coli* model. At the protein level, Ogt_{*B. abortus*} is predicted to be 33 % identical to Ogt_{*E. coli*} and the methyl-acceptor C139 residue is conserved (**Fig 22A**). In *B. abortus*, the residue corresponding to Ogt_{*E. coli*} S134 is a proline (**Fig 22A**). Remarkably, in *E. coli*, the mutation of S134 into a proline confers a broader specificity to the protein by increasing the size of its active site (Schoonhoven *et al.*, 2017).

The two genes predicted to code for Ada proteins also possess the conserved C38 and C321 residues, involved in its activation into a transcription factor and the capture of O⁶meG or O⁴meT, respectively (**Fig 22B**). Nevertheless, the deletion of the *ada1* and *ada2* genes did not change drastically the sensitivity of *B. abortus* to alkylating agents (**Fig 21**), so one could wonder if the supposed Ada proteins are actually functional as transcription factors of a hypothetical adaptive system. Quantitative reverse transcription polymerase chain reaction (RT-qPCR) experiments were performed on liquid cultures of *B. abortus* in the presence or absence of MMS and several DNA repair genes were compared for their RNA levels in these conditions (**Fig 23**). Interestingly, the RNA levels of the two *ada* genes were not statistically increased after MMS exposure. At the opposite, the ones that did have a high fold induction were *alkA*, *tagA* and *lexA* (**Fig 23**). In fact, the only overexpressed alkylation-specific genes were *alkA* and *tagA*, which are predicted to code for proteins of similar function. The absence of induction of the *ada* genes (**Fig 23**) and their marginal role in coping with alkylating stress *in vitro* (**Fig 21**) suggest that *B. abortus* is not relying on an Ada-dependent adaptive system to face alkylating stress. It has been proposed that the absence of an acidic residue as the 106th amino acid position of Ada_{*S. enterica*}, contrarily to Ada_{*E. coli*} (corresponding to D107), could explain the absence of an adaptive response in *S. enterica* Typhimurium, as it is part of the helix-turn-helix motif (Hakura *et al.*, 1991). Similarly, in *B. abortus*, the corresponding position is occupied by either a N116 (Ada1) or a V105 (Ada2) (**Fig 22B**), so this could be the key as to why *B. abortus* does not possess a functional adaptive system. Instead, it seems that it is relying on the non-inducible *ogt* and the inducible *alkA* and *tagA*, as well as the SOS system via *lexA* to face alkylating stress.

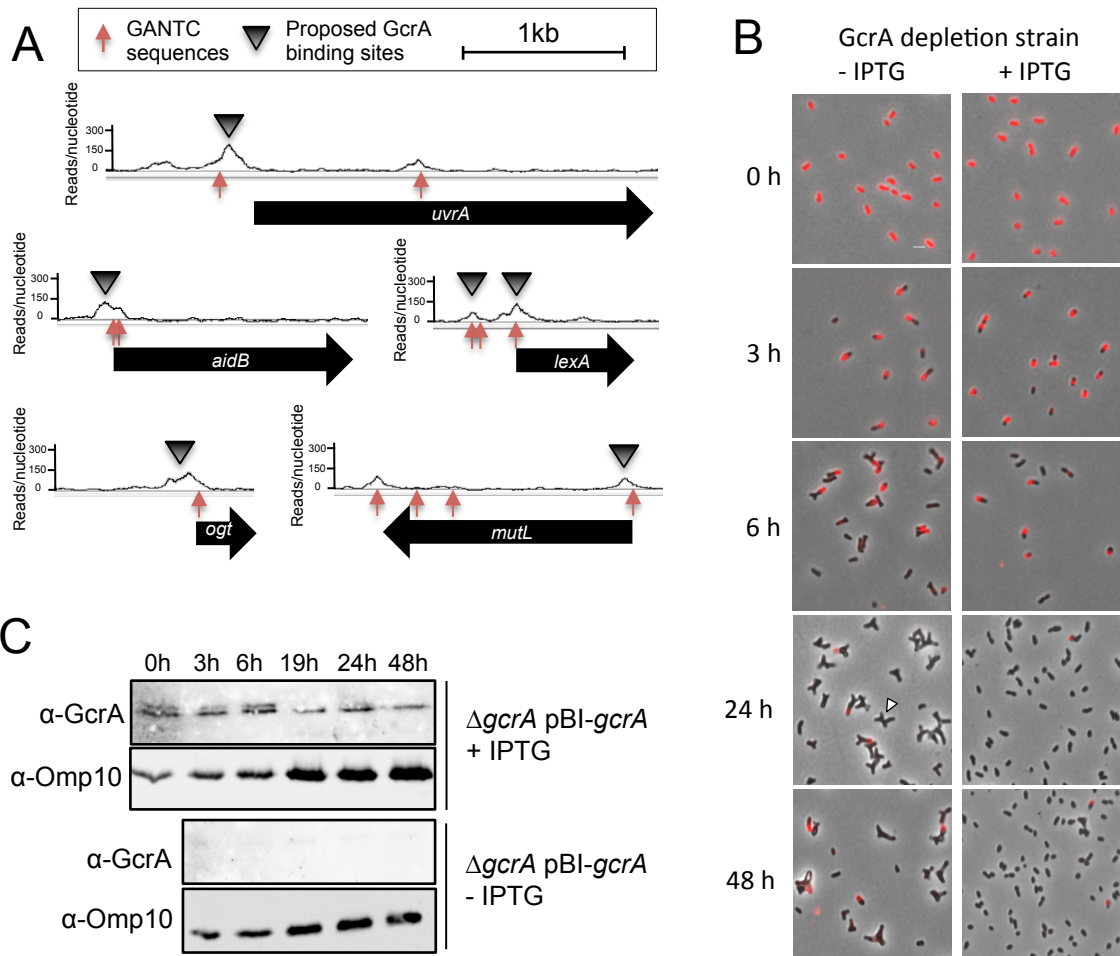


Fig 24. Targets of the transcription factor GcrA. **A)** *In vivo* GcrA binding sites detected by ChIP-seq. The number of reads per nucleotide is plotted for five promoter regions enriched by GcrA pull-down. **B)** GcrA depletion generates growth and division defects in *B. abortus*. Bacteria were labeled with TRSE to covalently bind Texas Red to amine groups present at the bacterial surface. Non labeled area thus correspond to newly incorporated envelope material. Grown in rich medium in presence of IPTG (+ IPTG), bacteria have a normal morphology. Upon IPTG removal (- IPTG), bacteria elongate (3 h), then form branches (6 h). At 24 h post IPTG removal, many bacteria present Y-shapes or more complex branched phenotypes (white arrow). **C)** Western blot against GcrA in the presence or absence of IPTG, with different timings post IPTG removal. Omp10 was used as loading control, as it was not amongst GcrA targets according to the ChIP-seq experiment.

II.2. The expression of *ogt* is dependent on the transcription factor GcrA

One striking characteristic of *ogt* is the presence, right after the start codon, of a GANTC motif. This sequence is known to be a site of epigenetic regulation in α -proteobacteria. Indeed, GANTC sites have been shown to be methylated by CcrM in a cell-cycle dependent manner in the α -proteobacterium *Caulobacter crescentus* (Collier *et al.*, 2007; Kozdon *et al.*, 2013; Gonzalez *et al.*, 2014), and probably also in *B. abortus* (Robertson *et al.*, 2000; Francis *et al.*, 2017). Interestingly, the gene coding for the alkylation-specific DNA repair AlkB protein is regulated throughout the cell cycle in *C. crescentus* (Colombi & Gomes, 1997). Since the cell cycle-dependent transcription factor GcrA is known to be a sensor of methylated GANTC sites on *C. crescentus* DNA (Fioravanti *et al.*, 2013; Haakonsen *et al.*, 2015), we identified the ortholog of *gcrA* in *B. abortus* (BAB1_0329), a gene previously shown to be essential (Sternon *et al.*, 2018). We performed a ChIP-seq against *B. abortus* GcrA to identify its direct targets in *B. abortus* genome. As many as 232 hits were found for the first chromosome of *B. abortus* and 110 for the second one. Note that this is a lot more than the number of hits (109 with the same threshold) for a ChIP-seq against *B. abortus* CtrA, another cell cycle transcription factor (Francis *et al.*, 2017). This discrepancy suggests that, like in *C. crescentus*, GcrA could be a co-factor of the housekeeping σ^{70} (Haakonsen *et al.*, 2015). Amongst GcrA targets, several genes involved in DNA repair were found (*ogt*, *lexA*, *uvrA* and *mutL*, but also *aidB*) (**Fig 24A**). Compared to the rest of the chromosomes, we found a significantly higher (4.4 and 4.7 fold in chromosomes I and II, respectively) frequency of GANTC sites in the peaks of this ChIP-seq ($p < 0.001$ according to a Poisson distribution).

In order to test if genes involved in DNA repair could be regulated by GcrA, a depletion strain based on an IPTG-inducible promoter was constructed for this transcription factor ($\Delta gcrA$ pBI-*gcrA*). In the absence of IPTG, the $\Delta gcrA$ pBI-*gcrA* strain mainly forms Y-shaped bacteria after the first six hours of growth, suggesting that their division is impaired. TRSE labeling (Brown *et al.*, 2012) suggests that later the bacteria slow down their growth (**Fig 24B**). Importantly, this last observation would need to be confirmed by time-lapse experiments, for example. After 3 h in the absence of IPTG, the bacteria are efficiently depleted from leftover GcrA, as attested by western blot experiments (**Fig 24C**). RT-qPCR was performed on DNA repair genes after culturing *B. abortus* $\Delta gcrA$ pBI-*gcrA* in the presence or absence of IPTG. With this technique, we could confirm that GcrA regulates the expression of *ogt* and *mutL* (**Fig 25A**). The induction of *lexA* is still happening after MMS treatment when the bacteria are depleted in GcrA (**Fig 25B**), which indicates that the activation of the SOS response under exogenous stress is regulated through a GcrA-independent mechanism.

WT and GcrA depletion strains were cultured in liquid medium supplemented or not with IPTG and/or MMS to test if GcrA control is crucial for survival and growth in alkylating conditions. Aliquots were taken at different time points and plated on rich medium agar plates supplemented with IPTG in order to evaluate the surviving population. As seen with TRSE

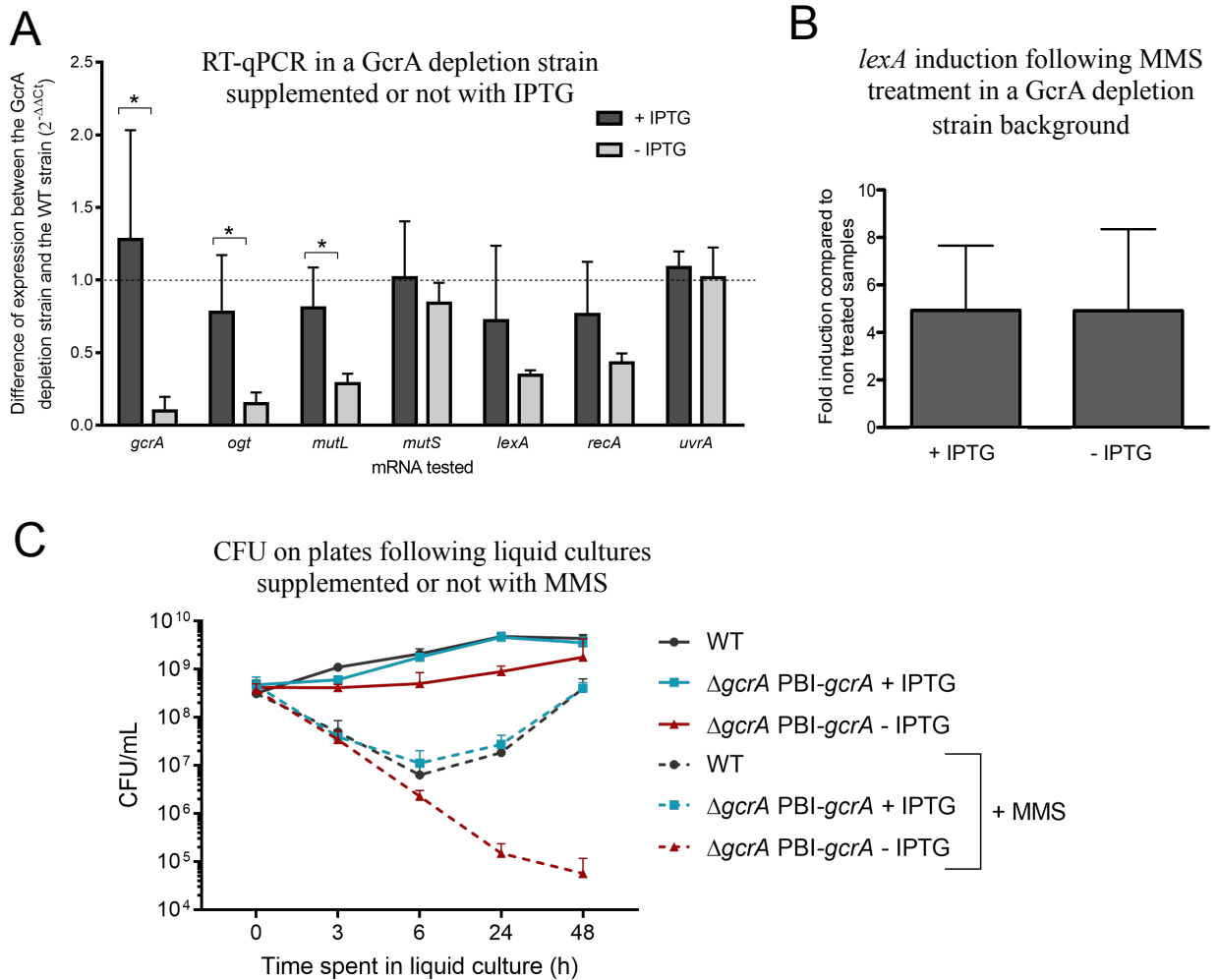


Fig 25. Phenotype of GcrA depletion strain after alkylating stress. **A)** Gene expression in the GcrA depletion strain. The mRNA levels of several genes coding for DNA repair proteins were calculated through RT-qPCR experiments for the GcrA depletion strain. As predicted by ChIP-seq experiment, *ogt* and *mutL* expression are both affected by the absence of GcrA (- IPTG). The expression of the other genes was not statistically different (Student's t test) between the two conditions (+/- IPTG) (n = 3). **B)** RT-qPCR data of *lexA* gene expression in a GcrA depletion background in presence (+) or absence (-) of IPTG, after 2.5 mM MMS exposure for 5 h, compared to non exposed bacteria. Experiments were repeated three times. Error bars represent standard deviation from the mean. Student's t test was performed with $p > 0.05$ (NS). **C)** Survival of GcrA depletion strain in presence of *in vitro* alkylating stress. Bacteria were cultured in liquid medium supplemented or not with IPTG and in the presence or absence of 5 mM of MMS. Samples were taken after 0, 3, 6, 24 and 48 h of culture and plated on rich medium supplemented with IPTG. Colony forming units were counted to evaluate survival. Error bars represent standard deviation (n = 3).

Infection in RAW 264.7 macrophages

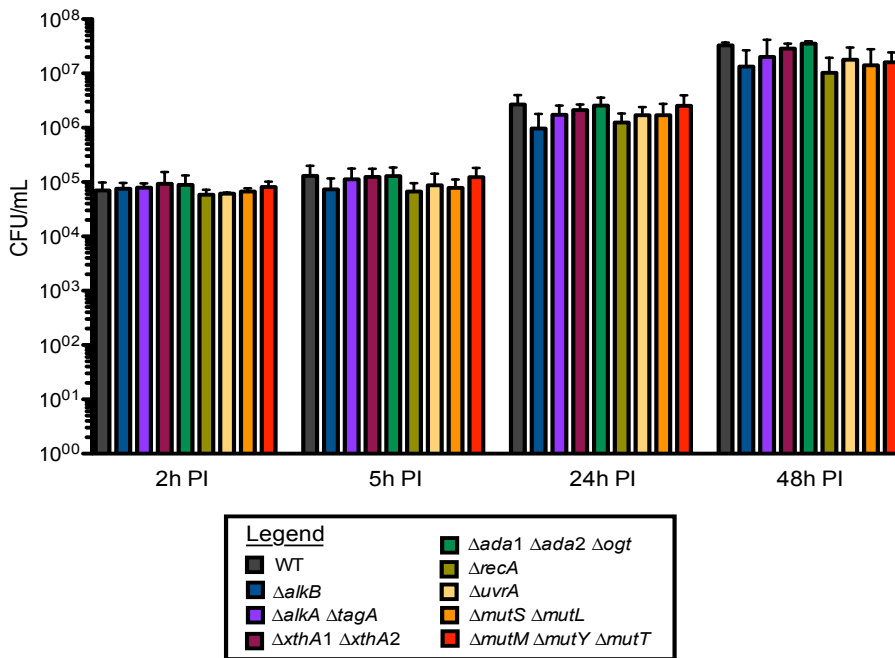


Fig 26. Infection of RAW 264.7 macrophages with deletion strain. Colony forming units were counted after 2, 5, 24 and 48 h post infection. Error bars represent standard deviations (n = 3). A Scheffe statistical analysis reveals that, in this model, none of the tested strains were attenuated in infection ($p > 0.05$, NS).

Infection in RAW 264.7 macrophages

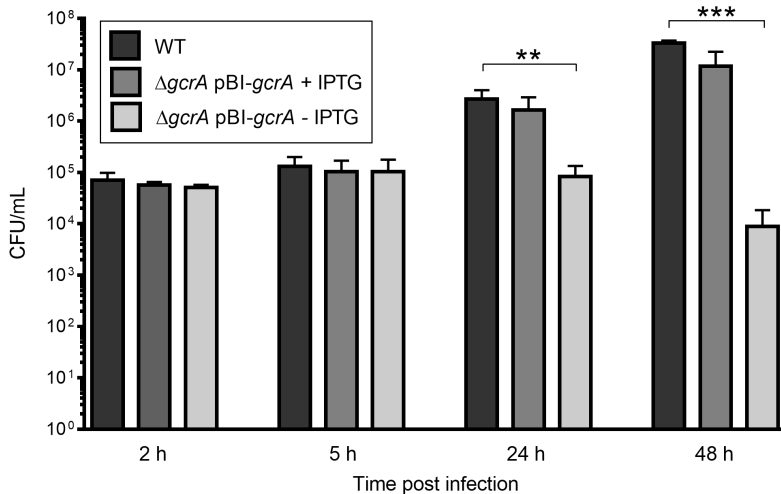


Fig 27. Infection of RAW 264.7 macrophages with the GcrA depletion strain. Colony forming units were counted after 2, 5, 24 and 48 h post infection for the WT and the GcrA depletion strains incubated with or without IPTG (+ IPTG or - IPTG, respectively). Error bars represent standard deviations (n = 3). A Scheffe statistical analysis reveals that, in the absence of IPTG, the GcrA depletion strain is attenuated at 24 ($p < 0.01$) and 48 h ($p < 0.001$) post infection in this cell type.

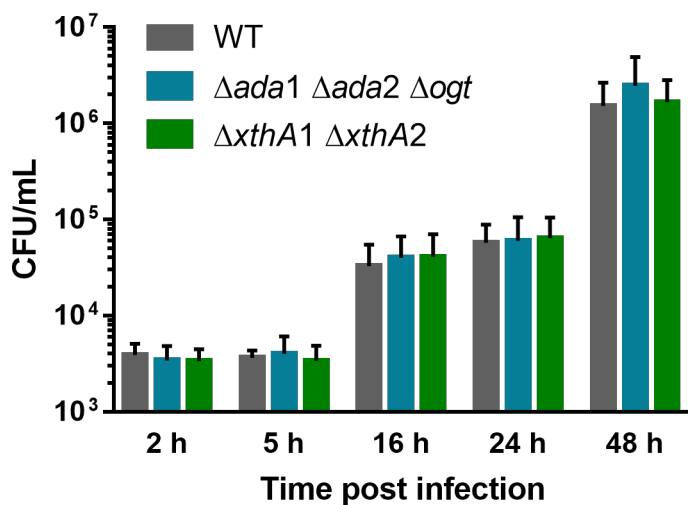


Fig 28. Infection in HeLa cells. This experiment has been performed in biological triplicates. Error bars represent standard deviation from the means.

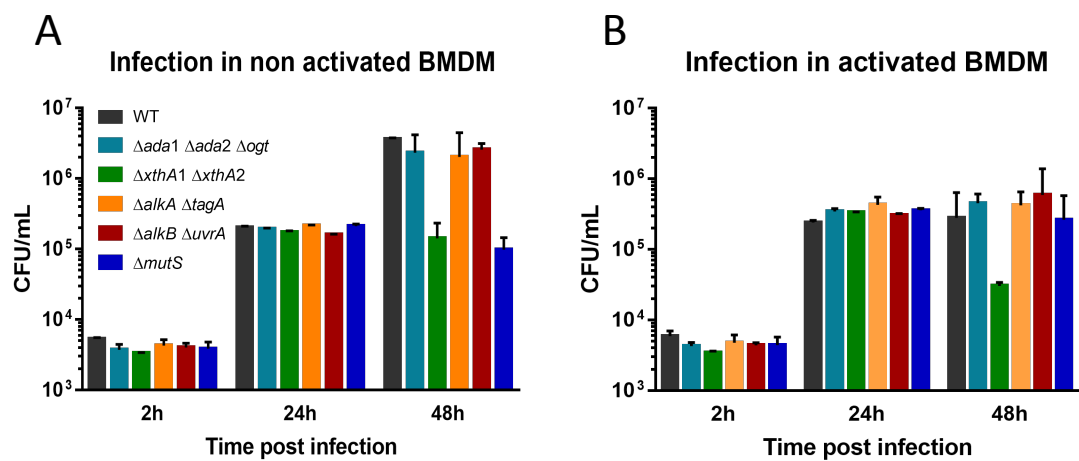


Fig 29. Infection of **A)** non activated and **B)** activated bone marrow derived macrophages (BMDM) with DNA repair deletion strains. Importantly, this experiment has only been done twice, so statistical analysis has not been performed.

labeling (**Fig 24B**), the $\Delta gcrA$ pBI-*gcrA* strain that was cultured without IPTG is not multiplying but it survives (at least up to two days) since bacteria recovered once plated on medium supplemented with IPTG (**Fig 25C**). When bacteria were cultured in the presence of MMS, the WT and GcrA depletion strains first underwent a massive drop of CFU, independently of the presence or absence of IPTG. Then, both the WT and the $\Delta gcrA$ pBI-*gcrA*, if supplemented with IPTG, were able to overcome the stress and started recovering with time, as attested by the raise in CFU (**Fig 25C**). When *B. abortus* was depleted in GcrA, bacteria were unable to recover from the stress and kept on dying (**Fig 25C**), indicating that the presence of GcrA is required for *B. abortus* to efficiently cope with high exogenous alkylating stress.

II.3. Individual DNA repair pathways are not essential for *B. abortus* infection

Previous attempts at detecting alkylating stress on other intracellular bacteria, based on deletion mutants for DNA repair pathways, were unsuccessful (Durbach *et al.*, 2003; Alvarez *et al.*, 2010). The deletion strains that were tested for *B. abortus* during RAW 264.7 macrophages infection also failed to show attenuation (**Fig 26**). These strains comprise the alkylation-specific triple mutant $\Delta ada1 \Delta ada2 \Delta ogt$, double mutant $\Delta alkA \Delta tagA$ and single mutant $\Delta alkB$. Similarly, an *aidB* mutant had previously been shown to be unaffected in infection (Dotreppe *et al.*, 2011). Other DNA repair mutants were also tested, such as the BER deficient mutant $\Delta xthA1 \Delta xthA2$, the NER deficient mutant $\Delta uvrA$, the MR deficient mutant $\Delta mutS \Delta mutL$ and the homologous recombination deficient mutant $\Delta recA$. In addition, the triple mutant $\Delta mutM \Delta mutY \Delta mutT$, impaired for oxidative damage (8-oxoguanine) repair and Fapy-7meG repair, was also tested. Amongst them all, none of the mutants were attenuated in infection (**Fig 26**).

According to RT-qPCR data, GcrA is involved in the regulation of at least two DNA repair pathways: direct repair through *ogt* and MR through *mutL* (**Fig 25A**). In RAW 264.7 macrophages, it was observed that the GcrA depletion strain keeps a stable number of CFU until 24 h PI, before to drop at 48 h PI (**Fig 27**). This indicates that GcrA is required for long-term survival in this model of infection. However, it would be hasty to attribute this attenuation to the sole disruption of DNA repair pathways, as GcrA also regulates many other functions.

II.4. Unpublished data

II.4.1. DNA repair deletion strains in other infection models

During RAW 264.7 macrophages infection, no DNA repair deletion strain was attenuated (**Fig 26**). As infection models may be very different between each other (Andreu *et al.*, 2017), we decided to try infection in other conditions. First, we infected HeLa cells with the WT strain, the triple methyltransferase mutant $\Delta ada1 \Delta ada2 \Delta ogt$ and the double AP endonuclease mutant $\Delta xthA1 \Delta xthA2$. It appeared that none of the strains were attenuated during HeLa cells infection (**Fig 28**). Next, we tested infection in non-activated and activated

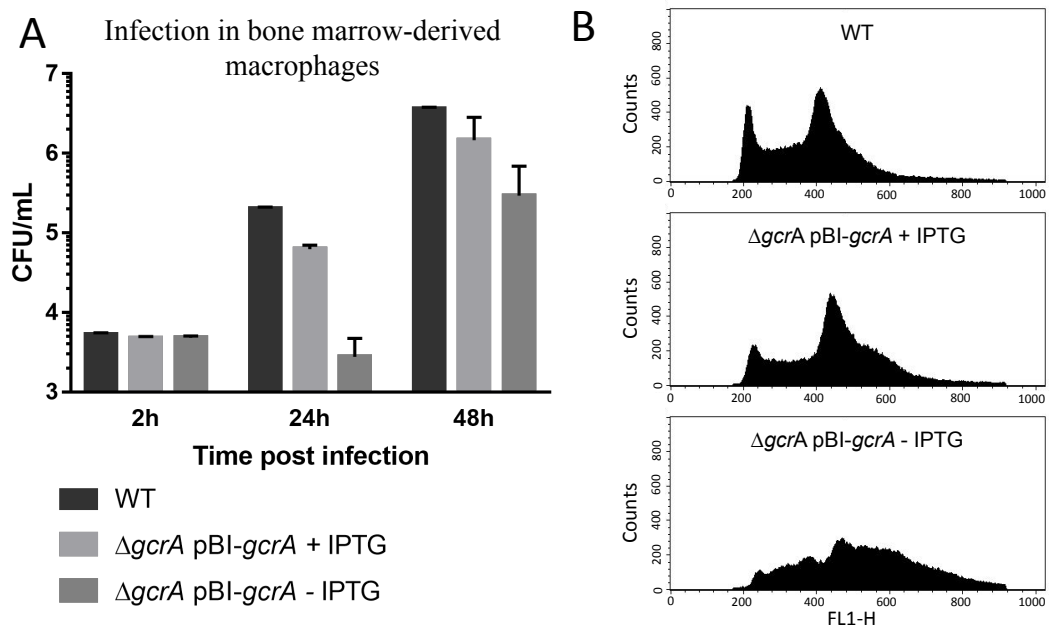


Fig 30. Data about GcrA depletion strain. **A)** Infection of non activated BMDM with GcrA depletion strain. Note that this experiment has been done with the same cells than in **Fig 24**, so WT data are the same between the two figures. **B)** DNA content of *B. abortus* GcrA depletion strain. This experiment represent flow cytometry data obtained after SytoxGreen labeling of bacterial DNA. This experiment has only been done once.

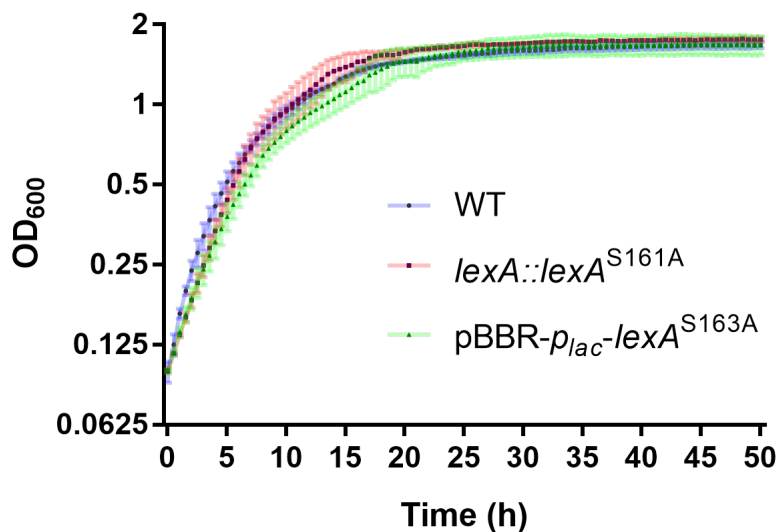


Fig 31. Growth curves of different strains of *B. abortus* in rich medium (TSB). This graph was obtained with exponential phase bacteria, normalized at OD₆₀₀ 0.1 to start the experiments. The OD600 were calculated every 30 minutes with a Bioscreen. This graph represents the mean values of three different experiments. Error bars represent standard deviation from the means.

bone marrow-derived macrophages (BMDM). To activate the cells, we incubated them overnight with 10 ng/mL of LPS and 20 ng/mL of IFN γ . They were then infected with bacteria. Importantly, this experiment has only been done twice, so a statistical analysis has not been performed and data should be considered with caution. Apparently, no attenuation was observable at 24 h PI, but some strains seemed attenuated at 48 h PI. In non-activated BMDM, it was the case of the $\Delta xthA1 \Delta xthA2$ BER deficient mutant and of the $\Delta mutS$ mismatch repair deficient mutant (**Fig 29A**). In activated BMDM, all strains, including the WT one, had a low CFU count at 48 h post infection compared to the non-activated condition (**Fig 29B**). This suggests that the host cells are better at controlling bacterial growth between 24 and 48h of infection when they are activated. In activated macrophages, the $\Delta xthA1 \Delta xthA2$ strain was the only one that was clearly attenuated compared to the WT strain. Indeed, in this context, the $\Delta mutS$ strain looked no worse than the WT strain (**Fig 29B**). Importantly, none of the alkylation-specific mutants were attenuated.

II.4.2. GcrA depletion strain is also attenuated in BMDM... but recovers

BMDM were also infected with GcrA depletion strain. Again, this experiment has only been done twice, so a statistical analysis has not been performed and data should be considered with caution (**Fig 30A**). At 24 h PI, the GcrA depletion strain (without IPTG) is clearly not growing, but at 48 h PI, it is surprising to see that it seems to recover (**Fig 30A**). This recovery is very striking and could mean that the intracellular environment of the rBCV is different between RAW 264.7 macrophages and BMDM. On that note, it has been shown that GcrA is dispensable in *C. crescentus* when bacteria are grown in minimal medium or starved in phosphate (Murray *et al.*, 2013; Haakonsen *et al.*, 2015). Alternatively, it is possible that suppressor mutants appeared during the infection. One way to know if it is the case would be to repeat the experiment, then to plate bacteria on medium with and without IPTG. If suppressors appeared, bacteria should be able to grow without IPTG.

II.4.3. GcrA depletion strain is impaired for normal DNA content

In *C. crescentus*, GcrA is involved in cell cycle regulation (Fioravanti *et al.*, 2013). The cell growth defect phenotype of *B. abortus* GcrA depletion strain also suggests that it is the case in *B. abortus* (**Fig 30B**). In *C. crescentus*, a GcrA depletion strain is elongated and has extra chromosomes because the rate of cell division is too slow compared to the rate of DNA replication (Haakonsen *et al.*, 2015). Here, we found that *B. abortus* GcrA depletion strain also accumulates extra copies of chromosomes, as shown with flow cytometry experiment (**Fig 30B**). Note that in *C. crescentus*, the GcrA depletion strain is still able to grow, as it makes filamentous bacteria (Murray *et al.*, 2013; Haakonsen *et al.*, 2015). At the opposite, in *B. abortus*, the growth appears to be impaired after 24 hours (**Fig 24B**), contrarily to the elongated and branched phenotype that could be observed with *B. abortus* CtrA depletion strain (Francis *et al.*, 2017).

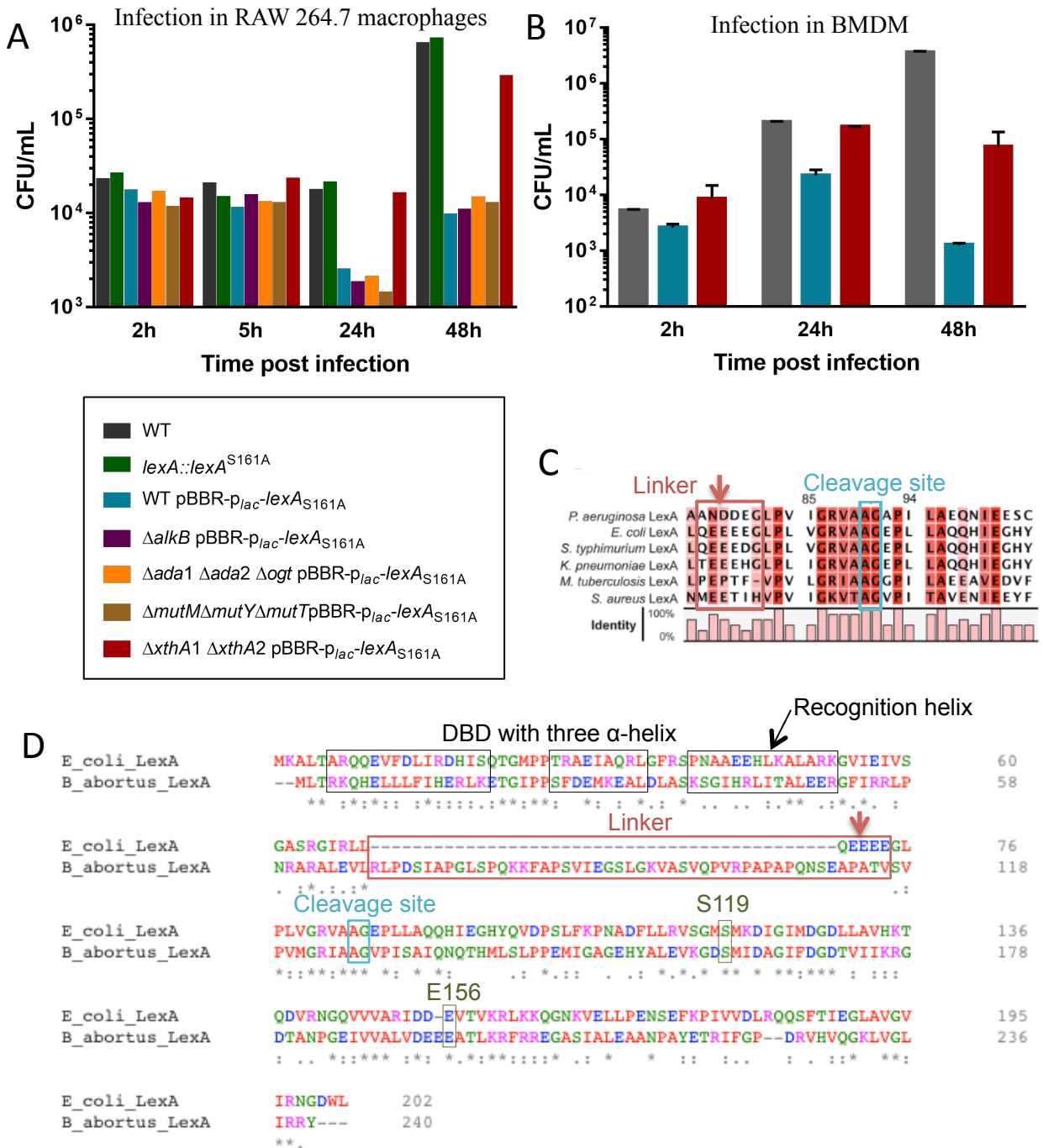


Fig 32. Data about *B. abortus* SOS system. Infection with SOS deficient strains in **A**) activated RAW 264.7 macrophages and **B**) bone marrow derived macrophages (BMDM). Cells were infected with *B. abortus* strains producing a mutated version of the SOS repressor *lexA* (*LexA^{S161A}*). This mutation is supposed to confer LexA a higher stability. The mutation was introduced either in the genomic DNA (*lexA::lexA_{S161A}*) or on a medium copy plasmid (pBBR-*p_{lac}-lexA_{S161A}*) in different genetic backgrounds. Importantly, the experiment has only been done once in activated RAW 264.7 macrophages and twice in BMDM, so statistical analyses have not been performed. **C**) Partial alignment of LexA amino acid sequences from different bacteria (from Mo *et al.*, 2014). **D**) Alignment of *B. abortus* and *E. coli* LexA performed with Clustal Omega. Important sequences are highlighted based on *E. coli* data.

II.4.4. The SOS system could be required for intracellular survival

In the study of Uphoff *et al.* (2018), it was shown that, in *E. coli*, the SOS system is required very early following alkylating stress. Our data also showed that *B. abortus* is overexpressing the SOS mediator *lexA* after MMS treatment (**Fig 23**). In *E. coli*, the S119 amino acid position has been reported to be a catalytic residue of LexA that is required for its self-cleavage (Slilaty & Little, 1987). Its mutation into an alanine (S119A) is known to make LexA non-cleavable while still making it able to interact with RecA* and without destabilizing its structure (Slilaty & Little, 1987). As for *B. abortus*, it is proposed to have a constitutive SOS response, with only a slight induction possible after DNA damage (Roux *et al.*, 2006) (**introduction section II.3.5**). This mutation in *B. abortus lexA* should thus render the bacteria unable to start a SOS response, as LexA would be unresponsive to the natural RecA* activity. We therefore changed this residue in *B. abortus lexA* gene (BAB1_1167) at the genomic level (*lexA::lexA_{S161A}*) or on a medium copy plasmid (pBBR-*p_{lac}-lexA_{S161A}*) in different genetic backgrounds. The growth of both strains was tested *in vitro* in rich medium to ensure that the mutation in *lexA* and its overexpression was not toxic to *B. abortus* (**Fig 31**). The two strains were then used for infecting activated RAW 264.7 macrophages and non-activated BMDM (**Fig 32A, B**). Note that these experiments have not been done three times (see legend) so data should be considered with caution. In both models of infection, the WT strain carrying the pBBR-*p_{lac}-lexA_{S161A}* plasmid (in blue) was clearly attenuated at 24 and 48 h PI. This attenuation was unexpectedly less stringent in the $\Delta xthA1 \Delta xthA2$ background (in red). In activated RAW 264.7 macrophages, the pBBR-*p_{lac}-lexA_{S161A}* plasmid was also tested in other genetic backgrounds: the alkylation-specific $\Delta alkB$ and $\Delta ada1 \Delta ada2 \Delta ogt$ mutants, as well as the $\Delta mutM \Delta mutY \Delta mutT$ mutant, impaired for oxidative damage repair. These strains did not look worse than in the WT background (**Fig 32A**). It is possible that the inability of *B. abortus* to perform a normal SOS response is already so deleterious that the absence of genes coding for specific DNA repair systems is inconsequential. Alternatively, it could be a sign that alkylating and oxidative stresses are not very high in these host cells. Note that the phenotype of attenuation was only observable with *lexA* overexpressing strains. Indeed, the strain for which the genomic *lexA* has been replaced by its mutated version (*lexA::lexA_{S161A}*) was not attenuated in activated RAW 264.7 macrophages infection (in green in **Fig 32A**).

A closer look at LexA amino acids sequences revealed that there are a few important differences between the canonical *E. coli* LexA and *B. abortus* LexA. Mainly, the linker region is much longer in *B. abortus* protein than it is in *E. coli* (red box in **Fig 32D**). The short linker of *E. coli* is known to be sufficient for the protein to make a 180° reorientation between the bound and the unbound form (Mo *et al.*, 2014), but a longer linker could have an impact on the kinetics of this reaction. Importantly, *E. coli* linker sequence seems to be partially conserved in other bacteria, especially for the central EE amino acids, but it is not the case in *B. abortus* (red arrow in **Fig 32C, D**). Another difference between *E. coli* LexA and *B. abortus* LexA is the non-conservation in the sequence of the third α -helix of the DNA binding domain (black boxes in **Fig 32D**). This sequence is known to be involved in the recognition of

ORF	seqID	Function	Start	End	score	strand
-	BAB_RS16000	branched chain amino acid ABC transporter substrate-binding protein	-74	-58	0.94	-
BAB1_0015	BAB_RS31930	hypothetical protein	-165	-149	0.94	+
BAB1_0068	BAB_RS16250	imuAB-dnaE2 (operon) (≈UmuDC)	-34	-18	0.94	-
BAB1_0271	BAB_RS32100	abortive infection protein	-372	-356	0.94	+
BAB1_0273	BAB_RS17215	transcriptional regulator	-399	-383	0.94	+
BAB1_0276	BAB_RS17230	hypothetical protein	-293	-277	0.94	-
BAB1_0416	BAB_RS17915	DUF85:Elongator protein 3/MiaB/NifB:Radical SAM	-86	-70	1.00	+
BAB1_0276	BAB_RS17920	hypothetical protein	-66	-50	1.00	-
-	BAB_RS32235	hypothetical protein	-130	-114	0.94	-
BAB1_0488	BAB_RS18245	hypothetical protein (YicC-like)	-257	-241	0.94	-
BAB1_0524	BAB_RS18415	glyoxalase	-31	-15	0.94	-
BAB1_0525	BAB_RS18420	pyruvate, phosphate dikinase PpdK	-249	-233	0.94	+
BAB1_0738	BAB_RS19450	lactate permease LldP	-292	-276	0.94	+
BAB1_2195	BAB_RS19455	tRNA-Pro	-23	-7	0.94	-
BAB1_0739	BAB_RS19460	ETC complex I subunit region	-258	-242	0.94	-
BAB1_0845	BAB_RS19960	DNA polymerase III subunit alpha (dnaE)	-399	-383	0.94	-
BAB1_0853	BAB_RS20000	inositol monophosphatase	-400	-384	0.94	+
BAB1_0905	BAB_RS20250	5'-nucleotidase SurE	-94	-78	0.94	-
BAB1_1126	BAB_RS21320	single-stranded DNA-binding protein SSB	-203	-187	0.94	-
BAB1_1127	BAB_RS32630	hypothetical protein	-381	-365	0.94	+
BAB1_1128	BAB_RS21325	excinuclease ABC subunit A UvrA	-157	-141	1.00	+
BAB1_1167	BAB_RS21510	LexA repressor	-72	-56	1.00	-
BAB1_1224	BAB_RS21770	DNA recombination/repair protein RecA	-139	-123	0.94	-
-	BAB_RS23255	hypothetical protein	-137	-121	0.94	-
BAB1_1856	BAB_RS24745	N-acetyltransferase	-399	-383	0.94	-
BAB1_1967	BAB_RS25305	universal stress protein	-253	-237	0.94	+
-	BAB_RS33035	hypothetical protein	-64	-48	0.94	-
BAB1_2186	BAB_RS26350	30S ribosomal protein S20, polyamine inhibitor	-346	-330	0.94	-
BAB2_0045	BAB_RS26590	lysophospholipase PldB	-38	-22	0.94	-
BAB2_0282	BAB_RS27710	ABC transporter permease	-201	-185	0.94	+
BAB2_0283	BAB_RS27715	LysR family transcriptional regulator	-80	-64	0.94	-
BAB2_0625	BAB_RS29305	DNA polymerase IV (dinB)	-36	-20	0.94	+
BAB2_0632	BAB_RS29335	MFS transporter (nitrite antiporter)	-93	-77	0.94	+
BAB2_0659	BAB_RS29470	DNA helicase RecG	-72	-56	1.00	-
BAB2_0660	BAB_RS29475	succinate dehydrogenase assembly factor 2 family protein	-95	-79	1.00	+
BAB2_0661	BAB_RS29480	transcription-repair coupling factor Mfd	-393	-377	1.00	+
BAB2_0997	BAB_RS31030	peptide deformylase	-68	-52	0.94	-
BAB2_0998	BAB_RS31035	DNA recombination-limiting protein RmuC	-51	-35	0.94	+

Fig 33. Proposed *B. abortus* LexA regulon. These hits were obtained by looking for a TGTTTC-N6-TGTTCT motif in *B. abortus* genome, with one substitution allowed, using RSATool (Van Helden, 2003). Targets that have been proposed to be part of the core regulon of LexA in α -proteobacteria (Erill *et al.*, 2004) are highlighted.

the SOS-boxes on target DNA (Mo *et al.*, 2014). In the α -proteobacterium *C. crescentus*, a TG TTC-N₆-TG TTC motif, which is different from the one of *E. coli*, as been determined for SOS-boxes (da Rocha *et al.*, 2008). We noticed that the predicted recognition domains of *B. abortus* LexA and *C. crescentus* LexA have 100% of identity (data not shown), suggesting that *B. abortus* LexA recognizes the same DNA sequence than *C. crescentus* LexA, as previously suggested (Erill *et al.*, 2004). This allowed us to propose a LexA regulon for *B. abortus*, using the online software RSAT (van Helden, 2003) (**Fig 33**). Fortunately, several hits were expected and seem to confirm that *B. abortus* and *C. crescentus* do share the same consensus sequence for SOS-boxes. Amongst those hits, there were the promoters of *lexA* itself, *recA*, *dnaE* (coding for DNA polymerase III subunit α), *dinB* (coding for DNA polymerase IV) and the operon *imuA-imuB-dnaE2/imuC* (coding for proteins of similar function than the DNA polymerase V, absent in *B. abortus* and *C. crescentus*). Importantly, da Rocha *et al.* (2008) proposed to look for a less stringent consensus sequence for SOS-boxes, *i.e.* GTTC-N₇-GTTC. Using this sequence with one substitution allowed, many other potential targets emerged. We found for example *sodA*, *sodC*, *clpX*, *uvrC*, *uvrD*, *ruvC*, *parE*, *xthA2*, *alkA* and *ada2*, leading to the finding of the complete proposed core regulon of α -proteobacteria (Erill *et al.*, 2004). Nevertheless, these hits should be taken with caution, as many of them are probably false positives.

Conversely, we also wondered if the particularity of *B. abortus* RecA to be constitutively in a RecA* state (Roux *et al.*, 2006) could be a shared characteristic with other α -proteobacteria. In *E. coli*, a M164Q mutation in RecA seems to be make it naturally better at launching the auto-cleavage of LexA without affecting its function in homologous recombination (Henry *et al.*, In preparation). This is very reminiscent of the phenotype of *B. abortus* RecA. We were thus positively surprised to see that *B. abortus* and other Rhizobiales (*Sinorhizobium* and *Agrobacterium* at least), as well as *C. crescentus*, bore a proline mutation at this particular position (black box in **Fig 34**), which could indicate that they also possess a constitutive SOS response. This is of course hypothetical and needs experimental evidences to be proven, but it seems worth mentioning.

II.4.5. We could not determine if CtrA was involved in DNA repair after alkylating stress

Considering that we had a CtrA depletion strain in the lab (Francis *et al.*, 2017), we figured we could try to do the same experiments with this strain than with the GcrA depletion strain. We thus performed RT-qPCR on liquid cultures supplemented or not with IPTG in order to determine if the absence of CtrA would have an impact on gene expression. Indeed, based on our previously published ChIP-seq experiment, we could predict that the expression of *tagA*, *mutM* and *uvrC* should be affected by the absence of CtrA (Francis *et al.*, 2017). However, we never managed to properly set up RT-qPCR experiments with this strain, as the level of *ctrA* mRNA was very high even in the absence of IPTG (**Fig 35**). Note that the team of *E. Biondi* apparently as the same problem with *S. meliloti* CtrA (personal communication).

Fig 35. Gene expression in the CtrA depletion strain. The mRNA levels of several genes coding for DNA repair proteins were calculated through RT-qPCR experiments for the CtrA depletion strain, in presence or absence of IPTG. Note that this experiment has been performed once, so there is no statistical analysis.

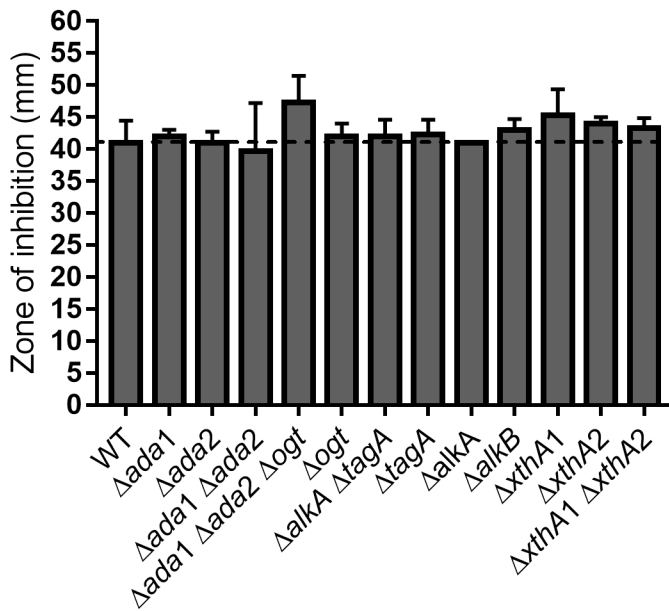
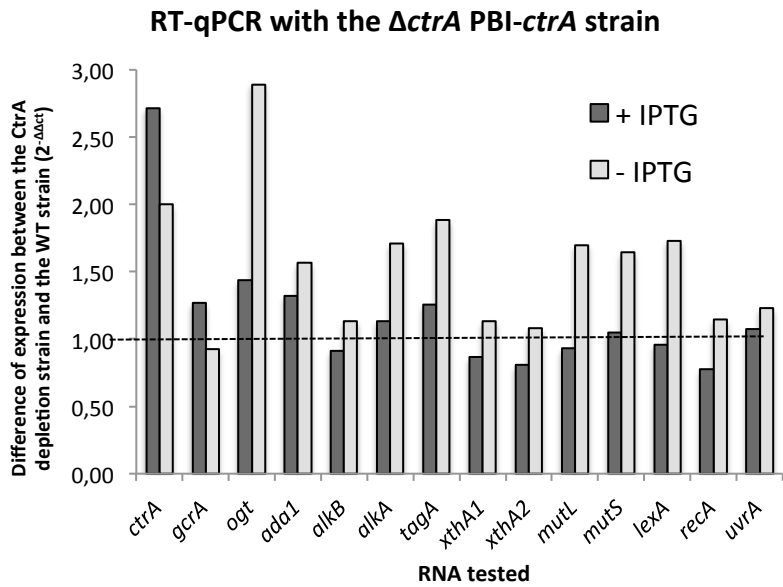


Fig 36. Disk assay with H₂O₂. Bacteria were plated on 2YT rich medium and a disk wetted with 30 % H₂O₂ was placed in the center of each petri dish. Diameters of inhibition were measured after 3 days of incubation at 37°C. Experiments were repeated three times. A Scheffe statistical analysis was performed with p > 0.05 (NS).

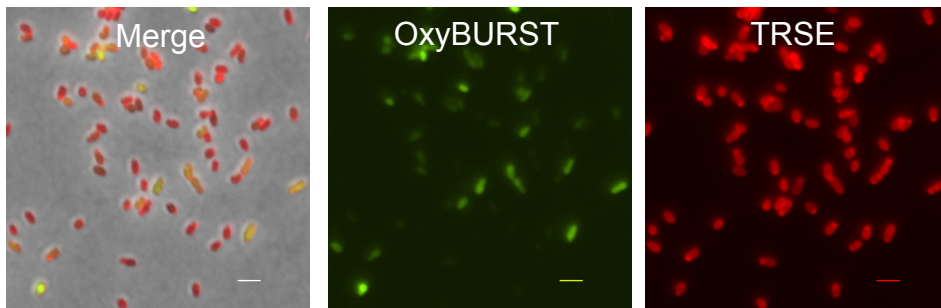


Fig 37. OxyBURST and TRSE labeling of *B. abortus* in liquid culture after H₂O₂ challenge. It is obvious that the signal emitted by OxyBURST is not homogenous, which suggest that oxidative stress is not felt homogenously by the bacterial population. Scale bars represent 2 μ m.

We also investigated the survival potential of the CtrA depletion strain in liquid culture supplemented with MMS by performing the survival assay. However, we were confronted with another problem. Actually, the CtrA depletion strain is unable to survive for long periods in liquid cultures, even in the absence of alkylating agents (data not shown). Therefore, it was impossible to tell if the growth defect that we observed with the addition of MMS was caused by a deregulation of DNA repair pathways or by the accumulation of lethal factors.

II.4.6. Genes coding for alkylated DNA repair are not required against H₂O₂

One could wonder how specific the genes that code for proteins involved in alkylated DNA repair are. To investigate this question, the survival of several deletion strains was tested against oxidative stress. More precisely, disk assays were performed on deletion strains plated on 2YT-agar. Whatman paper disks were humidified with 30% H₂O₂ and placed in the center of each plate. Zones of growth inhibition were measured after 3 days and revealed that there were no statistical differences between the growths of the different strains tested (**Fig 36**). One surprise was that the double mutant $\Delta xthA1 \Delta xthA2$, impaired for BER, was also not worse than the WT strain. Considering that the specificity of the BER pathway comes from its DNA glycosylases (e.g. *mutM*, *mutY*, *alkA*), the suppression of the AP endonucleases (XthA enzymes) should result in the complete deficiency in BER and in an accumulation of AP sites. Thus, it was expected that this strain would have a greater zone of inhibition than the other strains. Considering that it was not the case, it is possible that H₂O₂ did not significantly damage *B. abortus* DNA, as superoxide dismutase and catalase activities are known to be very efficient in *B. abortus* (Steele *et al.*, 2010). It would thus be very interesting to do this experiment again with another oxidative agent.

II.4.7. Set up of a probe to detect oxidative stress on *B. abortus*

The lack of phenotype of the triple mutant $\Delta mutM \Delta mutY \Delta mutT$ in infection (**Fig**), led us to question the occurrence of oxidative stress on *B. abortus* in our model of infection. Since the use of a N-nitrosation sensitive probe was conclusive, we decided to set up a probe that could similarly be attached at the bacterial surface and that would report the oxidative status of the eBCV. Luckily, such a probe was already available on the market, but had never been used for this purpose at the single cell level. We thus performed a series a set up experiments with the OxyBURST reagent (D2935 H₂DCFDA-SE, Thermo Fisher Scientific), which does not emit green fluorescence except when it is oxidized. The pictures presented in **Fig 37** were taken after labeling the bacteria with the OxyBURST and TRSE probes for one hour, then activating the OxyBURST probe with 1.5 M hydroxylamine (pH 8.5) for one hour and finally challenging the bacteria in 2YT rich medium supplemented with 0.6% H₂O₂ after 15 and 30 minutes. Interestingly, the FITC signal obtained by the OxyBURST-labeled bacteria was not homogenous (**Fig 37**), and a positive signal was also observable with a few non-stressed bacteria (data not shown). Importantly, LB medium is known to chemically generate H₂O₂ (Seaver & Imlay, 2001) and it should be no different in 2YT medium as it is the equivalent of LB medium, but with double amount of yeast extract. This could thus be the reason why non-stressed labeled bacteria also emit fluorescence. As for the heterogeneous

signal given by bacteria after H_2O_2 treatment, it is possible that it comes from a difference in the availability and amount of bacterial ROS scavengers between bacteria. It is also possible that the probe did not label the bacterial population evenly but that seems less likely as TRSE labeling (**Fig 37**) was efficient for all bacteria.

Material and methods

I. Bacterial strains and media

I.1. Growth conditions

E. coli strains DH10B and S17-1, as well as *S. enterica* serovar Typhimurium were grown in Luria-Bertani (LB) medium at 37°C. *B. abortus* 544 Nal^R strain and its derivatives were grown in either 2YT rich medium (1% yeast extract, 1.6% peptone, 0.5% NaCl) or TSB rich medium (3% Bacto tryptic soy broth) at 37°C. Antibiotics were used at the following concentrations: ampicillin, 100 µg/ml; kanamycin, 10 µg/ml with integrative plasmids or 50 µg/ml with replicative plasmids; chloramphenicol, 20 µg/ml; nalidixic acid, 25 µg/ml; rifampicin, 20 µg/ml; gentamicin, 10 or 50 µg/ml as indicated. When required, isopropyl β-D-1-thiogalactopyranoside (IPTG) was used at a concentration of 1 mM in bacterial culture and at 10 mM in the culture medium during cellular infections.

Note that the doses of alkylating agents are specified below for each experiment when they were required. The choice of those doses was based on early experiments on 2YT medium. At that time, we noticed that doses of 2 mM of MMS or below did not lead to a drop of CFU in the WT strain, nor did they lead to a change in the percentage of G1-phase bacteria in the population (data not shown). We thus decided to work mainly with 2.5-5 mM of MMS. The dose for MNNG was attributed with similar criteria.

I.2. Deletion, depletion and overexpression strains construction

B. abortus deletion strains were constructed by allelic exchange, via pNPTS138 vectors (M. R. K. Alley, Imperial College of Science, London, UK) carrying a kanamycin resistance cassette and a sucrose sensitivity cassette, as previously described (Deghelt *et al.*, 2014). Note that in the case of the $\Delta xthA2$ strain, 204 nucleic acids were kept on each side of the gene, as there was a previous report that the full deletion of the gene was not feasible (Hornback & Roop, 2006).

B. abortus GcrA depletion strain was constructed similarly than CtrA depletion strain (Francis *et al.*, 2017). Briefly, the *p_{lacI}-lacI-p_{lac}* sequence was amplified from the pSRK-Kan plasmid (Khan *et al.*, 2008) using Phusion High-Fidelity DNA Polymerase (New England BioLabs). The PCR product was then cloned into a pBBR-MCS1 plasmid using *SacI* and *BamHI* restriction enzymes. This modified pBBR-MCS1 is referred to as pBI. The *gcrA* coding sequence was amplified from *B. abortus* 544 genome with Phusion High-Fidelity DNA Polymerase (New England BioLabs) and then cloned into pBI using *BamHI* and *KpnI* enzymes in order to orient the insert opposite to the *p_{lac}* promoter already present in pBBR-MCS1. This final plasmid (pBI-*gcrA*) was transferred to *B. abortus* by mating, after inserting

the deletion plasmid (pNPTS138- $\Delta gcrA$), then *gcrA* was removed from the chromosome of *B. abortus* as previously described (Deghelt *et al.*, 2014).

B. abortus *lexA::lexA_{S161A}* was constructed by allelic exchange, similarly to deletion strains, using a pNPTS138 plasmid. The sequence of *lexA_{S161A}* was ordered as a GBlocks gene fragment (Integrated DNA Technologies), with NheI and ApaI sequences (in capital letters) following the start codon and BamHI sequence (in capital letters) downstream of the gene:

```
atGCTAGCGGGCCCatgttgaccgtaagcagcagagcttctgctgttcattcatgaacgtcttaaagaacgggc
attcctcctcttttgacgagatgaaggaagctctggaccttgcgtccaaatcaggtattcaccgcctcatcacggcgctggaagaacgt
ggcttcattcgcaggctgccaaccgggcgcgcgactcgaagtgtccgctgccggattcgatcgtcccggctcagcccgcag
aagaaatcgacaccagtgaattgaaggaagcctcggaaaagtagcttccgttcagcccgtgcgcctgccccggctccacaaaaca
gcgaggcgccagccactgtctctgtgccggtatggggcgtattgctgccggtgtgccgatctctgccatccagaaccagaccat
gctgagcctgccaccggaaatgatcggcgcgggcgaacattatgcgctggaagtcaaaggcgcgatgcatgatcgcgggaat
cgacggcgatacggatcatcaaacgcgcgatacggccaatccgggagaaattgctgtggcactggtggatgaagaggaagcaa
ccttgaagcgttccgccgagggcgcttccatcgcactggaagcagccaatccggcctatgaaaccggatttccggcctgatcg
ggtgcatgttcagggaagcttggggcttgatccgccgtattgaGGATCCat
```

This GBlock was ligated into a linearized pGEMT plasmid (EcoRV), then amplified before to be extracted with NheI and BamHI enzymes, and finally ligated in a PNPTS (for allelic replacement) or in a pBBRMCS1 (for the overexpression strain).

Primers, plasmids and ORF of studied genes are listed in the table below.

Gene	Corresponding ORF
<i>ogt</i>	BAB1_0185
<i>ada1</i>	BAB1_0398
<i>ada2</i>	BAB2_0347
<i>xthA1</i>	BAB1_0892
<i>xthA2</i>	BAB1_2004
<i>tagA</i>	BAB2_0179
<i>alkA</i>	BAB1_1661
<i>alkB</i>	BAB2_0704
<i>mutS</i>	BAB1_0146
<i>mutL</i>	BAB2_0212
<i>mutM</i>	BAB1_2184
<i>mutY</i>	BAB1_0518
<i>mutT</i>	BAB1_1940
<i>recA</i>	BAB1_1224
<i>uvrA</i>	BAB1_1128
<i>lexA</i>	BAB1_1167
<i>narG</i>	BAB2_0904
<i>moaA</i>	BAB1_0973
<i>gcrA</i>	BAB1_0329
<i>ctrA</i>	BAB1_1614
<i>virB</i>	BAB2_0068-BAB2_0058

Primer	Sequence
F1-ada1	ggacaggtttcggaagaac
R1-ada1	cataaggttcatgtccgtatcc
F2-ada1	atacggacatgaaccttatggcatgatcgggcataagc
R2-ada1	gcagcaattaatatgtgcaagtg
Up-ada1	gcctgtctggcgataatcc
Down-ada1	ccatagccatgcatcggaa
F1-ada2	ctgcagggtctacgacacctacgaaat
R1-ada2	cggagcggcggttttatccgggttgccgccattcttaaactctg
F2-ada2	aaacccggataaaaacgcc
R2-ada2	gtcgactccagtcttatgacgcggtt
Up-ada2	tgacggggcggtttatttcg
Down-ada2	caccacctctgcatggttc
F1-alkA	cgtttcgttccagaatagc
R1-alkA	actttcaaatccgggttcg
F2-alkA	cgaacccggattgaaagtccgcttctgtagatcccat
R2-alkA	ggaaaagacggcccttattg
Up-alkA	cgcacgatatgggtgatgc
Down-alkA	agggtccagttcgacatc
F1-alkB	agccgtcaacgatgtctc
R1-alkB	gtctttcatcagcccctttt
F2-alkB	aaaaggggctgatgaaagacgcgttctagggcggtct
R2-alkB	gagcagacgaagccttacag
Up-alkB	gccggaacatcctacac
Down-alkB	caatccaactagggcttgtctg
F1-ogt	atcatcatccgcgctacc
R1-ogt	gattccatgaccgaataatagc
F2-ogt	attattcggctatggaatcgcagacaggctggtaatcagttc
R2-ogt	cttgagcttggcgaggaac
Up-ogt	ttcgcaagatgccgatgc
Down-ogt	cttccactggccgtctg
F1-tagA	ccgagcggattgttgatc
R1-tagA	ccatcgcctcatttccc
F2-tagA	ccgggaaatgagcगतatggttaattgccagccgatg
R2-tagA	gcaagtgcgggaaacatg
Up-tagA	agggttgaaccagataaagc
Down-tagA	ccgcgccttcatcttctg
F1-xthA1	ctgcagatgccgtataaagtcaact
R1-xthA1	ccggttaaaccggaatcgtttccataatgattatgcgct
F2-xthA1	aacgattccgttttaacc
R2-xthA1	gtcgacgtacttttctttcgatct
Up-xthA1	cggcaagcatatccagatagc
Down-xthA1	ccgtcaagatcgggtctcac
F1-xthA2	ctgcagggaagatccgcttcaatta
R1-xthA2	tagattttctggtcgccgcgaccccgatgataaccttc
F2-xthA2	gcggcggaccagaaaatc
R2-xthA2	gtcgacgcccgatgcaggtgtattg
Up-xthA2	tgttcttccccgttttcc

Down-xthA2	ggccgtactattctgattgtg
F1-mutS	agacgagctttgtcgtcttc
R1-mutS	cgttccatgtcacaacc
F2-mutS	aggtttgtgacatggaagcggggaaggcgtgaggttc
R2-mutS	caccgtcgagcttttgtg
Up-mutS	gcggcgatcggtctttactg
Down-mutS	ctattcggcggacgaatatgac
F1-mutL	aaggcaatcttcggcaatcc
R1-mutL	ggattgtcatgcggcgactata
F2-mutL	tagtcgcccatgacaatccgctaataatgcatgtctgccaac
R2-mutL	cgatctatcacgctcagttgc
Up-mutL	cgacaaaataccggacaacc
Down-mutL	ggctgcgattcatcattatgg
F1-mutM	ctgcagttgccattagccttgcgata
R1-mutM	ccggcatccagactttggcaaggcagggtttcttccgtcaaa
F2-mutM	aagtctggatgccggtccaat
R2-mutM	gtcgacgaccgcttcttggccatata
Up-mutM	gccccattgaaggctgatc
Down-mutM	ttcacgccggaggaaac
F1-mutY	ggcggttttgcttaatacg
R1-mutY	tgaaagcgtctggaatagcggggtcataaccagcgcagaag
F2-mutY	gtattccagacgctttcaaa
R2-mutY	gcgctcgaagtttcaaac
Up-mutY	gcgcgatgatcagttttcg
Down-mutY	cggttcaatccatcgattgg
F1-mutT	tgccaggtcttgctattgtc
R1-mutT	ggctgtcaaagcagatcgaccatgcgccgtttcttcac
F2-mutT	gtcgatctgctttgacagcc
R2-mutT	caagatggcgcagcatc
Up-mutT	atattcgcgtggcgcatcag
Down-mutT	ttcaaggaccaggagatgac
F1-recA	gtctcatcggtaactacatgg
R1-recA	catcttacaccatectcttctg
F2-recA	caagaggatgggtgaagatgatgtaaggcgtgttcatg
R2-recA	ctttggaaggccgaattcc
Up-recA	tgatctgtgccacattctg
Down-recA	gaaacgatcaccgtcttcc
F1-narG	gcataactggatcatgtg
R1-narG	gattatctctctcagttttctt
F2-narG	aaaactgagaggatataatctagtcgtcccagggttaag
R2-narG	ccagttgtagtaaatcttctg
Up-narG	gttcggcatgaacgacat
Down-narG	tagcagaagatgcacttctc
F1-moaA	gccaagattccgctctttgc
R1-moaA	attgcgcataaattaagccgttg
F2-moaA	cggcttaatttatgcgcaatggcggatgacgggatttag
R2-moaA	cctcaaatccgatatgctttgc
Up- moaA	acaagatgtccaaggcag

Down-moaA	ctgtaatgccgaagattttctg
F1-gcrA	gaatggccaagcgaattgac
R1-gcrA	ctcgtctgtccagttcattgc
F2-gcrA	gcaatgaactggacagacgagtggaattcaggaagecgtccc
R2-gcrA	gctttctcgacatcatgcaga
Up-gcrA	ttcagggtctcgaccagatg
Down-gcrA	cttcacgaaacgctgcaag
F-gcrA ⁺	ggatccatgaactggacagacgagc
R-gcrA ⁺	ggtacctctcgaattcagcgcgc
Reference	Plasmid name
This study	pNPTS138- Δ ogt
This study	pNPTS138- Δ ada1
This study	pNPTS138- Δ ada2
This study	pNPTS138- Δ xthA1
This study	pNPTS138- Δ xthA2
This study	pNPTS138- Δ tagA
This study	pNPTS138- Δ alkA
This study	pNPTS138- Δ alkB
This study	pNPTS138- Δ mutS
This study	pNPTS138- Δ mutL
This study	pNPTS138- Δ mutM
This study	pNPTS138- Δ mutY
This study	pNPTS138- Δ mutT
This study	pNPTS138- Δ recA
This study	pNPTS138- Δ uvrA
This study	pNPTS138- Δ narG
This study	pNPTS138- Δ moaA
Nijskens <i>et al.</i> , 2008	pJQ200- Δ virB
This study	pNPTS138- Δ gcrA
This study	pBI-gcrA
This study	pNPTS138- <i>lexA::lexA</i> _{S161A}
This study	pBBRMCS1- <i>p_{lac}-lexA</i> _{S161A}
This study	pBBRMCS1- <i>p_{ada}-ada-gfp</i>
This study	pBBRMCS1- <i>p_{ada}-ada^{C38A}-gfp</i>
Francis <i>et al.</i> , 2017	pBBRMCS1- <i>p_{pleC}-gfp_{asv}</i>
Francis <i>et al.</i> , 2017	pBBRMCS1- <i>p_{pleC}mut-gfp_{asv}</i>

I.3. Cloning of the reporter system for alkylating stress

The *p_{ada}-ada*_{*E. coli*} sequence, including the start codon of *alkB*_{*E. coli*}, was amplified from *E. coli* DH10B with Phusion High-Fidelity DNA Polymerase (New England BioLabs) using primers listed below. Note that capital letters represent *SpeI* and *XhoI* restriction sites, respectively.

Primer	Sequence
F-yojL _{<i>E. coli</i>}	aaACTAGTtgagctactgaagttaccgttc
R-serine2-ada _{<i>E. coli</i>}	ccttcgaCTCGAGgctcattacctctctcattttc

A superfolder *gfp* coding sequence, with a *XhoI* sequence after the start codon and a *PstI* sequence after the stop codon (see capital letters), was adapted to fit the codon usage of *B. abortus* 2308 (<http://www.kazusa.or.jp/codon/>) and ordered as gBlocks gene fragment (Integrated DNA Technologies):

```
taatgCTCGAGtcgaagggcgaagaactgttcaccggcgtggtgccgatcctggtggaactggatggcgatgtaatg
gccataagttctccgtgcgcggcgaaggcgaaggcgatgccaccaatggcaagctgacctgaagttcatctgcaccaccggcaag
ctgccggtgccgtggccgacctggtgaccaccctgacctatggcgtgcagtgttctcgcgctatccggatcatatgaagcgccatg
atttctcaagtcggccatgccggaaggctatgtgcaggaacgaccatctcgttcaaggatgatggcacctataagaccgcgccga
agtgaagttcgaaggcgataccctggtgaatcgatcgaactgaaggcgatcgattcaaggaagatggcaatatacctggccataag
ctggaatataattcaattcgataatgtgtatatacaccgccgataagcagaagaatggcatcaaggccaattcaagatccgcataatg
tggagatggctcggcgagctggccgatcattatcagcagaataccccgatggcgatggcccgggtgctgctgccggataatcattat
ctgtcgaccagtcggtgctgtcgaaggatccgaatgaaaagcgcgatcatatggtgctgctggaattcgtgaccgccggcgatca
cccatggcatggatgaactgtataagtgaCTGCAGaaaa
```

Both DNA products were cloned into a pBBR-MCS1 plasmid using *PstI*, *XhoI* and *SpeI* restriction enzymes in a triple ligation to orient the *p_{ada}-ada_{E. coli}-gfp* fusion opposite to the *p_{lac}* promoter of pBBR-MCS1.

II. Synthesis and binding of the probes to bacteria

II.1. N-nitrosation sensitive probe

The probe was designed based on Mio *et al* (2016), with the addition of a succinimidyl ester group in order to allow the binding of the probe on amines at the bacterial surface. The complete synthesis protocol can be found in the **appendix 1**.

One mL of bacteria (DO₆₀₀ 0.5) were centrifuged at 7000 rpm for 2 min and washed twice in phosphate buffered saline (PBS). They were incubated for 1 hour at 37°C with the probe (10 µM) in 1 mL of PBS supplemented with 100 µL of NaHCO₃ 1 M (pH 8.4). Bacteria were then washed three times with PBS and used either for RAW 264.7 infection or for *in vitro* experiments. In the case of *in vitro* experiments, labeled bacteria were left for 1 h on wheel in the dark with 1 M of KNO₂ (Thermo Fisher scientific) and 20 µL of HCl 3 M, before to be washed twice with PBS and fixed with paraformaldehyde (PFA) 2% for 20 min at 37°C.

II.2. Texas Red succinimidyl ester (TRSE)

One mL of bacteria (DO₆₀₀ 0.5) were centrifuged at 7000 rpm for 2 min and washed twice in PBS. Bacteria were resuspended in 1 mL of PBS and incubated with TRSE at a final concentration of 1 µg/mL (Invitrogen) for 15 min at room temperature, as previously described (Francis *et al.*, 2017).

II.3. OxyBURST

OxyBURST reagent (D2935 H₂DCFDA-SE, Thermo Fisher Scientific) was purchased and resuspended in DMSO at a concentration of 1 mg/mL, and then air was removed with a vacuum system. Aliquots of 300 µL were prepared in PCR tubes, sealed with Parafilm (VWR), and stocked at -80°C. Bacteria were washed three times in PBS, then labeled with OxyBURST reagent (D2935 H₂DCFDA-SE, Thermo Fisher Scientific) at a concentration of 1 µg/mL in NaHCO₃ 0.1 M buffer (pH 8.5) for 30 minutes at room temperature. The probe were then activated with 1.5 M hydroxylamine (pH 8.5) for one hour and finally the bacteria were challenged in 2YT rich medium supplemented with 0.6% H₂O₂ after 15 and 30 minutes.

III. Cell cultures and infections

III.1. RAW 264.7 macrophages

RAW 264.7 macrophages (ATCC) were cultured at 37°C in the presence of 5% CO₂ in DMEM (Invitrogen) supplemented with 4.5 g/L glucose, 1.5 g/L NaHCO₃, 4 mM glutamine and 10% fetal bovine serum (Gibco). RAW 264.7 macrophages were seeded in 24-well plates (with coverslips for immunolabeling) at a concentration of 10⁵ cells/mL and left in the incubator overnight. The next morning, late exponential phase cultures of *Brucella* (DO₆₀₀ 06-0.9) were washed twice in PBS in order to remove antibiotics and traces of growth medium, then they were prepared in DMEM at a multiplicity of infection of 50 (*i.e.* 50 bacteria for one eukaryotic cell). During that step, 10 mM of IPTG or 163 µM of ascorbate were added to the culture medium if required. Bacteria and cells were centrifuged at 400 g for 10 min at 4°C and then incubated for 1 h at 37°C with 5% CO₂ atmosphere before to be washed twice with PBS and then incubated in medium supplemented with 50 µg/mL of gentamicin to kill extracellular bacteria. One hour later, the medium was replaced by fresh medium supplemented with 10 µg/mL of gentamicin. Note that when working with activated cells, we first seeded the cells in 24-well plates, then after 7 hours, we changed the medium to incubate the macrophages overnight with DMEM (Invitrogen) supplemented with 10 ng/mL of *E. coli* LPS (Sigma-Aldrich) and 20 ng/mL of IFN γ (R&D system), then started the infection as usual, but with using this modified DMEM medium instead of the classical medium.

III.2. HeLa cells

HeLa cells (from the Centre d'Immunologie de Marseille-Luminy, Marseille, France) were cultivated at 37°C and in a 5% CO₂ atmosphere in DMEM (Invitrogen) supplemented with 0.1 g/L of non-essential amino acids, 0.1 g/L of sodium pyruvate (Invitrogen) and with 10% fetal bovine serum (Gibco). Infection with HeLa cells were carried out as with RAW 264.7 macrophages, but with a few differences: cells were plated in 24-well plates with a concentration of 6 x 10⁴ cells/mL; *B. abortus* cultures were diluted to reach a MOI of 300; and cells were left in 50 µg/mL of gentamicin until the end of the experiment.

III.3. Bone marrow-derived macrophages (BMDM)

Bone marrow-derived macrophages (BMDM) were prepared as previously described (Pireaux *et al.*, 2016). Briefly, they were obtained from femurs and tibia of 6 to 8 week old C57BL/6 mice, which were euthanized by cervical dislocation. Cells were incubated in cell culture Petri dishes (Greiner Bioscience) for 7 days with DMEM (Gibco) supplemented with 10% heat-inactivated low-endotoxin serum (Sigma-Aldrich) and 10% of L929 conditioned medium. This conditioned medium was obtained by recovering the supernatant of murine L-929 fibroblasts (ATCC) cultured for 6 days in DMEM supplemented with low-endotoxin serum (Sigma-Aldrich). The 3 first days only, the BMDM culture medium also contained 1% of penicillin/streptomycin (Life Technologies). On the 7th day, BMDM were seeded in 24-well plates and the infection was carried as for RAW 264.7 macrophages.

IV. Immunolabeling of infected cells

Cells were washed twice in PBS before to be fixed for 20 min in 2% PFA pH 7.4 at 37°C. They were then left in PBS in the dark at 4°C overnight before to be permeabilized in PBS with 0.1% Triton X-100 (Prolabo) for 10 min. Cells were incubated for 45 min with anti-*Brucella* LPS primary monoclonal antibody (A76-12G12, undiluted hybridoma culture supernatant) in PBS containing 0.1% Triton X-100 and 3% (w/v) bovine serum albumin (BSA, Sigma Aldrich). Next, cells were washed three times in PBS before to be incubated with goat anti-mouse secondary antibodies coupled to Texas Red (1:500) (Sigma Aldrich) in PBS containing 0.1% Triton X-100 and 3% bovine serum albumin. Coverslips were washed three times in PBS, once in ddH₂O and then mounted on Mowiol (Sigma).

V. Microscopy and analyses of fluorescence

We used a Nikon Eclipse E1000 (objective 100X, plan Apo) microscope connected to a ORCA-ER camera (Hamamatsu). The Hg lamp was set with ND filter at 4. Bacteria in culture were observed with the phase contrast on PBS-agarose (1%) pads. Bacteria inside host cells were observed with the TxRed channel (100 ms). The FITC channel (1 sec) was used to detect either the N-nitrosation sensitive probe or the GFP signal of the reporter systems. Pictures were encoded with NIS-element software and analyzed with the plug-in MicrobeJ in ImageJ (Ducret *et al.*, 2016). For bacteria on pads, mean fluorescence intensities (MFI) were obtained as the “mean_c” values with MicrobeJ for individual bacteria. For intracellular bacteria, MFI were obtained by subtracting the background fluorescence (defined here as the average value of fluorescence given by the Pixel Inspection Tool on three points randomly chosen around a bacterium) to the “mean” value of fluorescence obtained for each bacterium with MicrobeJ.

VI. Growth curves and colony forming units counts

VI.1. Growth curves

Growth curves were performed with a Bioscreen C (Oy Growth curves). Overnight cultures were washed twice in TSB, then they were diluted to an OD of 0.1 and resuspended in their final fresh medium. Wells were filled with 200 μ L of culture and OD were measured every 30 min during 72 h.

VI.2. CFU after infection

For CFU counts after infection, cells were washed twice in PBS, then lysed with 0.01% Triton X-100 in PBS for 10 min at 37°C. Several dilutions were plated on TSB supplemented with IPTG when required. Plates were incubated for 3 days at 37°C.

VI.3. CFU after liquid culture (survival assay)

For CFU counts in culture, wild type *B. abortus* and GcrA/CtrA depletion strain supplemented with IPTG were grown to mid exponential phase (OD₆₀₀ 0.3-0.6) and normalized to OD₆₀₀ 0.15. Cultures were divided in different aliquots to be tested with or without MMS 5 mM and with or without IPTG. Samples were taken at different time points (3, 6, 20, 24 and 48 h) and plated with serial dilutions on 2YT plates, supplemented with 1 mM of IPTG for the depletion strain.

VI.4. CFU on plates supplemented with alkylating agents (plating assay)

For CFU counts on plates supplemented with MMS or MNNG, 100 μ L of bacteria in mid exponential phase (OD₆₀₀ 0.3-0.6) were plated after a normalization to OD₆₀₀ 0.1 of all bacterial cultures. All plates were prepared fresh, 1-2 hours before each experiment. MMS was added at a concentration of 2.5 mM in TSB-agar rich medium during plate preparation. MNNG was prepared in an acetate buffer (pH 5), and then added at a final concentration of 35 μ M in TSB-agar rich medium during plate preparation.

VII. Chromatin immunoprecipitation with anti-GcrA antibodies

VII.1. ChIP-seq

ChIP-seq experiment was conducted as previously described for CtrA (Francis *et al.*, 2017). Cultures of 80 mL of *B. abortus* (OD₆₀₀ 0.8) were harvested by centrifugation and proteins were cross-linked to DNA with 10 mM sodium phosphate buffer (pH 7.6) and 1% (v/v) formaldehyde for 10 min at RT and 30 min on ice. Bacteria were centrifuged and washed twice in cold PBS before to be resuspended in lysis buffer (10 mM Tris-HCl pH 7.5, 1 mM EDTA, 100 mM NaCl, 2.2 mg/ml lysozyme, 20 ml protease inhibitor solution from Roche). Bacteria were lysed, after the addition of 0.1 and 0.5 mm diameter Zirconia/Silica beads (Biospec Products), in the cell Disruptor Genie from Scientific Industries at maximal

amplitude (2800) for 25 min at 4°C. Bacteria were then incubated for 10 min in the presence of ChIP buffer (1.1% Triton X-100, 1.2 mM EDTA, 16.7 mM Tris-HCl pH 8.0, 167 mM NaCl, protease inhibitors). DNA fragments of about 300 base pairs were obtained by sonicating the lysate on ice (Branson Sonifier Digital cell disruptor S-450D 400W) by applying 15 bursts of 20 s (50% duty) at 30% amplitude. Debris were excluded in the pellet by centrifugation at 14,000 rpm for 3 min. The supernatant was normalized by protein content by measuring the absorbance at 280 nm and 7.5 mg of protein was diluted in 1 ml of ChIP buffer supplemented with 0.01% SDS and pre-cleared in 80 ml of protein A-agarose beads (Roche) and 100 µg BSA. Homemade anti-rabbit polyclonal GcrA antibodies (290.S3) were added to the supernatant (1/1000) and incubated over night at 4°C. The mix was then incubated with 80 ml of protein A-agarose beads pre-saturated with BSA for 2 h at 4°C. Beads were then washed in the following order: once with low salt buffer (0.1% SDS, 1% Triton X-100, 2 mM EDTA, 20 mM Tris-HCl pH 8.1, 150 mM NaCl), once with high salt buffer (0.1% SDS, 1% Triton X-100, 2 mM EDTA, 20 mM Tris-HCl pH 8.1, 500 mM NaCl), once with LiCl buffer (0.25 M LiCl, 1% NP-40, 1% sodium deoxycholate, 1 mM EDTA, 10 mM Tris-HCl pH 8.1) and twice with TE buffer (10 mM Tris-HCl pH 8.1 and 1 mM EDTA) before to be eluted with 500 µL of elution buffer (1% SDS and 0.1 M NaHCO₃). The reverse-crosslinking was performed with 500 mL of 300 mM of NaCl overnight at 65°C. Samples were then treated with Proteinase K (in 40 mM EDTA and 40 mM Tris-HCl pH 6.5) for 2 h at 45°C and DNA was finally extracted with QIAGEN MinElute kit to be resuspended in 30 µL of Elution buffer.

VII.2. Analyses

Illumina MySeq was used to sequence immunoprecipitated DNA. Data consisted of a number of reads per nucleotide. A Z score for each base pair (i.e. the number of standard deviation from the average) was calculated based on average and variance in a window of 1 million base pairs. A threshold of Z score above 4 was set to consider genomic regions as bound by GcrA. These sequences were mapped to the genome of *B. abortus* 2308 (table available on request). The GcrA binding peaks can also be visualized on Artemis (freely available at <http://www.sanger.ac.uk/science/tools/artemis>) with the genomic sequences (.gb files) available on request. To calculate the number of GANTC sequences in ChIP-seq peaks, we extracted peak sequences online with Emboss-extractseq (<http://emboss.bioinformatics.nl/cgi-bin/emboss/extractseq>) and looked for the presence of GANTC sites with the “pattern matching, dna-pattern” tool on RSATools (van Helden, 2003)(<http://embnet.ccg.unam.mx/rsa-tools/>) on both strands and with allowing overlapping matches. Results were normalized according to peak size to obtain the number of GANTC sites per kb (GANTC/kb). A similar analysis was performed for whole chromosomes with the “pattern matching, genome-scale dna-pattern” tool on RSATools. Ratios were calculated between data obtained (in GANTC/kb) for the peaks and for the whole chromosomes.

VIII. Whole genome sequencing after infection and liquid cultures

Ethics Statement: The animal handling and procedures of this study were in accordance with the current European legislation (directive 86/609/EEC) and the corresponding Belgian law “Arrêté royal relatif à la protection des animaux d’expérience du 6 avril 2010 publié le 14 mai 2010.” The Animal Welfare Committee of the Université de Namur (UNamur, Belgium) reviewed and approved the complete protocol for *Brucella* infections (Permit Number: 05-558).

Two liquid cultures of WT *B. abortus* were inoculated in 2YT rich medium from the same plate. One of them was divided in 5 subcultures and diluted (1:10) in liquid cultures twice every 24 h, before to be plated. The remaining original liquid culture was used to infect five C57BL/6 mice and RAW 264.7 macrophages. Mice were acquired from Harlan (Bicester, UK) and bred in the animal facility of the Gosselies campus of the Université Libre de Bruxelles (ULB, Belgium). Mice were injected intraperitoneally with a dose of 10^5 CFU/mL of *B. abortus* in 500 μ l of PBS. Infectious doses were validated by plating serial dilutions of inoculums. At 60 h post inoculation, mice were euthanized by cervical dislocation. Immediately after being killed, spleens were recovered in PBS with 0.1% Triton X-100 (Sigma) and plated on 2YT. RAW 264.7 macrophages were infected as described above and bacteria were plated at 6 and 48 h post infection. Five streaks were made from five isolated colonies obtained after passage in either liquid cultures, mice or RAW 264.7 macrophages from different wells. The five streaks served for inoculation of liquid cultures, from which genomic DNA was extracted (NucleoSpin Tissue extraction kit, Macherey-Nagel). Samples were sequenced with Illumina sequencing technique using NextSeq500 run Mid PE150 after preparing a TruSeq DNA library (performed by Genomics Core Leuven, Belgium). Sequencing hits were mapped on the genome of *B. abortus* 544 (performed by Genomics Core Leuven, Belgium) and mutations were counted for each strain, excluding regions corresponding to microsatellites.

IX. Reverse transcription followed by quantitative PCR

Bacterial cultures were grown in 2YT rich medium to exponential phase (OD_{600} 0.3), washed twice in PBS and allowed to grow in rich medium supplemented or not with IPTG and/or MMS 2.5 mM (Sigma) for 5 h. Bacteria were washed twice in PBS, then collected by centrifugation and immediately frozen and stored at -80°C until processing. RNA was extracted using TriPure isolation reagent (Roche) according to manufacturer’s instructions. Samples were treated with DNase I (Fermentas), then RNA was reverse transcribed with specific primers (see below), using the High capacity cDNA Reverse Transcription kit (Applied Biosystems). Specific cDNAs were amplified on a LightCycler 96 Instrument (Roche) using FastStart Universal SYBR Green Master (Roche). Results were normalized using 16S RNA as a reference.

Primers for RT-qPCR	
F-ada1	ttccatcgtgtttcaaggcc
R-ada1	atcccgatcatagatcgtatcc
F-ada2	caggttgatgccggtttgaatc
R-ada2	aaattgcgatcatggtgccaag
F-mutL	cgatagcggctttgaagtgtg
R-mutL	cccgatccgtcttcatgaattc
F-ogt	ccgctttcatcaggcaactatt
R-ogt	ccggtttcagtccagaatgatt
F-tagA	ctgtcgcgcaacccataacc
R-tagA	caatggcaaccctcgatatgatc
F-alkB	ggacaaggacgaacggaatttt
R-alkB	gccatggtgcaggatatatttgg
F-gcrA	cagtgatcgggaaagtgcac
R-gcrA	gggtgccgctattgttgttt
F-lexA	ccttgcgtccaaatcaggtattc
R-lexA	aatttcttctgcgggctgaga
F-mutS	tcgatatctcaaccggaaccttc
R-mutS	gccgcaattcctcatcatgaaa
F-alkA	gcggatcgatacattgagcgata
R-alkA	agccagactttcaaaccggg
F-recA	cattcccgttcaaactgcatg
R-recA	gaaccgaagcatagaacttgagc
F-uvrA	cgtttatgtgacctgcatg
R-uvrA	gaattcagcaccttcttccactg
F-xthA1	caagtcggtggatgagcaattt
R-xthA1	gaaggcctttattgatctcatccg
F-xthA2	agtttctgcgcgattatcagc
R-xthA2	cgaccccgatgataacctttct
F-16S	taataccgtatgtgcccttcgg
R-16S	tgatcatcctctcagaccagct

X. Western blot

Cultures of *B. abortus* in late exponential phase (OD₆₀₀ 0.7-1) were concentrated to an OD₆₀₀ of 10 in PBS, then inactivated for 1 h at 80°C. Loading buffer (1:4 of final volume) was added before to heat the sample at 95°C for 10 min. Ten µL of sample were loaded on each well of a 12% acrylamide gels. After migration, proteins were transferred with the semi-dry method onto a nitrocellulose membrane (GE Healthcare) which was blocked in PBS supplemented with 0.05% Tween 20 (VWR) and 5% (w/v) milk (Nestlé, foam topping) over night. The membrane was incubated for 1 h with polyclonal anti-GcrA (290.S3) or

monoclonal anti-Omp10 (A68/4B10/F05) primary antibodies (1:1000), then with secondary antibodies coupled to HRP (Dako Denmark) (1:5000), both in PBS 0.05% Tween 1% milk. The membrane was washed three times in PBS before to be revealed with The Clarity Western ECL Substrate (Biorad) and Image Quant LAS 4000 (General Electric).

XI. Flow cytometry

DNA content was measured using flow cytometry. Bacteria were washed twice in PBS, then fixed in ice-cold 70% ethanol and left for a day at -20°C. Fixed samples were then washed twice in FACS staining buffer (10 mM Tris pH 7.2, 1 mM EDTA, 50 mM NaCitrate, 0.01% Triton X-100) containing 0.1 mg/ml of RNaseA and incubated at room temperature for 30 min. Bacteria were then centrifuged for 2 min at 8000g, resuspended in 1 ml of FACS staining buffer supplemented with 0.5 μ M of Sytox Green Nucleic acid stain (Life Technologies), then incubated at room temperature in the dark for 5 min. Samples were analyzed by flow cytometry (FACS Calibur, BD Biosciences) at laser excitation of 488 nm. A minimum of 10^4 cells were recorded in triplicate for each experiment.

XII. Disk assays

Liquid cultures of bacteria in mid exponential phase (OD_{600} 0.3-0.6) were normalized to OD_{600} 0.15 in 2YT, then 100 μ L of each culture was plated on 2YT-agar plates. Wathman paper disks of 6 mm of diameters were pasteurized, then were humidified with 30% H_2O_2 (Sigma Aldrich) and placed in the center of each plate. Zones of growth inhibition (diameters) were measured after 3 days in the incubator at 37°C.

Discussion and perspectives

I. On the existence of intracellular alkylating stress

I.1. What are the sources of the detected alkylating stress?

Many environmental and pathogenic bacteria possess an adaptive system (Mielecki *et al.*, 2015), indicating that alkylating stress is widespread in the environment. Nevertheless, it was unknown if intracellular bacteria could also face this stress during infection.

To investigate this question, we developed a fluorescence-based reporter system to follow the occurrence of the stress on bacterial DNA at the single cell level. Here, using the class III pathogen *B. abortus* as a model of pathogenic intracellular bacterium, we were able to show that it does encounter alkylating stress inside host cells. *B. abortus* trafficking and replicative state inside host cells being well-characterized (Deghelt *et al.*, 2014; Celli, 2015), we could more specifically track the occurrence of alkylating stress in the intracellular environment. So not only can we say that alkylating stress is occurring, we can also propose that it happens when *B. abortus* is inside its endosome-derived compartment (eBCV), which is a common step to many intracellular bacteria (Kumar & Valdivia, 2009).

In order to understand if the stress was generated endogenously or exogenously, we first investigated whether N-nitroso compounds, which are alkylating agents, were produced by the host cells inside the eBCV. To do so, a probe was designed so it could be covalently attached at the bacterial surface and report, based on the emission of fluorescence, the level of N-nitrosation events occurring inside the eBCV. This technique is particularly interesting because it allowed us to examine the environment of each bacterium at a given time. Note that ultimately, this approach could be used for other questions, such as pH or oxidative stress occurrence in the environments met soon after internalization, before bacterial growth. In the case of alkylating stress, this technique revealed that N-nitrosation reactions do take place inside the eBCV, but only for a subset of the bacterial population. It could mean that exogenous N-nitrosation is not constant along time. For example, it could occur through waves with some bacteria being positive and other bacteria negative at a given time point. Alternatively, heterogeneity in the intracellular bacteria could generate a diversity of environments more or less prone to N-nitrosation. Another important point is that N-nitrosation reaction is favored by acidic pH (Mirvish, 1975), which is a characteristic of the eBCV (Porte *et al.*, 1999). Yet, even if this affirmation is true at the population level, it has been very recently proposed that acidification inside phagosomes is a stochastic mechanism with the final pH being very variable between vacuoles (Dragotakes *et al.*, 2018). Therefore, it is possible that the 23% of the population for which we detected N-nitrosation events correspond to the subsets of the eBCV with the most favorable pH for this reaction to occur. To know whether this is the case, it would be very interesting to test the endosomal pH of *Brucella* in parallel with our N-nitrosation reporter probe. Actually, a double labeling of the

bacteria should be possible, so we could imagine using a second probe with a pH-dependent fluorescent signal in order to test both signals at the single-cell level. At the opposite, we could also inhibit vacuolar acidification by using Bafilomycin A to see whether acidic pH is involved in N-nitrosation reactions in the eBCV or not.

Importantly, the addition of ascorbate to the cell culture medium diminished the level of exogenous N-nitrosation (**Fig 20C**), but not the level of alkylating stress detected with the Ada-based reporter system (**Fig 20D**). In addition to exogenous N-nitrosation, lipid peroxidation should also have been - at least partially - prevented by the addition of the antioxidant ascorbate, too. These results thus indicate that the alkylating stress signal that we detected with our reporter system does not reflect exogenous N-nitrosation or lipid peroxidation events, but more probably an endogenous event. Notably, the occurrence of external N-nitrosation events is relevant for alkylating stress only if metabolites are present in the environment. Indeed, alkylating stress is generated by those modified metabolites, and not by N-nitrosation *per se* (Archer, 1989). It has been proposed that the eBCV is very poor in metabolites (Kohler *et al.*, 2002; Lamontagne *et al.*, 2009; Rossetti *et al.*, 2011), which could explain why the production of alkylating agents by the host cells is innocuous compared to the endogenous generation of the stress. If this observation is true for cultured cells, we should keep in mind that it could be different in a more physiological environment, *i.e.* inside the host.

Another important point is that N-nitrosation reactions are dependent on RNS levels (Ohshima *et al.*, 1991) and *B. abortus* is known to be very weakly immunogenic, as it prevents proinflammatory responses in macrophages and neutrophils (Barquero-Calvo *et al.*, 2007). Interestingly, a study revealed that *Salmonella* is meeting sublethal RNS stresses early during macrophages, with patchy iNOS localization, which is reminiscent of what we observed with our N-nitrosation probe (Burton *et al.*, 2014). It could thus be very interesting to explore the effects of external N-nitrosation on intracellular bacteria that induce higher amounts of RNS, or in a more aggressive cell type, such as voluntarily activated bone marrow-derived macrophages.

We also have to keep in mind that even if N-nitroso compounds are generated by the host cells inside the eBCV, it is possible that they never reach *Brucella*'s DNA. Indeed, those modified metabolites would have to pass through the membranes of *B. abortus*, either via an active mechanism or via diffusion. Not much is known about how alkylating agents go through membranes, so this would be an interesting topic for future research.

Considering that external N-nitrosation was not a major source of alkylating stress, we decided to study the endogenous N-nitrosation potential of *Brucella*. In the case of *E. coli* and most of the other bacteria tested, the formation of N-nitroso compounds seems to be directly linked to nitrate reductase activity (Taverna & Sedgwick, 1996). Nevertheless, there are exceptions, such as in the case of *Pseudomonas aeruginosa*, where nitrite reductase activity is the key (Calmels *et al.*, 1988). As for *Pseudomonas denitrificans*, its N-nitrosation capacity is

apparently dependent on nitrate reductase activity, but modulated negatively by high nitrite concentrations (Calmels *et al.*, 1988).

Logically, we first tested the involvement of *B. abortus* nitrate reductase enzyme in the formation of endogenous alkylating stress. To do so, we tested our Ada_{*E. coli*}-based reporter system in a $\Delta narG$ deletion background. Surprisingly, the signal of our reporter system did not decrease (**Fig 20D**). We also decided to try this experiment again but in a $\Delta moaA$ strain. Indeed, *moaA* codes for an enzyme involved in the molybdenum cofactor biosynthesis pathway (**Fig 4**). In *E. coli*, a Δmoa mutant was shown to be greatly reduced in its ability to form N-nitroso compounds and therefore endogenously-produced mutations (Taverna & Sedgwick, 1996). The authors suggested that this was due to the inhibition of the activity of the three nitrate reductases of *E. coli* at once, as they all require this cofactor to be active (Taverna & Sedgwick, 1996). Since *B. abortus* possesses only one nitrate reductase, which is also dependent on molybdenum cofactor, we were expecting to obtain similar results between the $\Delta narG$ and the $\Delta moaA$ strains. Surprisingly, that was not the case, as the signal detected with the Ada_{*E. coli*}-based reporter system did decrease with the $\Delta moaA$ strain, contrarily to what we observed with the $\Delta narG$ strain (**Fig 20D**). Firstly, these results strongly suggest that the endogenous formation of N-nitroso compounds were indeed responsible for most of the alkylating stress that we could detect with our reporter system. Secondly, they indicate that the nitrate reductase of *Brucella* is not responsible for this stress, or at least not alone. Thus, it is probable that the phenotype of the $\Delta moaA$ mutant comes from other enzymes depending on the molybdenum cofactor. It could for example be the case of MSF, a nitrate-nitrite antiporter, which is probably part of *B. abortus* LexA regulon (**Fig 33**), as well as FdnG, a formate dehydrogenase involved in nitrate respiratory chain (Stewart, 1988).

As for the part played SAM, it is still unknown. Its involvement would need to be investigated but it probably won't be easy. Indeed, SAM is involved in many important processes and playing on its abundance to study its effects might generate many polar effects.

1.2. Could *B. abortus* actively avoid alkylating stress?

1.2.1. What we can expect

Importantly, the signal that we detected with our Ada-based reporter system was never very high compared to what we could obtain *in vitro* with alkylating agents. This suggests that, even though it is present, alkylating stress on intracellular *B. abortus* is probably very weak. This is not that surprising considering that *Brucella* has been selected through evolution to be able to survive and even thrive inside macrophages. The avoidance of the stress by the bacterium must thus be part of its adaption to its intracellular lifestyle. The two main sources of alkylating agents generated by the host cells would be lipid peroxidation and N-nitroso compounds formation. Since we know that both sources are not very present in the case of *Brucella* infection (in our model at least), we could suppose that the bacterium has evolved to actively avoid their generation.

1.2.2. The case of oxidative stress

Lipid peroxidation can arise from oxidative or nitrosative stress (Tudek *et al.*, 2017) (Fig 2A). As oxidative stress is also a direct-acting mechanism of defense against pathogens, it has been extensively studied over the last decades. There is a lot to learn from these studies. One main finding is that in one given type of host cell, oxidative stress and its consequences can be very diverse, owing to the bacterium that entered it. Indeed, bacteria are more or less prone to activate macrophages depending on the antigens they provide to their host, and some can even hijack their host so as to avoid stresses.

One particularly interesting study, reported by Schlosser-Silverman *et al.* (2000), revealed that *E. coli* and *S. enterica* Typhimurium do not share the same fate, in many aspects, inside J774 macrophages. Even though *S. enterica* Typhimurium was known to be able to multiply inside macrophages, they postulated that it must also encounter oxidative stress as *recA* and *recBC* mutants showed increased sensitivity in macrophages and attenuation in mice. However, while comparing the mutation frequencies of both bacteria inside host cells, they realized that *E. coli*, but not *S. enterica* Typhimurium, was affected by oxidative stress on this aspect (Schlosser-Silverman *et al.*, 2000). They also found that *E. coli* had a 20-fold increase of 8-oxodG adducts while *S. enterica* Typhimurium did not display any increase compared to the culture medium (Schlosser-Silverman *et al.*, 2000). Finally, they noticed that both bacteria were actually alive during the first 90 minutes, but that *E. coli* had arrested gene expression at that time. This phenotype was also observable with enteropathogenic *E. coli* but not with *S. enterica* Typhimurium (Schlosser-Silverman *et al.*, 2000). Other groups later completed these observations by proposing mechanisms of survival for *S. enterica* Typhimurium. First, it was demonstrated that the bacterium is relying on its Type-III secretion system to divert the localization of NADPH oxidases, so they do not settle on the *Salmonella*-containing vacuole (Vazquez-Torres *et al.*, 2000). Then, it was shown that *S. enterica* Typhimurium is particularly well equipped against oxidative stress and that its arsenal of detoxifying enzymes is essential for efficient detoxification following oxidative burst, even in the presence of a functional Type-III secretion system (Aussel *et al.*, 2011).

Intriguingly, it had been reported that very few NADPH oxidase complexes were found to localize on the eBCV in murine peritoneal macrophages (Gay *et al.*, 1984), suggesting that *B. abortus* could use a similar tactic than *S. enterica* Typhimurium to decrease oxidative stress. It was also shown that *B. abortus* uses an active mechanism to inhibit respiratory burst in neutrophils (Canning *et al.*, 1985) and prevents their degranulation (Kreutzer *et al.*, 1979). Note that despite *B. abortus* potential ability to delocalize NADPH oxidase, the phagocytosis of the bacteria does induce a raise in the production of superoxide anions by the host cells, but mainly in the extracellular environment (Gay *et al.*, 1984). *B. abortus* is weakly immunogenic, but even in non-activated macrophages, a *sodC* mutant, unable to produce a periplasmic superoxide dismutase, is attenuated at early (3 h PI) and later times (27 h and 51 h) of infection (Gee *et al.*, 2005). This indicates that oxidative stress is happening inside

host cells and that the bacterium does need some detoxifying enzyme in order to thrive inside its host.

In conclusion, both *S. enterica* Typhimurium and *B. abortus* seem to rely on mechanisms to decrease the direct source of oxidative stress and to protect themselves against its effects.

1.2.2. Are RNS produced against *B. abortus*?

As the formation of N-nitroso compounds is directly dependent on RNS levels (Ohshima *et al.*, 1991), it could be very interesting for a bacterium to inhibit the iNOS function in the host cells. Such ability is for example reported for *Burkholderia pseudomallei*. Indeed, this bacterium can suppress the iNOS activity in human hepatocyte via a *rpoS*-dependent mechanism (Sanongkiet *et al.*, 2016). *S. enterica* serovar Typhimurium and *M. tuberculosis* can also directly interfere with the localization of the iNOS proteins to prevent their arrival on phagosomal membranes (Chakravorty *et al.*, 2002; Miller *et al.*, 2004).

As stated earlier, the exogenous production of N-nitroso compounds was not detrimental enough to generate an alkylating stress that was detectable with our reporter system. However, we could detect N-nitrosation events for about 23 % of the labeled bacteria (**Fig 20C**), so NO must be present in the eBCV. Actually, *B. abortus* has never been reported to possess an active mechanism to inhibit iNOS, but it is well known that its LPS is naturally less prone to activate iNOS production than *E. coli* LPS (Lopez-Urrutia *et al.*, 2000). In addition, *B. abortus* is known to take advantage of its internalization by a TREM-2 mediated-phagocytosis to decrease the level of macrophages NO (Wei *et al.*, 2015). Indeed, for most bacteria, TREM-2 receptors stimulate phagocytosis while increasing intracellular oxidative stress, but for *B. abortus*, the receptors instead decrease the level of NO via the MAPK pathways (Wei *et al.*, 2015). These reports thus indicate that *B. abortus* does possess means to decrease the level of RNS that it will encounter inside these host cells.

Nevertheless, NO is a potent antibacterial tool against *Brucella*, as NOS2⁻ mice were delayed for their control of *B. abortus* infection (Ko *et al.*, 2002) and intracellular development of *B. suis* was impaired in human macrophages that produced NO (Gross *et al.*, 2004). Note that the preexisting existence of anti-*Brucella* antibodies seems to have a big influence on the production of microbicidal NO levels, as non-opsonized *B. suis* are subjected to lower level of NO than opsonized ones (Gross *et al.*, 1998). Nevertheless, murine spleen cells have been reported to generate high level of NO after non-opsonized *B. abortus* infection (Zhan *et al.*, 1996). Actually, inside the spleen and the liver of mice, *B. melitensis* was found to localize mainly in cells expressing iNOS (Copin *et al.*, 2012). Notably, the level of NO of previously stimulated macrophages is known to drop by more than two-fold once cells have internalized *B. abortus* (Wang *et al.*, 2001), so the bacterium must have expressed genes to counteract the effect of a high NO environment. Incidentally, *B. ovis* is the only *Brucella* species that does not possess a complete *tagA* gene (**Fig 16B**), but it is also the only

known exception of *Brucella* species that are all able to perform nitrate and nitrite reduction (Pickett & Nelson, 1954), but more importantly, to reduce nitric oxide (via Nor proteins) and nitrous oxide (via Nos proteins) (Haine *et al.*, 2006; Tsolis *et al.*, 2009; Ronneau *et al.*, 2016). Interestingly, a *norE* mutant is known to be attenuated in mice, bovine macrophages and HeLa cells (Lestrade *et al.*, 2003). In addition, mutants for *norB* and *nnrA* (coding for a transcriptional regulator of *nir*, *nor* and *nos*) are also attenuated in activated macrophages but their survival defect can be suppressed by the addition of an inhibitor of iNOS (Haine *et al.*, 2006). This suggests that, in addition to their role in respiration, the Nor proteins also help to detoxify the intravacuolar nitric oxide. Note that in addition to *narG*, *norB* and *nosZ* are also known to be overexpressed at 4 h and 12 h PI in host cells (Rossetti *et al.*, 2011), indicating that NO production could happen early during infection.

Considering all those data, it seems that *B. abortus* does meet RNS inside its BCV, but also that the bacterium has evolved to minimize the amount of NO that will eventually reach it inside the BCV. This could be part of the reason why exogenous alkylating agents were too scarce to create a detectable amount of stress in our experiments. The circle is now complete: by avoiding exogenous sources of alkylating stress, *B. abortus* is generating an endogenous one. Indeed, as *B. abortus* activates its nitrate respiration/denitrification pathway inside host cells, it would probably also automatically generate endogenous N-nitroso compounds and thus endogenous alkylating agents.

II. On the genes that are required to face alkylating stress *in vitro*

II.1. Inducible genes

To cope with the endogenous alkylating stress that its metabolism is generating, *B. abortus* must most probably rely on some DNA repair pathways. To better understand what role individual pathways were playing in repairing alkylated DNA, we first performed *in vitro* experiments. RT-qPCR were executed in the presence or absence of MMS in order to see which genes were upregulated after 5 hours of high alkylating stress and deletion strains were tested for their ability to grow on plates supplemented with MMS or MNNG.

As a reminder, in *E. coli*, the alkylation-specific adaptive response is characterized by Ada activation, leading to the upregulation of *ada* itself, *alkA*, *alkB* and *aidB* (**Fig 5A**). RT-qPCR experiments revealed that none of the two *B. abortus* *ada* genes was overexpressed following MMS treatment, indicating that *Brucella* is not relying on an adaptive response to cope with alkylating stress. Similarly, the expression of *alkB* was not induced in our experiment (**Fig 23**). As for *aidB*, we did not check its level of expression. At the opposite, we did find that *alkA*, but also *tagA*, were overexpressed after MMS treatment (**Fig 23**). The fact that these two genes were overexpressed was a surprise, as they are supposed to code for DNA glycosylases of similar function, which was also suggested by plating experiments (**Fig 21**). Actually, in *E. coli* and many other bacteria, *tagA* is known to be expressed constitutively, while *alkA* is the only one of the two genes to be inducible (Mielecki & Grzesiuk, 2014). In *E. coli*, AlkA is known to have much broader substrate specificity than

tagA, including unmodified bases (Berdal *et al.*, 1998). TagA, on the other hand, has a preference for 3meA (Thomas *et al.*, 1982) and is naturally inhibited by free 3meA, which is not the case of AlkA (Tudek *et al.*, 1998). In *B. abortus*, the deletion of *alkA* only was not deleterious for survival on plate with either MMS or MNNG, contrarily to the *tagA* deletion strain which was impaired for normal growth in presence of MMS (**Fig 21**). This suggests that, of the two genes, the most important one is *tagA*. It is thus possible that, in *B. abortus*, TagA substrate specificity evolved to be broader than AlkA.

Regarding their induction, we can only make assumptions. The fact that the two *ada* genes were not overexpressed after alkylating stress exclude their regulation via an adaptive response, so other mechanisms of regulation must be at play. The promoter of *tagA* was bound by CtrA in a ChIP-seq experiment (Francis *et al.*, 2017), but it is probable that its overexpression upon alkylating stress is due do another mechanism. One possibility is that *tagA* could be upregulated by the presence of a stress-induced σ factor, such as the general stress response σ^{E1} . However, the level of expression of *tagA* did not change in a $\Delta rpoE1$ strain, which is deprived of σ^{E1} , under *in vitro* stress conditions (Kim *et al.*, 2014). Since the regulons of the other σ factors are not yet known in *Brucella*, it would be interesting to keep an eye on future research in this filed, as it could provide answers to our interrogations. As for *alkA*, we found a degenerated LexA-binding box in its promoter, which suggests that its overexpression following alkylating stress could be due to the induction of the SOS response. As a matter of fact, the *lexA* gene, coding for the SOS response repressor and being one of the first genes to be expressed following SOS induction, was overexpressed after MMS treatment (**Fig 23**). This strongly suggests that the SOS response is indeed triggered by high exogenous alkylating stress on *B. abortus*. This is not surprising as it is also the case in other bacteria (Jeggo *et al.*, 1977; Uphoff, 2018). One way to know if *alkA* was really activated via the SOS response in *B. abortus* would be to mutate the LexA-binding box in the promoter of *alkA* and check by RT-qPCR if the gene is still upregulated following MMS exposure. In addition, a way to confirm that SOS induction is required against high exogenous alkylating stress would be to do the MMS/MNNG plating experiments with a *lexA* overexpression strain.

Importantly, there is a report on the fact that *B. abortus* could possess a constitutively active RecA* activity, which would lead to a basal constitutive SOS response that can be slightly more activated upon stress exposure (Roux *et al.*, 2006). As a reminder, this hypothesis is based on the facts that (1) the expression of a $p_{recA-B.abortus}$ -*lacZ* reporter system was greatly reduced in a *B. abortus* $\Delta recA$ strain, independently of mitomycin C addition, suggesting that *B. abortus* RecA is involved in its own high basal activation without a requirement for high DNA damage and (2) that *B. abortus* RecA led to a high constitutive expression of the $p_{recA-E.coli}$ -*lacZ* reporter system in *E. coli*, with a 2-fold induction achieved after mitomycin C treatment (Roux *et al.*, 2006) (see **introduction section II.3.5.** for a complete description of this paper). Since *recA* expression is conditioned by the presence of RecA* itself, we can assume that the high basal expression of *B. abortus* *recA* is dependent on the SOS system (Roux *et al.*, 2006). In this case, it would mean that some genes of the SOS regulon of *Brucella* would also be more highly expressed than in other bacteria. Notably, in

E. coli, translesion synthesis is known to generate spontaneous mutations, mostly because of the action of the DNA polymerase V, encoded by *umuDC* (Kato & Shinoura, 1977). Therefore, a *E. coli recA730* mutant, which exhibits a constitutively active SOS system, presents a mutator phenotype that can be abolished by mutations in the *umuC* gene (Caillet-Fauquet & Maenhaut-Michel, 1988). As *Brucella* does not possess *umuDC* genes but relies on *imuABC* genes instead, it can be expected that this problem would not happen. Indeed, in *C. crescentus*, the ImuABC system was shown to have no effect on spontaneous mutagenesis on undamaged DNA, even if the expression of *imuABC* was artificially overexpressed by 28-fold compared to the WT conditions (Alves *et al.*, 2017). This also implies that the idea of a high basal de-repression of *Brucella* SOS system proposed by Roux *et al.* (2006) would be viable. In addition, since the strength of LexA binding depends on the conservation of the SOS-boxes, we can also imagine that some DNA repair genes, such as the ones coding for the translesion synthesis polymerases, could still be tightly repressed in non-stressing conditions.

In *B. abortus*, Roux *et al.* (2006) found that *recA* expression could only be overexpressed by two fold at best. It is interesting to note that our RT-qPCR experiments seem to confirm this data, as *recA* was not statistically overexpressed after alkylating stress (**Fig 23**). Note that RecA is important for *Brucella* to survive against alkylating stress, as attested by our plating experiments (**Fig 21**), but since its basal expression level is supposed to be naturally high (Roux *et al.*, 2006), a higher induction might not be biologically necessary. The gene coding for UvrA, which we believe is part of LexA regulon in *B. abortus* (**Fig 33**), was also not statistically overexpressed after alkylating stress (**Fig 23**). Still, there is a marked difference between *recA* and *uvrA* expression patterns (**Fig 23**), suggesting that other LexA targets might be released from the repressor with different kinetics. It would be very interesting to test if other DNA repair genes, and more particularly those coding for translesion DNA polymerases, are overexpressed under alkylating stress conditions. Obviously, the list of our putative SOS-dependent genes (**Fig 33**) would first have to be confirmed experimentally. We could do this by playing on the SOS-binding boxes of the promoters, as proposed earlier, or with different genetic backgrounds, such as *lexA* deletion and overexpression strains.

Note that a constitutive de-repression of the SOS regulon, due to the absence of a *lexA* homologue, has also been proposed for the intracellular pathogens *Coxiella burnetii*, *Rickettsia prowazekii* and *Legionella pneumophila* (Mertens *et al.*, 2008). A high expression of DNA repair genes could thus be a common strategy in several intracellular pathogens.

II.2. Non-inducible genes

In the plating experiments, the non-inducible genes *ogt* and *xthA1* appeared to be particularly important for survival against alkylating stress (**Fig 21**). These mutant strains were always systematically sicker on plates with MMS, than on plates with MNNG. MMS being a S_N2 type of alkylating agent, it mainly induces methylation on N atoms (**Fig 1**). As for MNNG, which is a S_N1 agent, it generates both N- and O-methylations (Beranek, 1990).

The worse phenotype of the mutant strains on MMS is thus surprising, as we would expect the opposite. In the case of *alkB*, this was expected, as *E. coli* AlkB had been demonstrated to be insensitive to MNNG (Dinglay *et al.*, 2000), but for *xthA1* and *recA*, it was not anticipated. Actually, in *E. coli*, a Δ *ogt* strain is known to be completely unaffected by MNNG (Rebeck & Samson, 1991), but it does not match with our result, as *B. abortus* Δ *ogt* strain was slightly affected by MNNG (and even more so in the triple methyltransferase mutant Δ *ada1* Δ *ada2* Δ *ogt*) (**Fig 21**). Importantly, experiments on *S. enterica* Typhimurium revealed that, in this bacterium devoid of a functional adaptive system, Ogt plays a more crucial role in dealing with MNNG than Ada (Yamada *et al.*, 1995), which is also what we observed in *B. abortus*. Yamada *et al* (1995) also showed that *S. enterica* Typhimurium Ogt has much broader substrate specificity than *E. coli* Ogt. We believe it is also the case for *B. abortus* Ogt, as it possesses a proline as its 127th amino acid position (**fig 22A**). Indeed, in *E. coli*, this position is occupied by a serine (S134), which, if mutated into a proline, confers broader substrate specificity to the protein by increasing the size of its active site (Schoonhoven *et al.*, 2017). As for the difference between the phenotypes in presence of MMS and in presence of MNNG, one simple explanation could be that the chosen doses for each alkylating agent were not equivalent in their damaging potentials. The doses used for the plating experiments had been chosen to be sublethal for the WT strain, so that we would obtain information about the most important DNA repair pathways under “low” alkylating stress. It might be worth repeating the experiments with doses of MMS and MNNG leading to a slightly lethal effect on the WT strain, so that the two alkylating agents could be better compared.

III. On the absence of attenuation of the mutant strains inside host cells

III.1. Alkylating agents induce a non-linear dose response

With the *in vitro* experiments, we found several deletion strains that were sensitive to alkylating stress, such as the triple methyltransferase mutant Δ *ada1* Δ *ada2* Δ *ogt*, the double DNA glycosylase mutant Δ *alkA* Δ *tagA* or the single mutant Δ *recA* (**Fig 21**). The next step was thus to test those mutants during infection. Surprisingly, these strains were not attenuated in RAW 264.7 macrophages (**Fig 26**), despite the fact that low alkylating stress had been detected in these host cells at 5 h post infection (**Fig 18D**). This apparent discrepancy could be explained by the fact that the intensity of the alkylating stress is much lower inside macrophages compared to the addition of alkylating agents in culture or on plates. Looking at more aggressive models of infection would thus be a good idea. Indeed, when working in BMDM, we did manage to detect attenuation phenotypes with some DNA repair deficient strains (**Fig 29**).

One very important aspect of alkylating agents is that they do not induce a linear dose response. Actually, it has been shown that on eukaryotic cells, alkylating agents are innocuous until they reach a certain dose, called LOGEL (lowest observed genotoxic effect level) (Doak *et al.*, 2007). This LOGEL is not fixed, as it can be shifted depending on available DNA repair proteins (Thomas *et al.*, 2013). DNA repair pathways can be functionally redundant

and *B. abortus* is particularly well equipped against alkylating stress (**Fig 16**), so it could explain why the deletion of a single DNA repair pathway is not enough to generate an attenuated phenotype during infection. At the opposite, in culture, we probably systematically exceeded the LOGEL. This is consistent with the much higher activation of the reporter system in culture (**Fig 18B, C**), compared to infection experiments (**Fig 18D**). In fact, the redundancy in DNA repair pathways could have been predicted for *B. abortus*. Indeed, a Tn-seq study showed that no DNA repair gene is essential for *B. abortus* to infect and proliferate inside macrophages, at the exception of *recF* (Sternon *et al.*, 2018) (see **appendix 3**). Tn-seq is a high throughput technique that allows the detection of essential (*i.e.* required for survival or growth) genes in a given condition based on the analysis of transposon mutant libraries. Importantly, one of the major flaws of this technique is its inability to detect functional redundancy, which is in line with what we hypothesize here.

One way to see if the LOGEL can be displaced according to *Brucella* DNA repair capacities would be to try our *Ada*_{*E. coli*}-based reporter system in our DNA repair deletion backgrounds. Indeed, if it is the case, we should be able to observe a higher induction of the reporter system.

III.2. Did we look at the right phenotype?

If the LOGEL was attained inside host cells, the effect of alkylating stress would be cytotoxic and/or mutagenic. We looked at cytotoxic events through CFU counting and we were not able to detect any statistical difference between the WT and the various deletion strains (**Fig 26**). This indicates that, even in DNA repair deficient strains, the stress is not enough to generate a detectable cytotoxic effect. Note that in the case of the *recA* mutant, a previous report states that this strain was slightly attenuated in peritoneal murine macrophages, with half a log of difference with the WT strain (Roux *et al.*, 2006). Our data (**Fig 26**) are very similar to those but were not confirmed statistically. Looking into a more hostile and physiological model of infection might thus reveal attenuation phenotypes that are currently uncertain.

Another aspect of stresses that is often underestimated is their potential to be bacteriostatic. For example, oxidative stress has often be considered as bactericidal, when in reality its main purpose in host defense could be to stall bacterial multiplication (Imlay, 2013). Since *B. abortus* has evolved to block its cell cycle in the G1 phase during the first hours inside host cells (Deghelt *et al.*, 2014), there is no way to actually observe a potential bacteriostatic effect at that time. As for the mutagenic potential of the stress met by *B. abortus*, it appears to be null if we refer to culture conditions in our whole genome sequencing experiments (**Fig 19**). However, as stated above, the LOGEL is not fixed and should depend on functional DNA repair pathways (Thomas *et al.*, 2013). Therefore, it is possible that the absence of high mutation rates in the WT strain inside host cells does not reflect what happens in mutant strains. For example, the fact that the triple mutant $\Delta mutM \Delta mutY \Delta mutT$ was not attenuated in RAW 264.7 macrophages infection (**Fig 26**) might be

because this DNA repair system is involved in coping with 8-oxodG, which is very mutagenic but weakly cytotoxic. It would thus be interesting to do mutagenesis assays on intracellular bacteria with different genetic backgrounds.

III.3. On the role of the SOS response inside host cells

III.3.1. What part does the SOS system play in *Brucella* infectious process?

Since all of the mutant strains that we tested were impaired for a single DNA repair pathway at a time, we decided to investigate the impact of the inhibition of several repair pathways at the same time. Combining deletion mutants was a way to do it. We did try this technique with the $\Delta alkB \Delta uvrA$ double mutant, but it was infructuous (**Fig 29**). We then decided to suppress the expression of the SOS regulon, as this system affects several DNA repair pathways simultaneously. To do so, we generated a *lexA* overexpressing strain, and checked that it was not toxic *in vitro* (**Fig 31**). We decided to work with a theoretically stable form of LexA (via the S161A mutation), but it would definitely be very interesting to use a control strain that overexpresses the natural form of *B. abortus* *lexA*, which we do not have at present. The result obtained with our *lexA* overexpressing strain was very clear: the de-repression of the SOS system is required by *B. abortus* inside macrophages. Since the attenuation was visible at 24 h post infection (**Fig 32A,B**), we can expect that the DNA repair pathways that are under the control of LexA were necessary to cope with the post-replicative phase of the infection, when mutations have started to arise.

We also constructed a *lexA::lexA_{S161A}* strain, for which the genomic *lexA* had been replaced by its mutated version. Importantly, this strain was not attenuated in activated RAW 264.7 macrophages infection (in green in **Fig 32A**). It is difficult to determine why the phenotype of this strain was so different from the one of the overexpressing strain, but we can make speculations. (1) First of all, it is possible that the S161A mutation does not confer the same phenotype to *B. abortus* LexA than it does to *E. coli*. If both LexA are structurally very different, this mutation could thus potentially have no effect in *B. abortus* and our strain would be the equivalent of a “normal” *lexA* overexpression strain. (2) It is also possible that *B. abortus* LexA possesses intrinsic characteristics to allow the bacterium to monitor tightly which promoters to release under which conditions. Indeed, the absence of attenuation of the *lexA::lexA_{S161A}* *B. abortus* strain (**Fig 32A**) could be explained if *B. abortus* LexA has globally less affinity for its targets than *E. coli* LexA. The S161A mutation that plays on LexA stability only would therefore not greatly affect *B. abortus* SOS response, as target genes would often be free from LexA binding anyway. At the opposite, the overproduction of LexA (via the pBBR-*p_{lac}-lexA_{S161A}* plasmid) would sterically hinder the expression of the target genes. (3) Importantly, if *B. abortus* *lexA* behaves like *R. sphaeroides* LexA on *recA* promoter (see **introduction section I.2.2.**), its mode of action itself could also be a reason for the absence of attenuation of the *lexA::lexA_{S161A}* *B. abortus* strain. Indeed, if that is the case, under high LexA concentrations (like with our pBBR-*p_{lac}-lexA_{S161A}* plasmid), the RNA polymerase would be stalled, preventing the expression of the SOS regulon (Tapias *et al.*, 2002). At the opposite, if the intracellular level of LexA is naturally low (that would be

possible if proteins are diluted by division events), LexA greater stability (via the S161A mutation) would not prevent the SOS response. Instead, it would act as an activator on some genes by recruiting the RNA polymerase (Tapias *et al.*, 2002).

III.3.2. Why would a BER deficient mutant help when the SOS system is repressed?

One surprising phenotype was that the attenuation of the *lexA* overexpressing strain was less stringent in the $\Delta xthA1 \Delta xthA2$ background than in the WT background (**Fig 32A, B**). It seems that *B. abortus* is trying to compensate the absence of a functional SOS system by relying on the BER pathway. The absence of the XthA endonucleases should lead to an accumulation of AP sites, which are cytotoxic but also mutagenic (Troll *et al.*, 2014). The accumulation of mutations through deficient BER could thus compensate for the absence of the SOS response-derived mutagenesis.

III.3.3. What about phages?

Incidentally, the idea of a basal constitutively active SOS system developed by Roux *et al.* (2006) raises the question as to how phages do not spontaneously excise. Indeed, prophages can sense the activation of the SOS response and usually consider it as a signal to go lytic, as it means that the host bacterium might not survive (Johnson *et al.*, 1981). This sensing has been best studied for phage λ , a temperate phage infecting *E. coli*. For this prophage to maintain lysogeny, it necessarily needs to repress several genes, for example those involved in replication and synthesis of structural proteins. Structurally, the phage repressor that plays this role is very similar to LexA. This is why when RecA* stimulates the autocleavage of the SOS repressor, it also does so for the phage repressor (Galkin *et al.*, 2009). Considering that *B. abortus* has a constitutive SOS system, how do its prophages detect that the bacterium is not necessarily dying? That question is still unanswered but the cell cycle regulator GcrA might have something to do with it. Indeed, several *Brucella* phages encode a gene homologous to *gcrA* (X. De Bolle & E. Biondi, personal communication), which is puzzling. It is also possible that the phages of *Brucella* possess a very high number of repressors, which would compensate for the theoretical basal RecA* activity of *B. abortus*.

IV. On the role of cell cycle transcription factors to regulate DNA repair

IV.1. GcrA and CtrA as regulators of DNA repair

The absence of an adaptive system in *B. abortus*, but also in some other α -proteobacteria (Kaufman & Walker, 1990; Fernandez de Henestrosa & Barbe, 1991; Colombi & Gomes, 1997), led us to investigate which other factors could regulate genes involved in alkylating stress response. We found that *B. abortus* is relying on the essential and well-conserved transcription factor GcrA to control the expression of a series of genes involved in DNA repair. Those genes comprise *mutL* and *ogt*. In the free-living *C. crescentus*, GcrA is known to participate in cell cycle regulation (Holtzendorff *et al.*, 2004) and both *mutL* and

mutS are considered to be part of its regulon (Haakonsen *et al.*, 2015). In addition, the alkylation-specific *alkB* has been shown to be cell cycle-regulated in *C. crescentus* (Colombi & Gomes, 1997) and in this bacterium, *alkB* mRNA levels go down by more than two-fold in a GcrA depletion strain (Haakonsen *et al.*, 2015). It is unknown if GcrA also participates in the regulation of the cell cycle in other α -proteobacteria, but it is likely considering its high conservation in other bacteria of this class (Brilli *et al.*, 2010; Poncin *et al.*, 2018). In favor of this hypothesis, *B. abortus* GcrA depletion strain was impaired for division, growth and virulence, suggesting that it does play a role in *B. abortus* cell cycle regulation.

In *E. coli*, *ada* is known to be overexpressed in stationary phase, independently of the methylation of its C38 residue but through the activity of the alternative sigma factor RpoS (Taverna & Sedgwick, 1996). In this bacterium, the activity of Ogt is also known to be particularly important in non-dividing cells when endogenous alkylating agents are most produced (Rebeck & Samson, 1991; Mackay *et al.*, 1994). Of note, there is no gene homologous to *rpoS* in *B. abortus* and other α -proteobacteria (Staron & Mascher, 2010). Knowing this and taking into account the fact that *B. abortus* GcrA was found to regulate the expression of *ogt* and *mutL*, it reinforces the hypothesis that α -proteobacteria selected systems in which cell cycle regulators control DNA repair. During *B. abortus* infection, it has been shown that the expression level of *mutL* is five times higher at 4 h PI in HeLa cells than in liquid culture (Rossetti *et al.*, 2011). Thus, it would be particularly interesting to see if *gcrA* or *ogt* are also overexpressed at that time. Another gene that would merit more attention is *aidB*, as it is a potential target of *B. abortus* GcrA according to the ChIP-seq experiment (**Fig 24A**). Note that in *M. tuberculosis*, *ogt*, *alkA* and *tagA* are overexpressed early inside macrophages (Schnappinger *et al.*, 2003).

Incidentally, one other characteristic of GcrA in *C. crescentus* is its ability to sense CcrM-dependent methylation on DNA (Fioravanti *et al.*, 2013). Knowing that this epigenetic methylation is cell cycle regulated in *C. crescentus* (Stephens *et al.*, 1996) and probably also in *B. abortus* (Robertson *et al.*, 2000; Francis *et al.*, 2017), there could exist a functional link between both damage and epigenetic types of methylation. Importantly, in human cells, the promoter of the eukaryotic *ogt* gene (called *MGMT*) is regulated by epigenetic methylation (Esteller *et al.*, 2000). Indeed, its hypermethylation leads to *MGMT* silencing (Esteller *et al.*, 2000). It would be very interesting to confirm that *B. abortus* CcrM-dependent methylation pattern also has an effect on bacterial gene regulation. One way to know if it is the case for *ogt*, *mutL*, or even *aidB* would be to put these genes under the control of another promoter. We could also directly mutate the GANTC boxes in their promoters, provided that these sequences are indeed recognized by *B. abortus* GcrA. Considering the high percentage of GANTC boxes in the anti-GcrA ChIP-seq peaks (**Fig 24A**), we believe it should be the case. In addition, *in vitro* experiments show that *B. abortus* GcrA is able to discriminate non-, hemi- and fully-methylated DNA sequences, which is a good indication that its regulation must be similar than in *C. crescentus* (Fioravanti *et al.*, 2013). Importantly, we should also keep in mind that the attenuated phenotype of the GcrA depletion in infection is probably due to more than its inability to properly regulate DNA repair. One way to know if the

deregulation of DNA repair genes is the cause of this attenuation would be to overexpress those genes in a GcrA depletion background and repeat infection experiments.

Finally, it would also be very interesting to study the effects that aberrant methylation pattern, arising from alkylating stress, could have on gene expression. Indeed, if GcrA recognizes alkylation stress as a signal, it could activate the expression of some genes that would otherwise be non-induced. It is possible that alkylation stress would also prevent the normal CcrM-dependent methylation pattern. Indeed, a similar problem is known to arise with O⁶meG adducts, which can prevent the methylation of 5meC in eukaryotes by interfering with the binding of 5meC DNA methyltransferases and by pairing O⁶meG with thymine (Franco *et al.*, 2008).

In *C. crescentus*, several genes coding for proteins involved in DNA repair, such as LexA, RecN, RecA or MutS, are regulated along the cell cycle (Laub *et al.*, 2000). Importantly, most of these genes are overexpressed when bacteria exit the G1 stage and enter S-phase, then their expression levels go back to normal by the end of the S-phase (Laub *et al.*, 2000). Importantly, those genes are also overexpressed in a CtrA depletion background (Laub *et al.*, 2000). In *B. abortus*, where CtrA is thought to also be cell cycle-regulated, a ChIP-seq experiment revealed that CtrA binds to the promoters of *tagA*, *mutM* and *uvrC* (Francis *et al.*, 2017). The sole known function of TagA is to repair alkylated DNA, whereas MutM is mainly taking care of repairing oxidative damage on DNA, but also some alkylation lesions. (see **introduction section I.2.6.**) Note that SodC, which helps preventing oxidative DNA damage, appears to also be regulated by CtrA in *B. abortus* (Francis *et al.*, 2017). This indicates that alkylating stress and oxidative stress could be encountered at specific times during *B. abortus* cell cycle. As discussed earlier, each α -proteobacterium seems to have put different genes coding for DNA repair proteins under the control of CtrA, in a way that probably reflects their lifestyle (see **introduction section III.2.3.**). Thus, it is particularly interesting that *B. abortus* would have evolved to put precisely *tagA* and *mutM* under its control. Unfortunately, the role played by *B. abortus* CtrA on regulating genes coding for DNA repair proteins was very hard to decipher. We did try to perform RT-qPCR on a CtrA depletion strain to investigate which genes are effectively regulated by CtrA, but we never managed to properly set up the experiments (see **results section III.3.5.**). Nevertheless, the activity of *B. abortus* CtrA is not essential during the first hours of infection (Willett *et al.*, 2015; Francis *et al.*, 2017), which indicates that the probable part played by this transcription factor in the temporal regulation of DNA repair is not critical for the infection process.

IV.2. What would be the advantage of regulating DNA repair along the cell cycle?

If DNA repair is more active just after the G1 phase in *B. abortus*, as it is in *C. crescentus*, it could be relevant for what is happening inside the host cells. Indeed, *B. abortus* is blocked in a G1-like phase for several hours inside host cells before to reach its replicative niche (Deghelt *et al.*, 2014) (**Fig 12**).

One benefit of a G1 state is that, by definition, there is no ongoing replication fork. Therefore, there is no risk of a fork collapsing and leading to death at that stage, and the formation of double strand breaks is limited (Cox *et al.*, 2000). In addition, the absence of replication means that mutagenic adducts can accumulate on DNA without creating a lesion, as replication is necessary to generate mutations by mispairing bases (Fersht & Knill-Jones, 1981; Klapacz *et al.*, 2016). This protective effect can also be increased by diminishing the rate of transcription, which *Brucella* does during the first hours of infection (Rossetti *et al.*, 2011). Indeed, some positions on DNA are only accessible to genotoxic agents when DNA is in its single stranded form (**Fig 1B**) (Fix *et al.*, 2008). Moreover, intensive transcription in rapidly dividing bacteria can lead to the RNA polymerase stalling on DNA, which could become an obstacle to subsequent replication (Trautinger *et al.*, 2005; Lang & Merrikh, 2018). As for the absence of growth itself during the first hours of the infection, it could be a way for *B. abortus* to limit its PAMPs production and thus to limit its recognition by host cells. Not growing could also be a way for the bacterium to avoid using too many resources while it still resides in the eBCV, which is usually considered a nutrient-poor environment (Roop *et al.*, 2009).

Therefore, a G1 block could be a way to prevent mutations and conflicts to occur when *B. abortus* is still in the eBCV. The exit from this G1-block by *B. abortus* would require to be able to perform DNA repair rapidly at this time, so as to not fix mutations. A genetically encoded cell cycle-dependent regulation of DNA repair would thus favor the smooth functioning of this process. It is probable that this layer of regulation is not essential for *Brucella* to survive inside its host, as attested by infection experiments (see **Fig 27, 30** and Francis *et al.*, 2017), but rather that it contributes to the general fitness of the pathogen under stressing conditions.

Note also that *B. abortus* is devoid of genes coding for proteins of the non-homologous end joining repair pathway (see **introduction section II.3.5.**), which can be used during the G1 phase of the cell cycle, at the opposite of homologous recombination, for example. Thus, the existence of a basal activation of DNA repair genes during the G1 phase is also clearly advantageous in this situation. Importantly, the G1 block of *B. abortus* does not seem to happen inside all models of infection, as our team found that, inside trophoblasts, *B. abortus* grows at first, then stops growing for several hours before to finally restart growth (P. Thi Ong's PhD thesis, 2017). Knowing if DNA repair mutants have the same phenotype in this model would therefore be really interesting, as it could give an indication about the importance of the cell cycle stage regarding the generation of alkylating stress.

V. Model for *Brucella* resistance to alkylating stress

By crosschecking the information on the pathways typically involved in alkylated DNA repair and our experimental results, we can propose a model for *B. abortus* system of defense against alkylation damage (**Fig 38**).

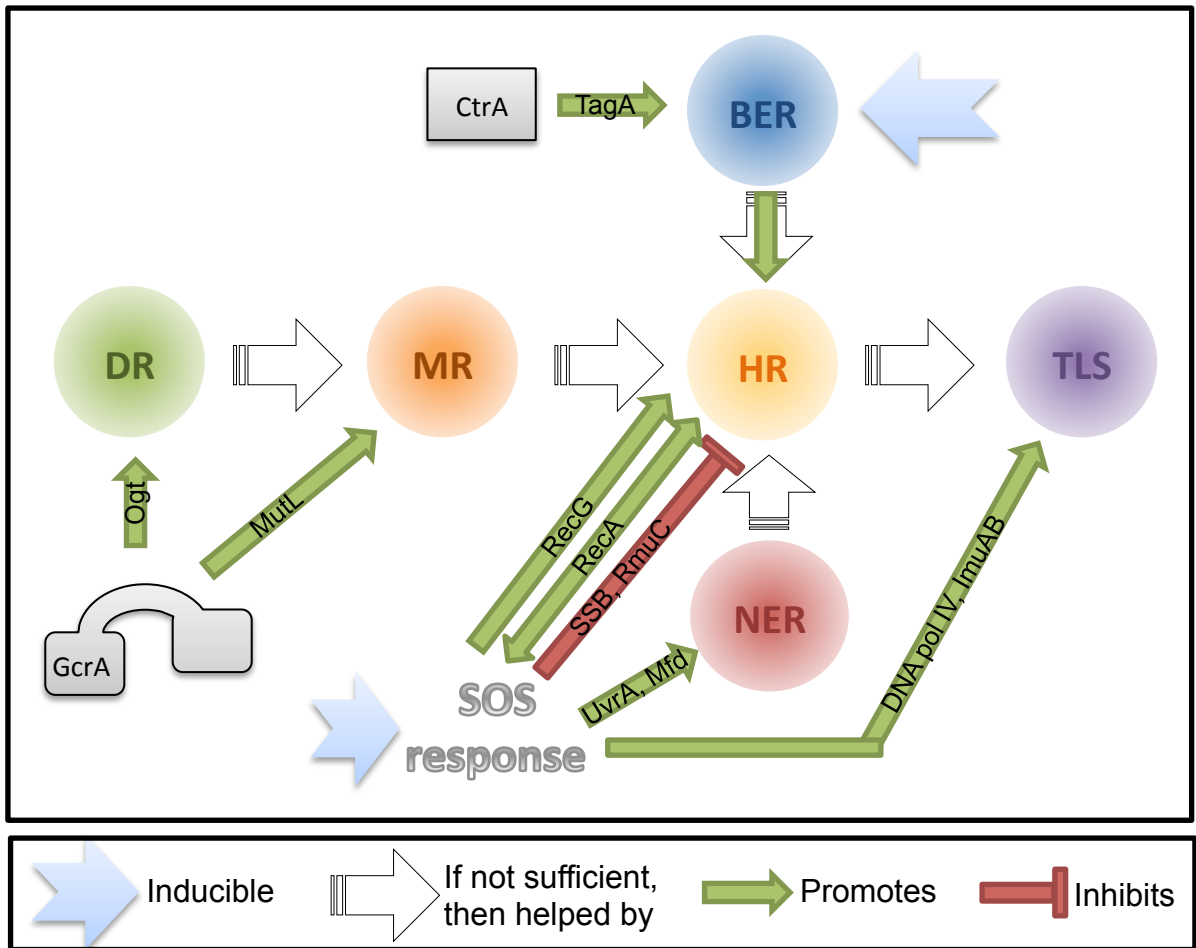


Fig 38. Model for the DNA repair pathways that are used by *B. abortus* under alkylating stress. DR stands for direct repair, MR for mismatch repair, HR for homologous recombination, TLS for translesion synthesis, BER for base excision repair and NER for nucleotide excision repair.

Typically, the first line of defense could be operated by the repair proteins TagA (involved in BER) and Ogt (involved in direct repair), as in *E. coli* (Uphoff, 2018). Interestingly, *B. abortus* seems to have put the two genes coding for these proteins under the control of the transcription factors CtrA and GcrA, respectively. If their regulation is similar to what is observed in *C. crescentus* (Laub *et al.*, 2000), this added layer of regulation could help the bacterium to produce more DNA repair proteins in anticipation of DNA replication. Indeed, contrarily to most other DNA repair pathways, BER and direct repair can be used at any time of the cell cycle, which makes *tagA* and *ogt* particularly important in the context of the G1-block. Note that the NER pathway, which can also be helpful when adducts are large (Mazon *et al.*, 2010), could also be used by *Brucella* during the eBCV stage. As explained earlier, *Brucella* transcription is globally downregulated early inside host cells, but it is not completely shut down (Rossetti *et al.*, 2011), thus still making it possible for the bacterium to couple its NER pathway to transcription via TRCF/Mfd (Deaconescu *et al.*, 2006).

Of note, inside host cells, *Brucella* is known to restart growth just before leaving the eBCV compartment, but it is unknown whether replication also restart at that time or later in the rBCV (Deghelt *et al.*, 2014) (**Fig 12**). Still, if the alkyl group on DNA has not been detected on time or if TagA and Ogt were saturated, the first round of replication will either stall or make errors and generate mismatches. As a post-replicative mechanism, the MR system could then serve as a backup pathway to prevent the occurrence of a mutation (Taira *et al.*, 2008; Kondo *et al.*, 2010; Uphoff, 2018). In *B. abortus*, GcrA also regulates *mutL*, so MR could participate in the basal handling of alkylation damage. If the alkyl adducts (typically O⁴meT) remain in the template, futile cycles of MR can lead to the formation of mutations and potentially also to single strand breaks (Kondo *et al.*, 2010; Nakano *et al.*, 2017). In that case, homologous recombination is particularly useful, as it enables replication forks to bypass alkylation lesions. Note that homologous recombination is also a post-replicative pathway and it is promoted by a functional BER pathway, as BER generates transient single strand breaks (Király *et al.*, 2014). Another way to bypass cytotoxic lesions is by relying on the translesion polymerases encoded by *dinB* and *imuABC*. In *Pseudomonas*, both DNA polymerases have been shown to be required by the bacterium to face alkylating stress (Jatsenko *et al.*, 2017). Their involvement is even more important in a $\Delta alkA \Delta tagA$ background, suggesting that translesion synthesis is used as a backup strategy by *Pseudomonas* if BER is insufficient (Jatsenko *et al.*, 2017). Note that in addition to its replisomal function, *dinB* could also have other functions (Henrikus *et al.*, 2018), and thus play a role at other moments of the cell cycle. Indeed, it was also found to be active at stalled transcription complexes (Cohen & Walker, 2010). In addition, in *E. coli*, the expression of genes coding for translesion polymerases is induced during the transition from exponential to stationary-phase growth in the absence of induction of the SOS system (Corzett *et al.*, 2013).

By bioinformatics, we predicted the regulon of LexA in *B. abortus* (**Fig 33**). If we can trust those predictions, we expect that the SOS system helps in tightly regulating homologous recombination. Indeed, among LexA regulon we found genes coding for RecA and RecG,

which are active players of the system, and SSB and RmuC, which are inhibitors. Importantly, the SOS system seems to also promote NER and translesion synthesis. The potential to further activate the SOS system when stresses increase has probably been kept to reinforce specific DNA pathways. On that note, cell cycle transcription factors and the SOS system seem to be regulating distinct DNA repair pathways. In addition, CtrA and GcrA are only involved in the first line of defense (early in the eBCV), whereas the SOS system might be needed at all times, as it can get further activated if necessary (**Fig 23**).

Altogether, the interconnection between the different layers of regulation of DNA repair pathways might be the reason why we could not observe any phenotype of attenuation with our mutant strains. Indeed, the absence of only one pathway should not be a problem as long as the others are present. At the opposite, when the SOS system is strongly repressed, many DNA repair pathways should be impacted, which could explain why the *lexA* overexpressing strain was attenuated in infection (**Fig 32A, B**). Incidentally, as *B. abortus* is known to inhibit its replication during the first five hours inside macrophages (Deghelt et al., 2014), it is no surprise that the phenotype of attenuation was only visible at latter timings, when replication had restarted (**Fig 32A, B**).

VI. What about other intracellular bacteria?

The main question brought out by this thesis is whether our conclusions also apply to other intracellular pathogens. First of all, it should be noted that there is good evidence that other bacteria precisely regulate their cell cycle during infection. One striking example is *Legionella pneumophila*, which has been found to occupy a compartment that avoids fusion with lysosomes if it infects the cells when it is in stationary phase. At the opposite, when macrophages are fed with replicative *L. pneumophila*, the bacteria are rapidly killed (Molofsky & Swanson, 2004). There even exists a specialized infectious non-replicative form of *L. pneumophila* that is ten times more infectious than stationary phase bacteria and that is produced exclusively in the intracellular environment (Garduno *et al.*, 2002). The obligate intracellular *Chlamydia trachomatis* is also known to rely on a biphasic infection process, with the infectious form being non-replicative (Cosse *et al.*, 2018). This infectious form will stay as such for at least 8 hours inside host cells before to differentiate into a replicative form (Wolf *et al.*, 2000). Other bacteria that are known to display biphasic infection steps are *Salmonella* and *Francisella*, with a relatively long non-proliferative period followed by a phase of massive proliferation (Salcedo & Holden, 2005).

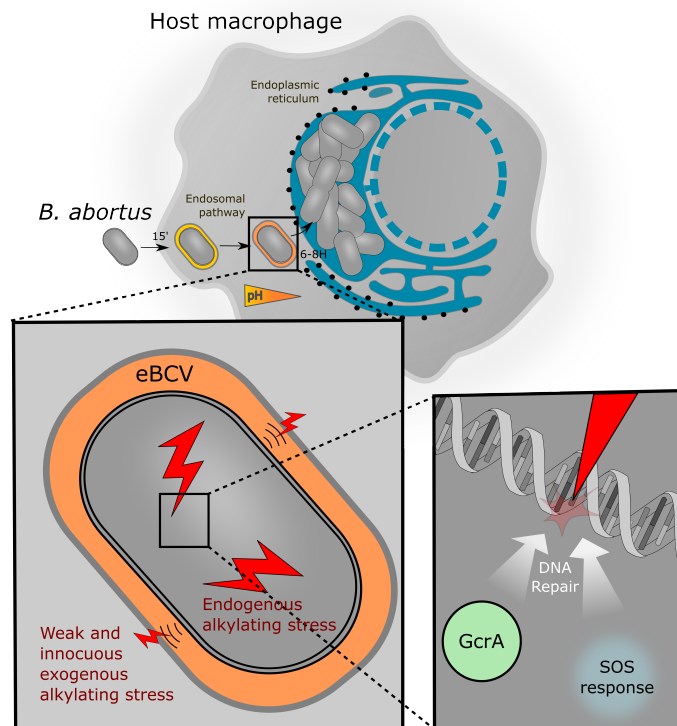
It is clear that only α -proteobacteria possess genes coding for CtrA and GcrA (Brilli *et al.*, 2010), so our finding about these transcription factors regulating DNA repair cannot be broadened to many other bacteria. However, we believe that other organisms could use other ways to end up with the same results. Indeed, even *E. coli* has evolved so that *ada* is overexpressed during stationary phase, independently of the real alkylation status of its DNA (Taverna & Sedgwick, 1996). It is doing so via the very well-conserved RpoS protein, which

is the stationary phase-specific σ subunit of RNA polymerase (Taverna & Sedgwick, 1996). As virtually all intracellular bacteria transit through the endosomal pathway (Kumar & Valdivia, 2009), we believe that most of them could be exposed to extracellular alkylating stress. However, millions of years of co-evolution with their host probably led them to develop strategies to counter the production and/or the effect of exogenous N-nitroso compounds, as *Brucella* is proposed to do.

There remains the question of endogenous alkylating stress by other bacteria. It is expected that the endogenous formation of N-nitroso compounds by bacteria happens because of a side reaction of nitrate reductase activity (Taverna & Sedgwick, 1996). However, other enzymes, such as nitrite reductase, can also be at play (Calmels *et al.*, 1988). In theory, looking at the presence of those two enzymes in the genome of a given species should be a good indicator of its ability to generate N-nitroso compounds. However, it is extremely complicated to infer conclusions with this criterion only. For example, *Salmonella enterica* serovar Typhimurium possesses both enzymes (Sparacino-Watkins *et al.*, 2014) but has been reported to be a poor N-nitrosating bacterium *in vitro* (Calmels *et al.*, 1985). Importantly, the N-nitrosation abilities of bacteria also seem to vary within the same genus or even within the same species (Calmels *et al.*, 1985), similarly to the very different fates that several related bacteria can encounter inside host cells (Schwan *et al.*, 2000). Nevertheless, we can assume that some intracellular bacteria do meet alkylating stress, as we found that genes coding for specialized DNA repair proteins have been conserved in many pathogens, including obligate intracellular ones (**Fig 16**). In addition, the human pathogen *M. tuberculosis* is known to upregulate genes coding for alkylated DNA repair enzymes early during infection (Schnappinger *et al.*, 2003), so it is a good indication that this bacterium probably meets the stress in the intracellular environment.

Conclusion

As a picture is worth a thousand words, we could summarize the principal findings of this thesis as follows:



During my thesis, we found that *B. abortus* is exposed to a weak alkylating stress inside macrophages, and more particularly during the first stage of the infection, when it is residing inside its endosome-derived compartment (eBCV). We also found that the host cell is able to generate N-nitroso compounds, which are natural alkylating agents, inside the eBCV. However, the production of N-nitroso compounds is minimal and heterogeneous against *B. abortus* and the bacteria do not seem to suffer from their presence. We believe that *B. abortus*, like many other pathogens, has learnt to divert and minimize the stresses that are produced by its host. Indeed, *B. abortus* is equipped with RNS detoxifying enzymes, which are part of the nitrate respiration enzymes used by the bacterium inside host cells (Lestrade *et al.*, 2003; Haine *et al.*, 2006). It is therefore not surprising that *Brucella* are not directly affected by exogenous alkylating agents, as they have evolved to cope with such agents at their source. Paradoxically, the use of denitrifying enzymes by *B. abortus* inside host cells is probably also part of the cause of the generation of endogenous alkylating agents, similarly to other bacteria (Calmels *et al.*, 1988). To cope with alkylating stress, we propose that *B. abortus* is relying on the transcription factors GcrA and CtrA, as well as on the SOS system. In conclusion, this thesis brought to light the existence of a stress that affects intracellular bacteria and that had been neglected for too long.

Bibliography

- Abdou E, Deredjian A, Jimenez de Bagues MP, *et al.* (2013) RegA, the regulator of the two-component system RegB/RegA of *Brucella suis*, is a controller of both oxidative respiration and denitrification required for chronic infection in mice. *Infect Immun* **81**: 2053-2061.
- Al Dahouk S, Loisel-Meyer S, Scholz HC, *et al.* (2009) Proteomic analysis of *Brucella suis* under oxygen deficiency reveals flexibility in adaptive expression of various pathways. *Proteomics* **9**: 3011-3021.
- Alexander B, Schnurrenberger PR & Brown RR (1981) Numbers of *Brucella abortus* in the placenta, umbilicus and fetal fluid of two naturally infected cows. *The Veterinary record* **108**: 500.
- Alvarez G, Campoy S, Spricigo DA, *et al.* (2010) Relevance of DNA alkylation damage repair systems in *Salmonella enterica* virulence. *J Bacteriol* **192**: 2006-2008.
- Alves IR, Lima-Noronha MA, Silva LG, *et al.* (2017) Effect of SOS-induced levels of imuABC on spontaneous and damage-induced mutagenesis in *Caulobacter crescentus*. *DNA Repair (Amst)* **59**: 20-26.
- Anderson ES, Paulley JT, Gaines JM, *et al.* (2009) The manganese transporter MntH is a critical virulence determinant for *Brucella abortus* 2308 in experimentally infected mice. *Infect Immun* **77**: 3466-3474.
- Andreu N, Phelan J, de Sessions PF, *et al.* (2017) Primary macrophages and J774 cells respond differently to infection with *Mycobacterium tuberculosis*. *Scientific reports* **7**: 42225.
- Appelberg R (2006) Macrophage nutritive antimicrobial mechanisms. *Journal of Leukocyte Biology* **79**: 1117-1128.
- Archambaud C, Salcedo SP, Lelouard H, *et al.* (2010) Contrasting roles of macrophages and dendritic cells in controlling initial pulmonary *Brucella* infection. *European journal of immunology* **40**: 3458-3471.
- Archer MC (1989) Mechanisms of action of N-nitroso compounds. *Cancer surveys* **8**: 241-250.
- Arimoto-Kobayashi S & Hayatsu H (1998) Formation of direct-acting mutagens from mixtures of N-nitrosomorpholine and carboxylates by UVA irradiation. *Environ Mol Mutagen* **31**: 163-168.
- Ausmees N & Jacobs-Wagner C (2003) Spatial and temporal control of differentiation and cell cycle progression in *Caulobacter crescentus*. *Annual review of microbiology* **57**: 225-247.
- Aussel L, Zhao W, Hébrard M, *et al.* (2011) *Salmonella* detoxifying enzymes are sufficient to cope with the host oxidative burst. *Molecular Microbiology* **80**: 628-640.
- Baharoglu Z & Mazel D (2014) SOS, the formidable strategy of bacteria against aggressions. *FEMS Microbiol Rev* **38**: 1126-1145.
- Bandara AB, Contreras A, Contreras-Rodriguez A, *et al.* (2007) *Brucella suis* urease encoded by ure1 but not ure2 is necessary for intestinal infection of BALB/c mice. *BMC Microbiol* **7**: 57.
- Barquero-Calvo E, Chaves-Olarte E, Weiss DS, *et al.* (2007) *Brucella abortus* uses a stealthy strategy to avoid activation of the innate immune system during the onset of infection. *PLoS One* **2**: e631.
- Barrionuevo P, Delpino MV, Pozner RG, *et al.* (2013) *Brucella abortus* induces intracellular retention of MHC-I molecules in human macrophages down-modulating cytotoxic CD8(+) T cell responses. *Cell Microbiol* **15**: 487-502.
- Bellaire BH, Roop RM, 2nd & Cardelli JA (2005) Opsonized virulent *Brucella abortus* replicates within nonacidic, endoplasmic reticulum-negative, LAMP-1-positive phagosomes in human monocytes. *Infect Immun* **73**: 3702-3713.
- Beranek DT (1990) Distribution of methyl and ethyl adducts following alkylation with monofunctional alkylating agents. *Mutat Res* **231**: 11-30.
- Berdal KG, Johansen RF & Seeberg E (1998) Release of normal bases from intact DNA by a native DNA repair enzyme. *Embo j* **17**: 363-367.
- Berdis AJ, Lee I, Coward JK, *et al.* (1998) A cell cycle-regulated adenine DNA methyltransferase from *Caulobacter crescentus* processively methylates GANTC sites on hemimethylated DNA. *Proc Natl Acad Sci U S A* **95**: 2874-2879.
- Bergmiller T & Ackermann M (2011) Pole age affects cell size and the timing of cell division in *Methylobacterium extorquens* AM1. *J Bacteriol* **193**: 5216-5221.
- Bielski BH, Arudi RL & Sutherland MW (1983) A study of the reactivity of HO₂/O₂⁻ with unsaturated fatty acids. *J Biol Chem* **258**: 4759-4761.
- Billard E, Cazevielle C, Dornand J, *et al.* (2005) High susceptibility of human dendritic cells to invasion by the intracellular pathogens *Brucella suis*, *B. abortus*, and *B. melitensis*. *Infect Immun* **73**: 8418-8424.
- Biondi EG, Reisinger SJ, Skerker JM, *et al.* (2006) Regulation of the bacterial cell cycle by an integrated genetic circuit. *Nature* **444**: 899-904.

- Bobo RA & Eagon RG (1968) Lipids of cell walls of *Pseudomonas aeruginosa* and *Brucella abortus*. *Canadian journal of microbiology* **14**: 503-513.
- Bodell WJ & Singer B (1979) Influence of hydrogen bonding in DNA and polynucleotides on reaction of nitrogens and oxygens toward ethylnitrosourea. *Biochemistry* **18**: 2860-2863.
- Boffa LC & Bolognesi C (1985) Methylating agents: their target amino acids in nuclear proteins. *Carcinogenesis* **6**: 1399-1401.
- Boschiroli ML, Ouahrani-Bettache S, Foulongne V, *et al.* (2002) The *Brucella suis virB* operon is induced intracellularly in macrophages. *Proc Natl Acad Sci U S A* **99**: 1544-1549.
- Boschiroli ML, Ouahrani-Bettache S, Foulongne V, *et al.* (2002) Type IV secretion and *Brucella* virulence. *Veterinary microbiology* **90**: 341-348.
- Boutte CC & Crosson S (2013) Bacterial lifestyle shapes stringent response activation. *Trends Microbiol* **21**: 174-180.
- Bowles T, Metz AH, O'Quin J, *et al.* (2008) Structure and DNA binding of alkylation response protein AidB. *Proc Natl Acad Sci U S A* **105**: 15299-15304.
- Boylan JA, Lawrence KA, Downey JS, *et al.* (2008) *Borrelia burgdorferi* membranes are the primary targets of reactive oxygen species. *Mol Microbiol* **68**: 786-799.
- Brilli M, Fondi M, Fani R, *et al.* (2010) The diversity and evolution of cell cycle regulation in alpha-proteobacteria: a comparative genomic analysis. *BMC Syst Biol* **4**: 52.
- Brown PJ, de Pedro MA, Kysela DT, *et al.* (2012) Polar growth in the Alphaproteobacterial order Rhizobiales. *Proc Natl Acad Sci U S A* **109**: 1697-1701.
- Burton Neil A, Schürmann N, Casse O, *et al.* (2014) Disparate Impact of Oxidative Host Defenses Determines the Fate of *Salmonella* during Systemic Infection in Mice. *Cell Host & Microbe* **15**: 72-83.
- Butala M, Klose D, Hodnik V, *et al.* (2011) Interconversion between bound and free conformations of LexA orchestrates the bacterial SOS response. *Nucleic Acids Res* **39**: 6546-6557.
- Caillet-Fauquet P & Maenhaut-Michel G (1988) Nature of the SOS mutator activity: genetic characterization of untargeted mutagenesis in *Escherichia coli*. *Molecular & general genetics : MGG* **213**: 491-498.
- Calmels S, Ohshima H & Bartsch H (1988) Nitrosamine formation by denitrifying and non-denitrifying bacteria: implication of nitrite reductase and nitrate reductase in nitrosation catalysis. *Journal of general microbiology* **134**: 221-226.
- Calmels S, Ohshima H, Vincent P, *et al.* (1985) Screening of microorganisms for nitrosation catalysis at pH 7 and kinetic studies on nitrosamine formation from secondary amines by *E. coli* strains. *Carcinogenesis* **6**: 911-915.
- Candeias LP & Steenken S (1993) Electron transfer in di(deoxy)nucleoside phosphates in aqueous solution. Rapid migration of oxidative damage (via adenine) to guanine. *Journal of the American Chemical Society* **115**: 2437-2440.
- Canning PC, Roth JA, Tabatabai LB, *et al.* (1985) Isolation of components of *Brucella abortus* responsible for inhibition of function in bovine neutrophils. *The Journal of infectious diseases* **152**: 913-921.
- Carrica Mdel C, Fernandez I, Sieira R, *et al.* (2013) The two-component systems PrpBA and NtrYX coordinately regulate the adaptation of *Brucella abortus* to an oxygen-limited environment. *Mol Microbiol* **88**: 222-233.
- Carvalho Neta AV, Mol JP, Xavier MN, *et al.* (2010) Pathogenesis of bovine brucellosis. *Veterinary journal (London, England : 1997)* **184**: 146-155.
- Castaneda-Roldan EI, Avelino-Flores F, Dall'Agnol M, *et al.* (2004) Adherence of *Brucella* to human epithelial cells and macrophages is mediated by sialic acid residues. *Cell Microbiol* **6**: 435-445.
- Catsburg CE, Gago-Dominguez M, Yuan JM, *et al.* (2014) Dietary sources of N-nitroso compounds and bladder cancer risk: findings from the Los Angeles bladder cancer study. *International journal of cancer* **134**: 125-135.
- Celli J (2015) The changing nature of the *Brucella*-containing vacuole. *Cell Microbiol* **17**: 951-958.
- Celli J, Salcedo SP & Gorvel JP (2005) *Brucella* coopts the small GTPase Sar1 for intracellular replication. *Proc Natl Acad Sci U S A* **102**: 1673-1678.
- Celli J, de Chastellier C, Franchini DM, *et al.* (2003) *Brucella* evades macrophage killing via VirB-dependent sustained interactions with the endoplasmic reticulum. *J Exp Med* **198**: 545-556.
- Chain PS, Comerci DJ, Tolmasky ME, *et al.* (2005) Whole-genome analyses of speciation events in pathogenic *Brucellae*. *Infect Immun* **73**: 8353-8361.
- Chakravorty D, Hansen-Wester I & Hensel M (2002) *Salmonella* pathogenicity island 2 mediates protection of intracellular *Salmonella* from reactive nitrogen intermediates. *J Exp Med* **195**: 1155-1166.
- Cheng Z, Miura K, Popov VL, *et al.* (2011) Insights into the CtrA regulon in development of stress resistance in obligatory intracellular pathogen *Ehrlichia chaffeensis*. *Mol Microbiol* **82**: 1217-1234.

- Chetsanga CJ, Lozon M, Makaroff C, *et al.* (1981) Purification and characterization of Escherichia coli formamidopyrimidine-DNA glycosylase that excises damaged 7-methylguanine from deoxyribonucleic acid. *Biochemistry* **20**: 5201-5207.
- Childers WS, Xu Q, Mann TH, *et al.* (2014) Cell fate regulation governed by a repurposed bacterial histidine kinase. *PLoS Biol* **12**: e1001979.
- Cirl C, Wieser A, Yadav M, *et al.* (2008) Subversion of Toll-like receptor signaling by a unique family of bacterial Toll/interleukin-1 receptor domain-containing proteins. *Nature medicine* **14**: 399-406.
- Cohen SE & Walker GC (2010) The transcription elongation factor NusA is required for stress-induced mutagenesis in Escherichia coli. *Current biology : CB* **20**: 80-85.
- Collier J (2012) Regulation of chromosomal replication in Caulobacter crescentus. *Plasmid* **67**: 76-87.
- Collier J, McAdams HH & Shapiro L (2007) A DNA methylation ratchet governs progression through a bacterial cell cycle. *Proc Natl Acad Sci U S A* **104**: 17111-17116.
- Colombi D & Gomes SL (1997) An alkB gene homolog is differentially transcribed during the Caulobacter crescentus cell cycle. *J Bacteriol* **179**: 3139-3145.
- Comerci DJ, Martinez-Lorenzo MJ, Sieira R, *et al.* (2001) Essential role of the VirB machinery in the maturation of the *Brucella abortus*-containing vacuole. *Cell Microbiol* **3**: 159-168.
- Copin R, De Baetselier P, Carlier Y, *et al.* (2007) MyD88-dependent activation of B220-CD11b+LY-6C+ dendritic cells during Brucella melitensis infection. *Journal of immunology (Baltimore, Md : 1950)* **178**: 5182-5191.
- Copin R, Vitry MA, Hanot Mambres D, *et al.* (2012) In situ microscopy analysis reveals local innate immune response developed around Brucella infected cells in resistant and susceptible mice. *PLoS Pathog* **8**: e1002575.
- Corzett CH, Goodman MF & Finkel SE (2013) Competitive fitness during feast and famine: how SOS DNA polymerases influence physiology and evolution in Escherichia coli. *Genetics* **194**: 409-420.
- Cosse MM, Hayward RD & Subtil A (2018) One Face of Chlamydia trachomatis: The Infectious Elementary Body. *Current topics in microbiology and immunology* **412**: 35-58.
- Costa de Oliveira R, Laval J & Boiteux S (1987) Induction of SOS and adaptive responses by alkylating agents in Escherichia coli mutants deficient in 3-methyladenine-DNA glycosylase activities. *Mutat Res* **183**: 11-20.
- Courcelle J, Khodursky A, Peter B, *et al.* (2001) Comparative gene expression profiles following UV exposure in wild-type and SOS-deficient Escherichia coli. *Genetics* **158**: 41-64.
- Cox M, Goodman M, Kreuzer K, *et al.* (2000) The importance of repairing stalled replication forks. *Nature* **404**: 37-41.
- Craig M & Slauch JM (2009) Phagocytic superoxide specifically damages an extracytoplasmic target to inhibit or kill Salmonella. *PLoS One* **4**: e4975.
- Culyba MJ, Kubiak JM, Mo CY, *et al.* (2018) Non-equilibrium repressor binding kinetics link DNA damage dose to transcriptional timing within the SOS gene network. *PLoS Genet* **14**: e1007405.
- Cunningham RP, Saporito SM, Spitzer SG, *et al.* (1986) Endonuclease IV (nfo) mutant of Escherichia coli. *J Bacteriol* **168**: 1120-1127.
- da Rocha RP, Paquola AC, Marques Mdo V, *et al.* (2008) Characterization of the SOS regulon of Caulobacter crescentus. *J Bacteriol* **190**: 1209-1218.
- De Bolle X, Crosson S, Matroule JY, *et al.* (2015) Brucella abortus Cell Cycle and Infection Are Coordinated. *Trends Microbiol* **23**: 812-821.
- Deaconescu AM, Chambers AL, Smith AJ, *et al.* (2006) Structural basis for bacterial transcription-coupled DNA repair. *Cell* **124**: 507-520.
- Dean AS, Crump L, Greter H, *et al.* (2012) Clinical manifestations of human brucellosis: a systematic review and meta-analysis. *PLoS Negl Trop Dis* **6**: e1929.
- Dees S, Thanabalasundrum S, Moss CW, *et al.* (1980) Cellular fatty acid composition of group IVe, a nonsaccharolytic organism from clinical sources. *Journal of clinical microbiology* **11**: 664-668.
- Deghelt M, Mullier C, Sternon JF, *et al.* (2014) The newborn *Brucella abortus* blocked at the G1 stage of its cell cycle is the major infectious bacterial subpopulation. *Nature Communications* **5**: 4366.
- Di Pasquale P, Caterino M, Di Somma A, *et al.* (2016) Exposure of E. coli to DNA-Methylating Agents Impairs Biofilm Formation and Invasion of Eukaryotic Cells via Down Regulation of the N-Acetylneuraminase Lyase NanA. *Front Microbiol* **7**: 147.
- Dinglay S, Treweek SC, Lindahl T, *et al.* (2000) Defective processing of methylated single-stranded DNA by E. coli AlkB mutants. *Genes & development* **14**: 2097-2105.
- Doak SH, Jenkins GJ, Johnson GE, *et al.* (2007) Mechanistic influences for mutation induction curves after exposure to DNA-reactive carcinogens. *Cancer research* **67**: 3904-3911.

- Domian IJ, Quon KC & Shapiro L (1997) Cell type-specific phosphorylation and proteolysis of a transcriptional regulator controls the G1-to-S transition in a bacterial cell cycle. *Cell* **90**: 415-424.
- Domian IJ, Reisenauer A & Shapiro L (1999) Feedback control of a master bacterial cell-cycle regulator. *Proc Natl Acad Sci U S A* **96**: 6648-6653.
- Dotreppe D, Mullier C, Letesson JJ, *et al.* (2011) The alkylation response protein AidB is localized at the new poles and constriction sites in *Brucella abortus*. *BMC Microbiol* **11**: 257.
- Dozot M, Boigegrain RA, Delrue RM, *et al.* (2006) The stringent response mediator Rsh is required for *Brucella melitensis* and *Brucella suis* virulence, and for expression of the type IV secretion system virB. *Cell Microbiol* **8**: 1791-1802.
- Dragotakes Q, Stouffer K, Fu MS, *et al.* (2018) Chance is an important element in phagolysosomal acidification that favors the macrophage. *Preprints BioRxiv*.
- Ducret A, Quardokus EM & Brun YV (2016) MicrobeJ, a tool for high throughput bacterial cell detection and quantitative analysis. *Nature microbiology* **1**: 16077.
- Durbach SI, Springer B, Machowski EE, *et al.* (2003) DNA Alkylation Damage as a Sensor of Nitrosative Stress in *Mycobacterium tuberculosis*. *Infection and Immunity* **71**: 997-1000.
- Eisenbrand G, Denkel E & Pool B (1984) Alcoholdehydrogenase as an activating enzyme for N-nitrosodiethanolamine (NDELA): in vitro activation of NDELA to a potent mutagen in *Salmonella typhimurium*. *Journal of cancer research and clinical oncology* **108**: 76-80.
- Endley S, McMurray D & Ficht TA (2001) Interruption of the *cydB* locus in *Brucella abortus* attenuates intracellular survival and virulence in the mouse model of infection. *J Bacteriol* **183**: 2454-2462.
- Erill I, Jara M, Salvador N, *et al.* (2004) Differences in LexA regulon structure among Proteobacteria through in vivo assisted comparative genomics. *Nucleic Acids Res* **32**: 6617-6626.
- Eskra L, Canavessi A, Carey M, *et al.* (2001) *Brucella abortus* genes identified following constitutive growth and macrophage infection. *Infect Immun* **69**: 7736-7742.
- Espey MG, Miranda KM, Thomas DD, *et al.* (2001) Distinction between nitrosating mechanisms within human cells and aqueous solution. *J Biol Chem* **276**: 30085-30091.
- Esser C, Ahmadinejad N, Wiegand C, *et al.* (2004) A genome phylogeny for mitochondria among alpha-proteobacteria and a predominantly eubacterial ancestry of yeast nuclear genes. *Molecular biology and evolution* **21**: 1643-1660.
- Esteller M, Toyota M, Sanchez-Cespedes M, *et al.* (2000) Inactivation of the DNA repair gene O6-methylguanine-DNA methyltransferase by promoter hypermethylation is associated with G to A mutations in K-ras in colorectal tumorigenesis. *Cancer research* **60**: 2368-2371.
- Fernandez de Henestrosa AR & Barbe J (1991) Induction of the *alkA* gene of *Escherichia coli* in gram-negative bacteria. *J Bacteriol* **173**: 7736-7740.
- Fernandez de Henestrosa AR, Rivera E, Tapias A, *et al.* (1998) Identification of the *Rhodobacter sphaeroides* SOS box. *Mol Microbiol* **28**: 991-1003.
- Fernandez De Henestrosa AR, Ogi T, Aoyagi S, *et al.* (2000) Identification of additional genes belonging to the LexA regulon in *Escherichia coli*. *Mol Microbiol* **35**: 1560-1572.
- Fersht AR & Knill-Jones JW (1981) DNA polymerase accuracy and spontaneous mutation rates: frequencies of purine.purine, purine.pyrimidine, and pyrimidine.pyrimidine mismatches during DNA replication. *Proc Natl Acad Sci U S A* **78**: 4251-4255.
- Fioravanti A, Fumeaux C, Mohapatra SS, *et al.* (2013) DNA binding of the cell cycle transcriptional regulator GcrA depends on N6-adenosine methylation in *Caulobacter crescentus* and other Alphaproteobacteria. *PLoS Genet* **9**: e1003541.
- Fix D, Canugovi C & Bhagwat AS (2008) Transcription increases methylmethane sulfonate-induced mutations in *alkB* strains of *Escherichia coli*. *DNA Repair (Amst)* **7**: 1289-1297.
- Fontecave M, Atta M & Mulliez E (2004) S-adenosylmethionine: nothing goes to waste. *Trends in biochemical sciences* **29**: 243-249.
- Forestier C, Deleuil F, Lapaque N, *et al.* (2000) *Brucella abortus* lipopolysaccharide in murine peritoneal macrophages acts as a down-regulator of T cell activation. *Journal of immunology (Baltimore, Md : 1950)* **165**: 5202-5210.
- Foster JT, Beckstrom-Sternberg SM, Pearson T, *et al.* (2009) Whole-genome-based phylogeny and divergence of the genus *Brucella*. *J Bacteriol* **191**: 2864-2870.
- Fowler RG, White SJ, Koyama C, *et al.* (2003) Interactions among the *Escherichia coli* *mutT*, *mutM*, and *mutY* damage prevention pathways. *DNA Repair (Amst)* **2**: 159-173.
- Frage B, Dohlemann J, Robledo M, *et al.* (2016) Spatiotemporal choreography of chromosome and megaplasmids in the *Sinorhizobium meliloti* cell cycle. *Mol Microbiol* **100**: 808-823.
- Francis N, Poncin K, Fioravanti A, *et al.* (2017) CtrA controls cell division and outer membrane composition of the pathogen *Brucella abortus*. *Mol Microbiol* **103**: 780-797.

- Franco R, Schoneveld O, Georgakilas AG, *et al.* (2008) Oxidative stress, DNA methylation and carcinogenesis. *Cancer letters* **266**: 6-11.
- Friedberg EC, Friedberg E, Walker G, *et al.* (1995) *DNA Repair and Mutagenesis*. ASM Press.
- Fu D, Calvo JA & Samson LD (2012) Balancing repair and tolerance of DNA damage caused by alkylating agents. *Nat Rev Cancer* **12**: 104-120.
- Fumeaux C, Radhakrishnan SK, Ardisson S, *et al.* (2014) Cell cycle transition from S-phase to G1 in *Caulobacter* is mediated by ancestral virulence regulators. *Nat Commun* **5**: 4081.
- Galhardo RS, Rocha RP, Marques MV, *et al.* (2005) An SOS-regulated operon involved in damage-inducible mutagenesis in *Caulobacter crescentus*. *Nucleic Acids Res* **33**: 2603-2614.
- Galibert F, Finan TM, Long SR, *et al.* (2001) The composite genome of the legume symbiont *Sinorhizobium meliloti*. *Science* **293**: 668-672.
- Galkin VE, Yu X, Bielnicki J, *et al.* (2009) Cleavage of bacteriophage lambda cI repressor involves the RecA C-terminal domain. *J Mol Biol* **385**: 779-787.
- Garduno RA, Garduno E, Hiltz M, *et al.* (2002) Intracellular Growth of *Legionella pneumophila* Gives Rise to a Differentiated Form Dissimilar to Stationary-Phase Forms. *Infection and Immunity* **70**: 6273-6283.
- Gay B, Sanchez-Teff S & Caravano R (1984) Ultrastructural localization of NADPH-oxidase activity in murine peritoneal macrophages during phagocytosis of *Brucella*. Correlation with the production of superoxide anions. *Virchows Archiv B, Cell pathology including molecular pathology* **45**: 147-155.
- Gee JM, Valderas MW, Kovach ME, *et al.* (2005) The *Brucella abortus* Cu,Zn superoxide dismutase is required for optimal resistance to oxidative killing by murine macrophages and wild-type virulence in experimentally infected mice. *Infect Immun* **73**: 2873-2880.
- Gibson KE, Campbell GR, Lloret J, *et al.* (2006) CbrA is a stationary-phase regulator of cell surface physiology and legume symbiosis in *Sinorhizobium meliloti*. *J Bacteriol* **188**: 4508-4521.
- Giovannoni SJ, Tripp HJ, Givan S, *et al.* (2005) Genome streamlining in a cosmopolitan oceanic bacterium. *Science* **309**: 1242-1245.
- Godfroid J (2018) *Brucella* spp. at the Wildlife-Livestock Interface: An Evolutionary Trajectory through a Livestock-to-Wildlife "Host Jump"? *Veterinary sciences* **5**.
- Gong C, Bongiorno P, Martins A, *et al.* (2005) Mechanism of nonhomologous end-joining in mycobacteria: a low-fidelity repair system driven by Ku, ligase D and ligase C. *Nature Structural & Molecular Biology* **12**: 304-312.
- Gonzalez Carrero MI, Sangari FJ, Aguero J, *et al.* (2002) *Brucella abortus* strain 2308 produces brucebactin, a highly efficient catecholic siderophore. *Microbiology* **148**: 353-360.
- Gonzalez D, Kozdon JB, McAdams HH, *et al.* (2014) The functions of DNA methylation by CcrM in *Caulobacter crescentus*: a global approach. *Nucleic Acids Res* **42**: 3720-3735.
- Grisham MB, Ware K, Gilleland HE, Jr., *et al.* (1992) Neutrophil-mediated nitrosamine formation: role of nitric oxide in rats. *Gastroenterology* **103**: 1260-1266.
- Gross A, Bertholet S, Mauel J, *et al.* (2004) Impairment of *Brucella* growth in human macrophagic cells that produce nitric oxide. *Microbial Pathogenesis* **36**: 75-82.
- Gross A, Terraza A, Ouahrani-Bettache S, *et al.* (2000) In vitro *Brucella suis* infection prevents the programmed cell death of human monocytic cells. *Infect Immun* **68**: 342-351.
- Gross A, Spiesser S, Terraza A, *et al.* (1998) Expression and bactericidal activity of nitric oxide synthase in *Brucella suis*-infected murine macrophages. *Infect Immun* **66**: 1309-1316.
- Guarne A (2012) The functions of MutL in mismatch repair: the power of multitasking. *Prog Mol Biol Transl Sci* **110**: 41-70.
- Guttenplan JB (1987) N-nitrosamines: bacterial mutagenesis and in vitro metabolism. *Mutat Res* **186**: 81-134.
- Guttenplan JB & Milstein S (1982) On the effects of pH on mutagenesis induced by N-nitroso compounds. *Mutat Res* **93**: 249-250.
- Haakonsen DL, Yuan AH & Laub MT (2015) The bacterial cell cycle regulator GcrA is a sigma70 cofactor that drives gene expression from a subset of methylated promoters. *Genes & development* **29**: 2272-2286.
- Haine V, Dozot M, Dornand J, *et al.* (2006) NnrA is required for full virulence and regulates several *Brucella melitensis* denitrification genes. *J Bacteriol* **188**: 1615-1619.
- Hakura A, Morimoto K, Sofuni T, *et al.* (1991) Cloning and characterization of the *Salmonella typhimurium* ada gene, which encodes O6-methylguanine-DNA methyltransferase. *J Bacteriol* **173**: 3663-3672.
- Hallez R, Bellefontaine AF, Letesson JJ, *et al.* (2004) Morphological and functional asymmetry in alpha-proteobacteria. *Trends Microbiol* **12**: 361-365.
- Hallez R, Mignolet J, Van Mullem V, *et al.* (2007) The asymmetric distribution of the essential histidine kinase PdhS indicates a differentiation event in *Brucella abortus*. *EMBO J* **26**: 1444-1455.

- Hanna N, Ouahrani-Bettache S, Drake KL, *et al.* (2013) Global Rsh-dependent transcription profile of *Brucella suis* during stringent response unravels adaptation to nutrient starvation and cross-talk with other stress responses. *BMC Genomics* **14**: 459.
- Hanot Mambres D, Machelart A, Vanderwinden JM, *et al.* (2015) In Situ Characterization of Splenic *Brucella melitensis* Reservoir Cells during the Chronic Phase of Infection in Susceptible Mice. *PLoS One* **10**: e0137835.
- Hanot Mambres D, Machelart A, Potemberg G, *et al.* (2016) Identification of Immune Effectors Essential to the Control of Primary and Secondary Intranasal Infection with *Brucella melitensis* in Mice. *Journal of immunology (Baltimore, Md : 1950)* **196**: 3780-3793.
- Hansen MS, Rodolakis A, Cochonneau D, *et al.* (2011) *Coxiella burnetii* associated placental lesions and infection level in parturient cows. *Veterinary journal (London, England : 1997)* **190**: e135-139.
- Hecht SS (1999) DNA adduct formation from tobacco-specific N-nitrosamines. *Mutat Res* **424**: 127-142.
- Heinrich K, Sobetzko P & Jonas K (2016) A Kinase-Phosphatase Switch Transduces Environmental Information into a Bacterial Cell Cycle Circuit. *PLoS Genet* **12**: e1006522.
- Henrikus SS, Wood EA, McDonald JP, *et al.* (2018) DNA polymerase IV primarily operates outside of DNA replication forks in *Escherichia coli*. *PLoS Genet* **14**: e1007161.
- Henry C, Loiseau L, Mérida-Florian A, *et al.* (In preparation) Homeostasis of the DNA repair RecA protein is under redox control. *In preparation*.
- Hoffmann GR (1980) Genetic effects of dimethyl sulfate, diethyl sulfate, and related compounds. *Mutat Res* **75**: 63-129.
- Holtzendorff J, Hung D, Brende P, *et al.* (2004) Oscillating global regulators control the genetic circuit driving a bacterial cell cycle. *Science* **304**: 983-987.
- Hop HT, Arayan LT, Huy TXN, *et al.* (2018) Lipocalin 2 (Lcn2) interferes with iron uptake by *Brucella abortus* and dampens immunoregulation during infection of RAW 264.7 macrophages. *Cell Microbiol* **20**.
- Hornback ML & Roop RM, 2nd (2006) The *Brucella abortus* xthA-1 gene product participates in base excision repair and resistance to oxidative killing but is not required for wild-type virulence in the mouse model. *J Bacteriol* **188**: 1295-1300.
- Hottes AK, Shapiro L & McAdams HH (2005) DnaA coordinates replication initiation and cell cycle transcription in *Caulobacter crescentus*. *Mol Microbiol* **58**: 1340-1353.
- Imlay JA (2013) The molecular mechanisms and physiological consequences of oxidative stress: lessons from a model bacterium. *Nat Rev Microbiol* **11**: 443-454.
- Inami K, Shiino J, Hagiwara S, *et al.* (2015) Transnitrosation of non-mutagenic N-nitrosoproline forms mutagenic N-nitroso-N-methylurea. *Bioorganic & medicinal chemistry* **23**: 3297-3302.
- Iwasaki H, Nakata A, Walker GC, *et al.* (1990) The *Escherichia coli* polB gene, which encodes DNA polymerase II, is regulated by the SOS system. *J Bacteriol* **172**: 6268-6273.
- Iyengar R, Stuehr DJ & Marletta MA (1987) Macrophage synthesis of nitrite, nitrate, and N-nitrosamines: precursors and role of the respiratory burst. *Proc Natl Acad Sci U S A* **84**: 6369-6373.
- Jacobs C, Ausmees N, Cordwell SJ, *et al.* (2003) Functions of the CckA histidine kinase in *Caulobacter* cell cycle control. *Mol Microbiol* **47**: 1279-1290.
- James PE, Grinberg OY, Michaels G, *et al.* (1995) Intraphagosomal oxygen in stimulated macrophages. *Journal of cellular physiology* **163**: 241-247.
- Janion C (2008) Inducible SOS response system of DNA repair and mutagenesis in *Escherichia coli*. *International journal of biological sciences* **4**: 338-344.
- Jatsenko T, Sidorenko J, Saumaa S, *et al.* (2017) DNA Polymerases ImuC and DinB Are Involved in DNA Alkylation Damage Tolerance in *Pseudomonas aeruginosa* and *Pseudomonas putida*. *PLoS One* **12**: e0170719.
- Jeggo P, Defais TM, Samson L, *et al.* (1977) An adaptive response of *E. coli* to low levels of alkylating agent: comparison with previously characterised DNA repair pathways. *Molecular & general genetics : MGG* **157**: 1-9.
- Jenal U & Fuchs T (1998) An essential protease involved in bacterial cell-cycle control. *Embo j* **17**: 5658-5669.
- Jiang X, Leonard B, Benson R, *et al.* (1993) Macrophage control of *Brucella abortus*: role of reactive oxygen intermediates and nitric oxide. *Cellular immunology* **151**: 309-319.
- Jimenez de Bagues MP, Loisel-Meyer S, Liautard JP, *et al.* (2007) Different roles of the two high-oxygen-affinity terminal oxidases of *Brucella suis*: Cytochrome c oxidase, but not ubiquinol oxidase, is required for persistence in mice. *Infect Immun* **75**: 531-535.
- Johnson AD, Poteete AR, Lauer G, *et al.* (1981) lambda Repressor and cro--components of an efficient molecular switch. *Nature* **294**: 217-223.
- Kaasen I, Evensen G & Seeberg E (1986) Amplified expression of the tag+ and alkA+ genes in *Escherichia coli*: identification of gene products and effects on alkylation resistance. *J Bacteriol* **168**: 642-647.

- Kadyrov FA, Dzantiev L, Constantin N, *et al.* (2006) Endonucleolytic function of MutL α in human mismatch repair. *Cell* **126**: 297-308.
- Kahng LS & Shapiro L (2003) Polar localization of replicon origins in the multipartite genomes of *Agrobacterium tumefaciens* and *Sinorhizobium meliloti*. *J Bacteriol* **185**: 3384-3391.
- Kato T & Shinoura Y (1977) Isolation and characterization of mutants of *Escherichia coli* deficient in induction of mutations by ultraviolet light. *Molecular & general genetics : MGG* **156**: 121-131.
- Katzmann E, Muller FD, Lang C, *et al.* (2011) Magnetosome chains are recruited to cellular division sites and split by asymmetric septation. *Mol Microbiol* **82**: 1316-1329.
- Kaufman A & Walker GC (1990) A constitutive O6-methylguanine-DNA methyltransferase of *Rhizobium meliloti*. *Mutat Res* **235**: 165-169.
- Khan SR, Gaines J, Roop RM, 2nd, *et al.* (2008) Broad-host-range expression vectors with tightly regulated promoters and their use to examine the influence of TraR and TraM expression on Ti plasmid quorum sensing. *Appl Environ Microbiol* **74**: 5053-5062.
- Kikuchi H, Kim S, Watanabe K, *et al.* (2006) *Brucella abortus*-d-alanyl-D-alanine carboxypeptidase contributes to its intracellular replication and resistance against nitric oxide. *FEMS Microbiol Lett* **259**: 120-125.
- Kim HS, Willett JW, Jain-Gupta N, *et al.* (2014) The *Brucella abortus* virulence regulator, LovhK, is a sensor kinase in the general stress response signalling pathway. *Mol Microbiol* **94**: 913-925.
- Kim IG & Oh TJ (2000) SOS induction of the *recA* gene by UV-, gamma-irradiation and mitomycin C is mediated by polyamines in *Escherichia coli* K-12. *Toxicol Lett* **116**: 143-149.
- Kiraly O, Gong G, Roytman MD, *et al.* (2014) DNA glycosylase activity and cell proliferation are key factors in modulating homologous recombination in vivo. *Carcinogenesis* **35**: 2495-2502.
- Klapacz J, Pottenger LH, Engelward BP, *et al.* (2016) Contributions of DNA repair and damage response pathways to the non-linear genotoxic responses of alkylating agents. *Mutat Res Rev Mutat Res* **767**: 77-91.
- Ko J, Gendron-Fitzpatrick A & Splitter GA (2002) Susceptibility of IFN regulatory factor-1 and IFN consensus sequence binding protein-deficient mice to brucellosis. *Journal of immunology (Baltimore, Md : 1950)* **168**: 2433-2440.
- Kohler S, Porte F, Jubier-Maurin V, *et al.* (2002) The intramacrophagic environment of *Brucella suis* and bacterial response. *Veterinary microbiology* **90**: 299-309.
- Köhler S, Michaux-Charachon S, Porte F, *et al.* (2003) What is the nature of the replicative niche of a stealthy bug named *Brucella*? *Trends in Microbiology* **11**: 215-219.
- Kondo H, Nakabeppu Y, Kataoka H, *et al.* (1986) Structure and expression of the *alkB* gene of *Escherichia coli* related to the repair of alkylated DNA. *J Biol Chem* **261**: 15772-15777.
- Kondo N, Takahashi A, Ono K, *et al.* (2010) DNA damage induced by alkylating agents and repair pathways. *J Nucleic Acids* **2010**: 543531.
- Kosaka H, Wishnok JS, Miwa M, *et al.* (1989) Nitrosation by stimulated macrophages. Inhibitors, enhancers and substrates. *Carcinogenesis* **10**: 563-566.
- Kozdon JB, Melfi MD, Luong K, *et al.* (2013) Global methylation state at base-pair resolution of the *Caulobacter* genome throughout the cell cycle. *Proc Natl Acad Sci U S A* **110**: E4658-4667.
- Kreutzer DL, Dreyfus LA & Robertson DC (1979) Interaction of polymorphonuclear leukocytes with smooth and rough strains of *Brucella abortus*. *Infect Immun* **23**: 737-742.
- Kuma A, Hatano M, Matsui M, *et al.* (2004) The role of autophagy during the early neonatal starvation period. *Nature* **432**: 1032-1036.
- Kumar Y & Valdivia RH (2009) Leading a sheltered life: intracellular pathogens and maintenance of vacuolar compartments. *Cell Host Microbe* **5**: 593-601.
- Kunisaki N & Hayashi M (1979) Formation of N-nitrosamines from secondary amines and nitrite by resting cells of *Escherichia coli* B. *Appl Environ Microbiol* **37**: 279-282.
- Kunkel TA & Erie DA (2005) DNA mismatch repair. *Annual review of biochemistry* **74**: 681-710.
- Kuzminov A & Stahl FW (1999) Double-strand end repair via the RecBC pathway in *Escherichia coli* primes DNA replication. *Genes & development* **13**: 345-356.
- Lam H, Matroule J-Y & Jacobs-Wagner C (2003) The Asymmetric Spatial Distribution of Bacterial Signal Transduction Proteins Coordinates Cell Cycle Events. *Developmental Cell* **5**: 149-159.
- Lamontagne J, Forest A, Marazzo E, *et al.* (2009) Intracellular adaptation of *Brucella abortus*. *J Proteome Res* **8**: 1594-1609.
- Lang KS & Merrih H (2018) The Clash of Macromolecular Titans: Replication-Transcription Conflicts in Bacteria. *Annual review of microbiology* **72**: 71-88.
- Lapaque N, Takeuchi O, Corrales F, *et al.* (2006) Differential inductions of TNF- α and I κ B by structurally diverse classic and non-classic lipopolysaccharides. *Cell Microbiol* **8**: 401-413.

- Laub M, Chen S & McAdams LSH (2002) Genes directly controlled by CtrA, a master regulator of the Caulobacter cell cycle. *Proc Natl Acad Sci U S A* **99**: 4632-4637.
- Laub M, McAdams H, Feldblyum T, *et al.* (2000) Global analysis of the genetic network controlling a bacterial cell cycle. *Science* **290**: 2144-2148.
- Lee DJ, Minchin SD & Busby SJ (2012) Activating transcription in bacteria. *Annual review of microbiology* **66**: 125-152.
- Leimkühler S (2017) Shared function and moonlighting proteins in molybdenum cofactor biosynthesis. *Biological Chemistry* **398**.
- Lennon CW, Ross W, Martin-Tumasz S, *et al.* (2012) Direct interactions between the coiled-coil tip of DksA and the trigger loop of RNA polymerase mediate transcriptional regulation. *Genes & development* **26**: 2634-2646.
- Lesley JA & Shapiro L (2008) SpoT regulates DnaA stability and initiation of DNA replication in carbon-starved *Caulobacter crescentus*. *J Bacteriol* **190**: 6867-6880.
- Lestrade P, Dricot A, Delrue RM, *et al.* (2003) Attenuated Signature-Tagged Mutagenesis Mutants of *Brucella melitensis* Identified during the Acute Phase of Infection in Mice. *Infection and Immunity* **71**: 7053-7060.
- Li Z, Pearlman AH & Hsieh P (2016) DNA mismatch repair and the DNA damage response. *DNA Repair (Amst)* **38**: 94-101.
- Lindahl T, Sedgwick B, Sekiguchi M, *et al.* (1988) Regulation and expression of the adaptive response to alkylating agents. *Annual review of biochemistry* **57**: 133-157.
- Lips J & Kaina B (2001) Repair of O(6)-methylguanine is not affected by thymine base pairing and the presence of MMR proteins. *Mutat Res* **487**: 59-66.
- Little JW (1991) Mechanism of specific LexA cleavage: autodigestion and the role of RecA coprotease. *Biochimie* **73**: 411-421.
- Little JW & Mount DW (1982) The SOS regulatory system of *Escherichia coli*. *Cell* **29**: 11-22.
- Livny J, Yamaichi Y & Waldor MK (2007) Distribution of centromere-like *parS* sites in bacteria: insights from comparative genomics. *J Bacteriol* **189**: 8693-8703.
- Ljungquist S, Lindahl T & Howard-Flanders P (1976) Methyl methane sulfonate-sensitive mutant of *Escherichia coli* deficient in an endonuclease specific for apurinic sites in deoxyribonucleic acid. *J Bacteriol* **126**: 646-653.
- Loechler EL (1994) A violation of the Swain-Scott principle, and not SN1 versus SN2 reaction mechanisms, explains why carcinogenic alkylating agents can form different proportions of adducts at oxygen versus nitrogen in DNA. *Chem Res Toxicol* **7**: 277-280.
- Loisel-Meyer S, Jimenez de Bagues MP, Basseres E, *et al.* (2006) Requirement of *norD* for *Brucella suis* virulence in a murine model of in vitro and in vivo infection. *Infect Immun* **74**: 1973-1976.
- Lopez-Goni I, Moriyon I & Neilands JB (1992) Identification of 2,3-dihydroxybenzoic acid as a *Brucella abortus* siderophore. *Infect Immun* **60**: 4496-4503.
- Lopez-Urrutia L, Alonso A, Nieto ML, *et al.* (2000) Lipopolysaccharides of *Brucella abortus* and *Brucella melitensis* induce nitric oxide synthesis in rat peritoneal macrophages. *Infect Immun* **68**: 1740-1745.
- Lori C, Ozaki S, Steiner S, *et al.* (2015) Cyclic di-GMP acts as a cell cycle oscillator to drive chromosome replication. *Nature* **523**: 236-239.
- Lu SC (2000) S-Adenosylmethionine. *The international journal of biochemistry & cell biology* **32**: 391-395.
- Mackay WJ, Han S & Samson LD (1994) DNA alkylation repair limits spontaneous base substitution mutations in *Escherichia coli*. *J Bacteriol* **176**: 3224-3230.
- Mao Z, Bozzella M, Seluanov A, *et al.* (2008) DNA repair by nonhomologous end joining and homologous recombination during cell cycle in human cells. *Cell cycle (Georgetown, Tex)* **7**: 2902-2906.
- Martin DW, Baumgartner JE, Gee JM, *et al.* (2012) *SodA* is a major metabolic antioxidant in *Brucella abortus* 2308 that plays a significant, but limited, role in the virulence of this strain in the mouse model. *Microbiology* **158**: 1767-1774.
- Martins-Pinheiro M, Marques RC & Menck CF (2007) Genome analysis of DNA repair genes in the alpha proteobacterium *Caulobacter crescentus*. *BMC Microbiol* **7**: 17.
- Martirosyan A, Moreno E & Gorvel JP (2011) An evolutionary strategy for a stealthy intracellular *Brucella* pathogen. *Immunol Rev* **240**: 211-234.
- Maxam AM & Gilbert W (1980) Sequencing end-labeled DNA with base-specific chemical cleavages. *Methods in enzymology* **65**: 499-560.
- Mazon G, Philippin G, Cadet J, *et al.* (2010) Alkyltransferase-like protein (eATL) prevents mismatch repair-mediated toxicity induced by O6-alkylguanine adducts in *Escherichia coli*. *Proc Natl Acad Sci U S A* **107**: 18050-18055.
- McCarthy JG, Edington BV & Schendel PF (1983) Inducible repair of phosphotriesters in *Escherichia coli*. *Proc Natl Acad Sci U S A* **80**: 7380-7384.

- Melek IM, Erdogan S, Celik S, *et al.* (2006) Evaluation of oxidative stress and inflammation in long term *Brucella melitensis* infection. *Molecular and cellular biochemistry* **293**: 203-209.
- Mercer RG, Callister SJ, Lipton MS, *et al.* (2010) Loss of the response regulator CtrA causes pleiotropic effects on gene expression but does not affect growth phase regulation in *Rhodobacter capsulatus*. *J Bacteriol* **192**: 2701-2710.
- Mergaert P, Uchiumi T, Alunni B, *et al.* (2006) Eukaryotic control on bacterial cell cycle and differentiation in the *Rhizobium-legume* symbiosis. *Proc Natl Acad Sci U S A* **103**: 5230-5235.
- Mertens K, Lantsheer L, Ennis DG, *et al.* (2008) Constitutive SOS expression and damage-inducible AddAB-mediated recombinational repair systems for *Coxiella burnetii* as potential adaptations for survival within macrophages. *Mol Microbiol* **69**: 1411-1426.
- Mestankova H, Schirmer K, Canonica S, *et al.* (2014) Development of mutagenicity during degradation of N-nitrosamines by advanced oxidation processes. *Water Res* **66**: 399-410.
- Miao J, Huo Y, Lv X, *et al.* (2016) Fast-response and highly selective fluorescent probes for biological signaling molecule NO based on N-nitrosation of electron-rich aromatic secondary amines. *Biomaterials* **78**: 11-19.
- Mielecki D & Grzesiuk E (2014) Ada response - a strategy for repair of alkylated DNA in bacteria. *FEMS Microbiol Lett* **355**: 1-11.
- Mielecki D, Wrzesinski M & Grzesiuk E (2015) Inducible repair of alkylated DNA in microorganisms. *Mutat Res Rev Mutat Res* **763**: 294-305.
- Mielecki D, Saumaa S, Wrzesinski M, *et al.* (2013) *Pseudomonas putida* AlkA and AlkB proteins comprise different defense systems for the repair of alkylation damage to DNA - in vivo, in vitro, and in silico studies. *PLoS One* **8**: e76198.
- Miller BH, Fratti RA, Poschet JF, *et al.* (2004) Mycobacteria inhibit nitric oxide synthase recruitment to phagosomes during macrophage infection. *Infect Immun* **72**: 2872-2878.
- Miller CN, Smith EP, Cundiff JA, *et al.* (2017) A *Brucella* Type IV Effector Targets the COG Tethering Complex to Remodel Host Secretory Traffic and Promote Intracellular Replication. *Cell Host Microbe* **22**: 317-329 e317.
- Mirvish SS (1975) Formation of N-nitroso compounds: chemistry, kinetics, and in vivo occurrence. *Toxicology and applied pharmacology* **31**: 325-351.
- Miwa M, Stuehr DJ, Marletta MA, *et al.* (1987) Nitrosation of amines by stimulated macrophages. *Carcinogenesis* **8**: 955-958.
- Mo CY, Birdwell LD & Kohli RM (2014) Specificity determinants for autoproteolysis of LexA, a key regulator of bacterial SOS mutagenesis. *Biochemistry* **53**: 3158-3168.
- Mohana-Borges R, Pacheco AB, Sousa FJ, *et al.* (2000) LexA repressor forms stable dimers in solution. The role of specific dna in tightening protein-protein interactions. *J Biol Chem* **275**: 4708-4712.
- Molofsky AB & Swanson MS (2004) Differentiate to thrive: lessons from the *Legionella pneumophila* life cycle. *Mol Microbiol* **53**: 29-40.
- Moreno E & Moriyon I (2002) *Brucella melitensis*: a nasty bug with hidden credentials for virulence. *Proc Natl Acad Sci U S A* **99**: 1-3.
- Moreno E & Moriyon I (2006) The Genus *Brucella*. *Prokaryotes* **5**: 315-456.
- Morimatsu K & Kowalczykowski SC (2003) RecFOR proteins load RecA protein onto gapped DNA to accelerate DNA strand exchange: a universal step of recombinational repair. *Molecular cell* **11**: 1337-1347.
- Moser M & Leo O (2010) Key concepts in immunology. *Vaccine* **28 Suppl 3**: C2-13.
- Murray SM, Panis G, Fumeaux C, *et al.* (2013) Computational and genetic reduction of a cell cycle to its simplest, primordial components. *PLoS Biol* **11**: e1001749.
- Nakano K, Yamada Y, Takahashi E, *et al.* (2017) *E. coli* mismatch repair enhances AT-to-GC mutagenesis caused by alkylating agents. *Mutat Res* **815**: 22-27.
- Naslund M, Segerback D & Kolman A (1983) S-adenosylmethionine, an endogenous alkylating agent. *Mutat Res* **119**: 229-232.
- Nichols DS & McMeekin TA (2002) Biomarker techniques to screen for bacteria that produce polyunsaturated fatty acids. *Journal of microbiological methods* **48**: 161-170.
- Nowosielska A, Smith SA, Engelward BP, *et al.* (2006) Homologous recombination prevents methylation-induced toxicity in *Escherichia coli*. *Nucleic Acids Res* **34**: 2258-2268.
- Ohshima H, Tsuda M, Adachi H, *et al.* (1991) L-arginine-dependent formation of N-nitrosamines by the cytosol of macrophages activated with lipopolysaccharide and interferon-gamma. *Carcinogenesis* **12**: 1217-1220.
- Osborne MR & Phillips DH (2000) Preparation of a methylated DNA standard, and its stability on storage. *Chem Res Toxicol* **13**: 257-261.
- Ozaki S, Schalch-Moser A, Zumthor L, *et al.* (2014) Activation and polar sequestration of PopA, a c-di-GMP effector protein involved in *Caulobacter crescentus* cell cycle control. *Mol Microbiol* **94**: 580-594.

- Pandya GA, Yang IY, Grollman AP, *et al.* (2000) Escherichia coli responses to a single DNA adduct. *J Bacteriol* **182**: 6598-6604.
- Pappas G, Papadimitriou P, Akritidis N, *et al.* (2006) The new global map of human brucellosis. *Lancet Infect Dis* **6**: 91-99.
- Paul BJ, Barker MM, Ross W, *et al.* (2004) DksA: a critical component of the transcription initiation machinery that potentiates the regulation of rRNA promoters by ppGpp and the initiating NTP. *Cell* **118**: 311-322.
- Paul R, Jaeger T, Abel S, *et al.* (2008) Allosteric regulation of histidine kinases by their cognate response regulator determines cell fate. *Cell* **133**: 452-461.
- Paulley JT, Anderson ES & Roop RM, 2nd (2007) Brucella abortus requires the heme transporter BhuA for maintenance of chronic infection in BALB/c mice. *Infect Immun* **75**: 5248-5254.
- Pickett MJ & Nelson EL (1954) Speciation within the genus Brucella. III. Nitrate reduction and nitrite toxicity tests. *J Bacteriol* **68**: 63-66.
- Pillon MC, Lorenowicz JJ, Uckelmann M, *et al.* (2010) Structure of the endonuclease domain of MutL: unlicensed to cut. *Molecular cell* **39**: 145-151.
- Pini F, De Nisco NJ, Ferri L, *et al.* (2015) Cell Cycle Control by the Master Regulator CtrA in Sinorhizobium meliloti. *PLoS Genet* **11**: e1005232.
- Pini F, Frage B, Ferri L, *et al.* (2013) The DivJ, CbrA and PleC system controls DivK phosphorylation and symbiosis in Sinorhizobium meliloti. *Mol Microbiol* **90**: 54-71.
- Pinto UM, Pappas KM & Winans SC (2012) The ABCs of plasmid replication and segregation. *Nat Rev Microbiol* **10**: 755-765.
- Pireaux V, Sauvage A, Bihin B, *et al.* (2016) Myeloperoxidase-Oxidized LDLs Enhance an Anti-Inflammatory M2 and Antioxidant Phenotype in Murine Macrophages. *Mediators Inflamm* **2016**: 8249476.
- Pitzer JE, Zeczycki TN, Baumgartner JE, *et al.* (2018) The manganese-dependent pyruvate kinase PykM is required for wild-type glucose utilization by Brucella abortus 2308 and its virulence in C57BL/6 mice. *J Bacteriol*.
- Pizarro-Cerda J, Meresse S, Parton RG, *et al.* (1998) Brucella abortus transits through the autophagic pathway and replicates in the endoplasmic reticulum of nonprofessional phagocytes. *Infect Immun* **66**: 5711-5724.
- Poncin K, Gillet S & De Bolle X (2018) Learning from the master: targets and functions of the CtrA response regulator in Brucella abortus and other alpha-proteobacteria. *FEMS Microbiol Rev* **42**: 500-513.
- Porte F, Liautard JP & Kohler S (1999) Early acidification of phagosomes containing Brucella suis is essential for intracellular survival in murine macrophages. *Infect Immun* **67**: 4041-4047.
- Posnick LM & Samson LD (1999) Influence of S-adenosylmethionine pool size on spontaneous mutation, dam methylation, and cell growth of Escherichia coli. *J Bacteriol* **181**: 6756-6762.
- Puri RV, Reddy PV & Tyagi AK (2014) Apurinic/aprimidinic endonucleases of Mycobacterium tuberculosis protect against DNA damage but are dispensable for the growth of the pathogen in guinea pigs. *PLoS One* **9**: e92035.
- Qin QM, Pei J, Ancona V, *et al.* (2008) RNAi screen of endoplasmic reticulum-associated host factors reveals a role for IRE1alpha in supporting Brucella replication. *PLoS Pathog* **4**: e1000110.
- Quardokus EM & Brun YV (2003) Cell cycle timing and developmental checkpoints in Caulobacter crescentus. *Curr Opin Microbiol* **6**: 541-549.
- Quon K, Yang B, Domian I, *et al.* (1998) Negative control of bacterial DNA replication by a cell cycle regulatory protein that binds at the chromosome origin. *Proc Natl Acad Sci U S A* **95**: 120-125.
- Quon KC, Marczynski GT & Shapiro L (1996) Cell cycle control by an essential bacterial two-component signal transduction protein. *Cell* **84**: 83-93.
- Ralt D, Wishnok JS, Fitts R, *et al.* (1988) Bacterial catalysis of nitrosation: involvement of the nar operon of Escherichia coli. *J Bacteriol* **170**: 359-364.
- Rebeck GW & Samson L (1991) Increased spontaneous mutation and alkylation sensitivity of Escherichia coli strains lacking the ogt O6-methylguanine DNA repair methyltransferase. *J Bacteriol* **173**: 2068-2076.
- Reisenauer A, Quon K & Shapiro L (1999) The CtrA response regulator mediates temporal control of gene expression during the Caulobacter cell cycle. *J Bacteriol* **181**: 2430-2439.
- Rippa V, Duilio A, di Pasquale P, *et al.* (2011) Preferential DNA damage prevention by the E. coli AidB gene: A new mechanism for the protection of specific genes. *DNA Repair (Amst)* **10**: 934-941.
- Robertson GT, Reisenauer A, Wright R, *et al.* (2000) The Brucella abortus CcrM DNA methyltransferase is essential for viability, and its overexpression attenuates intracellular replication in murine macrophages. *J Bacteriol* **182**: 3482-3489.
- Rocha EP, Cornet E & Michel B (2005) Comparative and evolutionary analysis of the bacterial homologous recombination systems. *PLoS Genet* **1**: e15.
- Ronneau S, Petit K, De Bolle X, *et al.* (2016) Phosphotransferase-dependent accumulation of (p)ppGpp in response to glutamine deprivation in Caulobacter crescentus. *Nat Commun* **7**: 11423.

- Ronneau S, Moussa S, Barbier T, *et al.* (2016) Brucella, nitrogen and virulence. *Crit Rev Microbiol* **42**: 507-525.
- Roop RM, 2nd (2012) Metal acquisition and virulence in Brucella. *Animal health research reviews* **13**: 10-20.
- Roop RM, 2nd, Gaines JM, Anderson ES, *et al.* (2009) Survival of the fittest: how Brucella strains adapt to their intracellular niche in the host. *Med Microbiol Immunol* **198**: 221-238.
- Rossetti CA, Galindo CL, Garner HR, *et al.* (2011) Transcriptional profile of the intracellular pathogen *Brucella melitensis* following HeLa cells infection. *Microb Pathog* **51**: 338-344.
- Roux B, Rodde N, Jardinaud MF, *et al.* (2014) An integrated analysis of plant and bacterial gene expression in symbiotic root nodules using laser-capture microdissection coupled to RNA sequencing. *Plant J* **77**: 817-837.
- Roux CM, Booth NJ, Bellaire BH, *et al.* (2006) RecA and RadA proteins of Brucella abortus do not perform overlapping protective DNA repair functions following oxidative burst. *J Bacteriol* **188**: 5187-5195.
- Rydberg B & Lindahl T (1982) Nonenzymatic methylation of DNA by the intracellular methyl group donor S-adenosyl-L-methionine is a potentially mutagenic reaction. *Embo j* **1**: 211-216.
- Salcedo SP & Holden DW (2005) Bacterial interactions with the eukaryotic secretory pathway. *Curr Opin Microbiol* **8**: 92-98.
- Salcedo SP, Chevrier N, Lacerda TL, *et al.* (2013) Pathogenic *brucellae* replicate in human trophoblasts. *The Journal of infectious diseases* **207**: 1075-1083.
- Salcedo SP, Marchesini MI, Lelouard H, *et al.* (2008) Brucella control of dendritic cell maturation is dependent on the TIR-containing protein Btp1. *PLoS Pathog* **4**: e21.
- Samartino LE & Enright FM (1993) Pathogenesis of abortion of bovine brucellosis. *Comparative immunology, microbiology and infectious diseases* **16**: 95-101.
- Samson L & Cairns J (1977) A new pathway for DNA repair in Escherichia coli. *Nature* **267**: 281-283.
- Samson L, Thomale J & Rajewsky MF (1988) Alternative pathways for the in vivo repair of O6-alkylguanine and O4-alkylthymine in Escherichia coli: the adaptive response and nucleotide excision repair. *Embo j* **7**: 2261-2267.
- Sangari FJ, Seoane A, Rodriguez MC, *et al.* (2007) Characterization of the urease operon of Brucella abortus and assessment of its role in virulence of the bacterium. *Infect Immun* **75**: 774-780.
- Sanongkiet S, Ponnikorn S, Udomsangpetch R, *et al.* (2016) Burkholderia pseudomallei rpoS mediates iNOS suppression in human hepatocyte (HC04) cells. *FEMS Microbiol Lett* **363**.
- Sassanfar M & Roberts JW (1990) Nature of the SOS-inducing signal in Escherichia coli. The involvement of DNA replication. *J Mol Biol* **212**: 79-96.
- Schallies KB, Sadowski C, Meng J, *et al.* (2015) Sinorhizobium meliloti CtrA Stability Is Regulated in a CbrA-Dependent Manner That Is Influenced by CpdR1. *J Bacteriol* **197**: 2139-2149.
- Schlosser-Silverman E, Elgrably-Weiss M, Rosenshine I, *et al.* (2000) Characterization of Escherichia coli DNA lesions generated within J774 macrophages. *J Bacteriol* **182**: 5225-5230.
- Schnappinger D, Ehrh S, Voskuil MI, *et al.* (2003) Transcriptional Adaptation of Mycobacterium tuberculosis within Macrophages: Insights into the Phagosomal Environment. *J Exp Med* **198**: 693-704.
- Schoonhoven NM, O'Flaherty DK, McManus FP, *et al.* (2017) Altering Residue 134 Confers an Increased Substrate Range of Alkylated Nucleosides to the E. coli OGT Protein. *Molecules* **22**.
- Schwan WR, Huang XZ, Hu L, *et al.* (2000) Differential bacterial survival, replication, and apoptosis-inducing ability of Salmonella serovars within human and murine macrophages. *Infect Immun* **68**: 1005-1013.
- Seaver LC & Imlay JA (2001) Hydrogen peroxide fluxes and compartmentalization inside growing Escherichia coli. *J Bacteriol* **183**: 7182-7189.
- Sedgwick B (1987) Molecular signal for induction of the adaptive response to alkylation damage in Escherichia coli. *Journal of cell science Supplement* **6**: 215-223.
- Sedgwick B (1997) Nitrosated peptides and polyamines as endogenous mutagens in O6-alkylguanine-DNA alkyltransferase deficient cells. *Carcinogenesis* **18**: 1561-1567.
- Sedzicki J, Tschon T, Low SH, *et al.* (2018) 3D correlative electron microscopy reveals continuity of Brucella-containing vacuoles with the endoplasmic reticulum. *Journal of cell science*.
- Selby CP & Sancar A (1993) Molecular mechanism of transcription-repair coupling. *Science* **260**: 53-58.
- Shephard SE, Hegi ME & Lutz WK (1987) In-vitro assays to detect alkylating and mutagenic activities of dietary components nitrosated in situ. *IARC scientific publications* 232-236.
- Shivange G, Monisha M, Nigam R, *et al.* (2016) RecA stimulates AlkB-mediated direct repair of DNA adducts. *Nucleic Acids Res* **44**: 8754-8763.
- Siam R & Marczyński GT (2000) Cell cycle regulator phosphorylation stimulates two distinct modes of binding at a chromosome replication origin. *Embo j* **19**: 1138-1147.
- Simmons L, Foti J, Cohen S, *et al.* (2008) The SOS Regulatory Network. *EcoSal Plus*.
- Slilaty SN & Little JW (1987) Lysine-156 and serine-119 are required for LexA repressor cleavage: a possible mechanism. *Proc Natl Acad Sci U S A* **84**: 3987-3991.

- Smith H, Williams AE, Pearce JH, *et al.* (1962) Foetal erythritol: a cause of the localization of *Brucella abortus* in bovine contagious abortion. *Nature* **193**: 47-49.
- Smith JA, Khan M, Magnani DD, *et al.* (2013) *Brucella* induces an unfolded protein response via TcpB that supports intracellular replication in macrophages. *PLoS Pathog* **9**: e1003785.
- Smith MB & March J (2007) March's Advanced Organic Chemistry: Reactions, Mechanisms, and Structure. 6th edition. *Journal of Medicinal Chemistry* **50**: 2279-2280.
- Smith SC, Joshi KK, Zik JJ, *et al.* (2014) Cell cycle-dependent adaptor complex for ClpXP-mediated proteolysis directly integrates phosphorylation and second messenger signals. *Proc Natl Acad Sci U S A* **111**: 14229-14234.
- Sparacino-Watkins C, Stolz JF & Basu P (2014) Nitrate and periplasmic nitrate reductases. *Chemical Society reviews* **43**: 676-706.
- Speina E, Ciesla JM, Wojcik J, *et al.* (2001) The pyrimidine ring-opened derivative of 1,N6-ethenoadenine is excised from DNA by the *Escherichia coli* Fpg and Nth proteins. *J Biol Chem* **276**: 21821-21827.
- Sperry JF & Robertson DC (1975) Erythritol catabolism by *Brucella abortus*. *J Bacteriol* **121**: 619-630.
- Stackebrandt E (1988) Phylogenetic relationships vs. phenotypic diversity: how to achieve a phylogenetic classification system of the eubacteria. *Canadian journal of microbiology* **34**: 552-556.
- Staron A & Mascher T (2010) General stress response in alpha-proteobacteria: PhyR and beyond. *Mol Microbiol* **78**: 271-277.
- Starr T, Ng TW, Wehrly TD, *et al.* (2008) *Brucella* intracellular replication requires trafficking through the late endosomal/lysosomal compartment. *Traffic* **9**: 678-694.
- Starr T, Child R, Wehrly TD, *et al.* (2012) Selective subversion of autophagy complexes facilitates completion of the *Brucella* intracellular cycle. *Cell Host Microbe* **11**: 33-45.
- Steele KH, Baumgartner JE, Valderas MW, *et al.* (2010) Comparative study of the roles of AhpC and KatE as respiratory antioxidants in *Brucella abortus* 2308. *J Bacteriol* **192**: 4912-4922.
- Stephens C, Reisenauer A, Wright R, *et al.* (1996) A cell cycle-regulated bacterial DNA methyltransferase is essential for viability. *Proc Natl Acad Sci U S A* **93**: 1210-1214.
- Sternon JF, Godessart P, Goncalves de Freitas R, *et al.* (2018) Transposon Sequencing of *Brucella abortus* Uncovers Essential Genes for Growth In Vitro and Inside Macrophages. *Infect Immun* **86**.
- Stewart V (1988) Nitrate respiration in relation to facultative metabolism in enterobacteria. *Microbiological reviews* **52**: 190-232.
- Taguchi Y, Imaoka K, Kataoka M, *et al.* (2015) Yip1A, a novel host factor for the activation of the IRE1 pathway of the unfolded protein response during *Brucella* infection. *PLoS Pathog* **11**: e1004747.
- Taira K, Nakamura S, Nakano K, *et al.* (2008) Binding of MutS protein to oligonucleotides containing a methylated or an ethylated guanine residue, and correlation with mutation frequency. *Mutat Res* **640**: 107-112.
- Tapias A & Barbe J (1998) Mutational analysis of the *Rhizobium etli* recA operator. *J Bacteriol* **180**: 6325-6331.
- Tapias A, Fernandez S, Alonso JC, *et al.* (2002) *Rhodobacter sphaeroides* LexA has dual activity: optimising and repressing recA gene transcription. *Nucleic Acids Res* **30**: 1539-1546.
- Tatum FM, Morfitt DC & Halling SM (1993) Construction of a *Brucella abortus* RecA mutant and its survival in mice. *Microb Pathog* **14**: 177-185.
- Taverna P & Sedgwick B (1996) Generation of an endogenous DNA-methylating agent by nitrosation in *Escherichia coli*. *J Bacteriol* **178**: 5105-5111.
- Thanbichler M (2009) Spatial regulation in *Caulobacter crescentus*. *Curr Opin Microbiol* **12**: 715-721.
- Thomas AD, Jenkins GJ, Kaina B, *et al.* (2013) Influence of DNA repair on nonlinear dose-responses for mutation. *Toxicol Sci* **132**: 87-95.
- Thomas L, Yang CH & Goldthwait DA (1982) Two DNA glycosylases in *Escherichia coli* which release primarily 3-methyladenine. *Biochemistry* **21**: 1162-1169.
- Topham NJ & Hewitt EW (2009) Natural killer cell cytotoxicity: how do they pull the trigger? *Immunology* **128**: 7-15.
- Trautinger BW, Jaktaji RP, Rusakova E, *et al.* (2005) RNA polymerase modulators and DNA repair activities resolve conflicts between DNA replication and transcription. *Molecular cell* **19**: 247-258.
- Troll CJ, Adhikary S, Cueff M, *et al.* (2014) Interplay between base excision repair activity and toxicity of 3-methyladenine DNA glycosylases in an *E. coli* complementation system. *Mutat Res* **763-764**: 64-73.
- Truglio JJ, Croteau DL, Van Houten B, *et al.* (2006) Prokaryotic nucleotide excision repair: the UvrABC system. *Chemical reviews* **106**: 233-252.
- Tsokos CG, Perchuk BS & Laub MT (2011) A dynamic complex of signaling proteins uses polar localization to regulate cell-fate asymmetry in *Caulobacter crescentus*. *Dev Cell* **20**: 329-341.
- Tsolis RM, Seshadri R, Santos RL, *et al.* (2009) Genome degradation in *Brucella ovis* corresponds with narrowing of its host range and tissue tropism. *PLoS One* **4**: e5519.

- Tudek B, Van Zeeland AA, Kusmierek JT, *et al.* (1998) Activity of Escherichia coli DNA-glycosylases on DNA damaged by methylating and ethylating agents and influence of 3-substituted adenine derivatives. *Mutat Res* **407**: 169-176.
- Tudek B, Zdzalik-Bielecka D, Tudek A, *et al.* (2017) Lipid peroxidation in face of DNA damage, DNA repair and other cellular processes. *Free Radic Biol Med* **107**: 77-89.
- Ulusoy S, Ulusoy HI, Pleissner D, *et al.* (2016) Nitrosation and analysis of amino acid derivatives by isocratic HPLC. *RSC Advances* **6**: 13120-13128.
- Uphoff S (2018) Real-time dynamics of mutagenesis reveal the chronology of DNA repair and damage tolerance responses in single cells. *Proc Natl Acad Sci U S A* **115**: E6516-E6525.
- Uphoff S, Lord ND, Okumus B, *et al.* (2016) Stochastic activation of a DNA damage response causes cell-to-cell mutation rate variation. *Science* **351**: 1094-1097.
- Val ME, Soler-Bistue A, Bland MJ, *et al.* (2014) Management of multipartite genomes: the Vibrio cholerae model. *Curr Opin Microbiol* **22**: 120-126.
- Van der Henst C, Beaufay F, Mignolet J, *et al.* (2012) The histidine kinase PdhS controls cell cycle progression of the pathogenic alphaproteobacterium *Brucella abortus*. *J Bacteriol* **194**: 5305-5314.
- van Helden J (2003) Regulatory Sequence Analysis Tools. *Nucleic Acids Research* **31**: 3593-3596.
- Vaughan P, Lindahl T & Sedgwick B (1993) Induction of the adaptive response of Escherichia coli to alkylation damage by the environmental mutagen, methyl chloride. *Mutat Res* **293**: 249-257.
- Vazquez-Torres A, Jones-Carson J, Mastroeni P, *et al.* (2000) Antimicrobial Actions of the NADPH Phagocyte Oxidase and Inducible Nitric Oxide Synthase in Experimental Salmonellosis. I. Effects on Microbial Killing by Activated Peritoneal Macrophages in Vitro. *The Journal of Experimental Medicine* **192**: 227-236.
- Vazquez-Torres A, Xu Y, Jones-Carson J, *et al.* (2000) Salmonella pathogenicity island 2-dependent evasion of the phagocyte NADPH oxidase. *Science* **287**: 1655-1658.
- Vermeer ITM, Henderson LY, Moonen EJC, *et al.* (2004) Neutrophil-mediated formation of carcinogenic N-nitroso compounds in an in vitro model for intestinal inflammation. *Toxicology Letters* **154**: 175-182.
- Vitry MA, Hanot Mambres D, De Trez C, *et al.* (2014) Humoral immunity and CD4+ Th1 cells are both necessary for a fully protective immune response upon secondary infection with Brucella melitensis. *Journal of immunology (Baltimore, Md : 1950)* **192**: 3740-3752.
- Vitry MA, Hanot Mambres D, Deghelt M, *et al.* (2014) Brucella melitensis invades murine erythrocytes during infection. *Infect Immun* **82**: 3927-3938.
- Vodovotz Y, Russell D, Xie QW, *et al.* (1995) Vesicle membrane association of nitric oxide synthase in primary mouse macrophages. *Journal of immunology (Baltimore, Md : 1950)* **154**: 2914-2925.
- Wade JT, Reppas NB, Church GM, *et al.* (2005) Genomic analysis of LexA binding reveals the permissive nature of the Escherichia coli genome and identifies unconventional target sites. *Genes & development* **19**: 2619-2630.
- Wagner JK & Brun YV (2007) Out on a limb: how the Caulobacter stalk can boost the study of bacterial cell shape. *Mol Microbiol* **64**: 28-33.
- Wang H, Ziesche L, Frank O, *et al.* (2014) The CtrA phosphorelay integrates differentiation and communication in the marine alphaproteobacterium Dinoroseobacter shibae. *BMC Genomics* **15**: 130.
- Wang M, Qureshi N, Soeurt N, *et al.* (2001) High levels of nitric oxide production decrease early but increase late survival of Brucella abortus in macrophages. *Microb Pathog* **31**: 221-230.
- Wei P, Lu Q, Cui G, *et al.* (2015) The role of TREM-2 in internalization and intracellular survival of Brucella abortus in murine macrophages. *Vet Immunol Immunopathol* **163**: 194-201.
- Weller GR, Kysela B, Roy R, *et al.* (2002) Identification of a DNA nonhomologous end-joining complex in bacteria. *Science* **297**: 1686-1689.
- Wheeler RT & Shapiro L (1999) Differential localization of two histidine kinases controlling bacterial cell differentiation. *Molecular cell* **4**: 683-694.
- Wiese J, Thiel V, Gartner A, *et al.* (2009) Kiloniella laminariae gen. nov., sp. nov., an alphaproteobacterium from the marine macroalga Laminaria saccharina. *Int J Syst Evol Microbiol* **59**: 350-356.
- Wigley DB (2013) Bacterial DNA repair: recent insights into the mechanism of RecBCD, AddAB and AdnAB. *Nat Rev Microbiol* **11**: 9-13.
- Willett JW, Herrou J, Briegel A, *et al.* (2015) Structural asymmetry in a conserved signaling system that regulates division, replication, and virulence of an intracellular pathogen. *Proc Natl Acad Sci U S A* **112**: E3709-3718.
- Winczura A, Zdzalik D & Tudek B (2012) Damage of DNA and proteins by major lipid peroxidation products in genome stability. *Free Radic Res* **46**: 442-459.

- Wolf K, Fischer E & Hackstadt T (2000) Ultrastructural analysis of developmental events in Chlamydia pneumoniae-infected cells. *Infect Immun* **68**: 2379-2385.
- Wu J, Ohta N & Newton A (1998) An essential, multicomponent signal transduction pathway required for cell cycle regulation in Caulobacter. *Proc Natl Acad Sci U S A* **95**: 1443-1448.
- Wu J, Wang P & Wang Y (2018) Cytotoxic and mutagenic properties of alkyl phosphotriester lesions in Escherichia coli cells. *Nucleic Acids Res* **46**: 4013-4021.
- Wu X, Haakonsen DL, Sanderlin AG, *et al.* (2018) Structural insights into the unique mechanism of transcription activation by Caulobacter crescentus GerA. *Nucleic Acids Res* **46**: 3245-3256.
- Wyatt MD & Pittman DL (2006) Methylating agents and DNA repair responses: Methylated bases and sources of strand breaks. *Chem Res Toxicol* **19**: 1580-1594.
- Yagupsky P & Baron EJ (2005) Laboratory exposures to brucellae and implications for bioterrorism. *Emerging infectious diseases* **11**: 1180-1185.
- Yamada M, Sedgwick B, Sofuni T, *et al.* (1995) Construction and characterization of mutants of Salmonella typhimurium deficient in DNA repair of O6-methylguanine. *J Bacteriol* **177**: 1511-1519.
- Yamaguchi M, Dao V & Modrich P (1998) MutS and MutL activate DNA helicase II in a mismatch-dependent manner. *J Biol Chem* **273**: 9197-9201.
- Yang M, Aamodt RM, Dalhus B, *et al.* (2011) The ada operon of Mycobacterium tuberculosis encodes two DNA methyltransferases for inducible repair of DNA alkylation damage. *DNA Repair (Amst)* **10**: 595-602.
- Zano SP, Bhansali P, Luniwal A, *et al.* (2013) Alternative substrates selective for S-adenosylmethionine synthetases from pathogenic bacteria. *Archives of biochemistry and biophysics* **536**: 64-71.
- Zdzalik D, Domanska A, Prorok P, *et al.* (2015) Differential repair of etheno-DNA adducts by bacterial and human AlkB proteins. *DNA Repair (Amst)* **30**: 1-10.
- Zhan Y, Liu Z & Cheers C (1996) Tumor necrosis factor alpha and interleukin-12 contribute to resistance to the intracellular bacterium Brucella abortus by different mechanisms. *Infect Immun* **64**: 2782-2786.
- Zhang AP, Pigli YZ & Rice PA (2010) Structure of the LexA-DNA complex and implications for SOS box measurement. *Nature* **466**: 883-886.
- Zhang JZ, Popov VL, Gao S, *et al.* (2007) The developmental cycle of Ehrlichia chaffeensis in vertebrate cells. *Cell Microbiol* **9**: 610-618.
- Zhu Y, Wang PP, Zhao J, *et al.* (2014) Dietary N-nitroso compounds and risk of colorectal cancer: a case-control study in Newfoundland and Labrador and Ontario, Canada. *The British journal of nutrition* **111**: 1109-1117.

Appendix

Appendix 1: synthesis of the N-nitrosation sensitive probe.

This probe was synthesized by Dr. Ravikumar Jimmidi and Prof. Stéphane Vincent, both from the Unité de Chimie Organique in the University of Namur.

Appendix 2: paper on *B. abortus* CtrA

Francis N, Poncin K, Fioravanti A, Vassen V, Willemart K, Ong TA, Rappez L, Letesson JJ, Biondi EG, De Bolle X; CtrA controls cell division and outer membrane composition of the pathogen *Brucella abortus*; *Mol Microbiol* (2017) 103:780-797.

Appendix 3: paper on *B. abortus* essential genes

Sternon JF, Godessart P, Gonçalves de Freitas R, Van der Henst M, Poncin K, Francis N, Willemart K, Christen M, Christen B, Letesson JJ, De Bolle X; Transposon Sequencing of *Brucella abortus* Uncovers Essential Genes for Growth In Vitro and Inside Macrophages; *Infect Immun* (2018) 86.

Appendix 4: paper on CtrA in *B. abortus* and other alpha-proteobacteria

Poncin K, Gillet S, De Bolle X; Learning from the master: targets and functions of the CtrA response regulator in *Brucella abortus* and other alpha-proteobacteria; *FEMS Microbiol Rev.* (2018) 42:500-513.

Appendix 1

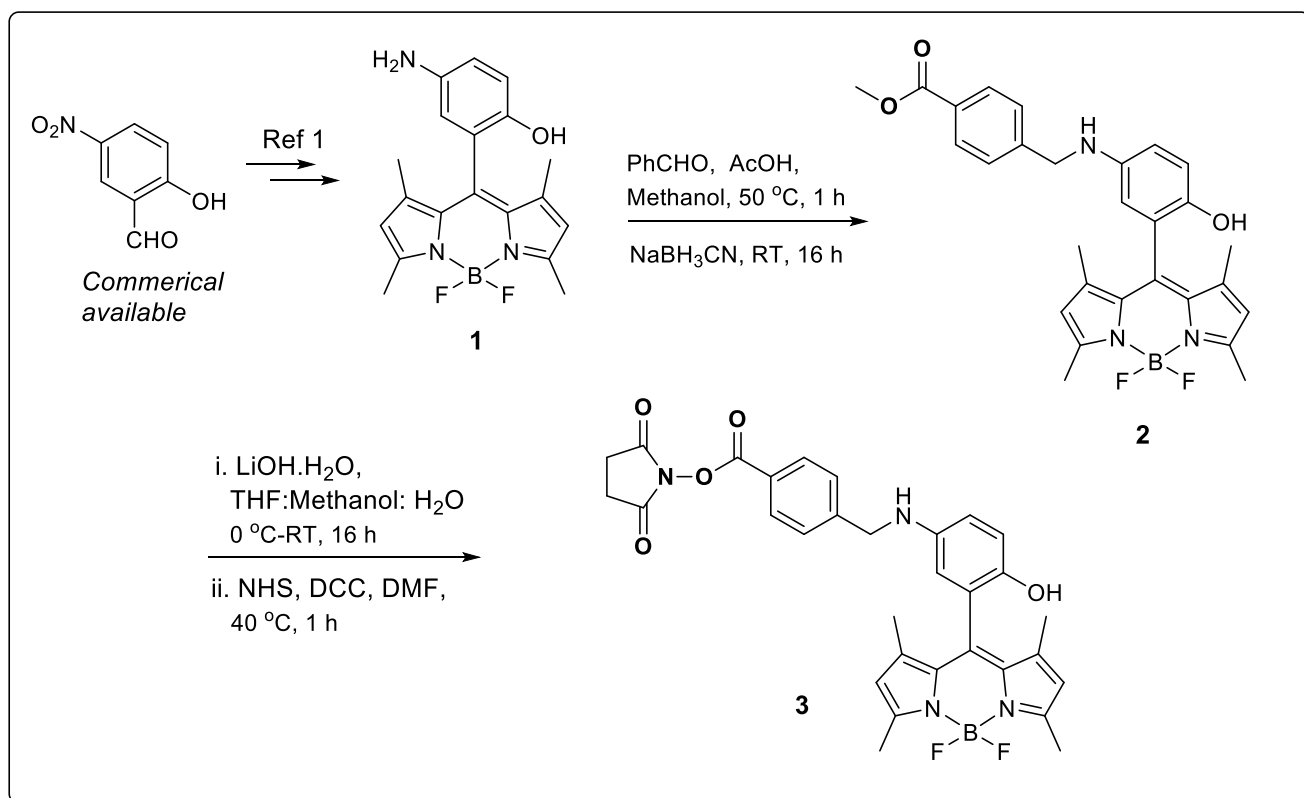
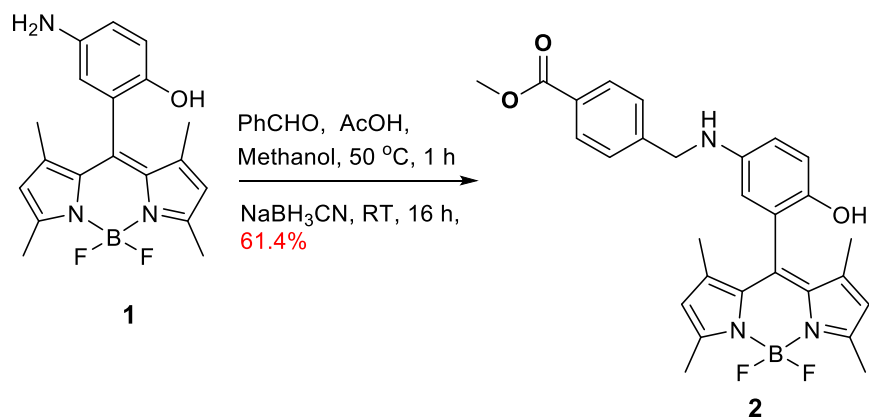
Protocol on the synthesis of the N-nitrosation sensitive probe

All reactions were carried out under an argon atmosphere. Yields refer to chromatographically and spectroscopically homogeneous materials. Reagents and chemicals were purchased from Sigma-Aldrich or Acros at ACS grade and were used without purification. All reactions were performed using purified and dried solvents: tetrahydrofuran (THF) was refluxed over sodium-benzophenone, dichloromethane (CH_2Cl_2), triethylamine (Et_3N), and pyridine were refluxed over calcium hydride (CaH_2). All reactions were monitored by thin-layer chromatography (TLC) carried out on Merck aluminum roll silica gel 60-F254 using UV light and a phosphomolybdic acid solution as revelator. Merck silica gel (60, particle size 40 -63 μm) was employed for flash column chromatography and preparative thin layer chromatography using technically solvent distilled prior to use as eluting solvents. Purification through adsorption silica chromatography columns were performed using Merck Gerduran silica gel 60 (40-63 \AA).

NMR Spectra were either recorded on a JEOL JNM EX-400 at 400 MHz for ^1H NMR and 100 MHz for ^{13}C NMR or on a JEOL JNM EX-500 at 500 MHz for ^1H NMR and 125 MHz for ^{13}C NMR. All the samples were prepared in a standard 5 mm quartz tube at room temperature (18-22°C) and without degassing, diluting the sample in deuterated solvents. Spectra were resolved with JEOL's Delta software. Chemical shifts (δ) are given in ppm referring to the partially deuteride nuclei of the used solvent (for ^1H NMR: 7.26 for CDCl_3 , 2.50 for $(\text{CD}_3)_2\text{SO}$, 3.31 for CD_3OD ; ^{13}C NMR: 77.16 for CDCl_3 , 39.52 for $(\text{CD}_3)_2\text{SO}$, 49.00 for CD_3OD). The coupling constants (J) are given in Hertz (Hz). The chemical shifts of signals featuring defined multiplicity were determined by arithmetic mean of the signal lines. Therefore, the following abbreviations were used: s = singlet, d = doublet, m = multiplet, br = broad and their combinations. Assignment of protons was accomplished by 1H-1H correlation COSY experiments. Assignment of carbons was accomplished by 1H-13C correlation HMQC, HMBC and DEPT experiments.

High-resolution mass spectra (HRMS) were performed on a Bruker maXis mass spectrometer Q-TOF by the "Fédération de Recherche" ICOA/CBM (FR2708) platform of Orléans in France. Melting points were performed on BOCHI Melting point B-545. The absorption spectra were acquired on a Perkin-Elmer Spectrum II FT-IR System UATR on neat compounds, mounted with a diamond crystal. Selected absorption bands are reported by wavenumber (cm^{-1}). The spectra were measured between wavenumbers of 4000-450 cm^{-1} .

Scheme S1

Synthesis of compound **2**:

A solution of **1** (130 mg, 0.366 mmol, 1 eq), methyl 4-formylbenzoate (48.0 mg, 0.292 mmol, 0.8 eq), and AcOH (0.2 mL) in dry Methanol (3 mL) was stirred at 50 °C for 1h, then NaBH₃CN (57.5 mg, 0.915 mmol, 2.5 eq) was added to the mixture at room temperature and stirring was continued for 16 h. The solvent was evaporated under vacuum and quenched with water and extracted with ethyl acetate. The organic layer was washed with brine and dried over Na₂SO₄. Filtration, evaporation and purification of the residue by silica gel flash chromatography (Cy/EtOAc 7:3) gave the desired product as red solid (113.1 mg, 61.4% yield).

Formula: C₂₈H₂₈BF₂N₃O₃

Mw: 503.35 g/mol

Rf: 0.34 (Cy/ EtOAc 1:1)

¹H NMR (CDCl₃, 400 MHz) δ ppm 1.49 (s, 6H, CH₃), 2.45 (s, 6H, CH₃), 3.87 (s, 3H, CH₃CO), 4.27 (bs, 2H), 5.96 (bs, 2H), 6.22 (d, *J* = 2.8 Hz, 1H), 6.60 (dd, *J* = 8.8, 2.8 Hz, 1H), 6.68 (d, *J* = 8.8, 1H), 7.35 (dd, *J* = 8.8, 2.8 Hz, 2H), 7.95 (*J* = 8.8, 2.8 Hz, 2H).

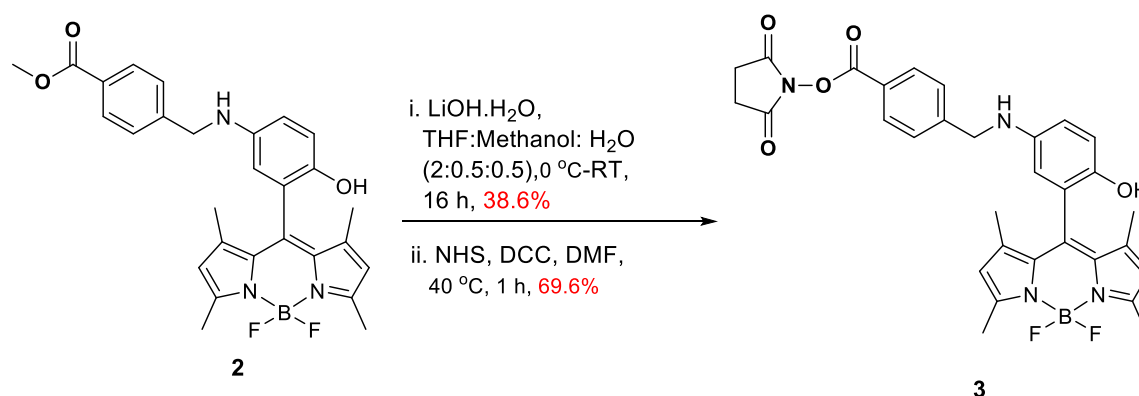
¹³C NMR (CDCl₃, 100 MHz) δ ppm 13.79 (CH₃), 14.70 (CH₃), 48.59 (CH₂Ar), 60.49(CH₃CO), 112.55, 116.57, 118.11, 121.47, 121.75, 127.21, 128.14, 129.26, 130.01, 131.72, 136.04, 142.60, 143.40, 144.41, 144.57, 156.32, 167.17.

HRMS: (ESI+-MS, m/z) calculated for C₂₈H₂₈BF₂N₃O₃ [M+H]⁺: 504.2270, found: 504.2269.

Melting point: 213-215 °C

IR: 3379 (N-H), 1688.48 (C=O), 1541, 1439 (C=C)_{Ar}, 1233 (C-O), 804, 735 cm⁻¹.

Synthesis of compound 3:



To a solution of compound **2** (80 mg, 0.158 mmol, 1 eq) in 3 mL of THF: MeOH: H₂O (2:0.5:0.5) was added LiOH.H₂O (20.0 mg, 0.476 mmol, 3 eq) at 0 °C. Then, the reaction mixture was stirred at room temperature for 16 h. After completion of the reaction, solvents were evaporated under reduced pressure. Then 5 ml of water were added and the solution was acidified with 1 N HCl and extracted with ethyl acetate (2 x 10 mL). The organic phases were combined and dried over MgSO₄, concentrated in vacuum to afford the crude intermediate acid as a red solid (30 mg, 38.6 %, 0.0613 mmol). The latter was dissolved in 1 mL dry DMF and DCC (15 mg, 0.073 mmol, 1.2 eq) and NHS (8.5 mg, 0.073 mmol, 1.2 eq) were added at room temperature and stirred at 40 °C. After disappearance of the starting material as monitored by TLC (1 h), the crude was directly subjected to flash chromatography eluted with cyclohexane to 50% Cy/EtOAc to get the desired product as red solid (25 mg, 69.6%).

Formula: C₃₁H₂₉BF₂N₄O₅

Mw: 586.40 g/mol

Rf: 0.4 (Cy/ EtOAc 1:1)

^1H NMR (CDCl_3 , 400 MHz) δ ppm 1.51 (s, 6H, CH_3), 2.52 (s, 6H, CH_3), 2.89 (bs, 4H, CH_2NCO), 4.37 (bs, 2H, Bn), 5.98 (bs, 2H), 6.34 (d, $J = 2.8$ Hz, 1H), 6.65 (dd, $J = 8.8$, 2.8 Hz, 1H), 6.82 (d, $J = 8.4$, 1H), 7.45 (d, $J = 8.8$, 2H), 8.05 ($J = 8.8$, 2H).

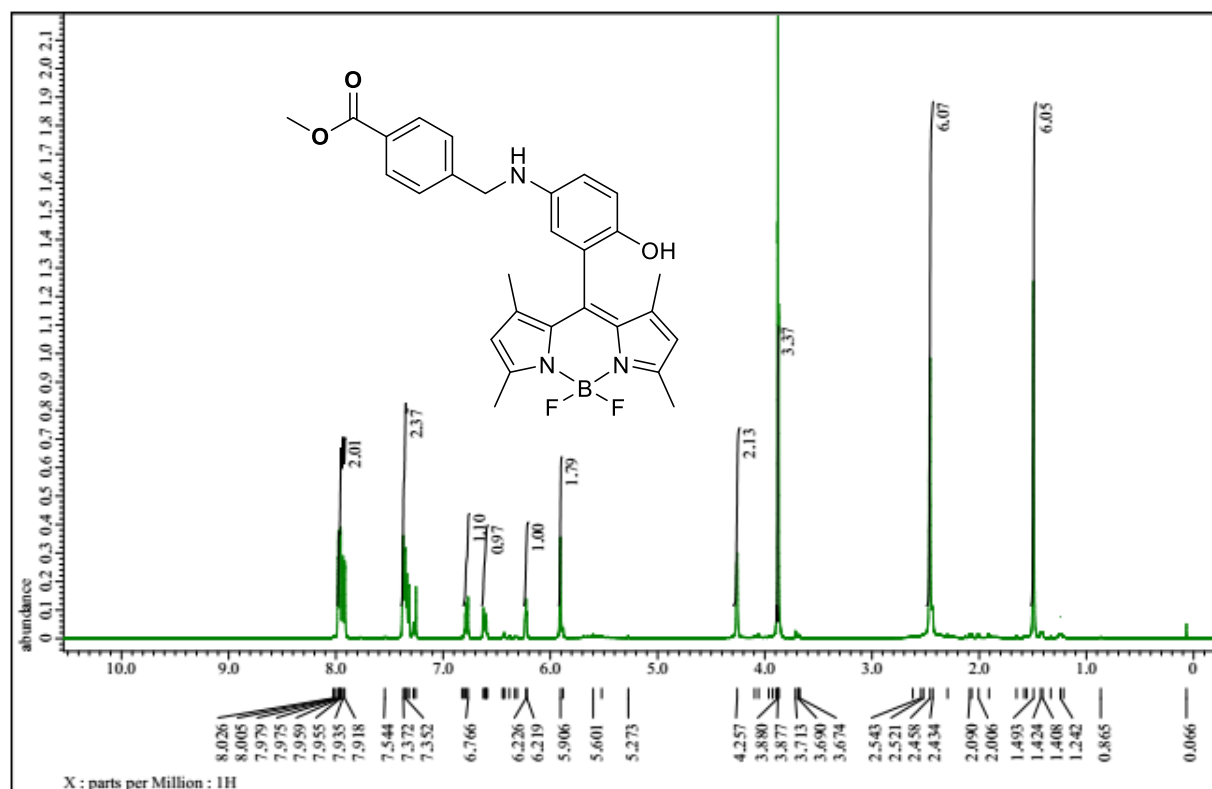
^{13}C NMR (CDCl_3 , 100 MHz) δ 13.78 (CH_3), 14.69 (CH_3), 25.75 (CH_2N), 48.55 (Bn), 113.06, 116.68, 117.80, 121.53, 121.77, 124.06, 127.63, 128.87, 131.01, 131.32, 136.01, 142.18, 143.44, 144.67, 147.23, 156.32, 161.72 (CO), 169.36 (NCO).

HRMS: (ESI+-MS, m/z) calculated for $\text{C}_{28}\text{H}_{28}\text{BF}_2\text{N}_3\text{O}_3$ $[\text{M}+\text{H}]^+$: 587.2277, found: 504.2271.

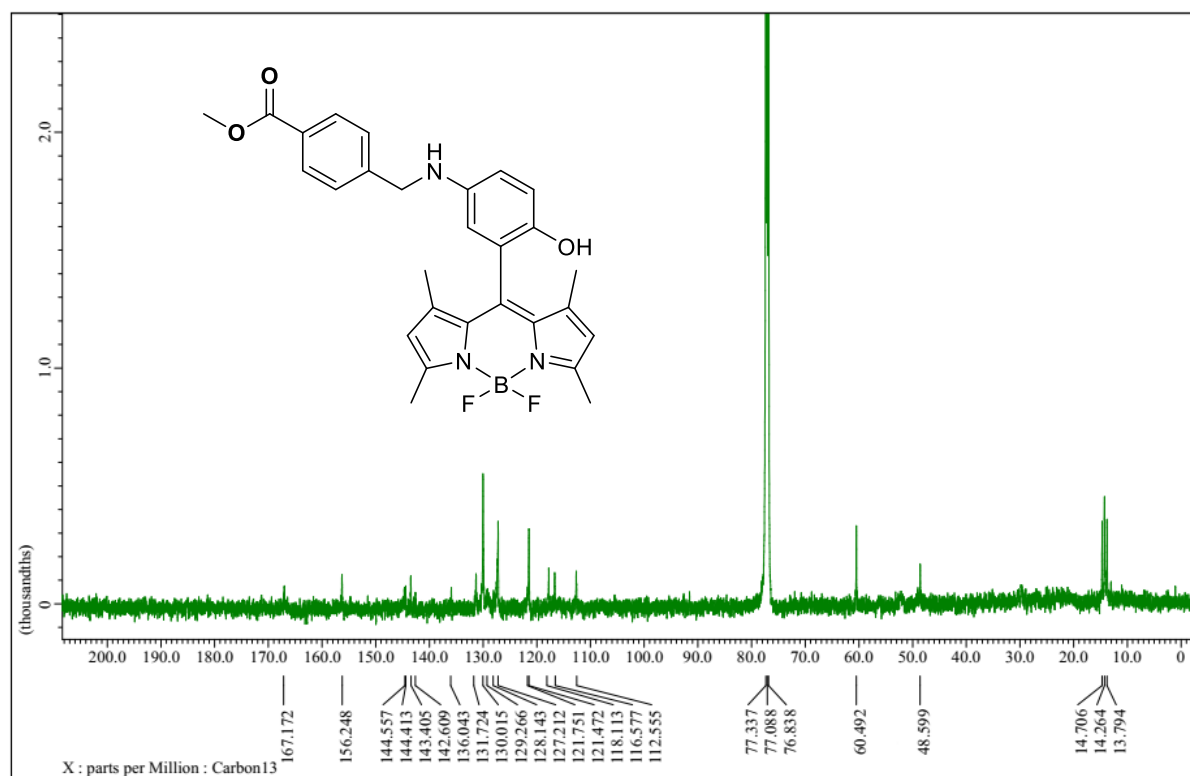
Melting point: 114-116 $^\circ\text{C}$

IR: 3370 (N-H), 2920 (C-H), 1732 (C=O), 1542.8, 1504 ($\text{C}=\text{C}$)_{Ar}, 1190 (C-O), 1306, 810.5 cm^{-1} .

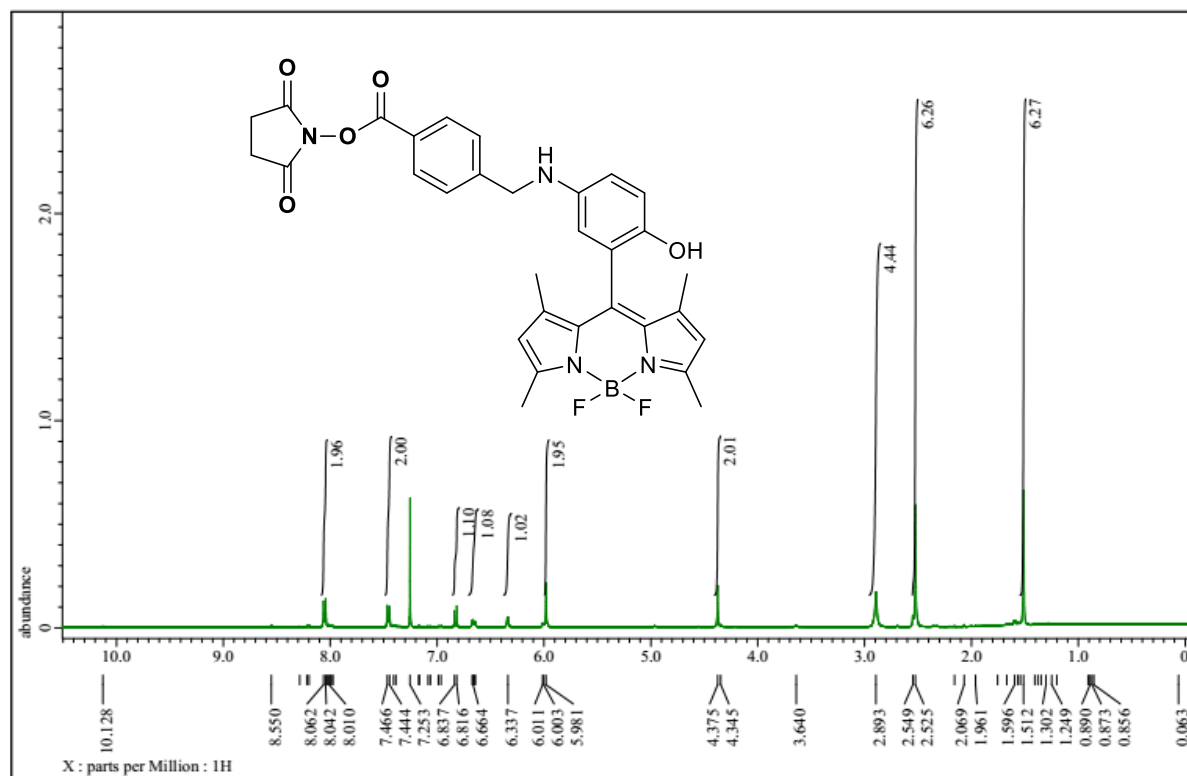
^1H NMR of compound **2** (400 MHz, CDCl_3)



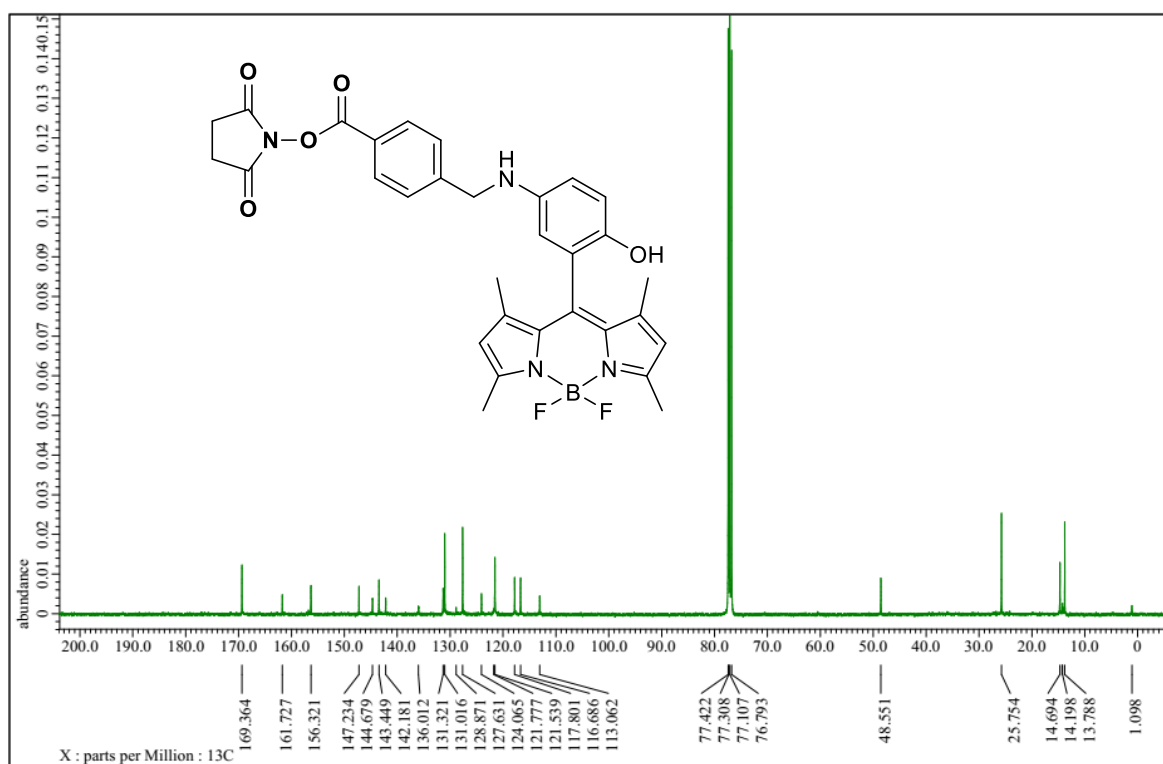
^{13}C NMR of compound **2** (100 MHz, CDCl_3)



^1H NMR of compound **3** (400 MHz, CDCl_3)



^{13}C NMR of compound **3** (100 MHz, CDCl_3)



Appendix 2

1 **CtrA Controls Cell Division and Outer Membrane**

2 **Composition of the Pathogen *Brucella abortus***

3

4 Nayla Francis,^a Katy Poncin,^a Antonella Fioravanti,^{b*} Victoria Vassen,^a Kevin Willemart,^a

5 Thi Anh Phuong Ong,^a Luca Rappez,^{a**} Jean-Jacques Letesson,^a Emanuele G. Biondi,^{bc}

6 Xavier De Bolle,^{a#}

7

8 University of Namur, Narilis, Microorganisms Biology Research Unit (URBM), Namur,

9 Belgium^a; Unité de Glycobiologie Structurale et Fonctionnelle, UMR8576 CNRS -

10 Université de Lille, 50 Avenue Halley, Villeneuve d'Ascq, France^b; Aix-Marseille

11 Université, CNRS, Laboratoire de Chimie Bactérienne, UMR 7283, Institut de

12 Microbiologie de la Méditerranée, Marseille, France^c

13

14 Running Title: CtrA regulon of the pathogen *Brucella abortus*

15 # Address correspondence to Xavier De Bolle, xavier.debolle@unamur.be

16 Phone : +32 81 72 44 38 Fax : +32 81 72 42 97

17 University of Namur, 61 rue de Bruxelles, 5000 Namur, Belgium

18 *Present address: Structural Biology Research Center, VIB, Vrije Universiteit Brussels,

19 Brussels, Belgium

20 **Present address: European Molecular Biology Laboratory (EMBL), Structural and

21 Computational Biology Department, Heidelberg, Germany

22

23 Keywords: *Brucella*, CtrA, cell cycle, cell division, intracellular trafficking,

24 alphaproteobacteria

25 **Summary**

26 *Brucella abortus* is a pathogen infecting cattle, able to survive, traffic and proliferate
27 inside host cells. It belongs to the *Alphaproteobacteria*, a phylogenetic group comprising
28 bacteria with free living, symbiotic and pathogenic lifestyles. An essential regulator of
29 cell cycle progression named CtrA was described in the model bacterium *Caulobacter*
30 *crenscentus*. This regulator is conserved in many alphaproteobacteria, but the evolution
31 of its regulon remains elusive. Here we identified promoters that are CtrA targets using
32 ChIP-seq and we found that CtrA binds to promoters of genes involved in cell cycle
33 progression, in addition to numerous genes encoding outer membrane components
34 involved in export of membrane proteins and synthesis of lipopolysaccharide. Analysis
35 of a conditional *B. abortus ctrA* loss of function mutant confirmed that CtrA controls cell
36 division. Impairment of cell division generates elongated and branched morphologies,
37 that are also detectable inside HeLa cells. Surprisingly, abnormal bacteria are able to
38 traffic to the endoplasmic reticulum, the usual replication niche of *B. abortus* in host
39 cells. We also found that CtrA depletion affected outer membrane composition, in
40 particular the abundance and spatial distribution of Omp25. Control of the *B. abortus*
41 envelope composition by CtrA indicates the plasticity of the CtrA regulon along
42 evolution.

43

44 **Introduction**

45 *Brucella abortus* is a facultative intracellular pathogen (Moreno & Moriyon, 2006)
46 preferentially infecting cattle, although humans can be accidental hosts. Infection by *B.*
47 *abortus* causes a disease called brucellosis, a worldwide zoonosis. *B. abortus* can infect
48 both epithelial cells (such as HeLa and Vero cells) (Detilleux *et al.*, 1990) and
49 professional phagocytes (macrophages and dendritic cells) (Archambaud *et al.*, 2010).
50 Once inside host cells, *B. abortus* resides in a membrane-bound compartment called BCV
51 for *Brucella* containing vacuole. *B. abortus* intracellular trafficking is biphasic; in a first a
52 non-proliferative phase the BCV interacts with early and then late endosomes (Chaves-
53 Olarte *et al.*, 2002, Pizarro-Cerda *et al.*, 1998a, Starr *et al.*, 2008), as shown by the
54 acquisition of Lamp1, a marker of late endosomes and lysosomes. Then, in most cell
55 types (Salcedo *et al.*, 2013), the second phase is characterized by bacterial proliferation
56 in a compartment harbouring endoplasmic reticulum (ER) markers (Celli *et al.*, 2003,
57 Celli *et al.*, 2005, Pizarro-Cerda *et al.*, 1998a). After this proliferation step, BCVs can
58 acquire autophagic markers and bacteria spread to neighbouring cells (Starr *et al.*,
59 2012).

60 Recently, new evidence showed that cell cycle and virulence of *B. abortus* are
61 coordinated (De Bolle *et al.*, 2015, Deghelt *et al.*, 2014). *B. abortus* cell cycle starts with
62 cell division, that generates two unequal daughter cells (Van der Henst *et al.*, 2013).
63 Each daughter cell has a period in which chromosome replication is not initiated, they
64 are proposed to be at the so-called G1 stage. When the chromosomal replication has
65 started, the bacteria are at the S (DNA synthesis) phase. The stage between the end of
66 chromosomal replication and cell division is G2. We recently developed tools to identify
67 *B. abortus* at the G1 stage, at the single cell level (Deghelt *et al.*, 2014). Bacteria in the G1
68 stage of their cell cycle are more infectious than their counterparts in S or G2 phases

69 (Deghelt et al., 2014). Furthermore, during the early non-proliferative phase of the
70 infection, bacteria remained in G1 phase for up to 6 h and were arrested for their growth
71 (Deghelt et al., 2014). *B. abortus* is thus able to block its cell cycle while trafficking
72 through the endocytic pathway. Around 8 h post-infection (PI) in HeLa cells, bacteria
73 resumed chromosome replication and growth while still residing in Lamp1+
74 compartments. However, the newly generated daughter cells were delivered into
75 Lamp1- BCVs (Deghelt et al., 2014).

76 *B. abortus* is a member of the *Alphaproteobacteria* class, and many key regulators
77 controlling the cell cycle progression of the model organism *Caulobacter crescentus* are
78 conserved in *B. abortus* (Brilli et al., 2010, Hallez et al., 2004). In particular the response
79 regulator and transcription factor CtrA is exclusively present in *Alphaproteobacteria* and
80 well conserved among them (Brilli et al., 2010). In *C. crescentus* this transcription factor
81 controls the expression of genes involved in polar morphogenesis, division, DNA
82 methylation and chemotaxis (Laub et al., 2002, Quon et al., 1998, Reisenauer et al.,
83 1999). CtrA also binds the replication origin of *C. crescentus* chromosome, thereby
84 preventing the initiation of its replication (Quon et al., 1998). CtrA regulates similar
85 processes in *Sinorhizobium meliloti*, a symbiont of legume plants (Pini et al., 2015). In
86 these two microorganisms, CtrA amount oscillates during cell cycle thanks to
87 regulations occurring at multiple levels (Domian et al., 1997, Holtzendorff et al., 2004,
88 Pini et al., 2015). In *B. abortus*, DNase I footprinting assays suggested that CtrA is also
89 involved in cell cycle regulation as it is able to bind the promoter of *ccrM* coding for an
90 essential DNA methyltransferase (Robertson et al., 2000), and promoters of *ftsE* and
91 *minC* genes, that are involved in division (Bellefontaine et al., 2002). CtrA also binds its
92 own promoter (Bellefontaine et al., 2002). In *C. crescentus* CtrA recognizes two
93 consensus sequences, the "TTAA(N₇)TTAAC" 9-mer box (Quon et al., 1998) and the

94 “TTAACCAT” 8-mer box (Laub et al., 2002), which are also found in predicted CtrA target
95 promoters in *B. abortus* (Bellefontaine et al., 2002, Hallez et al., 2004).

96 At the post-translational level, phosphorylation and proteolysis of CtrA are controlled by
97 a complex network (Curtis & Brun, 2010) that is predicted to be conserved in many
98 *Alphaproteobacteria* (Brilli et al., 2010). The phosphorylation cascade controlling CtrA
99 activity in *B. abortus* is conserved and functional (Willett *et al.*, 2015). Alteration of CtrA
100 control generates defects in intracellular survival and a shift in the abundance in *ccrM*
101 transcripts (Willett et al., 2015). However, the regulon of CtrA in *B. abortus* was poorly
102 explored until now.

103 Here we investigated the regulon of *B. abortus* CtrA by performing a chromatin
104 immunoprecipitation followed by deep sequencing (ChIP-seq) analysis. A detailed
105 analysis of CtrA binding sites on *B. abortus* genome not only revealed that CtrA binds to
106 the promoters of genes involved in cell cycle control and progression, but it also binds to
107 the promoters of genes involved in biogenesis of the outer membrane. We show that
108 CtrA is dispensable for elongation but is essential for division, CtrA absence generating
109 large branched morphologies both in culture and inside host cells. Moreover, CtrA is
110 involved in the control of outer membrane composition. Finally, we show that the
111 activity of two CtrA-bound promoters change according to bacterial cell size, suggesting
112 that CtrA is indeed a cell cycle regulator.

113

114 **Results**

115 *Investigating the CtrA regulon by ChIP-seq*

116 Since CtrA was recently proposed to control *B. abortus* cell cycle (Bellefontaine et al.,
117 2002, Willett et al., 2015), a ChIP-seq analysis was performed to map CtrA binding sites
118 on *B. abortus* 544 genome, when this bacterium is grown in rich medium until the mid-

119 exponential phase. The ChIP-seq data and the annotated genbank files are available as
120 Supplemental material (Chr1.gb, ChIP-seq_CtrA_chr1.txt, Chr2.gb and ChIP-
121 seq_CtrA_chr2.txt files). From this analysis, 109 CtrA binding regions were selected
122 (Table S1). CtrA binding sites are scattered on the two chromosomes (Fig. S1). Of these
123 regions, 71% had a predicted 9-mer or 8-mer consensus binding site with 0, 1 or 2
124 mismatches, and 97% mapped to intergenic regions. Among the CtrA-bound sequences
125 with no predicted 9-mer or 8-mer box, 57% had at least one “TTAA(C)” half site. CtrA
126 binding pattern to DNA showed a single peak coinciding with a predicted binding site
127 upstream of *cpdR* (BAB2_0042) and *ccrM* (BAB1_0516) (Fig. 1). CtrA binding upstream
128 of its own promoter showed two peaks of equal size overlapping multiple consensus
129 sequences (Fig 1). These peaks corresponded to the regions protected from DNase I
130 digestion by purified phosphorylated CtrA in an *in vitro* assay (Bellefontaine et al.,
131 2002). It should be noted that this intergenic region bound by CtrA could also serve to
132 regulate the expression of another gene (BAB1_1615), which has an opposite
133 orientation to *ctrA* (BAB1_1614). Similarly, CtrA binding between BAB2_1162 and *repA*
134 (BAB2_1163, a gene putatively involved in the segregation of chromosome II replication
135 origins) had a double peaks pattern, but the peaks were of unequal size, and the
136 apparently stronger binding site contains a half site TTAAC (Fig. 1). Some other CtrA
137 binding patterns to DNA were less expected. For instance, CtrA bound a region upstream
138 of *divK* (BAB2_0628, coding for a regulator of cell cycle (Hallez *et al.*, 2007b, Mignolet *et*
139 *al.*, 2010)) at the level of a TTAAC half site despite the presence of a 9-mer box around
140 300 base pairs upstream the actual binding site (Fig. 1). CtrA also bound a region inside
141 the *ddl* open reading frame (BAB1_1447), which is in operon with *ftsQ*, *ftsA* and *ftsZ*. Ddl
142 is a D-Ala-D-Ala ligase while FtsQ, FtsA and FtsZ are cell division proteins. Interestingly,
143 this binding site overlaps three TTAAC half sites. A similar binding profile was observed

144 in *C. crescentus*, where CtrA also bound a sequence within the *ddl* gene upstream of the
145 *ftsQA* operon (Laub et al., 2002).

146 The direct binding of CtrA to promoters identified in ChIP-seq was confirmed by
147 an electrophoretic mobility shift assay (EMSA), using *minC*, *dnaA*, *ftsQ*, *bamA*, *omp25* and
148 *tolQ* promoters as probes (Fig. S2), suggesting that –at least in the case of these target
149 genes– CtrA alone is able to directly bind these promoters.

150 The genome-wide analysis of the functional classes of CtrA-targeted genes
151 revealed an enrichment of genes involved in cell cycle (cell division, replication, DNA
152 methylation and cell cycle control) as expected, but also numerous genes involved in
153 envelope biogenesis/homeostasis. Indeed, genes predicted to be involved in envelope
154 composition and cell cycle are significantly enriched among CtrA targets, as they
155 constitute 33.3% and 11.5% of CtrA regulon respectively compared to 3.3% and 2.6% of
156 the whole genome of *B. abortus* ($p < 0.001$ in a χ^2 analysis).

157 CtrA is predicted to directly control many genes involved in cell division (Table
158 S1). These include the *minCDE* operon coding for the Min system (Meinhardt & de Boer,
159 2001), whose function is to control the mid-cell placement of the Z ring. This role in Z
160 ring placement is in agreement with the MinD oscillation reported in *B. abortus* (Hallez
161 et al., 2007a). The promoters of the genes coding for proteins involved in Z ring
162 formation and subsequent constriction (*ftsQAZ*, *ftsB*, *ftsEX*) are also directly bound by
163 CtrA. The genes (*pal* and *tolQRAB*) coding for proteins involved in the invagination of the
164 outer membrane during cell division (Gerding et al., 2007) are also direct targets of CtrA,
165 suggesting that CtrA potentially controls the whole cell division process. CtrA is also
166 binding the promoters of genes or operons involved in dNTP synthesis (*nrdHIEF*), the
167 initiation of chromosome I replication (*dnaA*), the partition of chromosome II origins

168 (*repAB*) (Deghelt et al., 2014), and the segregation of chromosomes at the termination of
169 replication (*ftsK*) (Stouf et al., 2013).

170 CtrA is binding many *B. abortus* promoters involved in envelope composition
171 (Table S1). Indeed, it is targeting genes involved in LPS biosynthesis (*lpxD-fabZ-lpxAB*
172 and *lpxE*), LPS export to the OM (*lptAB* and *lptFGD*), OM proteins composition (*omp2b*,
173 *omp25*, *ropB*, *omp19*, BAB1_0045, BAB1_0075, BAB1_1701 and BAB2_0314) and the
174 incorporation of proteins into the OM (*bamA*). Moreover, CtrA binds to the promoter of
175 six genes coding for L,D-transpeptidases homologs (BAB1_0047, BAB1_0138,
176 BAB1_0589, BAB1_0978, BAB1_1159, BAB1_1867), enzymes that link m-Dap residues
177 within the peptidoglycan mesh (Magnet et al., 2008). The function of these L,D-
178 transpeptidases is unexplored in *B. abortus*, but one of these L,D-transpeptidases
179 (homologous to BAB1_0589) was found to be localized at the growth pole in
180 *Agrobacterium tumefaciens* (Grangeon et al., 2015). PopZ is also localized at the growth
181 pole in *B. abortus* (Deghelt et al., 2014) and *A. tumefaciens* (Grangeon et al., 2015), and
182 its gene is also a direct target of CtrA in *B. abortus*. These observations suggest that polar
183 differentiation could be controlled by CtrA in *B. abortus*.

184 One striking feature of the CtrA regulon in *B. abortus* is the high proportion of
185 genes encoding proteins involved in the control of CtrA. As depicted in Fig. S3, the *divJ*,
186 *divK*, *divL*, *chpT*, *cpdR*, *rcdA*, *sciP* and *ccrM* genes are proposed to control CtrA, but our
187 data also suggest that these genes are direct targets of CtrA, highlighting the potential
188 circular topology of this regulation network, consistent with cell cycle control. CtrA was
189 reported to control *ccrM* transcripts levels in *B. abortus* (Willett et al., 2015), which is
190 consistent with its binding to the *ccrM* promoter *in vitro* (Bellefontaine et al., 2002) and
191 *in vivo* (Table S1). It is noteworthy that enrichment of reads at the *dnaA* promoter is

192 weak, suggesting either CtrA binding is infrequent or it happens only in a small fraction
193 of the bacterial population.

194 It is also worth mentioning that only few genes proposed to encode virulence
195 factors are directly bound by CtrA. These include a manganese transporter gene *mntH*
196 (Anderson *et al.*, 2009) and a periplasmic superoxide dismutase gene *sodC* (Gee *et al.*,
197 2005). CtrA proposed direct targets also comprise the main transcriptional regulator of
198 flagellar genes (*ftcR*) (Leonard *et al.*, 2007) and several putative DNA repair genes (*uvrC*,
199 *addBA*, *mutM* and *tagA*).

200 We decided to further investigate the role of CtrA in regulating cell division and
201 envelope composition by constructing a CtrA depletion strain and analysing its
202 phenotype in culture and in the context of a cellular infection.

204 *CtrA is crucial for B. abortus cell division*

205 In *C. crescentus*, CtrA is the master regulator controlling many important genes required
206 for cell cycle progression. Here we investigated the *B. abortus* CtrA function *in vivo* by
207 generating a *ctrA* depletion strain, as this gene was suggested to be essential
208 (Bellefontaine *et al.*, 2002). First, a wild type (WT) copy of *ctrA* was cloned on a
209 replicative plasmid as a fusion with an IPTG-inducible promoter; then the chromosomal
210 *ctrA* deletion was obtained by allelic replacement in the presence of IPTG. When the
211 growth medium was supplemented with IPTG, the $\Delta ctrA$ *p_{lac}-ctrA* strain harboured a WT
212 morphology (Fig. 2A). Upon IPTG removal, CtrA was cleared within 2 hours from the
213 cells (Fig. 2B). Abnormal morphologies appeared from 3 h post IPTG removal and
214 consisted of elongated cells and cells with mislocalized constrictions (Fig. 2A). At 3 h
215 post-IPTG removal, a fraction of CtrA-depleted bacteria (10.9 %) were longer than 2.75
216 μm while only 1.6% of WT bacteria and 1.3 % of the depletion strain grown with IPTG

217 exceeded this size ($p < 0.05$). A highly significant proportion ($p < 0.01$) of CtrA-depleted
218 bacteria (6.3%) had a mislocalized constriction, i.e. detectable septa located very close
219 to one pole (Fig. 2A; white arrow heads), compared to the WT strain (0.88%) and to the
220 CtrA depletion strain grown with IPTG (1.33%) (Fig. 2A). Seven hours after IPTG was
221 removed from the culture, we observed bacteria that grew to form multiple branches
222 while others generated small chains, interpreted as filamentation with aborted divisions
223 segmenting the bacteria (Fig. 2A). If the incubation in a CtrA-depleted state is prolonged
224 (15 h), bacteria kept on branching. These results suggest that in the absence of CtrA,
225 bacterial elongation is maintained but division is highly perturbed, since it is either
226 abolished (there are almost no visible constriction sites in branching bacteria) or
227 division is initiated at various positions but it is often not completed since bacteria form
228 chains.

229 We next characterized the viability of the CtrA depletion strain. The viability of the
230 CtrA depletion strain in rich culture medium was assessed by counting the number of
231 colony forming units (CFU) (Fig. 3A). In these assays, colonies were grown on plates in
232 the presence of IPTG, since this strain does not grow on plates without IPTG, consistent
233 with the essentiality of the *ctrA* gene. When the CtrA depletion strain was cultivated in
234 the presence of IPTG in liquid medium, a stable number of CFU was reached earlier than
235 the WT control, and the plateau was lower (Fig. 3A). In the absence of IPTG, the number
236 of CFU did not increase, and remained constant for 24 h before decreasing (Fig. 3A). The
237 high variability of CFU numbers after 48 h of depletion (Fig. 3A) could be due to a high
238 variability in the capacity of branched bacteria to divide and release viable bacteria.
239 These data suggest that CtrA is essential for *B. abortus* growth and long-term survival in
240 rich medium.

241 To test the reversibility of the CtrA depletion on cell division, the CtrA depletion
242 strain was grown overnight without IPTG, labeled with Texas Red Succinimidyl Ester
243 (TRSE) and inoculated in fresh medium supplemented with IPTG. The newly
244 incorporated envelope appears unlabeled with TRSE after growth and thus new division
245 sites appear as unlabeled rings (Brown *et al.*, 2012). After 3 h of repletion, we observed
246 a reaccumulation of CtrA (Fig. S4A) and several unlabeled constriction sites were visible
247 on the large bacteria (Fig. S4B). Six hours after IPTG was added to the medium, several
248 division events were completed as shown by the release of unlabeled or partially labeled
249 bacteria (Fig. S4B). Those bacteria were of different size and shapes, demonstrating that
250 the septa were formed at ectopic sites. These results further confirm that CtrA is
251 essential for division in *B. abortus*, and that CtrA depletion effect is reversible for the
252 generation of cell division events, but not for their correct positioning in the cell. It also
253 indicates that large branching bacteria generated in the absence of IPTG are not dead, at
254 least after an overnight depletion of CtrA.

255 In the ChIP-seq study reported above, only one condition was tested, and it is likely
256 that CtrA could be able to bind other targets in different conditions. Moreover is it also
257 likely that CtrA could be a crucial regulator in a fraction of its targets, but only an
258 accessory regulator for other promoters. The availability of a depletion strain for CtrA
259 allowed us to test some CtrA targets promoters for their dependence on CtrA. Using
260 reverse transcription followed by quantitative PCR (RT-qPCR), we found that the
261 abundance of *ccrM* transcript is strongly dependent on CtrA since after a CtrA depletion
262 condition (without IPTG) of 6 h, there is a significant ($p < 0.01$) 17.1 (± 0.8) fold decrease
263 of *ccrM* mRNA abundance compared to the control condition (with IPTG). RT-qPCR
264 analysis of other predicted CtrA targets (*omp25* and *ftsEX*) revealed statistically relevant

265 changes in mRNA abundance, but of very low amplitude (typically <40%), highlighting
266 the complexity of the regulation network involving CtrA.

267

268 *The activity of CtrA target promoters varies in function of bacterial cell size*

269 Since CtrA is a cell cycle regulator in *C. crescentus* (Laub et al., 2002, Quon et al., 1998,
270 Reisenauer et al., 1999) and *S. meliloti* (Pini et al., 2015), we wondered if CtrA is also
271 able to regulate its targets according to cell cycle. Because *B. abortus* is not
272 synchronizable as of yet, we monitored the activity of CtrA target promoters at the
273 single cell level, and we then sorted bacteria according to their size to reconstruct their
274 cell cycle. A reporter system was designed to monitor the activity of *ccrM* (p_{ccrM}), *repAB*
275 (p_{repAB}), *ctrA* (p_{ctrA}) and *pleC* (p_{pleC}) promoters by fusing each of them to a gene coding for
276 an unstable GFP (GFP-ASV) (Andersen et al., 1998) on a medium-copy replicative vector
277 (Terwagne et al., 2013). The *ccrM* and *ctrA* transcription follows a tightly regulated
278 profile throughout *C. crescentus* cell cycle while PleC protein amount remains stable
279 (Quon et al., 1996, Wheeler & Shapiro, 1999, Zweiger et al., 1994). The *repAB*, *ctrA* and
280 *ccrM* promoters are bound by CtrA in the ChIP-seq (Table S1), while the *pleC* promoter
281 is not, at least in the conditions tested here.

282 Currently, unlike *C. crescentus* cell cycle, the *B. abortus* cell cycle is not
283 synchronizable. In order to test if *ctrA*, *ccrM*, *repAB* and *pleC* promoters are controlled
284 along cell cycle, fluorescence intensity of the *B. abortus* reporter strains was measured
285 in three independent experiments and mean fluorescence intensity was plotted against
286 bacterial cell size (Fig. 4). The p_{ctrA} and p_{repAB} activities changed according to cell length,
287 and they display opposite profiles as maximal fluorescence intensity was measured in
288 intermediate bacteria for p_{repAB} and in small and large bacteria for p_{ctrA} reporters. These
289 data suggest that p_{ctrA} activity is maximal in large dividing bacteria, and this activity

290 decreases after division (Fig. 4). The maximal activity of p_{ctrA} in large bacteria is
291 consistent with cell division defect in the CtrA depletion strain (Fig. 2). On the contrary,
292 p_{repAB} seems to be turned on early in the cell cycle, leading to an accumulation of GFP-
293 ASV in intermediate bacteria (Fig. 4). These data correlate with the initiation of
294 replication of chromosome II at about half of the cell cycle of *B. abortus* (Deghelt et al.,
295 2014). The p_{ccrM} activity profile is similar to p_{ctrA} (Fig. 4); differences between bacterial
296 length classes are however not significant, probably due to the high variability of
297 fluorescence intensity between experiments, while variations of p_{repAB} and p_{ctrA} activities
298 according to cell length were significant (Fig. S5). The p_{pleC} did not show any significant
299 variation in its activity according to bacterial cell size (Fig. 4 and Fig. S5). Taken
300 together, these data suggest that two promoters bound by CtrA *in vivo* are differentially
301 regulated during *B. abortus* cell cycle, supporting the role of CtrA as a cell cycle
302 regulator.

303 The *ccrM* and *repAB* promoters contain two and one proposed CtrA binding sites,
304 respectively (Fig. S6). Using the p_{ccrM} - gfp_{asv} and p_{repAB} - gfp_{asv} fusions cited above, we
305 created mutants in the CtrA binding boxes (Fig. S6) and we were able to show that
306 mutagenesis of CtrA binding box 2 for p_{ccrM} and mutagenesis of the CtrA binding box in
307 p_{repAB} abolished activity of these promoters, strongly suggesting that CtrA is crucial to
308 activate them. Of course, we cannot exclude that these mutations also impair the binding
309 of other crucial factors required for the activity of *repAB* and *ccrM* promoters. The
310 mutation of CtrA binding box 1 in p_{ccrM} did not yield a significant effect, suggesting that
311 its role is either subtle or restricted to a condition that was not present in our
312 experiments.

313

314

315 *CtrA is required for B. abortus division and survival in HeLa cells.*

316 To assess the role of CtrA during infection, the depletion strain was used to infect HeLa
317 cells. Bacteria were incubated with HeLa cells for one hour with IPTG. Cells were then
318 washed and gentamycin was added to kill extracellular bacteria. The CtrA depletion
319 strain was able to infect HeLa cells and to replicate intracellularly almost to the same
320 extent as the WT when IPTG was kept in the medium (Fig. 3B). When IPTG was removed
321 after the initial hour of internalization, a similar number of CFU was recovered 3 h PI,
322 and then the CFU counts dropped dramatically and went below the detection limit at
323 48 h PI. We verified that the presence of Triton X-100, used for the extraction of bacteria
324 from host cells, did not decrease the CFU counts for the CtrA depletion strain in the
325 absence of IPTG (Fig. S7). Altogether, these data suggest that CtrA is crucial for *B.*
326 *abortus* viability during HeLa cells infection.

327 Similarly to the rich medium condition, we analysed the morphology of the CtrA
328 depletion strain during infection. As expected, this strain had WT morphology when
329 IPTG was kept in the medium (Fig. 5A). When the infection was performed in the
330 absence of IPTG, bacteria with aberrant morphologies appeared from 10h PI, but their
331 proportion was variable from one infection to the other. The intracellular branched
332 morphologies are similar to those observed after a long depletion in culture (Fig. 2). If
333 bacteria are labeled with TRSE prior to infection, they also display a Texas Red
334 fluorescence at the base of the branched morphology (Fig. 5B; white arrow head). The
335 emergence of abnormal morphologies late in the trafficking is consistent with the
336 previously reported biphasic trafficking of *B. abortus* in HeLa cells (Deghelt et al., 2014).
337 Indeed, *B. abortus* intracellular growth is detected between 6 and 8 h PI in HeLa cells,
338 suggesting a growth arrest of at least 6 hours (Deghelt et al., 2014). The CtrA depletion
339 generates elongated morphologies at 10 h PI, suggesting that growth was also arrested

340 for several hours before, otherwise these abnormal morphologies would have appeared
341 around 3 h PI. This suggests that CtrA is not crucial to control the timing of the
342 intracellular growth recovery.

343 We also investigated the intracellular trafficking of the CtrA depletion strain by
344 monitoring the labeling of BCV with Lamp1, a marker of late endosomes and lysosomes
345 that is excluded from the BCV during a normal trafficking in HeLa cells. Therefore, to test
346 the ability of the CtrA depletion strain to leave Lamp1+ compartments, we chose to
347 monitor the Lamp1 labeling of BCV with this marker at a time PI (10 h), when the WT
348 strain is expected to leave late endosomes (Deghelt et al., 2014, Pizarro-Cerda *et al.*,
349 1998b). As a control, we used a $\Delta virB$ strain known to stay in Lamp1+ compartments for
350 up to 12 h PI (Celli et al., 2003, Comerchi *et al.*, 2001). Our results showed indeed a low
351 proportion of Lamp1+ vacuoles for the WT strain compared to $\Delta virB$ ($p < 0.01$) (Fig. 6A
352 and 6B). The CtrA depletion strain supplemented or not with IPTG had a similar
353 proportion of Lamp1+ vacuoles compared to the WT (Fig 6A), suggesting that its
354 intracellular trafficking is similar to the WT. This suggested that CtrA depletion does not
355 profoundly affect trafficking of *B. abortus* in HeLa cells. Since an abnormal morphology
356 seems to be a typical feature of CtrA depletion (Fig. 2), we evaluated the proportion of
357 bacteria with abnormal morphology in ER compartments, compared to the proportion of
358 bacteria with a normal morphology in the same compartment. To label the ER, we chose
359 two markers, the translocon component Sec61 β (Fig. 6B) (Hartmann *et al.*, 1994) and
360 the dolichol kinase (DolK, Fig. 6C) (Shridas & Waechter, 2006), typical proteins of the
361 endoplasmic reticulum. The HeLa cells were infected with the CtrA depletion strain in
362 the absence of IPTG, Sec61 β positive (Sec61 β +) and DolK positive (DolK+) BCVs were
363 detected using immunofluorescence, and the proportion of Sec61 β + and DolK+ BCVs
364 was evaluated for normal and abnormal morphologies (Fig. 6B and 6C). If CtrA depletion

365 affects trafficking, one could expect a lower proportion of abnormal morphologies in the
366 ER compartments. Actually, we found that the proportion of Sec61 β + or DolK+ BCVs
367 containing abnormal morphologies was slightly higher compared to the Sec61 β + or
368 DolK + BCV containing bacteria with a normal morphology. The main interpretation of
369 these data is that CtrA depletion does not impair trafficking to the ER. The lower
370 proportion of bacteria with a normal morphology could be explained by the presence of
371 dead or non-growing bacteria, unable to traffic until ER compartments.

372

373 *CtrA depletion affects OMP amounts.*

374 One surprising feature of the CtrA regulon, according to ChIP-seq data (Table S1), is the
375 high proportion of direct targets corresponding to genes encoding outer membrane
376 components, particularly outer membrane proteins (OMPs). In order to reveal a possible
377 impact of CtrA depletion on the abundance of some of these OMPs, three integral OMPs
378 (Omp2b, Omp25 and BamA) and two proposed OM lipoproteins (Omp16 and Omp19)
379 were detected by Western blot on a *B. abortus* wild type strain, on the CtrA depletion
380 strain cultivated with IPTG and on the same strain depleted in CtrA overnight. While the
381 amount of Omp16 and Omp19 seems to remain unchanged in the absence of CtrA, a
382 slight decrease in the amount of Omp2b and BamA was observed (Fig. 7A). Omp25
383 abundance was lower in the absence of CtrA, and strongly decreased at longer depletion
384 times (Fig. 7B). Given that OMPs of group 2 and 3 (Omp2b and Omp25) are the major
385 OMPs in *Brucella* envelope (Dubray & Charriaut, 1983), their reduced abundance in the
386 absence of CtrA could lead to the perturbation of the envelope, which could have
387 dramatic consequences for the bacterium when it is inside host cells (Fig. 3C).

388 We also labeled Omp25 present at the surface of *B. abortus* by
389 immunofluorescence. The localization of Omp25 on the CtrA-depletion strain grown

390 overnight without IPTG was heterogeneous. This was observed with a monoclonal
391 antibody directed against Omp25 (Fig. S8). The labeling was often partial and
392 concentrated on the tip of the branches (Fig. 8A). For the wild type strain, 86.6 % of the
393 bacteria were either completely unlabeled or displayed an homogeneous labeling (Fig.
394 8B). The $\Delta ctrA$ $p_{lac-ctrA}$ depletion strain cultivated in the presence of IPTG displayed a
395 similar proportion of unlabeled or homogeneously labeled bacteria (82.2 %) (Fig. S8).
396 Partially labeled bacteria were counted in three independent experiments, and their
397 proportion is reported in Fig. 8C. The proportion of partially labeled bacteria was
398 significantly higher for the depletion strain compared to the wild type strain ($p < 2.1 \cdot 10^{-5}$
399 in a Scheffé statistical analysis). These data suggest that in the absence of CtrA, Omp25
400 localization on the surface of *B. abortus* is perturbed. Curiously, the Omp25 labeling
401 pattern was symmetric, meaning that if the tip of one branch is labeled, the tip of the
402 other branches are also labeled (Fig. 8A). One plausible explanation is that Omp25 is
403 incorporated in the outer membrane in a similar manner in all parts of the branched
404 cells that are generated at the same time. In this model, Omp25 proteins remain
405 immobile in the outer membrane, probably because they are directly or indirectly bound
406 to peptidoglycan (CloECKaert *et al.*, 1992).

407

408 Discussion

409 The essential transcription factor CtrA is known to be at the heart of a complex network
410 regulating the cell cycle progression of the model organism *C. crescentus*. CtrA is
411 essential and its regulon is also partially conserved in *Sinorhizobium meliloti* (Pini et al.,
412 2015). However, in phylogenetically more distant organisms such as *Rhodospirillales*
413 (Greene *et al.*, 2012) or *Rhodobacterales*, CtrA is not essential and has evolved to
414 regulate cell cycle-independent processes (Cheng *et al.*, 2011, Francez-Charlot *et al.*,
415 2015, Lang & Beatty, 2000, Mercer *et al.*, 2012). Analysis of the expression of CtrA
416 targets in *B. abortus* suggests that CtrA is involved in cell cycle-dependent regulation
417 (Fig. 4).

418 Here we show that CtrA regulon in *B. abortus* is partially conserved in comparison
419 with *C. crescentus* and *S. meliloti* CtrA regulons. They indeed share genes involved in cell
420 cycle regulation such as DNA methylation, chromosome replication and segregation and
421 division (Laub et al., 2002, Pini et al., 2015). However, as previously suggested by the
422 identification of a limited number of CtrA targets in *B. abortus* (Bellefontaine et al.,
423 2002), a similar process can be regulated through different target genes. For example,
424 CtrA is binding to the *mipZ* promoter in *C. crescentus* (Fumeaux *et al.*, 2014), allowing
425 the control of Z ring positioning, while this control is proposed to be mediated by the
426 binding to the *minCDE* promoter in *B. abortus* (Bellefontaine et al., 2002), as also
427 recently elucidated in *S. meliloti* (Pini et al., 2015). These comparisons underline the
428 plasticity of the CtrA regulon along evolution.

429 Depletion of CtrA leads to a severe (Fig. 2) and reversible (Fig. S4) cell division
430 defect in *B. abortus*. However, among the direct targets of CtrA found in the conditions
431 tested here, cell cycle-related genes are not restricted to cell division. Indeed, genes
432 involved in replication, the DivK-CtrA regulation network and the recruitment of

433 proteins to the poles (*popZ*) have also their promoter enriched by ChIP-seq. Besides cell
434 cycle-related genes, one obvious conclusion of the ChIP-seq experiment reported here is
435 the high proportion of genes involved in envelope biogenesis or homeostasis. Indeed,
436 CtrA predicted regulon is enriched in genes coding for LPS and outer membrane
437 proteins biosynthesis and export. The presence of CtrA is crucial for the production of
438 normal amounts of Omp25 (Fig. 7) and for an homogeneous distribution of Omp25 on
439 the surface of the bacterium (Fig. 8). We cannot exclude that alteration of Omp25
440 localization on the surface is an indirect effect of the inhibition of cell division. Indeed it
441 is likely that the generation of elongated and branched morphologies takes more time
442 than the generation of normal shaped bacteria, thus partially labeled bacteria could
443 reveal the oscillating nature of Omp25 incorporation in the outer membrane in these
444 cells. A *B. abortus* deletion strain for *omp25* was found to be attenuated in cattle
445 (Edmonds *et al.*, 2001), but more recent data suggested that this attenuation could be
446 explained by a higher internalization and a higher intracellular killing of the *omp25*
447 mutant compared to the wild type strain (Manterola *et al.*, 2007). The molecular
448 functions of the highly abundant Omp25 are still unknown; it was shown to inhibit TNF α
449 production in human macrophages (Jubier-Maurin *et al.*, 2001) and it could be involved
450 in defining the properties of the outer membrane by interacting with the LPS (Manterola
451 *et al.*, 2005). Interestingly, in *S. meliloti*, CtrA binds to the promoter of *ropB* gene (Pini *et*
452 *al.*, 2015), encoding an Omp25 homolog involved in outer membrane stability in
453 *Rhizobium leguminosarum* (Vanderlinde & Yost, 2012). It is thus possible that in
454 *Rhizobiales*, CtrA controls factors involved in outer membrane biogenesis or
455 homeostasis. Their control by CtrA would have been acquired after the divergence from
456 the common ancestor with *C. crescentus*, since CtrA regulon of *C. crescentus* is not

457 particularly enriched in genes involved in outer membrane biogenesis or homeostasis
458 (Fumeaux et al., 2014, Laub et al., 2002).

459 Depletion of CtrA results in a strong inhibition of cell division (Fig. 2A), possibly
460 explaining why the *ctrA* gene is essential in *B. abortus* as suggested in previous studies
461 (Bellefontaine et al., 2002, Willett et al., 2015). The inhibition of cell division results in
462 branched morphology or formation of small chains of cells, the latter being probably
463 produced by incomplete septation. It is noteworthy that the CtrA-loss of function
464 phenotype is reversible, as induction of *ctrA* expression after depletion resulted in the
465 reactivation of cell division (Fig. S4). Perturbation of division in the CtrA-depleted
466 condition is likely explained by the presence of numerous genes and operons involved in
467 division in the CtrA predicted regulon. Indeed, the *minCDE* operon is involved in Z ring
468 placement, and many genes and operons proposed to be involved in the cell division
469 process, like *ftsQAZ*, *ftsEX*, *ftsK* and the *pal(omp16)-tolQRAB* locus are detected as
470 possible direct targets of CtrA in *B. abortus* (Table S1). The deregulation of some of these
471 genes is probably sufficient to block the whole cell division process.

472 Depletion of CtrA also resulted in altered morphology of bacteria infecting host
473 cells (Fig. 5B). During infection elongated and branched morphologies can only be
474 generated by growth, suggesting that these bacteria are able to uptake nutrients during
475 cellular infection, after an initial stage of growth arrest that could be due to starvation
476 (see below). In host cells, the timing of the appearance of the altered morphologies is
477 different from the timing of their formation in bacteriological medium. Indeed, in HeLa
478 cells abnormal morphologies of the CtrA depletion strain appeared around or after 10 h
479 PI (Fig. 5B), mainly consisting of elongated cells (Fig. 5A) resembling bacteria recovered
480 3 h after IPTG removal in rich culture medium (Fig. 2A). At 15 h PI, branched bacteria
481 were observed (Fig. 5A), similarly to the 7 h depletion in culture (Fig. 2A). Interestingly,

482 *B. abortus* was shown to resume its intracellular growth around 8 h PI in HeLa cells
483 (Deghelt et al., 2014). The observation of elongated bacteria at or after 10 h PI for the
484 CtrA-depleted bacteria thus suggests that the absence of CtrA does not drastically
485 change the timing of growth arrest/resumption in HeLa cells. If CtrA is not required for
486 the control of the intracellular growth arrest/resumption, it is likely that other
487 regulation networks, like those triggered by starvation (Dozot *et al.*, 2006), could be
488 involved. Previous work also showed that *B. abortus* growth is resumed in Lamp1+
489 compartments around 8 h PI and that daughter cells are found almost exclusively in
490 Lamp1- compartment from 10 h PI (Deghelt et al., 2014). While CtrA depleted bacteria
491 with a normal morphology could be dead or non-growing bacteria unable to traffic until
492 the ER, bacteria that have grown to generate branching morphology are able to traffic to
493 the ER, demonstrating that they are able to perform this crucial step of intracellular
494 trafficking. This suggests that despite their morphological alterations, these bacteria are
495 probably still able to produce a functional VirB system, which is required for this step of
496 their intracellular trafficking (Comerci et al., 2001, Delrue *et al.*, 2001). Thus CtrA-
497 dependent cell cycle control and intracellular trafficking seem to be relatively
498 independent processes in *B. abortus*. The dramatic drop of the CFU counts at 48 h PI
499 (Fig. 3B) suggests that the branched bacteria are unable to survive for long periods in
500 host cells.

501 In conclusion, our data support the idea that along evolution of the CtrA regulon,
502 CtrA has kept the control of cell division in many *Alphaproteobacteria*. However, in *B.*
503 *abortus* and possibly in *Rhizobiales* it also acquired new functions, including the control
504 of envelope composition. It is interesting to realize that CtrA has to be cleared from *S.*
505 *meliloti* cells to allow them to differentiate into nitrogen-fixing bacteroids inside host
506 plants (Pini *et al.*, 2013), illustrating that fundamental processes of bacterial cell cycle

507 have been adapted to the lifestyle of pathogens and symbionts within the
508 *Alphaproteobacteria*.

509

510 **Experimental procedures**

511 *Bacterial strains and media*

512 *E. coli* strains DH10B, BL21 (DE3) and DB3.1 were grown in Luria-Bertani (LB) medium
513 at 37°C. Derivatives of the *Brucella abortus* 544 Nal^R strain were cultivated in 2YT rich
514 medium (1% yeast extract, 1.6% peptone, 0.5% NaCl) at 37°C. Antibiotic concentrations
515 are the following: ampicillin, 100µg/ml; kanamycin, 20 or 50 µg/ml; chloramphenicol,
516 20 µg/ml; nalidixic acid, 25 µg/ml; rifampicin, 20 µg/ml; gentamycin, 50 µg/ml. *B.*
517 *abortus* strains were constructed as previously described (Deghelt et al., 2014).
518 Plasmids are listed in Table S2.

519

520 *Cloning of the pBBR-MCS1-p_{lacI}-lacI-p_{lac}-ctrA*

521 The p_{lacI}-lacI-p_{lac} sequence was amplified from the pSRK-Kan vector (Khan *et al.*, 2008)
522 using Phusion High-Fidelity DNA Polymerase (New England BioLabs) and SacI-Kan3'
523 and p_{lac}-R1 primers (see Table S3). The *ctrA* coding sequence was amplified from *B.*
524 *abortus* 544 purified genomic DNA using *ctrA*-F2 and *KpnI*-*ctrA*-R2 primers. The PCR
525 product was fused to the p_{lacI}-lacI-p_{lac} sequence by joining PCR. The p_{lacI}-lacI-p_{lac}-*ctrA*
526 insert was then cloned in the pBBRMCS1 using SacI and *KpnI* restriction enzymes. By
527 using these enzymes, the insert was cloned in the opposite orientation to the p_{lac}
528 promoter of the pBBRMCS1.

529

530

531 *Cloning of a ctrA deletion for allelic exchange*

532 The *ctrA* gene was deleted from *B. abortus* 544 chromosome by allelic replacement. A
533 750 base pair (bp)-region upstream and another one downstream of *ctrA* were
534 amplified by PCR using *Pst*I-Up-*ctrA*-F/Up-*ctrA*-R and Down-*ctrA*-F/*Sal*I-Down-*ctrA*-R
535 pairs of primers respectively and both PCR products were fused together by joining PCR.
536 The PCR product was cloned in the pNPTS138 vector (M. R. K. Alley, Imperial College of
537 Science, London, UK) carrying a kanamycin resistance cassette and a sucrose sensitivity
538 cassette.

539

540 *Cloning of reporter vectors*

541 Promoter regions were amplified from *B. abortus* 544 purified genomic DNA using
542 Phusion High-Fidelity DNA Polymerase and fused by joining PCR to *gfp*(ASV). The pairs
543 of primers used to amplify the promoter regions are *Xba*I-p_{*ctrA*}-F1/p_{*ctrA*}-R1, *Xba*I-p_{*repAB*}-
544 F1/p_{*repAB*}-R1, *Xba*I-p_{*ccrM*}-F1/p_{*ccrM*}-R1 and *Xba*I-p_{*pleC*}-F1/p_{*pleC*}-R1. The pair of primers used
545 to amplify the *gfp*(ASV) gene is *gfp*(ASV)-F2/*Xho*I-*gfp*(ASV)-R2. *Xba*I and *Xho*I restriction
546 sites were added to the upstream and downstream primers. The fusion was first cloned
547 in pGEMT digested by *Eco*RV, generating blunt ends, and sequenced. A *Xba*I-*Xho*I
548 restriction allowed the transfer of the insert to a pBBRMCS1 vector, in the opposite
549 direction to the *lac* promoter of the vector.

550 Mutagenesis of the □CtrA boxes was generated in the same way, but using the
551 constructs with a wild type promoter as DNA template. The *Xba*I-p_{*gene*}-F1 and *Xho*I-
552 *gfp*(ASV)-R2 were kept as they were but their corresponding pair of primer (R1 and F2)
553 were modified to include the mutated CtrA-binding boxes. In the case of p_{*ccrM*}-mut1&2-
554 *gfp*(ASV), boxes were mutated sequentially (CtrA-binding box 1, followed by CtrA-
555 binding box 2). The wild type and mutated promoters are shown in figure S5.

556

557 *Chromatin immunoprecipitation with anti-CtrA antibodies*

558 An 80 ml culture of *B. abortus* 544 at an OD₆₀₀ of 0.8 was centrifuged to harvest the
559 bacteria. Protein-DNA crosslinking was performed in 10 µM sodium phosphate buffer
560 (pH 7.6) and 1% formaldehyde for 10 min at RT and 30 min on ice. Bacteria were
561 harvested by centrifugation at 8500 rpm for 5 min at 4°C, washed twice in cold PBS and
562 resuspended in lysis buffer (10 mM Tris-HCl pH 7.5, 1 mM EDTA, 100 mM NaCl, 2.2
563 mg/ml lysozyme, 20 µl protease inhibitor solution). Zirconia/Silica beads (Biospec
564 Products) of 0.1 and 0.5 mm diameter were added. Bacteria were lysed in the cell
565 Disruptor Genie from Scientific Industries at maximal amplitude (2800) for 25 min at
566 4°C. ChIP buffer was added (1.1% TritonX-100, 1.2 mM EDTA, 16.7 mM Tris-HCl pH 8.0,
567 167 mM NaCl, protease inhibitors) and bacteria were incubated at 37°C for 10 min for
568 further lysis. The lysate was sonicated on ice (Branson Sonifier Digital cell disruptor S-
569 450D 400W) by applying 15 bursts of 20 sec (50% duty) at 30% amplitude to cut the
570 DNA to fragments of about 300 base pairs and centrifuged at 14,000 rpm for 3 min to
571 pellet the debris. The supernatant was normalized by protein content by measuring the
572 absorbance at 280 nm. Around 7.5 mg of protein was diluted in 1 ml of ChIP buffer
573 supplemented with 0.01% SDS and pre-cleared in 80 µl of protein A-agarose beads
574 (Roche) and 100 µg BSA. Polyclonal anti-CtrA antibodies (Bellefontaine et al., 2002)
575 were added to the supernatant (dilution 1:1000) and incubated for one night at 4°C to
576 form immune complexes which were then incubated with 80 µl of protein A-agarose
577 beads pre-saturated with BSA for 2 h at 4°C. Beads were then washed once with low salt
578 buffer (0.1% SDS, 1% TritonX-100, 2 mM EDTA, 20 mM Tris-HCl pH 8.1, 150 mM NaCl),
579 high salt buffer (0.1% SDS, 1% TritonX-100, 2 mM EDTA, 20 mM Tris-HCl pH 8.1, 500
580 mM NaCl) and LiCl buffer (0.25 M LiCl, 1% NP-40, 1% sodium deoxycholate, 1 mM EDTA,

581 10 mM Tris-HCl pH 8.1) and twice with TE buffer (10 mM Tris-HCl pH 8.1 and 1 mM
582 EDTA). Protein-DNA complexes were eluted with 500 µl of elution buffer (1% SDS and
583 0.1M NaHCO₃). Reverse crosslinking was performed in presence of 300 mM of NaCl O/N
584 at 65°C. Samples were treated with 2 µg of Proteinase K for 2h at 45°C in 40 mM EDTA
585 and 40 mM Tris-HCl pH 6.5. DNA was extracted using QIAgen minelute kit and
586 resuspended in 30 µl of Elution Buffer. ChIP DNA was sequenced using Illumina MySeq.

587 *Analysis of the sequencing data*

588 Sequencing data consisted of a number of reads per nucleotide. Computing of average
589 and variance in a window of 1 million base pairs allowed the calculation of Z score pour
590 each base pair (i.e. the number of standard deviation from the average). Genomic
591 regions with reads numbers above the threshold ($Z > 4$) were kept and considered to be
592 bound by CtrA. These regions were mapped to the genome of *Brucella abortus* 2308, a
593 close relative to the *B. abortus* 544 strain. The mapping is available in the Supplemental
594 files ChIP-seq_CtrA_chr1.txt and ChIP-seq_CtrA_chr2.txt, that can be analysed using the
595 Chr1.gb and Chr2.gb genomic sequences respectively, with the Artemis program (freely
596 available at the following website <http://www.sanger.ac.uk/science/tools/artemis>).

597

598 *Electrophoretic mobility shift assay*

599 DNA probes of 50-70 pb were prepared by amplifying promoter regions from *B. abortus*
600 544 purified genomic DNA using Phusion High Fidelity DNA Polymerase (see Table S3
601 for list of primers, named as EMSA-F/R-promoter). Each PCR product was concentrated
602 and purified after migration on agarose gel eletrophoresis, using NucleoSpin® Gel and
603 PCR Clean-up (Macherey-Nagel) according to manufacturer's instructions. These
604 purified PCR products were then used as template for a new amplification with a
605 cyanine-5(Cy5)-labeled primer (Integrated DNA Technologies) (Table S3). The labeled

606 amplicons were purified after gel electrophoresis and quantified using a Qubit® 3.0
607 Fluorometer (Thermo Fisher Scientific).

608 His₆-CtrA was purified and phosphorylated as previously described (Bellefontaine et al,
609 2002). Binding reactions were prepared in a final volume of 20 µl with 0 to 340 µg of
610 CtrA, 3 ng of labeled probes and when necessary with 400 ng of competing probe (non-
611 labeled PCR product) in binding buffer (10 mM Tris pH 7.4, 10 mM MgCl₂, 50 mM NaCl,
612 10% glycerol). Samples were incubated for 30-45 minutes at 37°C and 10 µl were
613 loaded onto a 13.3% polyacrylamide gel (3.9 ml of ddH₂O, 700 µl of 5X TBE buffer, 2.3
614 ml of 40% acrylamide stock 19:1, 70 µl of 10% APS and 7 µl of TEMED). TBE is 89 mM
615 Tris, 89 mM boric acid and 2 mM EDTA, pH 8.3. Samples were run at 100V for 3h20 in
616 0.5 x TBE buffer at 4°C. Samples were revealed using an Amersham Imager 600 (GE
617 Healthcare Life Sciences) with the Cy5 fluorescence channel.

618

619 *Reverse transcription followed by quantitative PCR*

620 The *B. abortus* strains were grown in rich medium (2YT) until exponential phase,
621 washed and growth was restart in rich medium, with or without IPTG for 6 hours. Then
622 bacteria were washed in PBS, collected by centrifugation and immediately frozen and
623 stored at -80°C until processing. RNA was then extracted with TriPure isolation reagent
624 (Roche) according to the instructions of the manufacturer. DNA contamination was
625 eliminated by incubation with DNase I (Fermentas). RNA was reverse transcribed with
626 specific primers, using the High capacity cDNA Reverse Transcription kit (Applied
627 biosystems). Specific cDNAs were amplified using FastStart Universal SYBR Green
628 Master (Roche) with a LightCycler 96 Instrument (Roche). The specificity of the PCR was
629 assessed by melting-point analysis and gel electrophoresis. Results were normalized

630 using the housekeeping *groEL* gene as a reference. Primer sequences (with a name
631 starting by RT-qPCR) are available in Table S3.

632

633 *TRSE labeling*

634 Bacteria were harvested by centrifugation at 7000 rpm for 2 min. They were then
635 washed thrice with phosphate-buffered saline (PBS) and incubated with Texas Red
636 succinimidyl ester (TRSE) from Invitrogen diluted at 1 μ g/ml in PBS for 15 min at room
637 temperature (RT) in the dark. Bacteria were then washed once with PBS and twice with
638 the appropriate medium, 2YT for growth assays and Dulbecco's Modified Eagle's
639 Medium (DMEM) for HeLa cells infections.

640

641 *Microscopy and analysis of GFP fluorescence in the reporter systems using MicrobeTracker*

642 *B. abortus* strains labeled with TRSE were analysed by fluorescence microscopy as
643 previously reported (Deghelt et al., 2014). The pairwise comparisons of the proportions
644 of morphotypes such as elongated cells or bacteria with mislocalized constriction sites
645 were made using a Scheffe analysis. *B. abortus* strains expressing a promoter-*gfp* fusion
646 were observed using a Nikon 80i (objective phase contrast x 100, plan Apo) connected
647 to a Hammamatsu ORCA-ER camera. Cell meshes were obtained using the Matlab-based
648 MicrobeTracker software (Sliusarenko et al., 2011), determining the cell length and
649 quantifying the average amount of fluorescence per bacterium. Data were then
650 transferred to Excel files using the "XLStotmeansteparea.m" script. Data were sorted
651 according to bacterial cell length, and the mean cell length and mean fluorescence
652 intensity were calculated using a sliding window of 300 bacteria.

653

654

655 *HeLa cells culture and infection*

656 HeLa cells (from the Centre d'Immunologie de Marseille-Luminy, Marseille, France)
657 were cultivated at 37°C and in a 5% CO₂ atmosphere in DMEM (Invitrogen)
658 supplemented with 10% fetal bovine serum (Gibco), 0.1 g/l non-essential amino acids
659 and 0.1 g/l sodium pyruvate (Invitrogen). For the infection, HeLa cells were seeded in
660 24-well plates (on cover-slips for immunolabeling) at a concentration of 4.10⁴ cells/ml.
661 On the day of the infection, an O/N culture of *B. abortus* was diluted in DMEM to reach
662 an MOI (multiplicity of infection) of 300. Bacteria were added to HeLa cells and the 24-
663 well plates were centrifuged at 1200 rpm for 10 min at 4°C. Cells were then incubated at
664 37°C in a 5% CO₂ atmosphere for one hour. Cells were washed twice in PBS and fresh
665 medium supplemented with 50 µg/ml gentamycin was added.

666

667 *Immunolabeling of infected HeLa cells*

668 Cells were fixed in PBS 2% paraformaldehyde (Prolabo) for 20 min at RT then
669 permeabilized in PBS 0.1% Triton X-100 for 10 min. Cells were incubated for 45 min
670 with primary and secondary antibodies supplemented with 0.1% Triton X-100 and 3%
671 bovine serum albumin (BSA, Sigma Aldrich). *Brucella* were detected with the A76-12G12
672 monoclonal antibody (non-diluted hybridoma culture supernatant) followed by a
673 secondary anti-mouse antibodies coupled to Alexa-488 diluted 500 times (Sigma
674 Aldrich). Coverslips were washed thrice with PBS and once with ddH₂O and mounted
675 with Mowiol (Sigma). Antibodies are listed in Table S4.

676 For Lamp1 labeling, cells were fixed in methanol-acetone (80%-20%) for 20 min at
677 RT. Bacteria and Lamp1 were labeled with a rabbit anti-*Brucella* serum diluted 2000
678 times and mouse anti-Lamp1 antibodies diluted 200 times in PBS 2% BSA. Secondary
679 anti-rabbit antibodies coupled to Pacific Blue and anti-mouse antibodies coupled to

680 Alexa-488 (Sigma Aldrich) were diluted 500 times in PBS 2% BSA. Coverslips were
681 washed thrice in PBS 2% BSA and mounted with Mowiol. For each strain in each
682 condition (+/- IPTG), the number of BCVs analysed was as follows : 66 to 77 for the wild
683 type strain, 62 to 100 for the depletion strain with IPTG, 48 to 70 for the depletion strain
684 without IPTG, and 36 to 71 for the $\Delta virB$ strain.

685 For endoplasmic reticulum (ER) labeling, cells were fixed in PBS 2%
686 paraformaldehyde for 20 minutes at RT, then washed twice with PBS before to be
687 permeabilized with PBS 0.2% saponin (Sigma Aldrich) for 20 minutes at RT. Cells were
688 then blocked for 30 minutes with 0.2% saponin, 3% BSA, 50 mM NH₄Cl in 0.1% dPBS-
689 Tween20. ER was labeled either with primary anti-DOLK rabbit antibody (Abcam,
690 ab93609) diluted 200 times or with anti-Sec61 β rabbit antibody (B. Dobberstein,
691 Universität Heidelberg, Heidelberg, Germany) diluted 100 times, both in 3% BSA, 0.2%
692 saponin and 0.1% dPBS-Tween20. Secondary anti-rabbit coupled to Alexa-488 (Sigma
693 Aldrich) diluted 500 times were used for staining after washing thrice with PBS. *B.*
694 *abortus* were labeled using non-diluted A76-12G12 primary antibody obtained from
695 homemade hybridoma culture supernatant in 0.2% saponin and 3% BSA, followed by a
696 secondary anti-mouse antibody coupled to TxRed (Sigma Aldrich) diluted 500 times in
697 3% BSA, 0.2% saponin and 0.1% dPBS-Tween20. Coverslips were washed thrice in PBS
698 and once in ddH₂O before to be mounted on Mowiol. The infections were repeated three
699 times independently, and 167 to 317 BCVs were analyzed in each infection.

700

701 *Growth curve and CFU counts*

702 Growth curves were performed by using Bioscreen C from Oy Growth curves. O/N
703 cultures were diluted to an OD of 0.1 and the OD was measured every 30 min during 70

704 hours. For CFU counts in culture, wild type (WT) *B. abortus* 544 and the CtrA depletion
705 strain supplemented with IPTG were diluted to 10^{-6} or 10^{-7} in 2YT and 100 μ l were
706 plated on 2YT, supplemented with chloramphenicol and 1 mM IPTG for the depletion
707 strain. The depletion strain grown without IPTG was diluted to 10^{-4} or 10^{-5} . For CFU
708 counts after infection, HeLa cells were lysed with 0.01% TritonX-100 PBS for 10 min at
709 RT. Several dilutions were plated on 2YT supplemented with chloramphenicol and IPTG
710 if needed. Plates were incubated for 3 to 4 days at 37°C.

711

712 *Western blot analysis*

713 One ml of a *B. abortus* culture was concentrated to an OD₆₀₀ of 10 in PBS. Bacteria were
714 inactivated for one hour at 80°C and loading buffer was added. Fifteen μ l of bacterial
715 lysate was loaded in each well. After migration, proteins were transferred onto a
716 nitrocellulose membrane which was blocked in PBS supplemented with 0.05% Tween
717 and 5% milk for at least one hour. The membrane was incubated for 1 h with the
718 appropriate serum (diluted 10, 100 or 1000x depending on the serum) and secondary
719 antibodies coupled to HRP (diluted 5000x) (Dako Denmark) diluted in PBS 0.05%
720 Tween 1% milk. The membrane was washed for 3 times for 5 min. The Clarity Western
721 ECL Substrate (Biorad) and Image Quant LAS 4000 (General Electric) were used to
722 reveal the bands.

723

724 *Immunodetection of Omp25 on bacteria*

725 Bacteria grown overnight in rich culture medium were washed twice in PBS by
726 centrifugation at 4000 rpm for 2.5 min and resuspension. Washed bacteria were
727 resuspended in non-diluted hybridoma culture supernatant containing monoclonal anti-
728 Omp25 antibodies and secondary anti-mouse antibodies coupled to Alexa-488 diluted

729 500 times in PBS, and were incubated for 40 min at RT on a wheel. Bacteria were
730 washed twice in PBS and 2 µl were dropped on an agarose pad (1% PBS agarose) for
731 microscopy.

732

733 **Acknowledgements**

734 We thank Véronique Dhennin from the UMR8199 sequencing service LIGAN-PM
735 Equipex (Lille Integrated Genomics Advanced Network for personalized medicine) and
736 Aurélie Mayard for assistance in protein purification and Western blotting.

737 This research has been funded by the Interuniversity Attraction Poles Programme
738 initiated by the Belgian Science Policy Office (<https://www.belspo.be/>) to J.-J. Letesson
739 and by grants from Fonds de la Recherche Scientifique-Fonds National de la Recherche
740 Scientifique (FRS-FNRS, <http://www.fnrs.be>) (PDR T.0053.13 and PDR Brucell-cycle
741 T.0060.15, CDR J.0091.14 and FRFC 2.4.541.08 F) to X. De Bolle. We thank UNamur
742 (<https://www.unamur.be/>) for financial and logistic supports. This work was supported
743 by the French Agence Nationale de Recherche (ANR-JCJC-2011-Castacc)
744 (<http://www.agence-nationale-recherche.fr/>) and the Region Pas-De-Calais
745 (<http://www.nordpasdecalais.fr>) CPER to A. Fioravanti and Emanuele G. Biondi. N.
746 Francis held an Aspirant fellowship from FRS-FNRS. K. Poncin and V. Vassen are
747 supported by a Ph.D. grant from FRIA (FRS-FNRS). The authors declare no conflict of
748 interest.

749

750 **Author Contributions**

751 NF, KP, AV, VV, KW, TAPO and LR acquired and analyzed the data; NF, JLL, EB and XDB
752 designed the study; NF, JLL, EB and XDB wrote the manuscript.

753

754 **References**

- 755 Andersen, J. B., C. Sternberg, L. K. Poulsen, S. P. Bjorn, M. Givskov & S. Molin (1998) New
756 unstable variants of green fluorescent protein for studies of transient gene
757 expression in bacteria. *Appl Environ Microbiol* **64**: 2240-2246.
- 758 Anderson, E. S., J. T. Paulley, J. M. Gaines, M. W. Valderas, D. W. Martin, E. Menscher, T. D.
759 Brown, C. S. Burns & R. M. Roop, 2nd (2009) The manganese transporter MntH is
760 a critical virulence determinant for *Brucella abortus* 2308 in experimentally
761 infected mice. *Infect Immun* **77**: 3466-3474.
- 762 Archambaud, C., S. P. Salcedo, H. Lelouard, E. Devilard, B. de Bovis, N. Van Rooijen, J. P.
763 Gorvel & B. Malissen (2010) Contrasting roles of macrophages and dendritic cells
764 in controlling initial pulmonary *Brucella* infection. *Eur J Immunol* **40**: 3458-3471.
- 765 Bellefontaine, A. F., C. E. Pierreux, P. Mertens, J. Vandenhoute, J. J. Letesson & X. De Bolle
766 (2002) Plasticity of a transcriptional regulation network among alpha-
767 proteobacteria is supported by the identification of CtrA targets in *Brucella*
768 *abortus*. *Mol Microbiol* **43**: 945-960.
- 769 Brilli, M., M. Fondi, R. Fani, A. Mengoni, L. Ferri, M. Bazzicalupo & E. G. Biondi (2010) The
770 diversity and evolution of cell cycle regulation in alpha-proteobacteria: a
771 comparative genomic analysis. *BMC Syst Biol* **4**: 52.
- 772 Brown, P. J., M. A. de Pedro, D. T. Kysela, C. Van der Henst, J. Kim, X. De Bolle, C. Fuqua &
773 Y. V. Brun (2012) Polar growth in the Alphaproteobacterial order Rhizobiales.
774 *Proc Natl Acad Sci U S A* **109**: 1697-1701.
- 775 Celli, J., C. de Chastellier, D. M. Franchini, J. Pizarro-Cerda, E. Moreno & J. P. Gorvel (2003)
776 *Brucella* evades macrophage killing via VirB-dependent sustained interactions
777 with the endoplasmic reticulum. *J Exp Med* **198**: 545-556.
- 778 Celli, J., S. P. Salcedo & J. P. Gorvel (2005) *Brucella* coopts the small GTPase Sar1 for
779 intracellular replication. *Proc Natl Acad Sci U S A* **102**: 1673-1678.
- 780 Chaves-Olarte, E., C. Guzman-Verri, S. Meresse, M. Desjardins, J. Pizarro-Cerda, J. Badilla,
781 J. P. Gorvel & E. Moreno (2002) Activation of Rho and Rab GTPases dissociates
782 *Brucella abortus* internalization from intracellular trafficking. *Cellular*
783 *microbiology* **4**: 663-676.
- 784 Cheng, Z., K. Miura, V. L. Popov, Y. Kumagai & Y. Rikihisa (2011) Insights into the CtrA
785 regulon in development of stress resistance in obligatory intracellular pathogen
786 *Ehrlichia chaffeensis*. *Mol Microbiol* **82**: 1217-1234.
- 787 Cloeckert, A., M. S. Zygmunt, P. de Wergifosse, G. Dubray & J. N. Limet (1992)
788 Demonstration of peptidoglycan-associated *Brucella* outer-membrane proteins
789 by use of monoclonal antibodies. *J Gen Microbiol* **138**: 1543-1550.
- 790 Comerci, D. J., M. J. Martinez-Lorenzo, R. Sieira, J. P. Gorvel & R. A. Ugalde (2001)
791 Essential role of the VirB machinery in the maturation of the *Brucella abortus*-
792 containing vacuole. *Cell Microbiol* **3**: 159-168.
- 793 Curtis, P. D. & Y. V. Brun (2010) Getting in the loop: regulation of development in
794 *Caulobacter crescentus*. *Microbiology and molecular biology reviews : MMBR* **74**:
795 13-41.
- 796 De Bolle, X., S. Crosson, J. Y. Matroule & J. J. Letesson (2015) *Brucella abortus* Cell Cycle
797 and Infection Are Coordinated. *Trends Microbiol* **23**: 812-821.
- 798 Deghelt, M., C. Mullier, J. F. Sternon, N. Francis, G. Laloux, D. Dotreppe, C. Van der Henst,
799 C. Jacobs-Wagner, J. J. Letesson & X. De Bolle (2014) G1-arrested newborn cells
800 are the predominant infectious form of the pathogen *Brucella abortus*. *Nat*
801 *Commun* **5**: 4366.

- 802 Delrue, R. M., M. Martinez-Lorenzo, P. Lestrade, I. Danese, V. Bielarz, P. Mertens, X. De
803 Bolle, A. Tibor, J. P. Gorvel & J. J. Letesson (2001) Identification of *Brucella* spp.
804 genes involved in intracellular trafficking. *Cell Microbiol* **3**: 487-497.
- 805 Dettleux, P. G., B. L. Deyoe & N. F. Cheville (1990) Penetration and intracellular growth
806 of *Brucella abortus* in nonphagocytic cells in vitro. *Infect Immun* **58**: 2320-2328.
- 807 Domian, I. J., K. C. Quon & L. Shapiro (1997) Cell type-specific phosphorylation and
808 proteolysis of a transcriptional regulator controls the G1-to-S transition in a
809 bacterial cell cycle. *Cell* **90**: 415-424.
- 810 Dozot, M., R. A. Boigegrain, R. M. Delrue, R. Hallez, S. Ouahrani-Bettache, I. Danese, J. J.
811 Letesson, X. De Bolle & S. Kohler (2006) The stringent response mediator Rsh is
812 required for *Brucella melitensis* and *Brucella suis* virulence, and for expression of
813 the type IV secretion system virB. *Cell Microbiol* **8**: 1791-1802.
- 814 Dubray, G. & C. Charriaut (1983) Evidence of three major polypeptide species and two
815 major polysaccharide species in the *Brucella* outer membrane. *Annales de*
816 *recherches veterinaires. Annals of veterinary research* **14**: 311-318.
- 817 Edmonds, M. D., A. Cloeckert, N. J. Booth, W. T. Fulton, S. D. Hagius, J. V. Walker & P. H.
818 Elzer (2001) Attenuation of a *Brucella abortus* mutant lacking a major 25 kDa
819 outer membrane protein in cattle. *American journal of veterinary research* **62**:
820 1461-1466.
- 821 Francez-Charlot, A., A. Kaczmarczyk & J. A. Vorholt (2015) The branched CcsA/CckA-
822 ChpT-CtrA phosphorelay of *Sphingomonas melonis* controls motility and biofilm
823 formation. *Mol Microbiol* **97**: 47-63.
- 824 Fumeaux, C., S. K. Radhakrishnan, S. Ardisson, L. Theraulaz, A. Frandi, D. Martins, J.
825 Nesper, S. Abel, U. Jenal & P. H. Viollier (2014) Cell cycle transition from S-phase
826 to G1 in *Caulobacter* is mediated by ancestral virulence regulators. *Nat Commun*
827 **5**: 4081.
- 828 Gee, J. M., M. W. Valderas, M. E. Kovach, V. K. Grippe, G. T. Robertson, W. L. Ng, J. M.
829 Richardson, M. E. Winkler & R. M. Roop, 2nd (2005) The *Brucella abortus* Cu,Zn
830 superoxide dismutase is required for optimal resistance to oxidative killing by
831 murine macrophages and wild-type virulence in experimentally infected mice.
832 *Infect Immun* **73**: 2873-2880.
- 833 Gerding, M. A., Y. Ogata, N. D. Pecora, H. Niki & P. A. de Boer (2007) The trans-envelope
834 Tol-Pal complex is part of the cell division machinery and required for proper
835 outer-membrane invagination during cell constriction in *E. coli*. *Mol Microbiol* **63**:
836 1008-1025.
- 837 Grangeon, R., J. R. Zupan, J. Anderson-Furgeson & P. C. Zambryski (2015) PopZ identifies
838 the new pole, and PodJ identifies the old pole during polar growth in
839 *Agrobacterium tumefaciens*. *Proc Natl Acad Sci U S A* **112**: 11666-11671.
- 840 Greene, S. E., M. Brill, E. G. Biondi & A. Komeili (2012) Analysis of the CtrA pathway in
841 *Magnetospirillum* reveals an ancestral role in motility in alphaproteobacteria. *J*
842 *Bacteriol* **194**: 2973-2986.
- 843 Hallez, R., A. F. Bellefontaine, J. J. Letesson & X. De Bolle (2004) Morphological and
844 functional asymmetry in alpha-proteobacteria. *Trends Microbiol* **12**: 361-365.
- 845 Hallez, R., J. J. Letesson, J. Vandehaute & X. De Bolle (2007a) Gateway-based destination
846 vectors for functional analyses of bacterial ORFeomes: application to the Min
847 system in *Brucella abortus*. *Appl Environ Microbiol* **73**: 1375-1379.
- 848 Hallez, R., J. Mignolet, V. Van Mullem, M. Wery, J. Vandehaute, J. J. Letesson, C. Jacobs-
849 Wagner & X. De Bolle (2007b) The asymmetric distribution of the essential

- 850 histidine kinase PdhS indicates a differentiation event in *Brucella abortus*. *EMBO J*
851 **26**: 1444-1455.
- 852 Hartmann, E., T. Sommer, S. Prehn, D. Gorlich, S. Jentsch & T. A. Rapoport (1994)
853 Evolutionary conservation of components of the protein translocation complex.
854 *Nature* **367**: 654-657.
- 855 Holtzendorff, J., D. Hung, P. Brende, A. Reisenauer, P. H. Viollier, H. H. McAdams & L.
856 Shapiro (2004) Oscillating global regulators control the genetic circuit driving a
857 bacterial cell cycle. *Science* **304**: 983-987.
- 858 Jubier-Maurin, V., R. A. Boigegrain, A. Cloeckert, A. Gross, M. T. Alvarez-Martinez, A.
859 Terraza, J. Liautard, S. Kohler, B. Rouot, J. Dornand & J. P. Liautard (2001) Major
860 outer membrane protein Omp25 of *Brucella suis* is involved in inhibition of
861 tumor necrosis factor alpha production during infection of human macrophages.
862 *Infection and immunity* **69**: 4823-4830.
- 863 Khan, S. R., J. Gaines, R. M. Roop, 2nd & S. K. Farrand (2008) Broad-host-range
864 expression vectors with tightly regulated promoters and their use to examine the
865 influence of TraR and TraM expression on Ti plasmid quorum sensing. *Appl*
866 *Environ Microbiol* **74**: 5053-5062.
- 867 Lang, A. S. & J. T. Beatty (2000) Genetic analysis of a bacterial genetic exchange element:
868 the gene transfer agent of *Rhodobacter capsulatus*. *Proc Natl Acad Sci U S A* **97**:
869 859-864.
- 870 Laub, M. T., S. L. Chen, L. Shapiro & H. H. McAdams (2002) Genes directly controlled by
871 CtrA, a master regulator of the *Caulobacter* cell cycle. *Proc Natl Acad Sci U S A* **99**:
872 4632-4637.
- 873 Leonard, S., J. Ferooz, V. Haine, I. Danese, D. Fretin, A. Tibor, S. de Walque, X. De Bolle & J.
874 J. Letesson (2007) FtcR is a new master regulator of the flagellar system of
875 *Brucella melitensis* 16M with homologs in Rhizobiaceae. *Journal of bacteriology*
876 **189**: 131-141.
- 877 Magnet, S., L. Dubost, A. Marie, M. Arthur & L. Gutmann (2008) Identification of the L,D-
878 transpeptidases for peptidoglycan cross-linking in *Escherichia coli*. *J Bacteriol*
879 **190**: 4782-4785.
- 880 Manterola, L., C. Guzman-Verri, E. Chaves-Olarte, E. Barquero-Calvo, M. J. de Miguel, I.
881 Moriyon, M. J. Grillo, I. Lopez-Goni & E. Moreno (2007) BvrR/BvrS-controlled
882 outer membrane proteins Omp3a and Omp3b are not essential for *Brucella*
883 *abortus* virulence. *Infection and immunity* **75**: 4867-4874.
- 884 Manterola, L., I. Moriyon, E. Moreno, A. Sola-Landa, D. S. Weiss, M. H. Koch, J. Howe, K.
885 Brandenburg & I. Lopez-Goni (2005) The lipopolysaccharide of *Brucella abortus*
886 BvrS/BvrR mutants contains lipid A modifications and has higher affinity for
887 bactericidal cationic peptides. *Journal of bacteriology* **187**: 5631-5639.
- 888 Meinhardt, H. & P. A. de Boer (2001) Pattern formation in *Escherichia coli*: a model for
889 the pole-to-pole oscillations of Min proteins and the localization of the division
890 site. *Proc Natl Acad Sci U S A* **98**: 14202-14207.
- 891 Mercer, R. G., M. Quinlan, A. R. Rose, S. Noll, J. T. Beatty & A. S. Lang (2012) Regulatory
892 systems controlling motility and gene transfer agent production and release in
893 *Rhodobacter capsulatus*. *FEMS Microbiol Lett* **331**: 53-62.
- 894 Mignolet, J., C. Van der Henst, C. Nicolas, M. Deghelt, D. Dotreppe, J. J. Letesson & X. De
895 Bolle (2010) PdhS, an old-pole-localized histidine kinase, recruits the fumarase
896 FumC in *Brucella abortus*. *J Bacteriol* **192**: 3235-3239.
- 897 Moreno, E. & I. Moriyon (2006) The Genus *Brucella*. *Prokaryotes* **5**: 315-456.

- 898 Pini, F., N. J. De Nisco, L. Ferri, J. Penterman, A. Fioravanti, M. Brillì, A. Mengoni, M.
899 Bazzicalupo, P. H. Viollier, G. C. Walker & E. G. Biondi (2015) Cell Cycle Control by
900 the Master Regulator CtrA in *Sinorhizobium meliloti*. *PLoS Genet* **11**: e1005232.
- 901 Pini, F., B. Frage, L. Ferri, N. J. De Nisco, S. S. Mohapatra, L. Taddei, A. Fioravanti, F.
902 Dewitte, M. Galardini, M. Brillì, V. Villeret, M. Bazzicalupo, A. Mengoni, G. C.
903 Walker, A. Becker & E. G. Biondi (2013) The DivJ, CbrA and PleC system controls
904 DivK phosphorylation and symbiosis in *Sinorhizobium meliloti*. *Mol Microbiol* **90**:
905 54-71.
- 906 Pizarro-Cerda, J., S. Meresse, R. G. Parton, G. van der Goot, A. Sola-Landa, I. Lopez-Goni, E.
907 Moreno & J. P. Gorvel (1998a) *Brucella abortus* transits through the autophagic
908 pathway and replicates in the endoplasmic reticulum of nonprofessional
909 phagocytes. *Infect Immun* **66**: 5711-5724.
- 910 Pizarro-Cerda, J., E. Moreno, V. Sanguedolce, J. L. Mege & J. P. Gorvel (1998b) Virulent
911 *Brucella abortus* prevents lysosome fusion and is distributed within
912 autophagosome-like compartments. *Infect Immun* **66**: 2387-2392.
- 913 Quon, K. C., G. T. Marczyński & L. Shapiro (1996) Cell cycle control by an essential
914 bacterial two-component signal transduction protein. *Cell* **84**: 83-93.
- 915 Quon, K. C., B. Yang, I. J. Domian, L. Shapiro & G. T. Marczyński (1998) Negative control of
916 bacterial DNA replication by a cell cycle regulatory protein that binds at the
917 chromosome origin. *Proc Natl Acad Sci U S A* **95**: 120-125.
- 918 Reisenauer, A., K. Quon & L. Shapiro (1999) The CtrA response regulator mediates
919 temporal control of gene expression during the *Caulobacter* cell cycle. *Journal of*
920 *bacteriology* **181**: 2430-2439.
- 921 Robertson, G. T., A. Reisenauer, R. Wright, R. B. Jensen, A. Jensen, L. Shapiro & R. M. Roop,
922 2nd (2000) The *Brucella abortus* CcrM DNA methyltransferase is essential for
923 viability, and its overexpression attenuates intracellular replication in murine
924 macrophages. *J Bacteriol* **182**: 3482-3489.
- 925 Salcedo, S. P., N. Chevrier, T. L. Lacerda, A. Ben Amara, S. Gerart, V. A. Gorvel, C. de
926 Chastellier, J. M. Blasco, J. L. Mege & J. P. Gorvel (2013) Pathogenic *brucellae*
927 replicate in human trophoblasts. *The Journal of infectious diseases* **207**: 1075-
928 1083.
- 929 Shridas, P. & C. J. Waechter (2006) Human dolichol kinase, a polytopic endoplasmic
930 reticulum membrane protein with a cytoplasmically oriented CTP-binding site. *J*
931 *Biol Chem* **281**: 31696-31704.
- 932 Sliusarenko, O., J. Heinritz, T. Emonet & C. Jacobs-Wagner (2011) High-throughput,
933 subpixel precision analysis of bacterial morphogenesis and intracellular spatio-
934 temporal dynamics. *Mol Microbiol* **80**: 612-627.
- 935 Starr, T., R. Child, T. D. Wehrly, B. Hansen, S. Hwang, C. Lopez-Otin, H. W. Virgin & J. Celli
936 (2012) Selective subversion of autophagy complexes facilitates completion of the
937 *Brucella* intracellular cycle. *Cell Host Microbe* **11**: 33-45.
- 938 Starr, T., T. W. Ng, T. D. Wehrly, L. A. Knodler & J. Celli (2008) *Brucella* intracellular
939 replication requires trafficking through the late endosomal/lysosomal
940 compartment. *Traffic* **9**: 678-694.
- 941 Stouf, M., J. C. Meile & F. Cornet (2013) FtsK actively segregates sister chromosomes in
942 *Escherichia coli*. *Proc Natl Acad Sci U S A* **110**: 11157-11162.
- 943 Terwagne, M., A. Mirabella, J. Lemaire, C. Deschamps, X. De Bolle & J. J. Letesson (2013)
944 Quorum sensing and self-quorum quenching in the intracellular pathogen
945 *Brucella melitensis*. *PLoS One* **8**: e82514.

- 946 Van der Henst, C., M. de Barsy, A. Zorreguieta, J. J. Letesson & X. De Bolle (2013) The
947 *Brucella* pathogens are polarized bacteria. *Microbes Infect* **15**: 998-1004.
- 948 Vanderlinde, E. M. & C. K. Yost (2012) Mutation of the sensor kinase chvG in *Rhizobium*
949 *leguminosarum* negatively impacts cellular metabolism, outer membrane
950 stability, and symbiosis. *Journal of bacteriology* **194**: 768-777.
- 951 Wheeler, R. T. & L. Shapiro (1999) Differential localization of two histidine kinases
952 controlling bacterial cell differentiation. *Mol Cell* **4**: 683-694.
- 953 Willett, J. W., J. Herrou, A. Briegel, G. Rotskoff & S. Crosson (2015) Structural asymmetry
954 in a conserved signaling system that regulates division, replication, and virulence
955 of an intracellular pathogen. *Proc Natl Acad Sci U S A* **112**: E3709-3718.
- 956 Zweiger, G., G. Marczyński & L. Shapiro (1994) A *Caulobacter* DNA methyltransferase
957 that functions only in the predivisional cell. *J Mol Biol* **235**: 472-485.
- 958 -
- 959

For Peer Review

960 **Figure Legends**

961

962 **Fig. 1.** *In vivo* CtrA binding sites detected by ChIP-seq. The number of reads per nucleotide is
963 plotted for 6 promoter regions enriched by CtrA pull-down. Red bars surrounded by red
964 rectangles represent predicted 8-mer and 9-mer binding sites. Green bars surrounded by green
965 rectangles represent TTAA(C) half binding sites. Arrows under gene names represents the start
966 of the coding sequences.

967

968 **Fig. 2.** CtrA depletion generates cell division defects strain in *B. abortus*.

969 A. Phase contrast ("Phase") and fluorescence ("TexasRed") microscopy images of a CtrA
970 depletion strain labeled with TRSE and grown with IPTG ("+IPTG") show that bacteria have a
971 normal morphology. Upon IPTG removal ("-IPTG"), bacteria elongate (3 h), form chains and
972 branch (7 and 15 h). TRSE allows covalent binding of amine groups present at the bacterial
973 surface to Texas Red. Growth occurring after TRSE labeling results in the incorporation of
974 unlabeled envelope material. The scale bar corresponds to 2 μm .

975 B. CtrA detection by Western blot shows a quick decrease in CtrA amount and apparent
976 clearance 120 min post-IPTG removal.

977

978 **Fig. 3.** Viability of the CtrA depletion strain in rich medium and infection.

979 A. CFU count of wild type and CtrA depletion ($\Delta ctrA$ $p_{lac-ctrA}$) strains cultivated with or without
980 IPTG (+IPTG or -IPTG, respectively) in rich medium. Error bars correspond to standard
981 deviations (n = 3).

982 B) CFU count of wild type and CtrA depletion ($\Delta ctrA$ $p_{lac-ctrA}$) strains incubated with or without
983 IPTG (+IPTG or -IPTG, respectively) during a HeLa cell infection over a 48 h period of time.
984 Standard deviations are shown (n = 3).

985

986

987 **Fig. 4.** Activity profile of *repAB*, *ctrA*, *ccrM* and *pleC* promoters according to cell length.
988 Phase and fluorescence microscopy images of *B. abortus* reporter strains were analysed
989 with the MicrobeTracker program. Bacteria were ordered according to their cell length
990 and the mean cell length and mean fluorescence intensity was calculated for a sliding
991 window (from smallest to largest bacteria) of 300 bacteria. The mean fluorescence
992 intensities were normalized to the average fluorescence intensity of the whole
993 population of a given experiment, allowing the representation of results from three
994 independent experiments on the same plot. Each experiment is shown with a different
995 color. The number of bacteria analysed for p_{repAB} are 1632, 1402 and 2377; for p_{ctrA}
996 1456, 1487 and 1467; for p_{ccrM} 1446, 753 and 1678; for p_{pleC} 1888, 1297 and 1953.
997

998 **Fig. 5.** Morphology of the CtrA depletion strain during infection.

999 A. Immunofluorescence microscopy of HeLa cells infected for 15 h with the depletion strain in
1000 presence or in absence of IPTG. Phase contrast images were merged with anti-*Brucella* staining
1001 (cyan) to detect intracellular bacteria. The scale bars correspond to 5 μm . The absence of IPTG,
1002 bacteria with normal and abnormal morphologies can be found in variable proportions from one
1003 infection to the other.

1004 B. Representative image of an abnormal morphology generated by the CtrA depletion strain 15 h
1005 post-infection in HeLa cells, with bacteria labeled with TRSE before infection. The TRSE-labeled
1006 part corresponds to the old pole of the initial bacterium that invaded the host cell (white arrow
1007 head). DAPI (staining the nucleus in blue), anti-*Brucella* (green) and Texas Red are merged.
1008

1009 **Fig. 6.** Intracellular trafficking of the CtrA depletion strain.

1010 A. Three *B. abortus* strains, wild type, CtrA depletion (with or without IPTG) and $\Delta virB$, were
1011 used to infect HeLa cells. At 10 h PI, cells were fixed and immunofluorescence (IF) was
1012 performed to detect bacteria and Lamp1. The proportion of Lamp1+ BCV is shown for each

1013 strain/condition. The mean of three independent infections is indicated, the error bars
1014 correspond to standard deviation.

1015 B. The CtrA depletion strain was used to infect HeLa cells for 10 to 24 h (3 samples) in the
1016 absence of IPTG and IF was performed to detect bacteria and the ER marker Sec61 β . The
1017 abnormal morphology indicates that bacteria experienced a CtrA depletion inside host cells. The
1018 average and standard deviation are shown (497 normal and 153 abnormal bacteria were
1019 counted in total).

1020 C. The CtrA depletion strain was used to infect HeLa cells for 15 h (3 samples) in the absence of
1021 IPTG and immunofluorescence was applied to detect the proportion of ER-associated bacteria
1022 using the dolichol kinase (DolK) marker. The average and standard deviation are shown (235
1023 normal and 65 abnormal bacteria were counted in total).

1024

1025 **Fig. 7.** Effect of the CtrA depletion on outer membrane proteins abundance.

1026 A. Western blots on *B. abortus* lysates of the wild type (WT) strain and the CtrA depletion strain
1027 grown with or without IPTG for one night, using monoclonal antibodies recognizing OMPs
1028 whose genes were identified by ChIP-seq as being potentially regulated by CtrA.

1029 B. Western blots on lysates of the CtrA depletion strain grown without IPTG for 0, 7, 15 and 24 h,
1030 using a monoclonal anti-Omp25 antibody (A68/4B10/F05). Omp10 was detected by Western
1031 blot as a loading control.

1032

1033 **Fig. 8.** Effect of CtrA depletion on Omp25 localization.

1034 A. Phase contrast microscopy and associated fluorescent anti-Omp25 signal of the CtrA
1035 depletion strain cultivated in the absence of IPTG. In these bacteria, the Omp25 signal is
1036 localized at the tip of the branches, revealing the heterogeneity of the outer membrane
1037 composition in these bacteria. These localization patterns also suggest that Omp25 diffusion in
1038 the outer membrane is slow.

1039 B. Homogeneous localization of anti-Omp25 signal on the wild type strain. The scale bars
1040 correspond to 2 μ m.

1041 C. Proportion of partially labeled bacteria generated with the anti-Omp25 antibody, for the wild
1042 type strain or the depletion strain cultivated in the presence or in absence of IPTG. Standard
1043 deviations are shown (n = 3).

1044

1045 **Supporting information**

1046 Figure S1 : Distribution of CtrA binding sites on *B. abortus* chromosomes I and II

1047 Figure S2 : EMSA analysis of several CtrA targets

1048 Figure S3 : DivK-CtrA regulation network and its control by CtrA

1049 Figure S4 : Morphology of bacteria after CtrA repletion

1050 Figure S5 : Activity of promoters bound by CtrA as a function of cell length

1051 Figure S6 : Mutations of the CtrA binding boxes in *ccrM* and *repABC* promoters

1052 Figure S7 : Resistance of *B. abortus* strains to Triton X-100 treatment

1053 Figure S8 : Omp25 localization on *B. abortus*

1054 Table S1 : ChIP-seq based CtrA binding sites in *B. abortus* genome

1055 Table S2 : Plasmids list

1056 Table S3 : Primers list

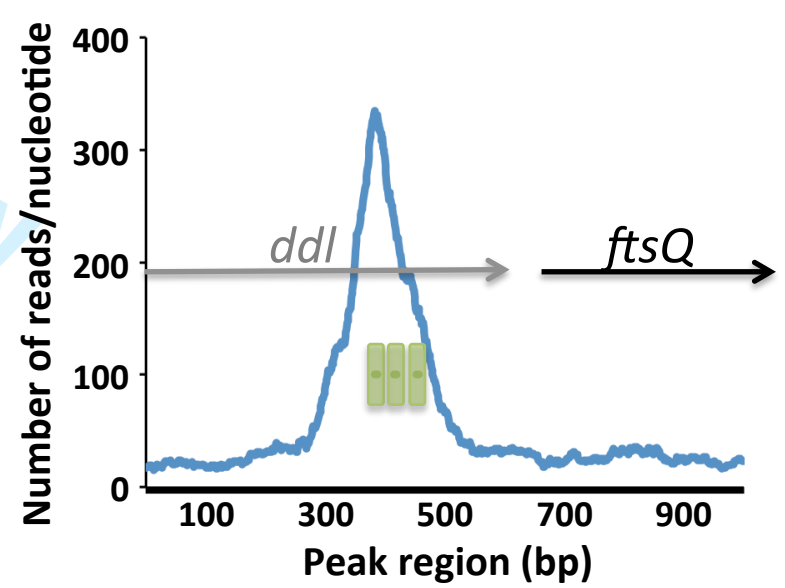
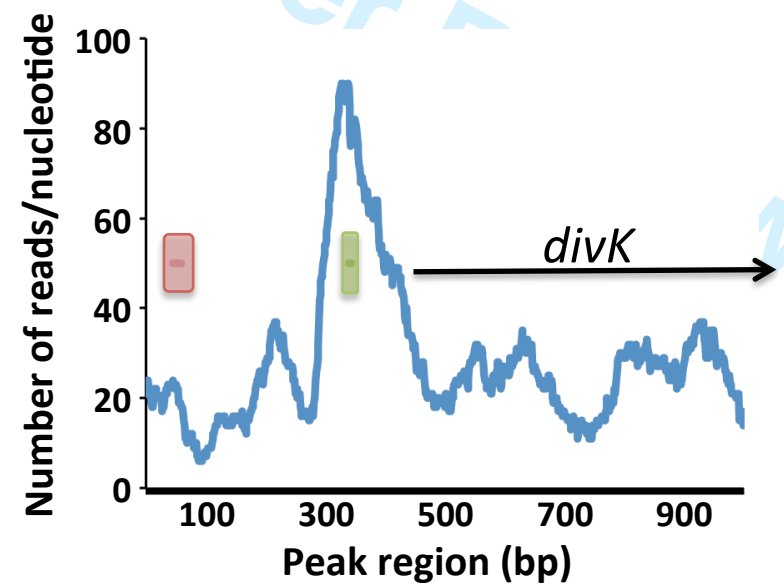
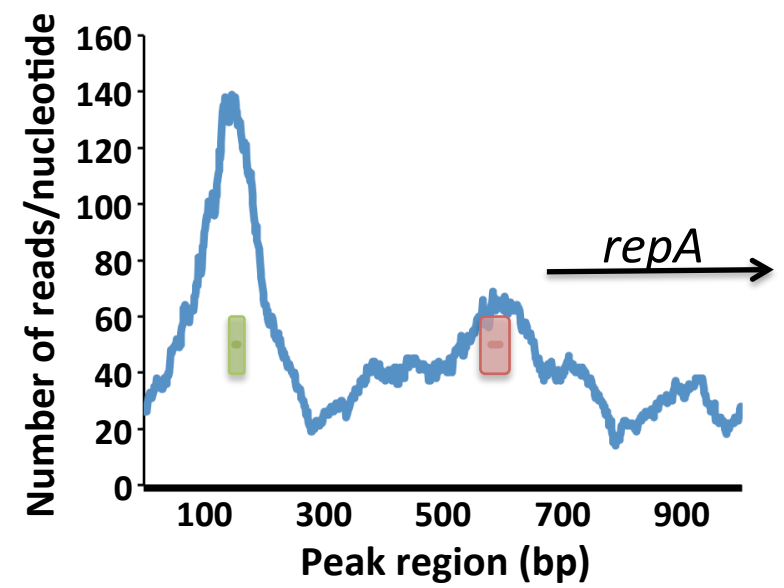
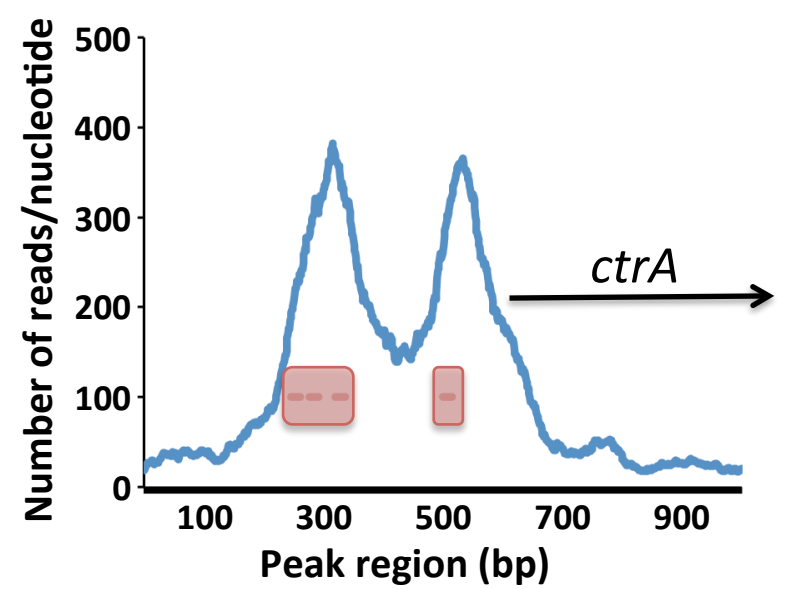
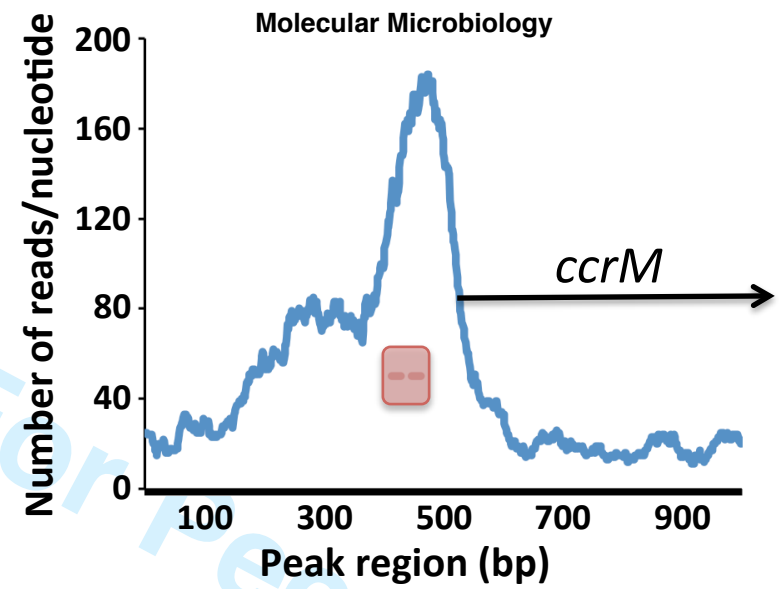
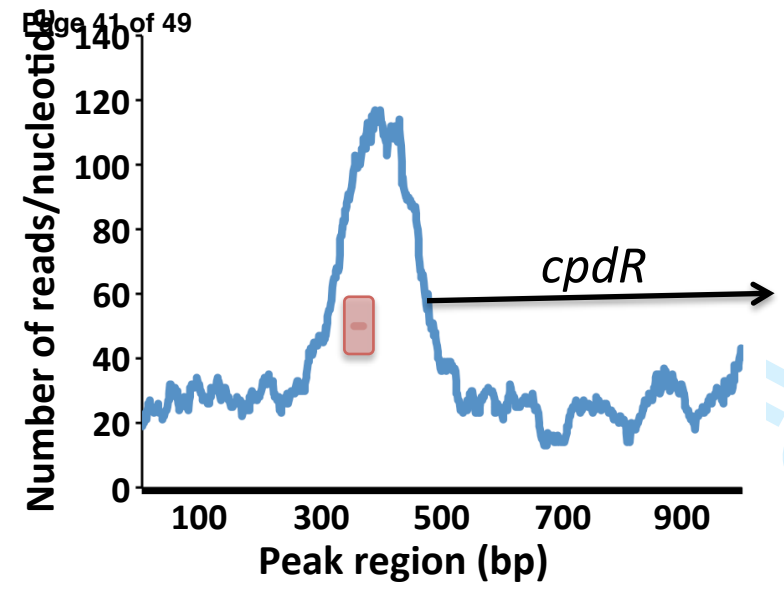
1057 Table S4 : Antibodies used in this study

1058 Chr1.gb : Annotated chromosome I of *B. abortus*

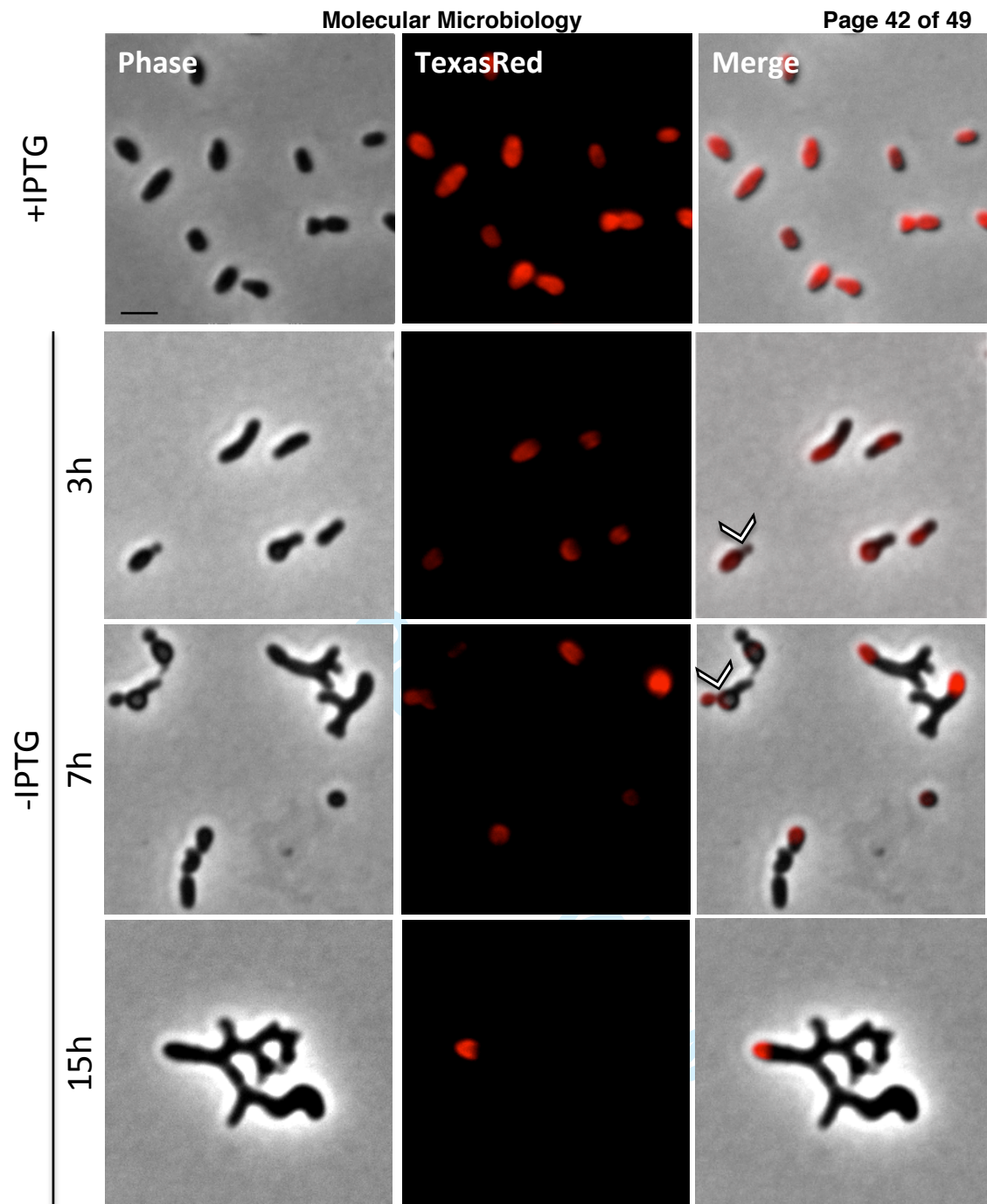
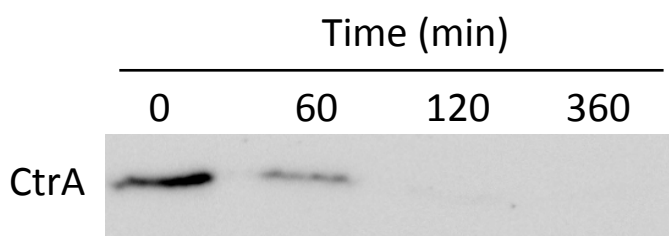
1059 ChIP-seq_CtrA_chr1.txt : ChIP-seq profile of CtrA on *B. abortus* chromosome I

1060 Chr2.gb : Annotated chromosome II of *B. abortus*

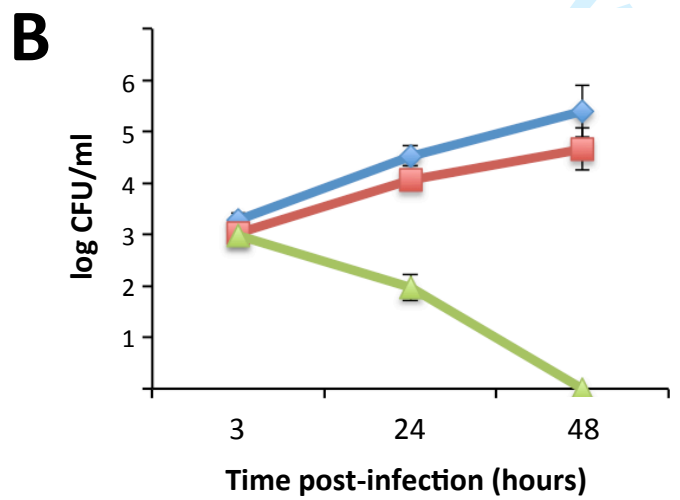
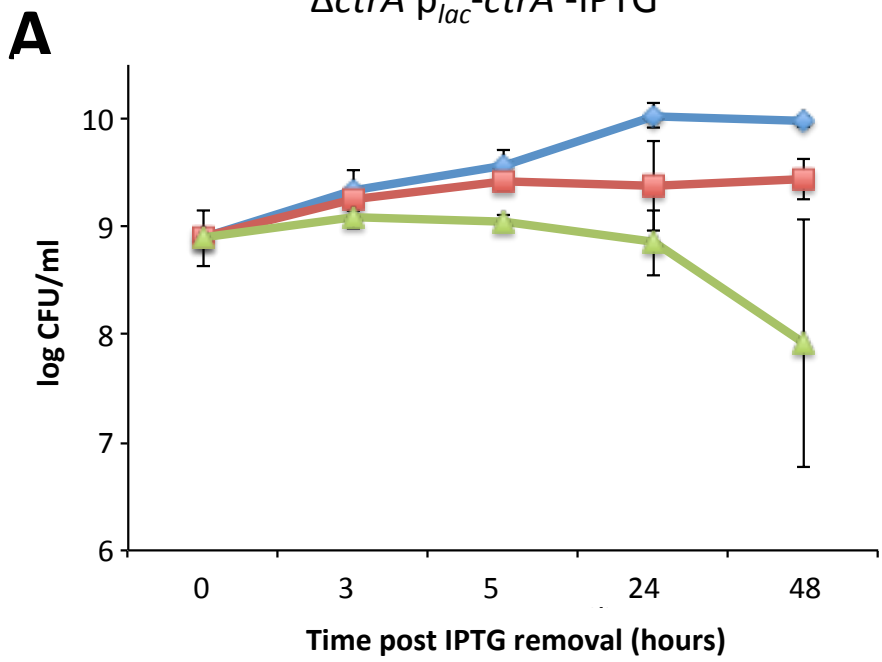
1061 ChIP-seq_CtrA_chr2.txt : ChIP-seq profile of CtrA on *B. abortus* chromosome II

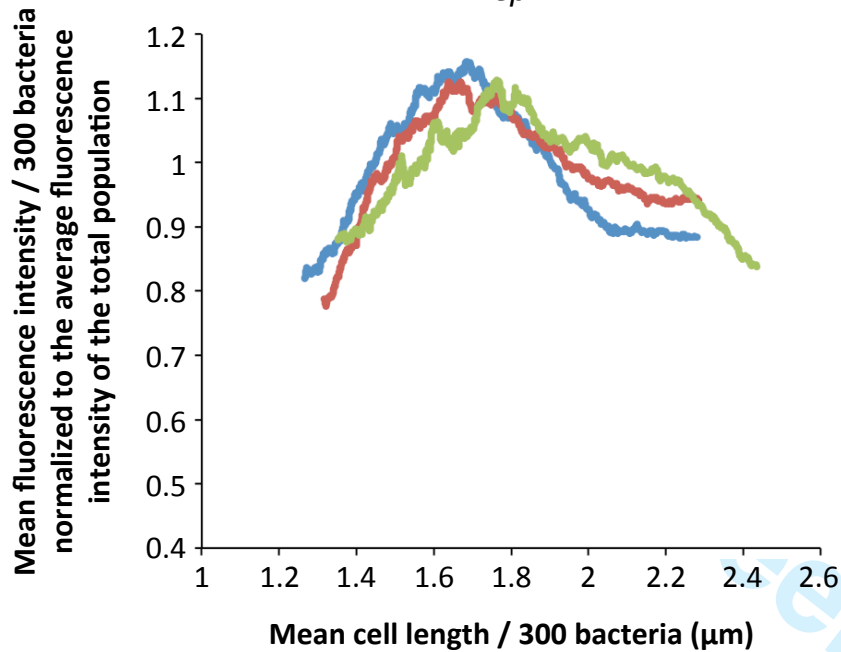
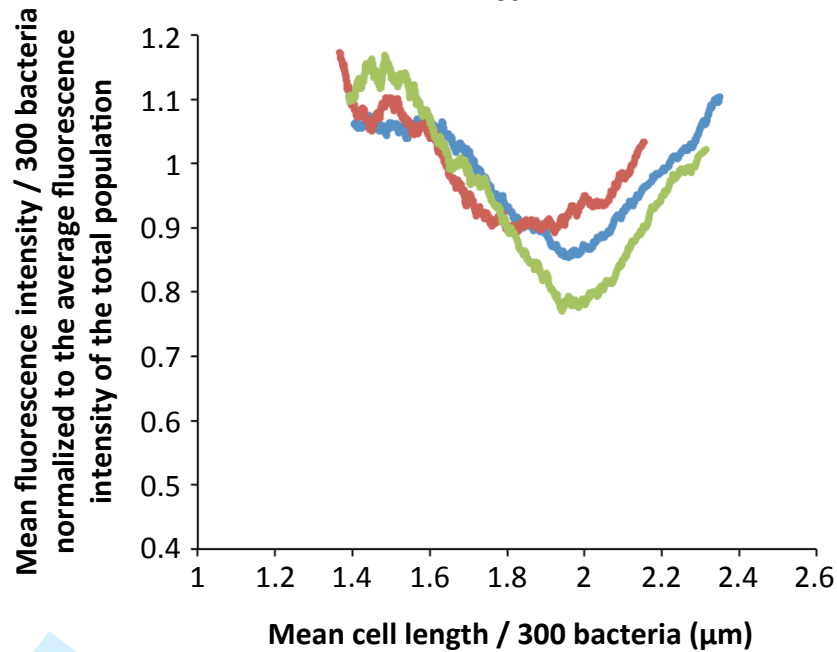
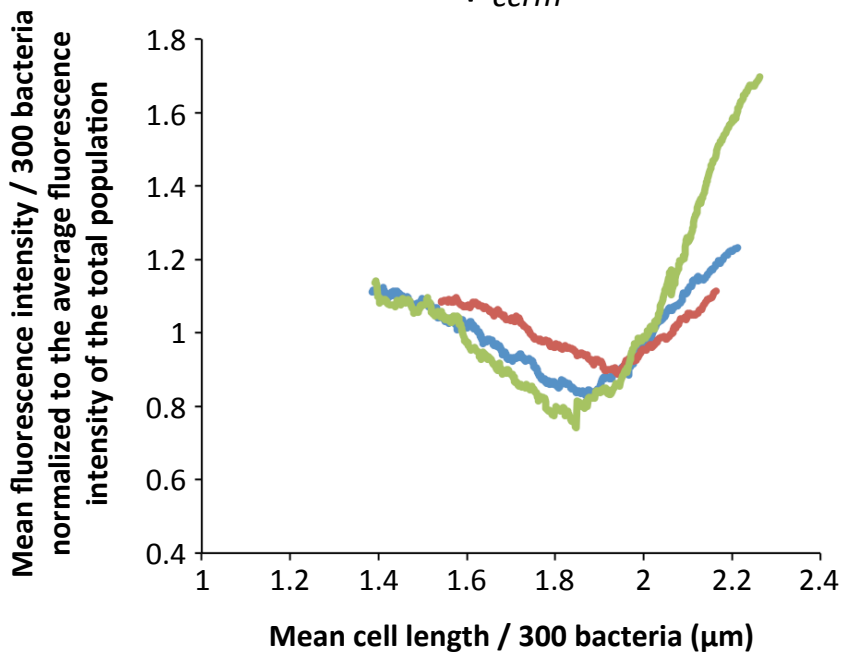
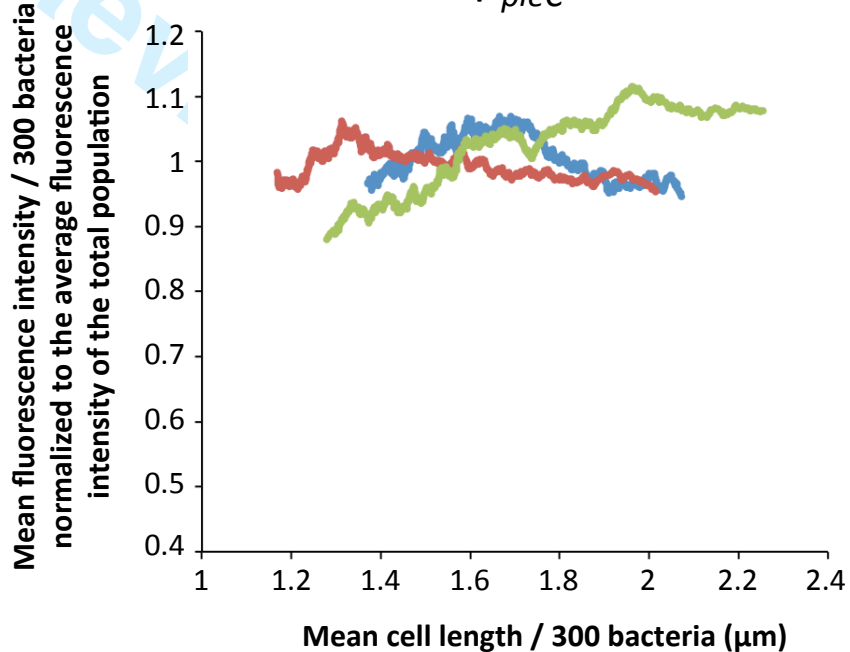


- 8-mer or 9-mer binding sites
- TTAA(C) half binding sites

A**B**

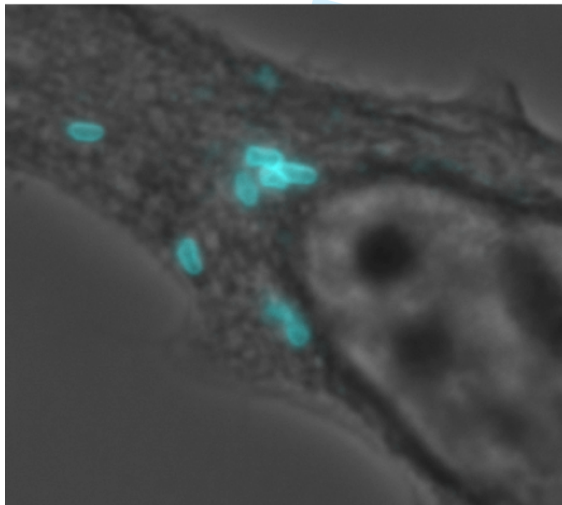
— Wild type
— $\Delta ctrA$ p_{lac}-ctrA +IPTG
— $\Delta ctrA$ p_{lac}-ctrA -IPTG



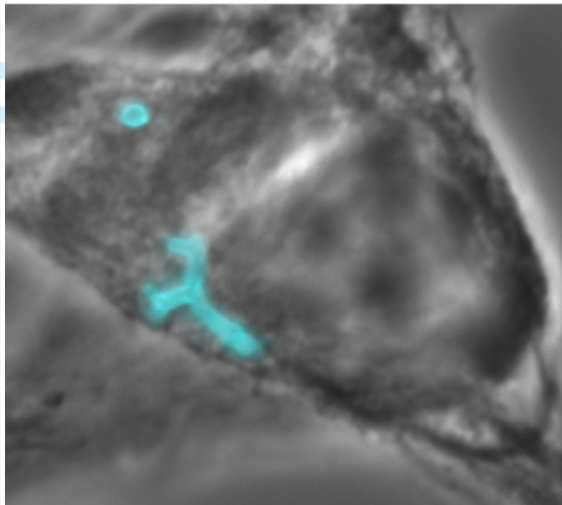
p_{repAB}  p_{ctrA}  p_{ccrm}  p_{pleC} 

A

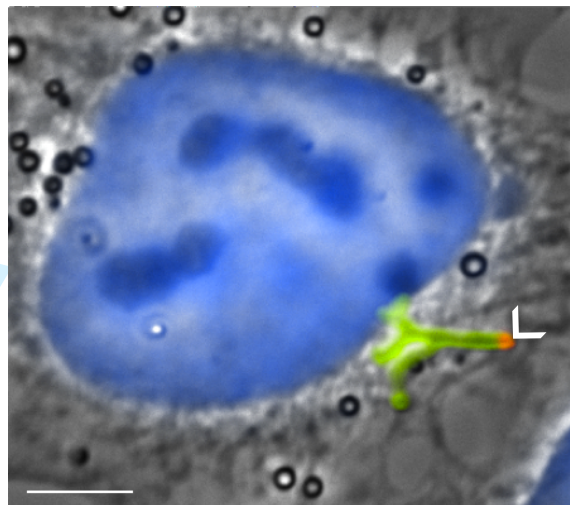
+IPTG

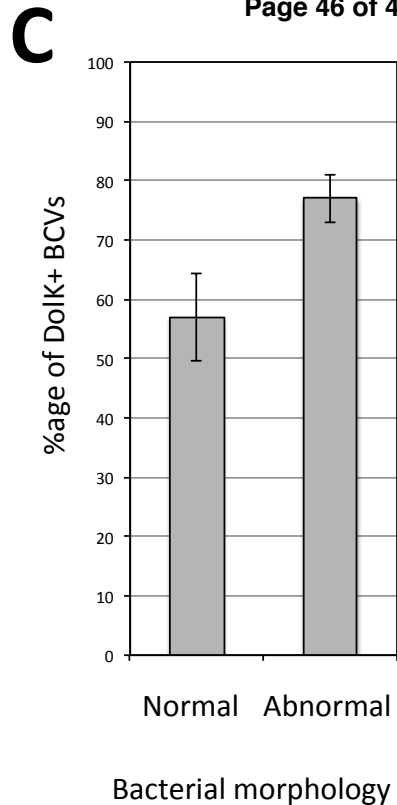
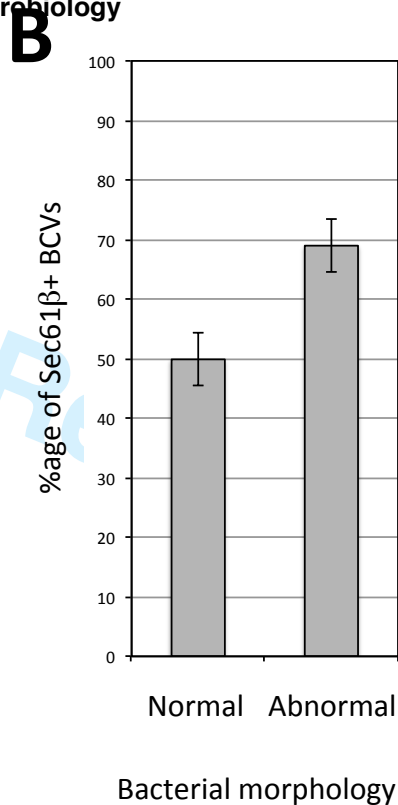
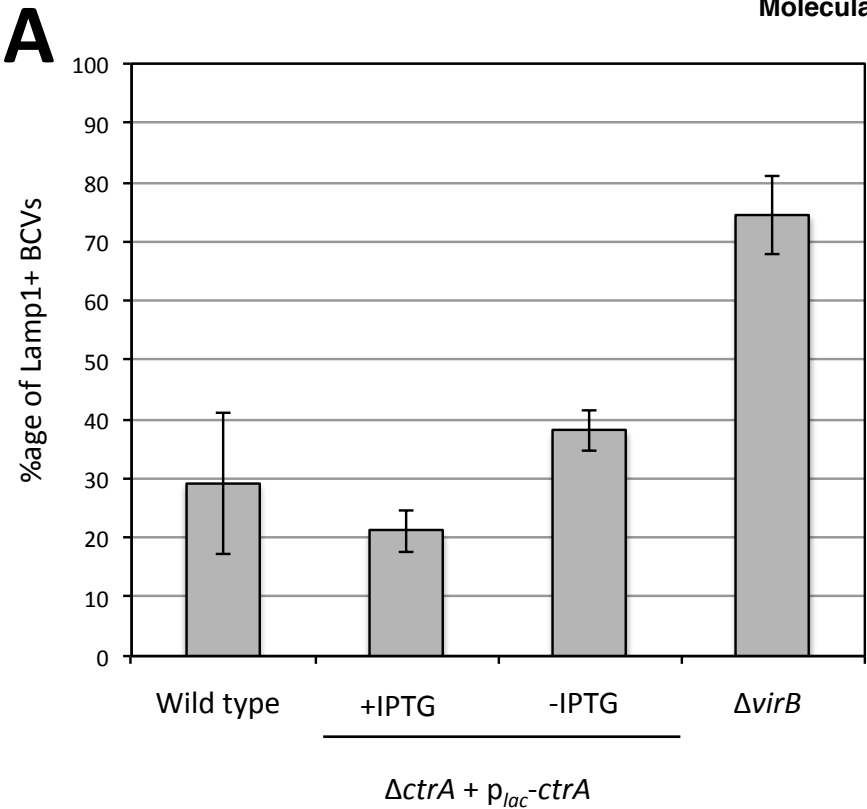


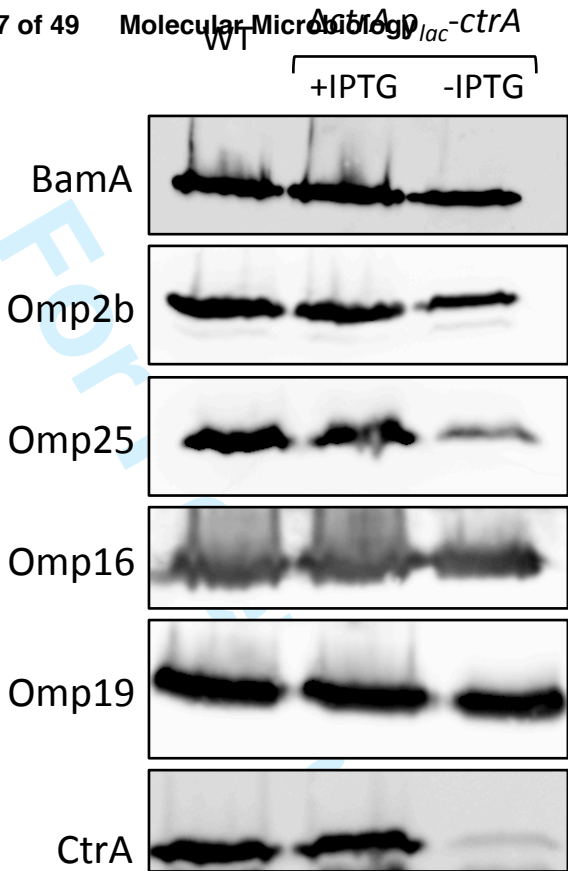
-IPTG



B





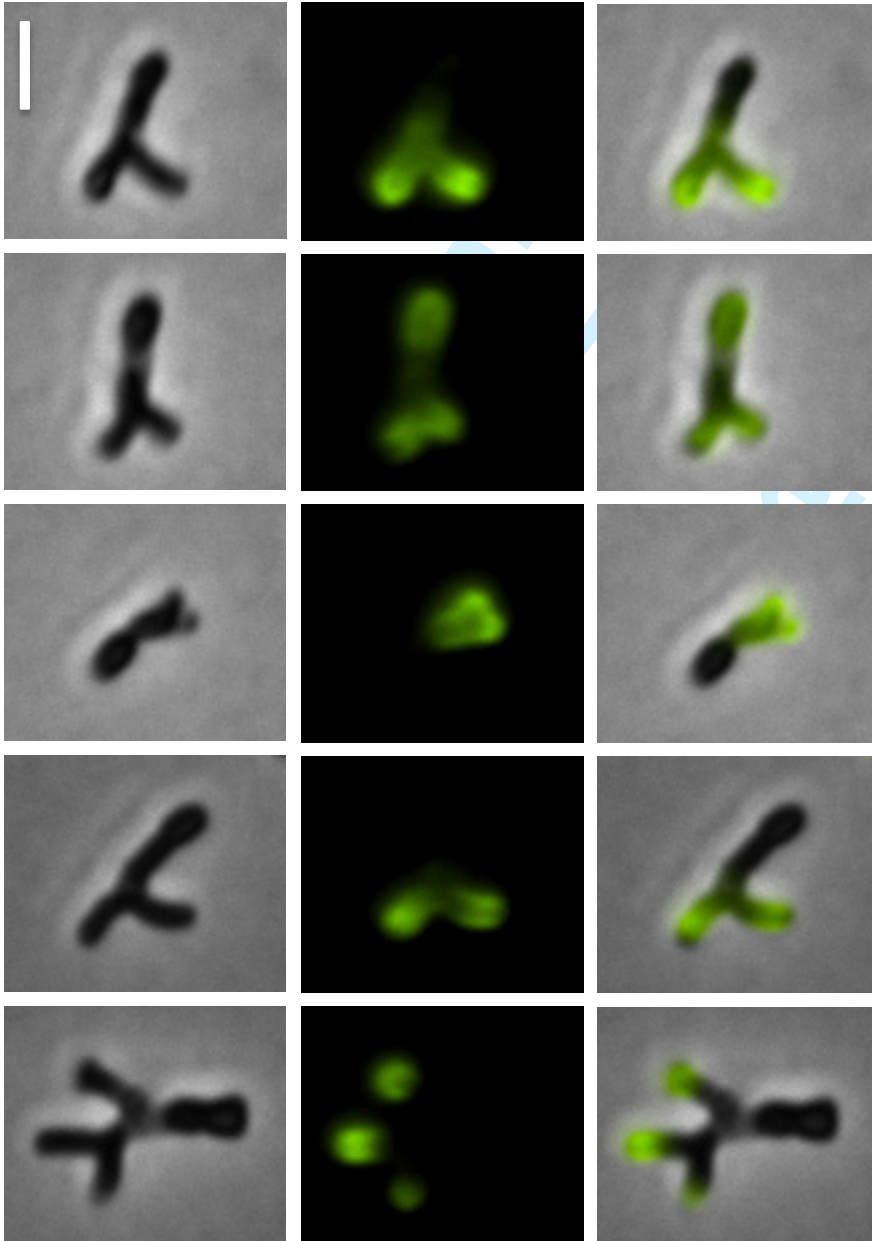
A**B**

0 7 15 24

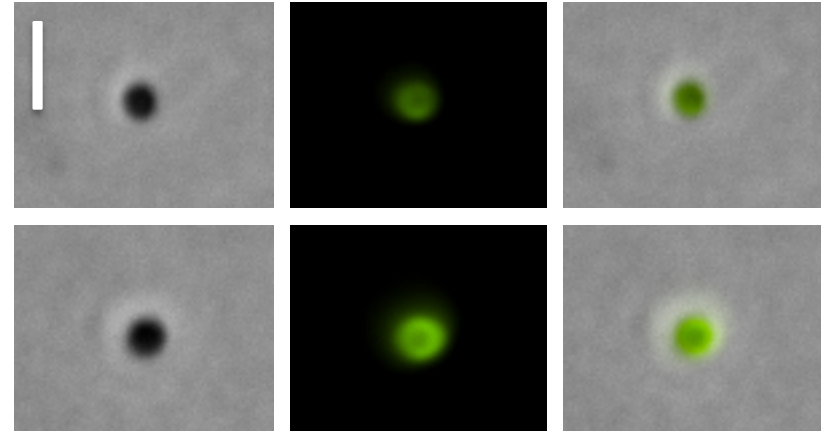
Omp25

Omp10

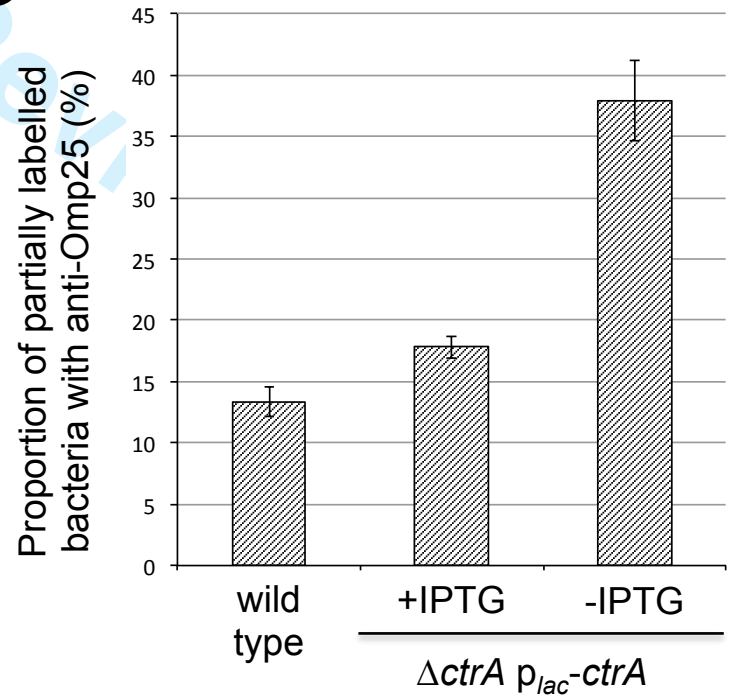
A phase contrast anti-Omp25 fluorescence Molecular Microbiology merge



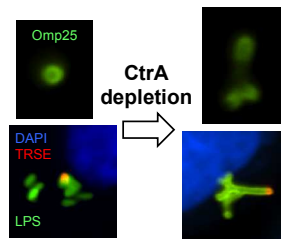
B phase contrast anti-Omp25 fluorescence merge



C



Graphical abstract



Abbreviated Summary

Brucella abortus is an alpha-proteobacterial pathogen responsible for worldwide zoonosis. Here we report that CtrA is essential for the cell division process, in culture and inside host cells. By characterizing the CtrA regulon, we found that CtrA not only controls cell cycle, but it also modulates the outer membrane composition.

Appendix 3

1 **Transposon sequencing of *Brucella abortus* uncovers essential genes for growth *in vitro***
2 **and inside macrophages**

3

4 **Running title** : Tn-seq analysis of *B. abortus*

5

6 Jean-François Sternon^{*}, Pierre Godessart^{*}, Rosa Gonçalves de Freitas^{*}, Mathilde Van der
7 Henst^{*}, Katy Poncin^{*}, Nayla Francis^{*}, Kevin Willemart^{*}, Matthias Christen[†], Beat Christen[†],
8 Jean-Jacques Letesson^{*}, Xavier De Bolle^{*‡}

9

10 ^{*}Research Unit in Microorganisms Biology (URBM), Narilis, University of Namur, 61 rue de
11 Bruxelles, 5000 Namur, Belgium

12 [†]Institute of Molecular Systems Biology, ETH Zürich, HPT E 71, Auguste-Piccard-Hof 1,
13 8093 Zürich, Switzerland

14

15 [‡]Corresponding author.

16 Prof. Xavier De Bolle

17 61 rue de Bruxelles

18 5000 Namur

19 Phone : +32 81 72 44 38

20 E-mail: xavier.debolle@unamur.be

21

22 **Summary**

23 *Brucella abortus* is a class III zoonotic bacterial pathogen able to survive and replicate inside
24 host cells, including macrophages. Here we report a multi-dimensional transposon sequencing
25 analysis to identify genes essential for *Brucella abortus* growth in rich medium and
26 replication in RAW 264.7 macrophages. The construction of a dense transposon mutants
27 library and mapping of 929,769 unique mini-Tn5 insertion sites in the genome allowed
28 identification of 491 essential coding sequences and essential segments in the *B. abortus*
29 genome. Chromosome II carries a lower proportion (5%) of essential genes compared to
30 chromosome I (19%), supporting the hypothesis of a recent acquisition of a mega-plasmid as
31 the origin of chromosome II. Temporally resolved transposon sequencing analysis as a
32 function of macrophage infection stages identified 79 genes with a specific attenuation
33 phenotype in macrophage, at either 2, 5 or 24 h post-infection, and 86 genes for which the
34 attenuated mutant phenotype correlated with a growth defect on plates. We identified 48
35 genes required for intracellular growth including the *virB* operon, encoding the type IV
36 secretion system, which supports the validity of the screen. The remaining genes encode
37 amino acid and pyrimidine biosynthesis, electron transfer systems, transcriptional regulators
38 and transporters. In particular, we report the need of an intact pyrimidine nucleotide
39 biosynthesis pathway in order for *B. abortus* to proliferate inside RAW 264.7 macrophages.

40

41 **Introduction**

42 *Brucella abortus* is a class III bacterial pathogen from the *Brucella* genus known for being the
43 causative agent of brucellosis, a worldwide anthro-po-zoonosis generating major economic
44 losses and public health issues (1). These bacteria are Gram-negative and belong to the
45 Rhizobiales order within the *Alphaproteobacteria* group and share common characteristics
46 such as the DivK-CtrA regulation network which governs cell cycle regulation (2) and
47 unipolar growth as observed in *Agrobacterium tumefaciens* and *Sinorhizobium meliloti* (3). A
48 specific feature of *B. abortus* compared to other *Alphaproteobacteria* is its multipartite
49 genome, composed of two replicons of 2.1 and 1.2 Mb named chromosome 1 (chr I) and
50 chromosome 2 (chr II), respectively (4). The chr I replication origin is similar to the one of *C.*
51 *crescentus*, while chr II replication origin resembles those found in megaplasmids of the
52 Rhizobiales (5, 6).

53 One main aspect of *B. abortus* infections is the ability of the bacteria to invade, survive, and
54 proliferate within host cells, including macrophages (7). Recently, the cellular infection
55 process of *B. abortus* in both RAW 264.7 macrophages and HeLa cells has been extensively
56 characterized at the single cell level in terms of growth and genome replication, highlighting a
57 typical biphasic infection profile (5). Indeed, during the course of cellular infections, *Brucella*
58 first enters host cells through the endosomal pathway where it remains in a “*Brucella*
59 containing vacuole” (BCV) for several hours without proliferating while preventing the
60 maturation of its compartment into a phagolysosome (7). During that period, typical markers
61 such as LAMP1 are acquired (7). In most cell types, surviving bacteria are able to control the
62 biogenesis of their vacuole into an endoplasmic reticulum (ER) derived compartment where
63 they actively proliferate (7-9). This process is dependent on the type IV secretion system
64 called VirB (10, 11). The chemical composition of the replicative BCV is difficult to study
65 directly, but mutant *Brucella* strains may be used as probes to gain a better knowledge of the

66 bacterial environment in these compartments. Screening of transposon mutants collections for
67 attenuated strains generated hypotheses, such as the availability of histidine that was proposed
68 to be limited (12), which is consistent with the ability of histidinol dehydrogenase inhibitors
69 to impair growth of *Brucella* in macrophages (13). However, a major drawback of previous
70 screenings for attenuated mutants was the size of the library, typically limited to a few
71 thousands of mutants, that does not allow saturation at the genome-wide level and therefore
72 cannot yield quantitative results. Moreover, several interesting hypotheses regarding
73 biosynthetic pathways required for intracellular proliferation have never been investigated.
74 In the present study, we have performed Tn-seq on *B. abortus* both before and after the
75 infection of RAW 264.7 macrophages using a highly saturating transposon mutant library.
76 This library was generated by plating on a rich medium and was subsequently used to infect
77 RAW 264.7 macrophages for 2, 5 and 24 h. At each stage, the transposon insertion sites were
78 mapped to identify genes in which the transposition insertion frequency is low, suggesting
79 that these genes are required for growth and/or survival. This approach allowed identification
80 of genes involved in several essential processes for growth on rich medium. The temporally
81 resolved transposon sequencing analysis allowed the identification of mutants attenuated at
82 three post-infection (PI) time points. Complete and near-complete pathways required for
83 trafficking to the ER and intracellular growth in host cells have been identified, including the
84 ability to synthesize pyrimidines when *B. abortus* is growing in RAW 264.7 macrophages.
85

86 **Results**

87 **Identification of essential genes in *B. abortus* 2308**

88 To gain genome-wide insights into the composition of essential genes necessary for growth of
89 *B. abortus* on rich medium, we carried a Tn-seq analysis. A *B. abortus* 2308 library of 3.10^6
90 random mutants was constructed using a *kan*^R derivative of mini-Tn5, a mini-transposon that
91 was previously used with *Brucella* (12, 14). A P_{xyl} promoter was present in the mini-Tn5
92 derivative to limit the potential polar effects (see Material and Methods). The mini-Tn5
93 derivatives transpose using a conservative mechanism, and a single insertion is found in each
94 mutant (14). Directly after mating, the library was grown on rich medium and transposon
95 insertion sites were identified by deep sequencing (Fig. 1). We identified 929,769 insertion
96 sites from 154,630,306 mapped reads, saturating the *B. abortus* genome with an insertion site
97 every 3.5 bp on average. To allow a genome-wide analysis independent of gene annotations,
98 we created a simple parameter assessing transposon insertion frequency termed R200 (see
99 Experimental procedures and Fig. S1), equal to the \log_{10} of the number of transposon
100 insertions + 1 found within a 200 bp sliding window (Fig. 2). According to the frequency
101 distribution of R200 values (see Fig. S2), a main peak of frequency is centered on an average
102 value of 4.05 with a standard deviation of 0.204. Since average values are strongly influenced
103 by extreme data and because the proportion of essential genes is very different between chr I
104 and chr II (see below), the average R200 values for chr I and II are 3.3 and 3.8 respectively.
105 The theoretical distribution of R200 values (Fig. S2) allows the definition of cutoffs to
106 consider growth alteration, expressed as the number of standard deviations from the average
107 of the main peak of R200 values. Simple statistics can also be applied to compare the R200
108 values of different genomic regions, as indicated in Fig. 2. As shown in Fig. 2 and the
109 Supplemental Data (SD) files (SD1 to SD14) showing the transposition tolerance maps
110 (TTMs), the essential genes and genes generating a fitness defect when mutated are very often

111 located in the coding sequences, validating the use of R200 values. One TTM was generated
112 for each chromosome, generating SD1 for chr I
113 (<https://figshare.com/s/bd0d4fa73ad8cf7737fe>) and SD2 for chr II
114 (<https://figshare.com/s/3219dfa7ac60d1cda34f>). Moreover, R200 and dense coverage offer an
115 analysis with high resolution to identify new essential genes and domains (see below).

116 We considered as essential all genes where at least one R200 value was equal to 0 in the
117 control condition (growth on rich medium), since the probability of such events to happen
118 randomly was estimated to be approximately $4 \cdot 10^{-15}$ (see Material and Methods) (15). In order
119 to test the validity of this analysis, we checked that genes required for supposedly essential
120 processes were indeed scored as essential if they do not have functional paralogs. As
121 expected, genes coding for all four RNA polymerase core subunits (α , β , β' and ω), the
122 housekeeping σ^{70} , and 51 out of the 54 ribosomal proteins were found as essential.
123 Additionally, the previously established essentiality of *pdhS*, *ccrM*, *omp2b*, *divK*, *cckA* and
124 *chpT* genes (16-20) was also confirmed.

125 Out of the 3419 predicted genes annotated on the *B. abortus* genome, 491 genes were
126 found to be essential for *in vitro* culture, *i.e.* 14.4% of the predicted genes. This percentage is
127 in agreement with those previously reported for other *Alphaproteobacteria* such as *C.*
128 *crescentus* (12.4%), *Brevundimonas subvibrioides* (13.4%), and *Agrobacterium tumefaciens*
129 (6.9%) (15, 21). A list of all essential genes for *in vitro* culture is available as Supplementary
130 Table S1.

131 Based on the presence of a plasmid-like replication and segregation system on chr II and
132 differences in gene content, it has been postulated that chr II could originate from an
133 ancestrally acquired mega-plasmid (5, 22). We thus tested the distribution of essential genes
134 between the two chromosomes of *B. abortus*. Accordingly, 429 out of the 2236 genes (19%)
135 of chr I were essential. This is 3.7 times more than the 5 % found on chr II with 62 essential

136 genes out of 1183. This result further supports the mega-plasmid hypothesis. One can thus
137 hypothesize that essential genes have started to be transferred from chr I to chr II but that the
138 frequency of this transfer was not sufficient to equilibrate the proportion of essential genes on
139 both chromosomes yet. Besides the *repABC* operon, essential for replication initiation and
140 segregation (5, 6), many essential genes of chr II could have been gained by recombination
141 events with chr I. In agreement with this hypothesis, a fraction of the essential genes of chr II
142 are clustered, such as the BAB2_0983 - BAB2_1013 region which contains 10 essential genes
143 potentially involved in housekeeping functions like diaminopimelate biosynthesis (*dapD* and
144 *dapE*), cell division (*fzIA*) and LPS export (*msbA*).

145 The high resolution of the mapping (200 bp) due to the high number of reads aligned to
146 many unique sites allow the identification of previously unannotated essential coding
147 sequences. Indeed, since R200 values clearly map to the position of coding sequences in
148 many instances in the genome, a drop of R200 values in a region where no gene has been
149 predicted could indicate that a gene is indeed present and functionally relevant. This is
150 conceptually validated by two examples shown in Fig. 3A. Interestingly, one of the two newly
151 identified genes codes for the antitoxin component of a homologue of the SocAB system first
152 identified in *C. crescentus* (Fig. 3A) (23). In *C. crescentus*, SocA is a proteolytic adaptor for
153 the degradation of the SocB toxin by the ClpXP machinery (23). The essentiality of ClpXP in
154 *C. crescentus* is due to the presence of the SocAB system (23). Therefore the essentiality of
155 *clpXP* genes in *B. abortus* (Fig. S3) could also be due to the presence of a SocAB homologue
156 in *B. abortus*. Moreover, this method also allows for the reannotation of genes as exemplified
157 by *ftsK*, where the open reading frame extends beyond the current *ftsK* locus in 5' and
158 matches with an essentiality region (see Fig. 3B). Furthermore, thanks to the high coverage of
159 this Tn-seq, our analysis also permits to map essentiality regions in genes corresponding to
160 protein domains, as displayed by genes showing essentiality on a fraction of their coding

161 sequence (see Fig. 3C). Taken together, these observations show that high resolution Tn-seq
162 could support genomic re-annotations and identification of essential protein domains.

163 Tn-seq allows for the reconstruction of essential pathways, complexes and systems. Here,
164 we specifically focused on pathways relative to *B. abortus* cell cycle, which will be divided
165 into four categories, the replication of DNA, the growth of the envelope, the cell division, and
166 the cell cycle regulation network. Regarding the replication of DNA, α , β , γ , δ , χ and τ
167 subunits of the DNA polymerase III as well as the helicase *dnaB* and the primase *dnaG* are
168 essential for growth. None of the three ϵ -subunits (BAB1_2072, BAB2_0617, and
169 BAB2_0967) were scored essential, which is likely due to functional redundancy. Genes
170 responsible for the initiation of DNA replication for chromosome I (*dnaA*) and for
171 chromosome II (*repC*) and for the segregation of chromosome I (*parA* and *parB*) and
172 chromosome II (*repA* and *repB*) were also essential. Interestingly, only one homolog of the
173 structural maintenance of chromosome gene (*smc*, BAB1_0522) could be found in the
174 genome and was not essential in our Tn-seq, either suggesting that a functional analog is
175 present, or that this function is not essential in *B. abortus*. Genes responsible for the synthesis
176 of peptidoglycan precursors from fructose-6-phosphate and their export to the periplasm
177 (namely, *glmS*, *glmM*, *glmU*, *murA*, *murB*, *murC*, *murD*, *murE*, *murF*, *murG*, *mraY*, *ftsW*)
178 were all scored essential. Out of three predicted class-A penicillin-binding proteins (PBP),
179 only one (BAB1_0932) was found to be essential for growth on rich medium as well as the
180 only predicted class-B PBP, *ftsI*. The two other class A PBPs were either only needed for
181 optimal growth on rich medium while not being strictly essential (BAB1_0607) or not
182 required at all (BAB1_0114).

183 The entire pathway responsible for the synthesis of lipopolysaccharide (LPS) lipid A
184 from UDP-GlcNAc (namely, *lpxA*, *lpxB*, *lpxC*, *lpxD*, *lpxK*, *lpxXL* and *kdtA*), as well as the
185 pathway responsible for its export to the outer membrane (namely, *msbA*, *lptA*, *lptB*, *lptC*,

186 *lptD*, *lptE*, *lptF*, *lptG*) appears to be essential for growth on rich medium. Conversely, no gene
187 known for being involved in the LPS core synthesis (24) was scored essential for culture on
188 plates. Moreover, none of the genes responsible for the LPS O-chain synthesis were scored
189 essential, with the exception of *wbkC* (see Discussion).

190 Genes involved in the export of outer membrane proteins (OMPs) such as *bamA*, *bamD*
191 and *bamE* were essential for growth on rich medium (see Discussion). However, no predicted
192 homolog of *bamB* nor *bamC* could be found. Interestingly, none of the three homologs of the
193 OMPs periplasmic chaperone *degP* were scored essential, which is probably due to functional
194 redundancy. It should be noted that no clear predicted homolog of the OMPs periplasmic
195 chaperones *skp* and *surA* could be identified *in silico*. Additionally, among the genes
196 responsible for lipoprotein export to the outer membrane, both *lgt* and *lspA* were essential, but
197 surprisingly *lnt* was not. *lnt* is the phospholipid/apolipoprotein transacylase, that is N-
198 acylating the N-terminal cysteine in the biogenesis of lipoproteins. The *lnt* gene is also not
199 essential in *B. subvibrioides*, suggesting that the dispensability of *lnt* could be a shared feature
200 among *Alphaproteobacteria*.

201 Genes coding for the divisome proteins *ftsZ*, *ftsA*, *ftsQ*, *ftsK*, *ftsW*, *ftsY*, *ftsI*, as well as for
202 the outer membrane invagination system *tolQRAB-pal* were all essential on plates. The cell
203 division regulatory operon *minCDE* as well as *ftsEX* were not essential, and no predicted
204 homologs could be found for *ftsB*, *ftsN* and *zipA*.

205 Regarding the regulation of the bacterial cell cycle in *Brucella*, one of the key features of
206 *Brucella* cell cycle is the DivK-CtrA pathway, conserved among many *Alphaproteobacteria*
207 (25). Most but not all members of the DivK-CtrA pathway were found to be essential for
208 growth on plates in Tn-seq. Indeed, *pdhS*, *divK*, *divL*, *cckA*, *chpT*, *ctrA*, *cpdR* and *clpXP* were
209 found to be essential (Fig. S3). Presumably redundant genes for c-di-GMP synthesis (*pdeA*
210 and *pleD*) and for DivK phosphorylation (*pleC* and *divJ*) were not essential (Fig. S3).

211 Taken together, these data demonstrate that Tn-seq enables the reconstitution of essential
212 pathways, in a single experiment. In particular, it allows the identification of a crucial
213 homolog within a family of several potential paralogs.

214

215 **Screening for genes required for macrophage infection**

216 Another main objective of this study was to identify genes specifically required for
217 macrophage infection. For this purpose, three large-scale infections of RAW 264.7
218 macrophages were carried out in parallel using the transposon mutants library described
219 above (Fig. 1). For each infection, a specific post-infection (PI) time point was selected in
220 order to have a better understanding of the specific gene requirement at different stages of the
221 cellular infection process. After each time point, bacteria were extracted from infected
222 macrophages and grown on rich medium prior to transposon insertion site identification and
223 R200 calculation as explained above (Fig. 1).

224 Attenuation corresponds to a decrease of fitness specific to infection. Therefore, in the
225 context of an attenuated mutant, one expects that the R200 values for the mutated gene would
226 be lower after infection compared to the control condition. Consequently, for analyzing post-
227 infection data, the control R200 values were subtracted from the corresponding PI R200 for
228 each PI dataset. This resulted in three lists of Delta-R200 values, namely “2 h PI - control”,
229 “5 h PI - control”, and “24 h PI - control”, corresponding to Delta-R200 2 h PI (SD3
230 <https://figshare.com/s/77195e0a2cc1a1933b7f> and SD4
231 <https://figshare.com/s/2475d4b00e6a58226e40>), Delta-R200 5 h PI (SD5
232 <https://figshare.com/s/93ce83ccea559a0de2f7> and SD6
233 <https://figshare.com/s/6f604b5eba5934c392f1>) and Delta-R200 24 h PI (SD7
234 <https://figshare.com/s/ea7871157f284d31eaed> and SD8
235 <https://figshare.com/s/958e728387a31b8ce139>), respectively. A total of 165 candidates have

236 been identified using the Delta-R200 analysis. Among these candidates, 75 were found at 2 h
237 PI, 98 were found at 5 h PI, and 165 were found at 24 h PI (see Tables 1 and 2).

238 In order to validate the Delta-R200 analysis, we checked for genes known to cause an
239 attenuation during a cellular infection when mutated. For this purpose, we have chosen one 2
240 h PI control, the response regulator *bvrR*, and two 24 h PI controls, the type IV secretion
241 system operon *virB* (10, 26), required for intracellular proliferation, and *vjbR*, an important
242 transcriptional activator of *virB* which is not part of the *virB* operon (27, 28). As expected, the
243 *bvrR* mutants were strongly attenuated from 2 h PI, and both *virB* and *vjbR* mutants were only
244 attenuated at 24 h PI (Fig. S4 and Table 1), which is in agreement with the timing required by
245 the bacterium to reach its replicative niche and proliferate. Taken together, these data lean
246 toward the validation of the candidates identified by the Delta-R200 analysis.

247 We decided to assess the validity of our datasets by testing for the reproducibility of the
248 observed phenotypes by mutating candidate genes and testing mutant survival by the counting
249 of colony forming units -CFU- after infection of RAW 264.7 macrophages for two hours. We
250 chose four candidates, two that displayed no attenuation in Tn-seq as negative controls
251 (*omp2a* and *ftsK*-like, corresponding to BAB1_0659 and BAB2_0709 coding sequences,
252 respectively), and two that displayed attenuation in Tn-seq as positive controls (*wadB* and
253 *pgk*, corresponding to BAB1_0351 and BAB1_1742, respectively). As expected, the two
254 negative control strains did not show any sign of attenuation compared to the wild type strain,
255 while the positive control strains exhibited a statistically significant attenuation phenotype
256 (Fig. 4A).

257 One can distinguish two categories of attenuated mutants. On the one hand, mutants can
258 be attenuated due to a failure to perform a successful infection, but on the other hand, mutants
259 can be attenuated due to growth impairments that are actually already observed when grown
260 on rich medium and amplified during infection. In fact, as opposed to candidates displaying a

261 typical attenuation profile such as the *wadB* mutant, others displayed attenuation in
262 conjunction with low control R200 values as exemplified by the *pgk* mutant (Fig. 4B). This
263 second type of profile suggested growth deficiencies independent of infection. In addition,
264 while the *pgk* mutant strain displayed a small but yet significant decrease in CFU (Fig. 4A), it
265 was clear that colonies were smaller in size than the wild type colonies (Fig. 4C). Therefore,
266 the attenuation of candidates sharing a *pgk*-like profile in Tn-seq is likely to be due, at least in
267 part, to growth impairments already present in the control condition. Actually, the second
268 round of culture taking place after the infection could simply amplify the disadvantage of
269 clones that already display growth delays on plates.

270 In order to investigate the effect of re-plating on Tn-seq candidates, we performed a
271 new Tn-seq experiment in which the colonies of the library of transposon mutants were
272 collected and re-plated prior to sequencing instead of infecting host cells. The TTMs obtained
273 for this control condition (SD9 <https://figshare.com/s/519aecf6ea1bea563510> and SD10
274 <https://figshare.com/s/266012d35d5780c5a1b3>) and the re-plating (SD11
275 <https://figshare.com/s/9282c05218ec976c4286> and SD12
276 <https://figshare.com/s/c5318e37bf294ff0cdde>) are available at the indicated URLs. Despite a
277 large difference in the average R200 values between the two control experiments (3.47 for the
278 first control and 5.21 for the second), a good correlation ($r = 0.86$) was found between the two
279 datasets. By comparing the control with the re-plating, we were able to monitor the fitness
280 loss of mutants due to a second growth on plate, independently of any infection. Surprisingly,
281 54 % of the candidates harboring attenuation at 2, 5 or 24 h PI in our initial Tn-seq also
282 displayed a similar attenuation after re-plating, thus meaning that the fitness loss of those
283 mutants could be due to a growth defect detectable after a simple re-plating instead of
284 infection. Consequently, attenuated candidates displaying pre-existing growth impairments
285 (listed in Table 2) should be carefully analyzed in future investigations (see Discussion). It is

286 striking that complete or almost complete pathways fall into this category, like the purine
287 biosynthesis (*purB*, *purC*, *purD*, *purF*, *purH*, *purL*, *purMN* and *purQ*) and the cytochrome c
288 maturation (*ccmABC* and *ccmIEFH*) pathways (Table 2).

289

290 **Identification of hyper-invasive mutants**

291 Tn-seq can theoretically highlight hyper-invasive mutants in addition to attenuated mutants.
292 Indeed, such mutants would display higher R200 values compared to the control, meaning
293 that proportionally more mutant bacteria would be found inside host cells when such genes
294 are disrupted, thus resulting in positive Delta-R200 values. Using this criterion, only nine
295 genes (namely *wbkD*, *wbkF*, *per*, *gmd*, *wbkA*, *wbkE*, *wboA*, *wboB*, and *manB_{core}*
296 [BAB2_0855]) were identified and remarkably all of them are part of the lipopolysaccharide
297 O-chain synthesis pathway (24). Indeed, such mutants have a rough LPS and rough mutants
298 are known to be more invasive than the smooth parental strain (29, 30). To confirm this using
299 our settings, a mutant of the GDP-mannose dehydratase gene (*gmd*) was constructed and CFU
300 were counted after infecting RAW 264.7 macrophages for 2 h. As expected, the resulting
301 strain displayed increased invasiveness typical of rough strains (Fig. S5).

302

303 **Identification of genes required for growth in RAW 264.7 macrophages**

304 The 24 h PI-specific candidates mainly include genes predicted to be involved in trafficking,
305 regulation, transport and metabolism, including amino acid and nucleic base biosynthesis (see
306 Table 1). The biosynthesis of histidine seems to be crucial, as well as the synthesis of
307 pyrimidines, suggesting that *B. abortus* cannot find or uptake enough of these compounds
308 from the ER compartments in which it is proliferating. The 24 h PI specific candidates also
309 comprise expected virulence genes such as the *virB* operon (11), transcriptional regulators
310 like *vjbR* (28) and *vtlR* (31), the cytochrome bd biosynthesis operon *cydABCD* (32). When

311 comparing our data with the list of attenuated transposon mutants from previous studies
312 performed on various infection models and *Brucella* species (33-37), it is striking that only 42
313 % of the attenuated mutants identified here had already been identified. Indeed, 33 of the 79
314 candidates attenuated in our time-resolved Tn-seq analysis were part of the 257 candidates
315 compiled from the previous studies. Therefore, the Tn-seq approach reported here has
316 generated 46 new candidates, suggesting that the comprehensive analysis of the *Brucella*
317 genome could yield new insights into the genes required for a macrophage infection (see
318 Discussion).

319

320

321 **The pyrimidine biosynthesis pathway allows intracellular proliferation**

322 One of the major hits of the 24 h PI dataset is the pyrimidine biosynthesis (here called “pyr”)
323 pathway. In fact, with the exception of genes already essential for culture on rich medium, all
324 pyr biosynthesis genes became strongly attenuated at 24 h PI (namely *pyrB*, *pyrC*, *pyrD*,
325 *pyrE*, and *pyrF*), while none of them were impacted when re-plated.

326 We further investigated the pyr pathway by creating a deletion mutant of its first non-
327 essential gene, the $\Delta pyrB$ strain. The $\Delta pyrB$ mutant grew as the wild type strain in rich
328 medium (Fig. S6). We then evaluated the infectious potential of the $\Delta pyrB$ strain and its
329 complementation strain by enumerating CFU in RAW 264.7 macrophages at both 2 h PI and
330 24 h PI. Estimation of the intracellular growth ratio (CFU at 24 h PI divided by CFU at 2 h
331 PI) clearly showed that the $\Delta pyrB$ strain is strongly attenuated compared to the wild type and
332 the complementation strains, validating the Tn-seq profile of the mutant (Fig. 5).
333 Consistently, deletion mutants for all other *pyr* genes ($\Delta pyrC$, $\Delta pyrD$, $\Delta pyrE$, and $\Delta pyrF$)
334 behaved as the wild type when cultured in rich medium (Fig. S6) and were impaired for
335 intracellular growth, further validating the involvement of the pyr pathway for proliferation
336 inside RAW 264.7 macrophages (Fig. 5).

337

338 **Discussion**

339 In this work, a multi-dimensional Tn-seq analysis has been performed with *B. abortus* to
340 identify genes essential for growth on rich medium as well as genes required for replication in
341 RAW 264.7 macrophages. The analysis of mutants at different times PI as well as the analysis
342 of re-plated library allowed the identification of genes specifically involved in the infection
343 model tested here, by comparison with the control condition (growth on rich medium). A
344 similar approach could be successfully applied to many other bacterial pathogens.

345 As most of the current therapies against bacterial pathogens aim at targeting essential
346 processes such as translation or cell wall biosynthesis, the collection of all essential genes for
347 growth on rich medium generates a baseline to identify novel therapeutic targets. In this
348 study, a total of 491 candidate genes were qualified as essential for growth on rich medium
349 plates. Interestingly, our quantitative analysis also highlights genome sections that show a
350 reduced fitness and statistical comparison of any regions (inside or outside predicted genes) in
351 the genome is thus also feasible (Fig. 2). The quantitative analysis also allows the
352 identification of regions in which mutagenesis generates a growth defect on the control plates,
353 and thus a category of attenuated mutants with growth defects on plates (Table 2) should be
354 distinguished from specifically attenuated mutants (Table 1). This type of discrimination is
355 supported by the possibility that a fraction of the attenuated mutants with growth defects on
356 plates could be non-specifically affected during the infection process. On the other hand, the
357 specificity of the attenuated mutants reported in Table 1 is expected to be medium-dependent
358 and could thus be challenged by other screenings. Additionally, it would be interesting to
359 apply Tn-seq to *B. abortus* grown in different media. In particular, it would be informative to
360 test chemically defined media.

361 While PG biosynthesis is obviously essential, only one of the three predicted class-A
362 penicillin-binding proteins, BAB1_0932, was found to be essential for growth on rich

363 medium, showing that Tn-seq could allow the identification of the main functional gene
364 among a group of paralogs. As expected, BAB1_0932 is the ortholog of Atu1341, which was
365 also identified as essential in *A. tumefaciens* (21). Comparison of essential genes in *B.*
366 *abortus*, *A. tumefaciens* and *B. subvibrioides* also reveals interesting observations. The D-Ala-
367 D-Ala ligase encoding gene *ddl* (BAB1_1447) located near the *murA-G*, *mraY* genes cluster
368 involved in cell wall synthesis, is not essential in *B. abortus* while it is essential in *A.*
369 *tumefaciens* and *B. subvibrioides*. This could be explained by the presence of a paralog for *ddl*
370 (BAB1_1291, also not essential) in *B. abortus*. MurI, a glutamate racemase that was found to
371 be essential in *C. crescentus* (15) and non-essential in *A. tumefaciens* (21), is actually required
372 for *B. abortus* growth in RAW 264.7 macrophages but not in rich medium (see below and
373 Table 1). Tn-seq also allowed to reshape essential processes compared to other bacteria, as
374 exemplified by the *bam* genes, responsible for the OMPs export system. *Brucella* possesses
375 an incomplete OMPs export system composed of only *bamADE* and lacking *bamB* and *bamC*,
376 and here, we showed that *bamE* was scored essential in Tn-seq, whereas it is not essential in
377 *E. coli* (38). One possibility would be that *bamE* is functionally redundant with another gene
378 in *E. coli*, while this redundancy is absent in *B. abortus*. At the level of the regulation network
379 involving CtrA (Fig. S1), it is interesting to note that *cpdR*, *sciP*, *gcrA* and *ccrM* are identified
380 here as essential genes, which is consistent with the previous identification of *ccrM* as an
381 essential gene in *B. abortus* (18), but surprisingly different compared to *A. tumefaciens* where
382 they are all non-essential, except for *gcrA* that is absent in *A. tumefaciens* C58 (21). In *C.*
383 *crescentus*, *cpdR* and *sciP* are not essential (39, 40), while *gcrA* and *ccrM* were first reported
384 as essential (41, 42), which was later questioned by the observation of a slow growth
385 phenotype for *C. crescentus* $\Delta gcrA$ and $\Delta ccrM$ strains (43). Essentiality of *cpdR*, *sciP*, *gcrA*
386 and *ccrM* genes could indicate that this part of the regulation network is less redundant with
387 other cell cycle control systems in *B. abortus* compared to *C. crescentus*.

388 Intriguingly, a few genes (*mucR*, *sodA*, *pgm* and *wbkC*) for which a viable deletion
389 mutant was previously reported (44-49) are actually scored as essential in our Tn-seq analysis.
390 A *pssA* gene (BAB1_0470) was also scored as essential but the corresponding viable mutant
391 was previously characterized (50). Interestingly, mutants for another *pssA* homolog
392 (BAB2_0668) were found to be attenuated from 2 h PI (Table 2), suggesting that these
393 enzymes are playing distinct roles. The absence of mini-transposon in dispensable genes has
394 already been observed in previous Tn-seq experiments performed on other bacterial species
395 (51). It is also possible that, in the Tn-seq protocol, suppressor mutations do not have the time
396 to be selected, and thus these genes appear as essential only in Tn-seq. Another possibility
397 would be that these mutants have a long lag phase for growth on plates or a very low growth
398 speed, and are thus wrongly detected as essential in the Tn-seq.

399 Remarkably, a second Tn-seq assessing the effects of re-plating revealed that 54 % of
400 these candidates displayed fitness decreases similar to those found in infection when
401 undergoing a second round of culture. Strikingly, 55 out of the 75 initial candidates identified
402 at 2 h PI are in the second category (Table 2) since they were already affected by re-plating.
403 Such observations suggest that it could be important to take into account growth defect in
404 culture before proposing a “specific” virulence attenuation for mutant strains. Interestingly,
405 this does not rule out that particular mutants could have an exacerbated growth defect
406 phenotype inside host cells. R200 analysis of the difference between 24 and 5 h PI (SD13
407 <https://figshare.com/s/44d2126e6c24ca1214d1> and SD14
408 <https://figshare.com/s/c6a0d65386f6edb2202b>) indicates that several *pur* genes (*purA*, *purB*,
409 *purC*, *purD*, *purF*, *purH*, *purL*, *purM*, *purN* and *purQ*) have lower R200 values at 24 h PI
410 compared to 5 h PI. These data suggest that even if a mutant has growth problems in a given
411 culture medium, Tn-seq analysis at different times post-infection allows to generate
412 hypotheses regarding attenuation at different times PI. Additionally, the reference culture

413 medium is of course important, and it would be interesting to test several rich media for the
414 growth colonies before and after infection.

415 When comparing our candidates to the list of 257 attenuated mutants previously available
416 from different infection models (33-37), it was surprising that only 33 genes could be found
417 in common (Table S3). This means that 46 additional candidates were identified by Tn-seq.
418 However, this also means that 214 attenuated mutants previously reported were not identified
419 using Tn-seq in a RAW 264.7 macrophages infection, which is not surprising since these
420 screening were done with different strains/species and different infection models. However, it
421 should be noted that intriguingly, out of the remaining 214 candidates, 80 were categorized
422 here as either strictly essential for growth on rich medium or essential when re-plated (Table
423 S3). It is thus possible that different strains and different culture media generate different
424 collections of essential genes, or that several attenuated mutants previously reported are
425 actually suppressors of mutants in essential genes that display a growth defect in the infection
426 model.

427 The 24 h PI time point revealed several pathways involved in trafficking and metabolism.
428 The type IV secretion system VirB was needed but the effectors proposed to be translocated
429 to the host cell (52) were untouched in our Tn-seq analysis, which is probably the result of
430 functional redundancy between effectors. Indeed, under the infection conditions used here,
431 there is usually one bacterium per infected cell, and thus trans-complementation (53) is
432 unlikely although it cannot be completely ruled out. Regarding metabolism, *glk* mutants were
433 attenuated at 24 h PI (see Table 2), suggesting that *B. abortus* could need to utilize glucose in
434 the replication niche of RAW 264.7 macrophages, which is consistent with the requirement of
435 glucose uptake in alternatively activated macrophages (54). The biosynthesis of histidine was
436 strongly impacted at 24 h PI, as previously suggested (55), and we found here that it is more
437 specifically the second part of the pathway that is important for bacterial proliferation inside

438 RAW 264.7 macrophages (namely, *hisB*, *hisC*, and *hisD*). This could be due to the fact that
439 the first half of the histidine biosynthesis pathway (composed of *hisZ*, *hisG*, *hisE*, *hisI*, *hisA*,
440 *hisH*, *hisF*) is also responsible for the production of 5'-phosphoribosyl-4-carboxamide-5-
441 aminoimidazole (AICAR) that contributes to purine biosynthesis. The first half of the
442 histidine biosynthesis pathway and the purine biosynthesis pathway are both impacted when
443 re-plated (Table 2). Therefore, Tn-seq suggests that genes responsible for the synthesis of
444 histidine, at least from imidazole-glycerol-3-phosphate, are required for the proliferation of *B.*
445 *abortus* in the endoplasmic reticulum of RAW 264.7 macrophages. The *ilvC* and *ilvD* genes,
446 coding for enzymes involved in the biosynthesis of isoleucine and valine, are also scored as
447 required for growth in RAW 264.7 macrophages. It is also noticeable that the glutamate
448 racemase (*MurI*) is required for growth in these macrophages. This enzyme converts L-Glu to
449 D-Glu, presumably to allow the synthesis of PG. The late attenuation of these *murI* mutants is
450 consistent with a late growth of *B. abortus* in RAW 264.7 macrophages (5). Another major hit
451 is the biosynthesis of pyrimidines. Indeed, Tn-seq showed that all non-essential pyr
452 biosynthesis genes (*i.e.* *pyrB*, *pyrC*, *pyrD*, *pyrE*, and *pyrF*) were consistently attenuated at
453 24 h PI in RAW 264.7 macrophages while none of the associated mutants display growth
454 defects on rich medium. Interestingly, none of the *pyr* genes were impacted when re-plated as
455 opposed to most genes involved in purine biosynthesis (*i.e.* *purB*, *purC*, *purD*, *purH*, *purL-1*,
456 *purL-2*, *purN*, *purM*). This is likely due to the composition of the culture medium and the heat
457 resistance of purines and pyrimidines during medium sterilization. The *hisD*, *hisF*, *pyrB*, *pyrC*
458 and *pyrD* genes were already hit in previous screenings for attenuated mutants (12, 56) but the
459 *pyr* mutants have not been complemented and the pyrimidines biosynthesis pathway was
460 never investigated in *B. abortus*. Here we show that all the mutants in genes of the pyr
461 pathway are attenuated for growth inside macrophages, hence validating the Tn-seq data. It
462 should be noted that a second homolog was found for *pyrC* (BAB1_0688, here called *pyrC2*),

463 however a *B. abortus* Δ *pyrC2* strain displays a growth defect in rich medium (Fig. S7) and
464 attenuation at 5 h PI in Tn-seq (Table 1), suggesting pleiotropic defects in this mutant
465 compared to the *pyr* mutants characterized in this work. Altogether, these results strongly
466 suggest that the ability of *B. abortus* to synthesize pyrimidines in the host cell is decisive for
467 its proliferation inside macrophages. It would be interesting to investigate the survival,
468 trafficking and proliferation of *pyr* mutants in different cell types as well as in other infection
469 models. If the inability of the *pyrB* mutant to proliferate inside several intracellular niches is
470 confirmed, this mutant could be a good candidate to start vaccinal tests.

471 Tn-seq data also generate unexpected observations, such as the attenuation of the *lnt*
472 mutants at 2 h PI, while *lnt* is not required for growth on rich medium, suggesting that a
473 redundant function is present for growth on plates but not for short term survival in
474 RAW 264.7 macrophages. Alternatively, it is also possible that the activity of Lnt is
475 dispensable in *B. abortus*, at least in the control condition. It is noticeable that *lnt* is also
476 dispensable for growth in *Francisella tularensis* (57), suggesting that the dispensability of Lnt
477 is widespread. Interestingly, our screening also revealed a role for a TamAB (BAB1_0045
478 and BAB1_0046) system homolog for intracellular proliferation, TamAB being proposed to
479 be involved in the translocation of outer membrane proteins (58). These data thus open new
480 investigations pathways to better understand the molecular processes required for *B. abortus*
481 survival and growth inside host macrophages.

482 In conclusion, Tn-seq is a comprehensive method that allowed the identification of
483 attenuated *B. abortus* mutants for macrophages infection. The high coverage of the genome
484 with transposons has allowed for identification of essential, attenuated and non-essential
485 genes, as well as genes or operons required for full growth on rich medium. It would be
486 interesting to perform such experiments on other *Brucella* strains as well as other host cell
487 types (including activated macrophages and trophoblasts (59)) and more complex infection

488 models such as animal models like a mouse intranasal infection (60). This would generate a
489 fundamental knowledge of the molecular arsenal required for *Brucella* survival and growth in
490 the course of infections.

491

492 **Material and Methods**

493 **Bacterial strains and media**

494 The wild type strain *Brucella abortus* 2308 NaI^R was cultivated in 2YT (1% yeast extract,
495 1.6% peptone, 0.5% NaCl). The conjugative *Escherichia coli* S17-1 strain was cultivated in
496 rich medium (Luria-Bertani broth). When required, antibiotics were used at the following
497 concentrations: ampicillin, 100 µg ml⁻¹; kanamycin 50 µg ml⁻¹ for *E. coli* and 10 µg ml⁻¹ for *B.*
498 *abortus*; Nalidixic acid, 25 µg ml⁻¹.

499 **RAW 264.7 macrophages culture**

500 Macrophages were cultivated in DMEM (Invitrogen) supplemented with 10% fetal bovine
501 serum (Gibco), 4.5 g l⁻¹ glucose, 1.5 g l⁻¹ NaHCO₃, and 4 mM glutamine at 37 °C with 5%
502 CO₂.

503 **Mini-Tn5 Kan^R plasmid construction**

504 The pXMCS-2 mini-Tn5 Genta^R plasmid (61) was manipulated to exchange the gentamycin
505 resistance cassette (Genta^R) with a Kan^R gene, using a dual joining PCR strategy. The region
506 upstream of the Genta^R cassette was amplified by PCR from the pXMCS-2 mini-Tn5 Genta^R
507 plasmid using primers “Tn-Kan part 1 F” and “Tn-Kan part 1 R” and fused by overlapping
508 PCR to the Kan^R coding sequence, amplified from the pNPTS138 plasmid using primers “Tn-
509 Kan part 2 F” and “Tn-Kan part 2 R”. Then, this DNA fragment was fused to the region
510 downstream of the Genta^R cassette amplified by PCR using primers “Tn-Kan part 3 F” and
511 “Tn-Kan part 3 R” from the pXMCS-2 mini-Tn5 Genta^R plasmid. In parallel, the pXMCS-2
512 mini-Tn5 Genta^R plasmid was restricted using *EcoRI* and *NdeI* to excise the Genta^R fragment.

513 The DNA fragment bearing the new Kan^R cassette was digested with *EcoRI* and *NdeI* was
514 then ligated in the previously restricted pXMCS-2 mini-*Tn5* Genta^R plasmid. Primers used for
515 this construct are listed in Table S2.

516 **Mutant library generation**

517 One ml of an overnight culture of *B. abortus* 2308 was mixed with 50 µl of an overnight
518 culture of the conjugative *E. coli* S17-1 strain carrying the pXMCS-2 mini-*Tn5* Kan^R plasmid.
519 This plasmid possesses a hyperactive *Tn5* transposase allowing the straightforward generation
520 of a high number of transposon mutants. The resulting *B. abortus* transposon mutants were
521 selected on 2YT plates (2% Agar) supplemented with both kanamycin and nalidixic acid. *Tn5*
522 mutagenesis generates insertion of the transposon in only one locus per genome, as
523 demonstrated previously for *Brucella* (14). Each *Tn5* derivative contains a *C. crescentus xyl*
524 promoter that is constitutively active in *B. abortus* since when it is fused to YFP coding
525 sequence on a pBBR1-derived plasmid, it generates a fluorescent signal of uniform intensity
526 similar to the *E. coli lac* promoter fused to YFP coding sequence.

527 **RAW 264.7 macrophages infection using the transposon mutants library**

528 Transposon mutants were pooled using 2YT medium, diluted in RAW 264.7 macrophages
529 culture medium to reach a MOI (Multiplicity of Infection) of 50, and added onto the
530 macrophages, which were previously seeded in 6-well plates to a concentration of 1.5×10^5
531 cells per ml. A total of 16 6-well plates were planned per time point. Macrophages were then
532 centrifuged 10 min at 400 g at 4°C and subsequently incubated for 1 hour at 37°C with 5%
533 CO₂. The culture medium was then removed and replaced with fresh medium containing
534 gentamycin 50 µg ml⁻¹ in order to kill extracellular bacteria, and macrophages were then
535 further incubated for 1, 4, and 23 hours at 37°C with 5% CO₂. For each time post-infection
536 (2 h, 5 h or 24 h PI), culture medium was removed, each well was washed twice with PBS,
537 and macrophages were lysed using PBS 0.1 % Triton X-100 for 10 min at 37°C. Macrophages

538 lysates were then plated on 100 2YT plates per time point, each supplemented with
539 kanamycin and incubated at 37°C for four days in order to obtain colonies that were collected
540 for genomic DNA (gDNA) preparation and sequencing of Tn5-gDNA junctions.

541 **RAW 264.7 macrophages infection and Colony Forming Units (CFU) counting**

542 The infection protocol for performing CFU is identical to the one described above with the
543 exception of the inoculum, which originates from an overnight liquid culture. After infection,
544 infected macrophages are lysed and the resulting extracts are cultivated on 2YT plates
545 supplemented with kanamycin. Once grown, colonies were counted to calculate the number of
546 colonies per ml of lysate.

547 **Analysis of essential genes for growth on plates**

548 In order to assess the overall transposon insertion across *B. abortus* genome, we have created
549 a parameter called R200, defined by the $\log_{10}(\text{number of Tn5 insertion} + 1)$ for a 200 bp
550 sliding window. This sliding window was shifted every 5 bp to generate a collection of R200
551 spanning the whole genome for the control condition, *i.e.* bacteria on plates. Given that *B.*
552 *abortus* genome is 3,278,307 bp, a list of 655,662 R200 values was created, with an average
553 value of 9481 transposon insertions mapped per window. As previously published (15), the
554 probability of obtaining a window of a given size with **no** transposon insertion event can be
555 estimated by the following formula: $P = (1-(w/g))^n$ where *w* is the window size, *g* is the
556 genome size, and *n* is the number of independent Tn5 insertion events. In our case, the
557 resulting probability was $3.8 \cdot 10^{-15}$, with $g = 3,278,307$; $w = 200$, and $n = 544,094$. It should be
558 noted that this value only accounts for a single window, whereas essential genes are typically
559 characterized by a series of overlapping empty windows rather than a single 200 bp window,
560 thus further lowering the probability of finding such profiles fortuitously. Essential genes
561 were defined as all genes having at least one R200 equal to 0. Defined essential genes usually
562 have many R200 equal to 0, as indicated in the Supplemental Datasets (SD) 1 to 14 (see the

563 list below). The TTMs can be aligned to the annotated Genbank files for chromosomes I and
564 II (SD15 and SD16) of *B. abortus* 2308 using Artemis (Sanger institute,
565 <http://www.sanger.ac.uk/science/tools/artemis>). Here is the list of Supplementary Datasets :

566 (SD1) TTM_ctrl_chrI.txt Transposon tolerance map (R200) for chromosome I when grown
567 on rich medium. Link : <https://figshare.com/s/bd0d4fa73ad8cf7737fe>

568 (SD2) TTM_ctrl_chrII.txt Transposon tolerance map (R200) for chromosome II when grow
569 on rich medium. Link : <https://figshare.com/s/3219dfa7ac60d1cda34f>

570 (SD3) Delta-R200_2hPI_chrI.txt Attenuation profile at 2 h post-infection for chromosome I.
571 Link : <https://figshare.com/s/77195e0a2cc1a1933b7f>

572 (SD4) Delta-R200_2hPI_chrII.txt Attenuation profile at 2 h post-infection for chromosome II.
573 Link : <https://figshare.com/s/2475d4b00e6a58226e40>

574 (SD5) Delta-R200_5hPI_chrI.txt Attenuation profile at 5 h post-infection for chromosome I.
575 Link : <https://figshare.com/s/93ce83ccea559a0de2f7>

576 (SD6) Delta-R200_5hPI_chrII.txt Attenuation profile at 5 h post-infection for chromosome II.
577 Link : <https://figshare.com/s/6f604b5eba5934c392f1>

578 (SD7) Delta-R200_24hPI_chrI.txt Attenuation profile at 24 h post-infection for chromosome I.
579 Link : <https://figshare.com/s/ea7871157f284d31eae>

580 (SD8) Delta-R200_24hPI_chrII.txt Attenuation profile at 24 h post-infection for chromosome
581 II. Link : <https://figshare.com/s/958e728387a31b8ce139>

582 (SD9) TTM_replated_ctrl_chrI.txt Transposon tolerance map (R200) for chromosome I when
583 grown on rich medium (prior to replating). Link :
584 <https://figshare.com/s/519aecf6ea1bea563510>

585 (SD10) TTM_replated_ctrl_chrII.txt Transposon tolerance map (R200) for chromosome II
586 when grown on rich medium (prior to replating). Link :
587 <https://figshare.com/s/266012d35d5780c5a1b3>

588 (SD11) TTM_replated_chrI.txt Transposon tolerance map (R200) for chromosome I when
589 replated on rich medium. Link : <https://figshare.com/s/9282c05218ec976c4286>

590 (SD12) TTM_replated_chrII.txt Transposon tolerance map (R200) for chromosome II when
591 replated on rich medium. Link : <https://figshare.com/s/c5318e37bf294ff0cdde>

592 (SD13) DD-R200_24-5hPI_chrI.txt Attenuation at 24 h PI compared to 5 h PI for
593 chromosome I. Link : <https://figshare.com/s/44d2126e6c24ca1214d1>

594 (SD14) DD-R200_24-5hPI_chrII.txt Attenuation at 24 h PI compared to 5 h PI for

595 chromosome II. Link : <https://figshare.com/s/c6a0d65386f6edb2202b>

596 (SD15) ChrI.gb Annotated chromosome I of *B. abortus* 2308. Link :

597 <https://figshare.com/s/ae37affea7e62601b553>

598 (SD16) ChrII.gb Annotated chromosome II of *B. abortus* 2308. Link :

599 <https://figshare.com/s/ddee5b11fe553d1a2052>

600 Statistical analysis is described in Fig. S2. Briefly, a main frequency peak centered on a R200
601 value of 4.05 was used to predict a theoretical distribution of R200 from which thresholds
602 corresponding to 2 (-2S), 4 (-4S) and 6 (-6S) standard deviations for the average of the
603 theoretical distribution were computed.

604 Analysis of the effect of re-plating on rich medium was tested in an independent Tn-seq in
605 which a new mutant library was constructed with the same mini-Tn5 derivative as described
606 above. All colonies were collected and the resulting suspension was used on the one hand for
607 control analysis (data in TTM_replated_ctrl_chrI and TTM_replated_ctrl_chrII) and on the
608 other hand for re-plating on the same rich medium. Colonies generated after re-plating were
609 collected and analyzed by Tn-seq as described above (data in TTM_replated_chrI and
610 TTM_replated_chrII).

611 **Attenuation in infection analysis**

612 For each post infection sample (2 h PI, 5 h PI and 24 h PI), a list of R200 values was
613 calculated as for the control condition. Then, the control R200 values list was subtracted from
614 each post infection sample R200 list separately, generating three Delta-R200 datasets,
615 available as Supplemental Datasets (SD3 to SD8). Therefore, regions with a neutral Delta-
616 R200 value have no impact during infection when mutated, while regions with a negative
617 Delta-R200 are attenuated during infection, and regions with a positive Delta-R200 depict
618 hyper-invasiveness for the corresponding mutants. For each time PI, the frequency
619 distribution of Delta-R200 value was computed to define a normal distribution with an
620 average and a standard deviation covering the main peak of this distribution. The threshold

621 for negative Delta-R200 values was set at $-0.75 \log_{10}$ for the “2 h - control” and “5 h -
622 control” Delta-R200 analyses, selecting respectively 5.5% and 6.7% of windows from the
623 total genome. The threshold for negative Delta-R200 values was set at $-1 \log_{10}$ for the “24h -
624 control” Delta-R200 analysis, allowing selection of 10.3% of the windows. The threshold for
625 positive Delta-R200 values for the “2 h - control” condition was set at $+0.6 \log_{10}$, selecting
626 1.1% of the windows. The genes covered by selected windows were considered as required
627 for the infection, with usually most of their coding sequences covered.

628 **Generation of the *B. abortus* targeted mutants**

629 Unless stated otherwise, all *B. abortus* mutants were generated by insertion of a plasmid in
630 the targeted gene, according to a previously published procedure (62). The primers sequences
631 used to generate PCR products cloned in the disruption plasmids are available in Table S2.

632 All deletion strains were constructed using a previously described allelic exchange strategy
633 (5). The primers used to amplify upstream and downstream regions of the target genes
634 required for homologous recombination are also available in Table S2.

635 **Growth curves**

636 Growth was monitored in 2YT medium at 37 °C during 72 h by measuring the Optical
637 Density at 600 nm using a permanently shaking plate reader (Epoch2 microplate
638 spectrophotometer, Biotek).

639

640 **Acknowledgments**

641 We would like to thank M. Waroquier for his flawless technical support, F. Tilquin for lab
642 managing, as well as Dr. F. Renzi, J.-Y. Matroule and R. Hallez for stimulating and helpful
643 discussions. This research has been funded by the Interuniversity Attraction Poles Programme
644 initiated by the Belgian Science Policy Office (<https://www.belspo.be/>) to J.-J. Letesson and
645 by grants from Fonds de la Recherche Scientifique-Fonds National de la Recherche

646 Scientifique (FRS-FNRS, <http://www.fnrs.be>) (PDR T.0053.13 and PDR Brucell-cycle
647 T.0060.15, and CDR J.0091.14) to X. De Bolle and grant 31003A_166476 from the Swiss
648 National Science Foundation to B. Christen. We thank UNamur (<https://www.unamur.be/>) for
649 financial and logistic supports. N. Francis held an Aspirant fellowship from FRS-FNRS. J.-F.
650 Sternon, P. Godessart, M. Van der Henst and K. Poncin are supported by a Ph.D. grant from
651 FRIA (FRS-FNRS). The funders had no role in study design, data collection and
652 interpretation, or the decision to submit the work for publication. JFS, PG, RGdF, MVdH,
653 KP, NF and KW made the experiments; JFS, PG, MC, BC, JIL and XDB designed the study
654 and JFS and XDB wrote the manuscript.

655

656 **References**

- 657 1. **Moreno E, Moriyon I.** 2006. The Genus *Brucella*. *Prokaryotes* **5**:315-456.
- 658 2. **De Bolle X, Crosson S, Matroule JY, Letesson JJ.** 2015. *Brucella abortus* Cell
659 Cycle and Infection Are Coordinated. *Trends Microbiol* **23**:812-821.
- 660 3. **Brown PJ, de Pedro MA, Kysela DT, Van der Henst C, Kim J, De Bolle X, Fuqua
661 C, Brun YV.** 2012. Polar growth in the Alphaproteobacterial order Rhizobiales. *Proc
662 Natl Acad Sci U S A* **109**:1697-1701.
- 663 4. **Michaux-Charachon S, Bourg G, Jumas-Bilak E, Guigue-Talet P, Allardet-
664 Servent A, O'Callaghan D, Ramuz M.** 1997. Genome structure and phylogeny in the
665 genus *Brucella*. *J Bacteriol* **179**:3244-3249.
- 666 5. **Deghelt M, Mullier C, Sternon JF, Francis N, Laloux G, Dotreppe D, Van der
667 Henst C, Jacobs-Wagner C, Letesson JJ, De Bolle X.** 2014. G1-arrested newborn
668 cells are the predominant infectious form of the pathogen *Brucella abortus*. *Nat
669 Commun* **5**:4366.
- 670 6. **Pinto UM, Pappas KM, Winans SC.** 2012. The ABCs of plasmid replication and
671 segregation. *Nat Rev Microbiol* **10**:755-765.
- 672 7. **Celli J.** 2015. The changing nature of the *Brucella*-containing vacuole. *Cell Microbiol*
673 **17**:951-958.
- 674 8. **Detilleux PG, Deyoe BL, Cheville NF.** 1990. Entry and intracellular localization of
675 *Brucella* spp. in Vero cells: fluorescence and electron microscopy. *Veterinary
676 pathology* **27**:317-328.
- 677 9. **Sedzicki J, Tschon T, Low SH, Willemart K, Goldie KN, Letesson JJ, Stahlberg
678 H, Dehio C.** 2018. 3D correlative electron microscopy reveals continuity of *Brucella*-
679 containing vacuoles with the endoplasmic reticulum. *J Cell Sci* **131**.
- 680 10. **Comerci DJ, Martinez-Lorenzo MJ, Sieira R, Gorvel JP, Ugalde RA.** 2001.
681 Essential role of the VirB machinery in the maturation of the *Brucella abortus*-
682 containing vacuole. *Cell Microbiol* **3**:159-168.
- 683 11. **O'Callaghan D, Cazevieille C, Allardet-Servent A, Boschioli ML, Bourg G,
684 Foulongne V, Frutos P, Kulakov Y, Ramuz M.** 1999. A homologue of the
685 *Agrobacterium tumefaciens* VirB and *Bordetella pertussis* Ptl type IV secretion
686 systems is essential for intracellular survival of *Brucella suis*. *Mol Microbiol* **33**:1210-
687 1220.
- 688 12. **Kohler S, Foulongne V, Ouahrani-Bettache S, Bourg G, Teyssier J, Ramuz M,
689 Liautard JP.** 2002. The analysis of the intramacrophagic virulome of *Brucella suis*
690 deciphers the environment encountered by the pathogen inside the macrophage host
691 cell. *Proc Natl Acad Sci U S A* **99**:15711-15716.
- 692 13. **Abdo MR, Joseph P, Mortier J, Turtaut F, Montero JL, Masereel B, Kohler S,
693 Winum JY.** 2011. Anti-virulence strategy against *Brucella suis*: synthesis, biological
694 evaluation and molecular modeling of selective histidinol dehydrogenase inhibitors.
695 *Org Biomol Chem* **9**:3681-3690.
- 696 14. **Lestrade P, Delrue RM, Danese I, Didembourg C, Taminiau B, Mertens P, De
697 Bolle X, Tibor A, Tang CM, Letesson JJ.** 2000. Identification and characterization
698 of in vivo attenuated mutants of *Brucella melitensis*. *Mol Microbiol* **38**:543-551.
- 699 15. **Christen B, Abeliuk E, Collier JM, Kalogeraki VS, Passarelli B, Coller JA, Fero
700 MJ, McAdams HH, Shapiro L.** 2011. The essential genome of a bacterium. *Mol
701 Syst Biol* **7**:528.
- 702 16. **Hallez R, Mignolet J, Van Mullem V, Wery M, Vandehaute J, Letesson JJ,
703 Jacobs-Wagner C, De Bolle X.** 2007. The asymmetric distribution of the essential

- 704 histidine kinase PdhS indicates a differentiation event in *Brucella abortus*. EMBO J
705 **26**:1444-1455.
- 706 17. **Laloux G, Deghelt M, de Barsy M, Letesson JJ, De Bolle X.** 2010. Identification of
707 the essential *Brucella melitensis* porin Omp2b as a suppressor of Bax-induced cell
708 death in yeast in a genome-wide screening. PLoS One **5**:e13274.
- 709 18. **Robertson GT, Reisenauer A, Wright R, Jensen RB, Jensen A, Shapiro L, Roop
710 RM, 2nd.** 2000. The *Brucella abortus* CcrM DNA methyltransferase is essential for
711 viability, and its overexpression attenuates intracellular replication in murine
712 macrophages. J Bacteriol **182**:3482-3489.
- 713 19. **Van der Henst C, Beaufay F, Mignolet J, Didembourg C, Colinet J, Hallet B,
714 Letesson JJ, De Bolle X.** 2012. The histidine kinase PdhS controls cell cycle
715 progression of the pathogenic alphaproteobacterium *Brucella abortus*. J Bacteriol
716 **194**:5305-5314.
- 717 20. **Willett JW, Herrou J, Briegel A, Rotskoff G, Crosson S.** 2015. Structural
718 asymmetry in a conserved signaling system that regulates division, replication, and
719 virulence of an intracellular pathogen. Proc Natl Acad Sci U S A **112**:E3709-3718.
- 720 21. **Curtis PD, Brun YV.** 2014. Identification of essential alphaproteobacterial genes
721 reveals operational variability in conserved developmental and cell cycle systems. Mol
722 Microbiol **93**:713-735.
- 723 22. **Paulsen IT, Seshadri R, Nelson KE, Eisen JA, Heidelberg JF, Read TD, Dodson
724 RJ, Umayam L, Brinkac LM, Beanan MJ, Daugherty SC, Deboy RT, Durkin AS,
725 Kolonay JF, Madupu R, Nelson WC, Ayodeji B, Kraul M, Shetty J, Malek J, Van
726 Aken SE, Riedmuller S, Tettelin H, Gill SR, White O, Salzberg SL, Hoover DL,
727 Lindler LE, Halling SM, Boyle SM, Fraser CM.** 2002. The *Brucella suis* genome
728 reveals fundamental similarities between animal and plant pathogens and symbionts.
729 Proc Natl Acad Sci U S A **99**:13148-13153.
- 730 23. **Aakre CD, Phung TN, Huang D, Laub MT.** 2013. A bacterial toxin inhibits DNA
731 replication elongation through a direct interaction with the beta sliding clamp. Mol
732 Cell **52**:617-628.
- 733 24. **Fontana C, Conde-Alvarez R, Stahle J, Holst O, Iriarte M, Zhao Y, Arce-Gorvel
734 V, Hanniffy S, Gorvel JP, Moriyon I, Widmalm G.** 2016. Structural studies of
735 lipopolysaccharide defective mutants from *Brucella melitensis* identify a core
736 oligosaccharide critical in virulence. J Biol Chem **291**:7727-7741.
- 737 25. **Brilli M, Fondi M, Fani R, Mengoni A, Ferri L, Bazzicalupo M, Biondi EG.** 2010.
738 The diversity and evolution of cell cycle regulation in alpha-proteobacteria: a
739 comparative genomic analysis. BMC Syst Biol **4**:52.
- 740 26. **Delrue RM, Martinez-Lorenzo M, Lestrade P, Danese I, Bielarz V, Mertens P, De
741 Bolle X, Tibor A, Gorvel JP, Letesson JJ.** 2001. Identification of *Brucella* spp.
742 genes involved in intracellular trafficking. Cell Microbiol **3**:487-497.
- 743 27. **Arocena GM, Sieira R, Comerci DJ, Ugalde RA.** 2010. Identification of the
744 quorum-sensing target DNA sequence and N-Acyl homoserine lactone responsiveness
745 of the *Brucella abortus virB* promoter. J Bacteriol **192**:3434-3440.
- 746 28. **Delrue RM, Deschamps C, Leonard S, Nijskens C, Danese I, Schaus JM, Bonnot
747 S, Ferooz J, Tibor A, De Bolle X, Letesson JJ.** 2005. A quorum-sensing regulator
748 controls expression of both the type IV secretion system and the flagellar apparatus of
749 *Brucella melitensis*. Cell Microbiol **7**:1151-1161.
- 750 29. **Detilleux PG, Deyoe BL, Cheville NF.** 1990. Penetration and intracellular growth of
751 *Brucella abortus* in nonphagocytic cells in vitro. Infect Immun **58**:2320-2328.

- 752 30. **Porte F, Naroeni A, Ouahrani-Bettache S, Liautard JP.** 2003. Role of the *Brucella*
753 *suis* lipopolysaccharide O antigen in phagosomal genesis and in inhibition of
754 phagosome-lysosome fusion in murine macrophages. *Infect Immun* **71**:1481-1490.
- 755 31. **Sheehan LM, Budnick JA, Blanchard C, Dunman PM, Caswell CC.** 2015. A
756 LysR-family transcriptional regulator required for virulence in *Brucella abortus* is
757 highly conserved among the alpha-proteobacteria. *Mol Microbiol* **98**:318-328.
- 758 32. **Endley S, McMurray D, Ficht TA.** 2001. Interruption of the *cydB* locus in *Brucella*
759 *abortus* attenuates intracellular survival and virulence in the mouse model of
760 infection. *J Bacteriol* **183**:2454-2462.
- 761 33. **Cha SB, Rayamajhi N, Lee WJ, Shin MK, Jung MH, Shin SW, Kim JW, Yoo HS.**
762 2012. Generation and envelope protein analysis of internalization defective *Brucella*
763 *abortus* mutants in professional phagocytes, RAW 264.7. *FEMS immunology and*
764 *medical microbiology* **64**:244-254.
- 765 34. **Delrue RM, Lestrade P, Tibor A, Letesson JJ, De Bolle X.** 2004. *Brucella*
766 pathogenesis, genes identified from random large-scale screens. *FEMS Microbiol Lett*
767 **231**:1-12.
- 768 35. **Kim DH, Lim JJ, Lee JJ, Kim DG, Lee HJ, Min W, Kim KD, Chang HH, Rhee**
769 **MH, Watarai M, Kim S.** 2012. Identification of genes contributing to the
770 intracellular replication of *Brucella abortus* within HeLa and RAW 264.7 cells. *Vet*
771 *Microbiol* **158**:322-328.
- 772 36. **Liautard J, Ouahrani-Bettache S, Jubier-Maurin V, Lafont V, Kohler S,**
773 **Liautard JP.** 2007. Identification and isolation of *Brucella suis* virulence genes
774 involved in resistance to the human innate immune system. *Infect Immun* **75**:5167-
775 5174.
- 776 37. **Wu Q, Pei J, Turse C, Ficht TA.** 2006. Mariner mutagenesis of *Brucella melitensis*
777 reveals genes with previously uncharacterized roles in virulence and survival. *BMC*
778 *Microbiol* **6**:102.
- 779 38. **Sklar JG, Wu T, Gronenberg LS, Malinverni JC, Kahne D, Silhavy TJ.** 2007.
780 Lipoprotein SmpA is a component of the YaeT complex that assembles outer
781 membrane proteins in *Escherichia coli*. *Proc Natl Acad Sci U S A* **104**:6400-6405.
- 782 39. **Gora KG, Tsokos CG, Chen YE, Srinivasan BS, Perchuk BS, Laub MT.** 2010. A
783 cell-type-specific protein-protein interaction modulates transcriptional activity of a
784 master regulator in *Caulobacter crescentus*. *Mol Cell* **39**:455-467.
- 785 40. **Iniesta AA, McGrath PT, Reisenauer A, McAdams HH, Shapiro L.** 2006. A
786 phospho-signaling pathway controls the localization and activity of a protease
787 complex critical for bacterial cell cycle progression. *Proc Natl Acad Sci U S A*
788 **103**:10935-10940.
- 789 41. **Holtzendorff J, Hung D, Brende P, Reisenauer A, Viollier PH, McAdams HH,**
790 **Shapiro L.** 2004. Oscillating global regulators control the genetic circuit driving a
791 bacterial cell cycle. *Science* **304**:983-987.
- 792 42. **Wright R, Stephens C, Shapiro L.** 1997. The CcrM DNA methyltransferase is
793 widespread in the alpha subdivision of proteobacteria, and its essential functions are
794 conserved in *Rhizobium meliloti* and *Caulobacter crescentus*. *J Bacteriol* **179**:5869-
795 5877.
- 796 43. **Murray SM, Panis G, Fumeaux C, Viollier PH, Howard M.** 2013. Computational
797 and genetic reduction of a cell cycle to its simplest, primordial components. *PLoS Biol*
798 **11**:e1001749.
- 799 44. **Caswell CC, Elhassanny AE, Planchin EE, Roux CM, Weeks-Gorospe JN, Ficht**
800 **TA, Dunman PM, Roop RM, 2nd.** 2013. Diverse genetic regulon of the virulence-

- 801 associated transcriptional regulator MucR in *Brucella abortus* 2308. Infect Immun
802 **81**:1040-1051.
- 803 45. **Godfroid F, Cloeckeaert A, Taminiau B, Danese I, Tibor A, de Bolle X, Mertens P,**
804 **Letesson JJ.** 2000. Genetic organisation of the lipopolysaccharide O-antigen
805 biosynthesis region of *Brucella melitensis* 16M (*wbk*). Res Microbiol **151**:655-668.
- 806 46. **Martin DW, Baumgartner JE, Gee JM, Anderson ES, Roop RM, 2nd.** 2012.
807 SodA is a major metabolic antioxidant in *Brucella abortus* 2308 that plays a
808 significant, but limited, role in the virulence of this strain in the mouse model.
809 Microbiology **158**:1767-1774.
- 810 47. **Mignolet J, Van der Henst C, Nicolas C, Deghelt M, Dotreppe D, Letesson JJ, De**
811 **Bolle X.** 2010. PdhS, an old-pole-localized histidine kinase, recruits the fumarase
812 FumC in *Brucella abortus*. J Bacteriol **192**:3235-3239.
- 813 48. **Mirabella A, Terwagne M, Zygmunt MS, Cloeckeaert A, De Bolle X, Letesson JJ.**
814 2013. *Brucella melitensis* MucR, an orthologue of *Sinorhizobium meliloti* MucR, is
815 involved in resistance to oxidative, detergent, and saline stresses and cell envelope
816 modifications. J Bacteriol **195**:453-465.
- 817 49. **Ugalde JE, Czibener C, Feldman MF, Ugalde RA.** 2000. Identification and
818 characterization of the *Brucella abortus* phosphoglucomutase gene: role of
819 lipopolysaccharide in virulence and intracellular multiplication. Infect Immun
820 **68**:5716-5723.
- 821 50. **Bukata L, Altabe S, de Mendoza D, Ugalde RA, Comerci DJ.** 2008.
822 Phosphatidylethanolamine synthesis is required for optimal virulence of *Brucella*
823 *abortus*. J Bacteriol **190**:8197-8203.
- 824 51. **Hubbard TP, Chao MC, Abel S, Blondel CJ, Abel Zur Wiesch P, Zhou X, Davis**
825 **BM, Waldor MK.** 2016. Genetic analysis of *Vibrio parahaemolyticus* intestinal
826 colonization. Proc Natl Acad Sci U S A **113**:6283-6288.
- 827 52. **Ke Y, Wang Y, Li W, Chen Z.** 2015. Type IV secretion system of *Brucella* spp. and
828 its effectors. Frontiers in cellular and infection microbiology **5**:72.
- 829 53. **Nijskens C, Copin R, De Bolle X, Letesson JJ.** 2008. Intracellular rescuing of a *B.*
830 *melitensis* 16M *virB* mutant by co-infection with a wild type strain. Microb Pathog
831 **45**:134-141.
- 832 54. **Xavier MN, Winter MG, Spees AM, den Hartigh AB, Nguyen K, Roux CM, Silva**
833 **TM, Atluri VL, Kerrinnes T, Keestra AM, Monack DM, Luciw PA, Eigenheer**
834 **RA, Baumler AJ, Santos RL, Tsolis RM.** 2013. PPARgamma-mediated increase in
835 glucose availability sustains chronic *Brucella abortus* infection in alternatively
836 activated macrophages. Cell Host Microbe **14**:159-170.
- 837 55. **Joseph P, Abdo MR, Boigegrain RA, Montero JL, Winum JY, Kohler S.** 2007.
838 Targeting of the *Brucella suis* virulence factor histidinol dehydrogenase by histidinol
839 analogues results in inhibition of intramacrophagic multiplication of the pathogen.
840 Antimicrob Agents Chemother **51**:3752-3755.
- 841 56. **Kim S, Watarai M, Kondo Y, Erdenebaatar J, Makino S, Shirahata T.** 2003.
842 Isolation and characterization of mini-Tn5Km2 insertion mutants of *Brucella abortus*
843 deficient in internalization and intracellular growth in HeLa cells. Infect Immun
844 **71**:3020-3027.
- 845 57. **LoVullo ED, Wright LF, Isabella V, Huntley JF, Pavelka MS, Jr.** 2015. Revisiting
846 the Gram-negative lipoprotein paradigm. J Bacteriol **197**:1705-1715.
- 847 58. **Selkig J, Mosbahi K, Webb CT, Belousoff MJ, Perry AJ, Wells TJ, Morris F,**
848 **Leyton DL, Totsika M, Phan MD, Celik N, Kelly M, Oates C, Hartland EL,**
849 **Robins-Browne RM, Ramarathinam SH, Purcell AW, Schembri MA, Strugnell**

- 850 **RA, Henderson IR, Walker D, Lithgow T.** 2012. Discovery of an archetypal protein
851 transport system in bacterial outer membranes. *Nat Struct Mol Biol* **19**:506-510, S501.
- 852 59. **Salcedo SP, Chevrier N, Lacerda TL, Ben Amara A, Gerart S, Gorvel VA, de**
853 **Chastellier C, Blasco JM, Mege JL, Gorvel JP.** 2013. Pathogenic *brucellae*
854 replicate in human trophoblasts. *The Journal of infectious diseases* **207**:1075-1083.
- 855 60. **Hanot Mambres D, Machelart A, Potemberg G, De Trez C, Ryffel B, Letesson JJ,**
856 **Muraille E.** 2016. Identification of Immune Effectors Essential to the Control of
857 Primary and Secondary Intranasal Infection with *Brucella melitensis* in Mice. *J*
858 *Immunol* **196**:3780-3793.
- 859 61. **Christen M, Beusch C, Bosch Y, Cerletti D, Flores-Tinoco CE, Del Medico L,**
860 **Tschan F, Christen B.** 2016. Quantitative Selection Analysis of Bacteriophage
861 phiCbK Susceptibility in *Caulobacter crescentus*. *J Mol Biol* **428**:419-430.
- 862 62. **Haine V, Sinon A, Van Steen F, Rousseau S, Dozot M, Lestrade P, Lambert C,**
863 **Letesson JJ, De Bolle X.** 2005. Systematic targeted mutagenesis of *Brucella*
864 *melitensis* 16M reveals a major role for GntR regulators in the control of virulence.
865 *Infect Immun* **73**:5578-5586.
- 866 63. **Anderson ES, Paulley JT, Gaines JM, Valderas MW, Martin DW, Menscher E,**
867 **Brown TD, Burns CS, Roop RM, 2nd.** 2009. The manganese transporter MntH is a
868 critical virulence determinant for *Brucella abortus* 2308 in experimentally infected
869 mice. *Infect Immun* **77**:3466-3474.
- 870 64. **Anderson ES, Paulley JT, Martinson DA, Gaines JM, Steele KH, Roop RM, 2nd.**
871 2011. The iron-responsive regulator irr is required for wild-type expression of the
872 gene encoding the heme transporter BhuA in *Brucella abortus* 2308. *J Bacteriol*
873 **193**:5359-5364.
- 874 65. **Delory M, Hallez R, Letesson JJ, De Bolle X.** 2006. An RpoH-like heat shock sigma
875 factor is involved in stress response and virulence in *Brucella melitensis* 16M. *J*
876 *Bacteriol* **188**:7707-7710.
- 877 66. **Gil-Ramirez Y, Conde-Alvarez R, Palacios-Chaves L, Zuniga-Ripa A, Grillo MJ,**
878 **Arce-Gorvel V, Hanniffy S, Moriyon I, Iriarte M.** 2014. The identification of
879 wadB, a new glycosyltransferase gene, confirms the branched structure and the role in
880 virulence of the lipopolysaccharide core of *Brucella abortus*. *Microb Pathog* **73**:53-59.
- 881 67. **Himeno H, Kurita D, Muto A.** 2014. tmRNA-mediated trans-translation as the major
882 ribosome rescue system in a bacterial cell. *Front Genet* **5**:66.

884

885 **TABLE 1 Attenuated *B. abortus* mutants in RAW 264.7 infection at 2, 5 or 24 h PI**

ORF	Gene name	2 h PI	5 h PI	24 h PI	Predicted functions
Secretion					
BAB2_0068	<i>virB1</i>	-	-	+	type IV secretion system
BAB2_0067	<i>virB2</i>	-	-	+	type IV secretion system
BAB2_0066	<i>virB3</i>	-	-	+	type IV secretion system
BAB2_0065	<i>virB4</i>	-	-	+	type IV secretion system
BAB2_0064	<i>virB5</i>	-	-	+	type IV secretion system
BAB2_0063	<i>virB6</i>	-	-	+	type IV secretion system
BAB2_0062	<i>virB7</i>	-	-	+	type IV secretion system
BAB2_0061	<i>virB8</i>	-	-	+	type IV secretion system
BAB2_0060	<i>virB9</i>	-	-	+	type IV secretion system
BAB2_0059	<i>virB10</i>	-	-	+	type IV secretion system
BAB2_0058	<i>virB11</i>	-	-	+	type IV secretion system
BAB1_0045	<i>tamA</i>	-	-	+	export of autotransporters (type V secretion system)
BAB1_0046	<i>tamB</i>	-	-	+	export of autotransporters (type V secretion system)
Protein synthesis and degradation					
BAB1_2087	<i>hisE</i>	-	-	+	histidine biosynthesis
BAB1_2082	<i>hisB</i>	-	-	+	histidine biosynthesis
BAB1_1988	<i>hisC</i>	-	-	+	histidine biosynthesis
BAB1_0285	<i>hisD</i>	-	-	+	histidine biosynthesis
BAB1_1399	<i>ilvC</i>	-	-	+	isoleucine, leucine and valine biosynthesis
BAB1_0096	<i>ilvD</i>	-	-	+	isoleucine, leucine and valine biosynthesis
BAB1_2158	<i>lnt</i>	+	+	+	lipoprotein synthesis
BAB1_1437	<i>pepP</i>	+	+	+	peptidase, Xaa-Pro aminopeptidase
BAB1_0162	<i>ibpA</i>	-	-	+	chaperone
BAB1_2025		+	+	+	DnaJ-like chaperone
BAB1_1115	<i>tgt</i>	+	+	+	tRNA modification
BAB1_0477	<i>rpII</i>	-	+	+	ribosomal protein L9
BAB1_0427		-	+	+	tRNA1(Val) A37 N6-methylase TrmN6
Nucleic acid synthesis and degradation					
BAB2_0641	<i>pyrB</i>	-	-	+	pyrimidines biosynthesis
BAB2_0640	<i>pyrC</i>	-	-	+	pyrimidines biosynthesis
BAB1_0341	<i>pyrD</i>	-	-	+	pyrimidines biosynthesis
BAB1_0673	<i>pyrE</i>	-	-	+	pyrimidines biosynthesis
BAB1_2132	<i>pyrF</i>	-	-	+	pyrimidines biosynthesis
BAB1_0688	<i>pyrC2</i>	-	+	+	pyrimidines biosynthesis
BAB1_1695	<i>purA</i>	-	-	+	purines biosynthesis
BAB1_1757	<i>purE</i>	+	+	+	purines biosynthesis
BAB1_0861	<i>purS</i>	-	-	+	purines biosynthesis
BAB1_0024	<i>cmk</i>	+	+	+	CDP synthesis from CMP
BAB1_0168	<i>ydjH</i>	-	-	+	adenosine kinase (AK)

BAB1_0172	<i>rph</i>	-	-	+	ribonuclease
BAB2_0643	<i>yqgF</i>	-	+	+	endonuclease, resolvase family
BAB1_0003	<i>recF</i>	-	-	+	recombination in response to DNA damage
BAB1_1206	<i>queF</i>	-	-	+	dehydrogenase, involved in queuosine biosynthesis

Electrons transfer and redox

BAB2_0727	<i>cydB</i>	-	-	+	cytochrome bd
BAB2_0728	<i>cydA</i>	-	-	+	cytochrome bd
BAB2_0729	<i>cydC</i>	-	-	+	ABC transporter, cytochrome bd biogenesis
BAB2_0730	<i>cydD</i>	-	-	+	ABC transporter, cytochrome bd biogenesis
BAB1_1435		-	+	+	related to cytochrome c oxidase synthesis
BAB1_0051	<i>pcuC</i>	-	+	+	incorporation of Cu(I) in cytochrome c oxidase
BAB1_0139	<i>nfuA</i>	-	-	+	Fe-S cluster biogenesis protein

Cell envelope

BAB1_0351	<i>wadB</i>	+	+	+	envelope, LPS core synthesis
BAB1_1217	<i>murl</i>	-	-	+	glutamate racemase
BAB1_1462	<i>ampD-like</i>	-	+	+	N-acetyl-anhydromuramyl-L-alanine amidase

Regulation

BAB1_2092	<i>bvrR</i>	+	+	+	two-component regulator
BAB1_1665	<i>rpoH2</i>	+	+	+	RNA polymerase sigma factor
BAB1_1669		+	+	+	signal transduction, HWE-family histidine kinase
BAB2_0678	<i>rirA</i>	-	+	+	transcriptional regulator, iron responsive
BAB1_1517	<i>vtlR</i>	-	-	+	LysR transcriptional regulator controlling sRNA expression
BAB2_0118	<i>vjbR</i>	-	-	+	quorum sensing transcriptional regulator
BAB2_0143	<i>deoR1</i>	-	-	+	transcriptional regulator
BAB1_0160	<i>ptsN</i>	+	+	+	pts, metabolism, carbon catabolite repression
BAB1_0638	<i>glnE</i>	-	-	+	glutamine pool regulation

Transport

BAB1_1460	<i>mntH</i>	+	+	+	manganese transport, ion transport
BAB2_0699	<i>oppA</i>	+	+	+	ABC transporter, substrate binding, oligopeptide transport
BAB2_0701	<i>oppB</i>	+	+	+	ABC transporter, permease, oligopeptide transport
BAB2_0702	<i>oppC</i>	+	+	+	ABC transporter, permease, oligopeptide transport
BAB2_0703	<i>oppD</i>	+	+	+	ABC transporter, ATPase
BAB1_2145	<i>phoU</i>	-	+	+	phosphate transport control
BAB1_1345		-	-	+	Kef-type potassium/proton antiport protein

Metabolism

BAB2_1010	<i>glk</i>	-	-	+	glucokinase
BAB1_0435	<i>glcD</i>	+	+	+	glycolate oxidase
BAB1_1918	<i>lpd</i>	+	+	+	dihydrolipoyl dehydrogenase
BAB1_0898	<i>bgIX</i>	-	+	+	beta-glucosylase-related glycosidase
BAB1_1476	<i>pldB</i>	-	+	+	lysophospholipase L2
BAB1_0113	<i>fabG</i>	-	-	+	3-oxoacyl-ACP reductase
BAB1_0318	<i>gph</i>	-	-	+	phosphoglycolate phosphatase

				Unknown functions	
BAB1_1485		+	+	+	inner membrane conserved protein (DUF475)
BAB1_1766	<i>hfaC</i>	+	+	+	duplicated ATPase domains
BAB1_0478		-	-	+	inner membrane conserved protein (DUF2232)
BAB1_1283		-	-	+	conserved periplasmic protein (DUF192)
BAB1_2069	<i>maf-2</i>	-	-	+	Maf-like nucleotide binding protein

886

887 *Note.* For each coding sequence (“ORF”), a reduced R200 value is indicated by “+”. If the
888 corresponding mutants also display a lower R200 after re-plating on rich medium, they are
889 reported in Table 2. If a similar R200 value is found between a given time PI and the control,
890 a “-“ is indicated in the table. The coding sequences untouched by previous screenings of
891 mutant libraries are shown in bold, including some (like *mntH*, *rirA*, *wadB* and *rpoH2*) that
892 were investigated by targeted mutagenesis (63-66). The R200 values (TTMs) and the genomic
893 maps are available as Supplementary Datasets (see Material and Methods for a complete list).

894 **TABLE 2** Attenuated *B. abortus* mutants in RAW 264.7 infection at 2, 5 or 24 h PI
 895 with a growth defect on plates

ORF	Gene name	2 h PI	5 h PI	24 h PI	Predicted function
Protein synthesis and degradation					
BAB1_1846		-	+	+	membrane bound metallopeptidase
BAB1_1191	<i>clpA</i>	+	+	+	protease-associated factor
BAB2_0183	<i>hisG</i>	-	-	+	histidine biosynthesis, first part of the pathway
BAB2_0182	<i>hisZ</i>	-	-	+	histidine biosynthesis, first part of the pathway
BAB1_1098	<i>hisI</i>	-	-	+	histidine biosynthesis, first part of the pathway
BAB1_2085	<i>hisA</i>	+	+	+	histidine biosynthesis, first part of the pathway
BAB1_2084	<i>hisH</i>	+	+	+	histidine biosynthesis, first part of the pathway
BAB1_2086	<i>hisF</i>	+	+	+	histidine biosynthesis, first part of the pathway
BAB1_0704	<i>ksgA</i>	-	+	+	16S ribosomal RNA methyltransferase
BAB1_1553	<i>ychF</i>	+	+	+	translation-associated GTPase
BAB1_2167	<i>truB</i>	-	+	+	tRNA modification
BAB1_1019	<i>rluA</i>	-	-	+	pseudouridylate synthase, 23S RNA-specific
BAB1_1657	<i>dsbB</i>	-	-	+	disulfide bond formation in periplasm
BAB1_0962		+	+	+	protein-L-isoAsp O-methyltransferase
Nucleic acid synthesis and degradation					
BAB1_0442	<i>purD</i>	+	+	+	purines biosynthesis
BAB1_0730	<i>purN</i>	+	+	+	purines biosynthesis
BAB1_0857	<i>purL</i>	+	+	+	purines biosynthesis
BAB1_0860	<i>purQ</i>	+	+	+	purines biosynthesis
BAB1_0731	<i>purM</i>	+	+	+	purines biosynthesis
BAB1_0862	<i>purC</i>	+	+	+	purines biosynthesis
BAB1_0868	<i>purB</i>	+	+	+	purines biosynthesis
BAB1_1824	<i>purH</i>	+	+	+	purines biosynthesis
Electrons transfer and redox					
BAB1_0091	<i>ccmA</i>	+	+	+	cytochrome c maturation
BAB1_0092	<i>ccmB</i>	+	+	+	cytochrome c maturation
BAB1_0093	<i>ccmC</i>	+	+	+	cytochrome c maturation
BAB1_0632	<i>ccmE</i>	+	+	+	cytochrome c maturation
BAB1_0633	<i>ccmF</i>	+	+	+	cytochrome c maturation
BAB1_0634	<i>ccmH</i>	+	+	+	cytochrome c maturation
BAB1_0631	<i>ccmI</i>	+	+	+	cytochrome c maturation
BAB2_0656	<i>ccdA</i>	+	+	+	cytochrome c maturation (<i>dsbD</i> homolog)
BAB1_0388	<i>ccoG</i>	-	+	+	cytochrome c oxidase
BAB1_0389	<i>ccoP</i>	-	+	+	cytochrome c oxidase
BAB1_0392	<i>ccoN</i>	-	+	+	cytochrome c oxidase
BAB1_1557		-	+	+	cytochrome c1 family
BAB1_1559		-	+	+	ubiquinol cytochrome c reductase, iron-sulfur component
BAB1_0739		+	+	+	Electron Transport Chain (ETC)- complex I subunit

BAB1_1030	<i>gor</i>	+	+	+	glutathione reductase
BAB2_0476	<i>gshA</i>	+	+	+	gamma-glutamylcysteine synthetase
BAB1_2135	<i>gshB</i>	+	+	+	glutathione synthetase
BAB1_0855		+	+	+	glutaredoxin-like protein
Cell envelope					
BAB1_1041	<i>miaA</i>	+	+	+	predicted lipoprotein
BAB1_1040	<i>miaD</i>	+	+	+	ABC transporter-associated inner membrane protein
BAB1_1038	<i>miaE</i>	+	+	+	ABC transporter, permease
BAB1_1039	<i>miaF</i>	+	+	+	ABC transporter, ATPase
BAB2_0076	<i>omp10</i>	+	+	+	outer membrane lipoprotein
BAB1_1930	<i>omp19</i>	-	-	+	outer membrane lipoprotein
BAB1_0491		+	+	+	invasion protein B (conserved periplasmic protein)
Regulation					
BAB1_0143	<i>glnD</i>	+	+	+	glutamine pool regulation
BAB1_0304	<i>cenR</i>	+	+	+	regulator for envelope composition
BAB1_2006	<i>cenR</i>	+	+	+	transcriptional regulator(also called <i>otpR</i>)
BAB1_1962	<i>gntR13</i>	-	+	+	transcriptional regulator
BAB1_0640	<i>pleC</i>	-	-	+	histidine kinase, regulation of cell cycle
BAB1_2093	<i>bvrS</i>	+	+	+	histidine kinase for BvrR regulator
BAB1_2094	<i>hprK</i>	+	+	+	kinase, regulator of phosphotransferase system (PTS)
BAB1_2159	<i>hipB</i>	+	+	+	transcriptional regulator
BAB1_2175	<i>irr</i>	+	+	+	transcriptional regulator, ferric uptake regulator
Transport and storage					
BAB1_0386	<i>copA</i>	+	+	+	cation metal exporter, ATPase
BAB1_0387		+	+	+	cation exporter associated protein
BAB2_1079	<i>znuA</i>	-	-	+	ABC transporter for zinc
BAB2_1080	<i>znuC</i>	-	-	+	ABC transporter for zinc
BAB2_1081	<i>znuB</i>	-	-	+	ABC transporter for zinc
BAB2_0411		+	+	+	conserved hypothetical
BAB2_0412	<i>tauE</i>	+	+	+	sulfite exporter
BAB1_1589		-	+	+	major facilitator superfamily (transporter)
BAB1_1045	<i>fdx</i>	+	+	+	ferredoxin
Metabolism					
BAB2_0366	<i>eryI</i>	+	+	+	erythritol metabolism (also called <i>rpiB</i>)
BAB2_0367	<i>eryH</i>	+	+	+	erythritol metabolism (also called <i>tpiA2</i>)
BAB2_0370	<i>eryC</i>	+	+	+	erythritol metabolism
BAB2_1013	<i>gpm</i>	+	+	+	phosphoglycerate mutase
BAB1_1761	<i>pykM</i>	-	-	+	pyruvate kinase
BAB2_0513	<i>gcvT</i>	-	-	+	glycine cleavage system
BAB2_0514	<i>gcvH</i>	-	-	+	glycine cleavage system
BAB2_0515	<i>gcvP</i>	-	-	+	glycine cleavage system
BAB1_2022	<i>cobT</i>	-	-	+	cobalamin biosynthesis

BAB1_2023	<i>cobS</i>	-	-	+	cobalamin biosynthesis
BAB2_1012	<i>dapB</i>	+	+	+	dihydrodipicolinate reductase
BAB1_0773	<i>gppA</i>	+	+	+	exopolyphosphatase
BAB1_2103		+	+	+	nucleotidyl transferase
BAB2_0442	<i>acaD</i>	+	+	+	acyl-CoA dehydrogenase
BAB2_0511		+	+	+	reductase
BAB2_0668	<i>pssA</i>	+	+	+	phosphatidylserine synthase
BAB1_0471		-	+	+	oxoacyl-(acyl carrier protein) reductase
BAB2_1027	<i>upp</i>	-	+	+	phosphoribosyl transferase

Unknown functions

BAB1_0084	<i>yccA</i>	-	-	+	inner membrane protein
BAB1_1670		-	-	+	hypothetical protein
BAB1_1092		-	-	+	hypothetical protein

896

897 *Note.* For each coding sequence (“ORF”), a reduced R200 value is indicated by “+”. If a
898 similar R200 value is found between a given time PI and the control, a “-“ is indicated in the
899 table. These mutants also display a lower R200 after re-plating on rich medium. The R200
900 values (TTMs) and the genomic maps are available as Supplementary Datasets (see Material
901 and Methods for a complete list).

902

903

904 **Figure Legends**

905 **FIG 1** Summary of the Tn-seq approach. A transposon mutants library was initially created
906 in *B. abortus* on plates using a mini-Tn5 derivative. Three million mutants were then pooled
907 and the resulting suspension was split in two. A first part of the pool underwent direct
908 sequencing of Tn5-gDNA junctions, allowing the identification of mini-Tn5 insertion sites by
909 mapping on the genomic sequence (see Fig. S1 for a detailed description of the mapping and
910 the subsequent computing), resulting in the control dataset. The second part of the pool was
911 used to infect RAW 264.7 macrophages in three separated infections. At given time points
912 post-infection (2 h, 5 h and 24 h PI), bacteria were extracted, grown on plates, colonies were
913 collected and their gDNA was subsequently extracted to be sequenced as for the control,
914 resulting in 2 h PI, 5 h PI and 24 h PI-specific datasets. Transposon tolerance maps (TTMs) in
915 the form of R200 values, and all post-infection lists were separately compared to the control
916 list using the Delta-R200 method (see Material and Methods). The number of mapped read (in
917 millions) for each dataset is displayed besides its respective mapping icon, and the number of
918 insertion sites is 929×10^3 for the control condition, and 742×10^3 , 713×10^3 , and 579×10^3
919 for the 2 h, 5 h and 24 h PI datasets, respectively.

920

921 **FIG 2** Sliding R200 values along a gene map. Statistical analysis of the R200 values is
922 indicated in Fig. S2. This analysis indicates a main peak of R200 centered on a value of 4.05.
923 Values of 2 (-2S), 4 (-4S) and 6 (-6S) standard deviations below 4.05 are indicated on the Y
924 axis. The region shown here is an example in which non-essential genes such as the *nikBCDE*
925 operon (red) are found close to the *acaD* gene (BAB2_0442, in green) and the *fadAJ* operon
926 (yellow) contributing to fitness. In the same region, an essential gene (*lysK*) is also identified.
927 The R200 values of *nikBCDE* are statistically different compared to *acaD* ($p < 10^{-3}$) and
928 *fadAJ* ($p < 10^{-19}$) according to a Scheffé pairwise comparison test with independent samples

929 (9 and 16 non-overlapping windows for the *nikBCDE-acaD* and *nikBCDE-fadAJ*
930 comparisons, respectively). The light grey horizontal bar is the average R200 for chr II (3.8).

931

932 **FIG 3** Genomic re-annotations and identification of essential domains according to Tn-seq.

933 The red line represents R200 values across the genome, the thin grey line represents the mean

934 R200 per chromosome, and the black size marker corresponds to 0.5 kb. (A) Tn-seq has

935 allowed to identify two previously unannotated essential genes as exemplified by the *ssrA*

936 gene (encoding tmRNA, allowing proteolysis of incomplete proteins) (67) between

937 BAB1_1419 and BAB1_1420. A coding sequence located between BAB2_0403 and

938 BAB2_0404, carrying a DUF4065 domain and well conserved (>90% identities at the protein

939 level) within Rhizobiales, was also found to be essential. This gene encodes the antitoxin

940 component of a toxin/antitoxin system called SocAB in *C. crescentus* (see text), and

941 BAB2_0403 is homologous to *socB*. Proposed reannotations are shown with a hatched line.

942 Old and new proposed annotation are shown. (B) Open reading frame extension and matching

943 essentiality region strongly suggest that *ftsK* (BAB1_1895) was misannotated. It should be

944 noted that this corrected annotation is supported by BLASTP of the resulting extended *ftsK*

945 gene against the Alphaproteobacterium model *C. crescentus*. Examples in (A) and (B) are

946 also supported by correct annotation in other genomic sequences. (C) Tn-seq is able to

947 identify domain-specific essentiality as shown for *polA* (BAB1_0120) and *dnaJ*

948 (BAB1_2130). In DnaJ, the Hsp70 interaction site seems essential, while in PolA, encoding

949 the DNA polymerase I, the 5'-3' exonuclease domain is proposed to be essential.

950

951 **FIG 4** Validation of Tn-seq data using reconstructed mutants. (A) CFUs counting after a 2 h

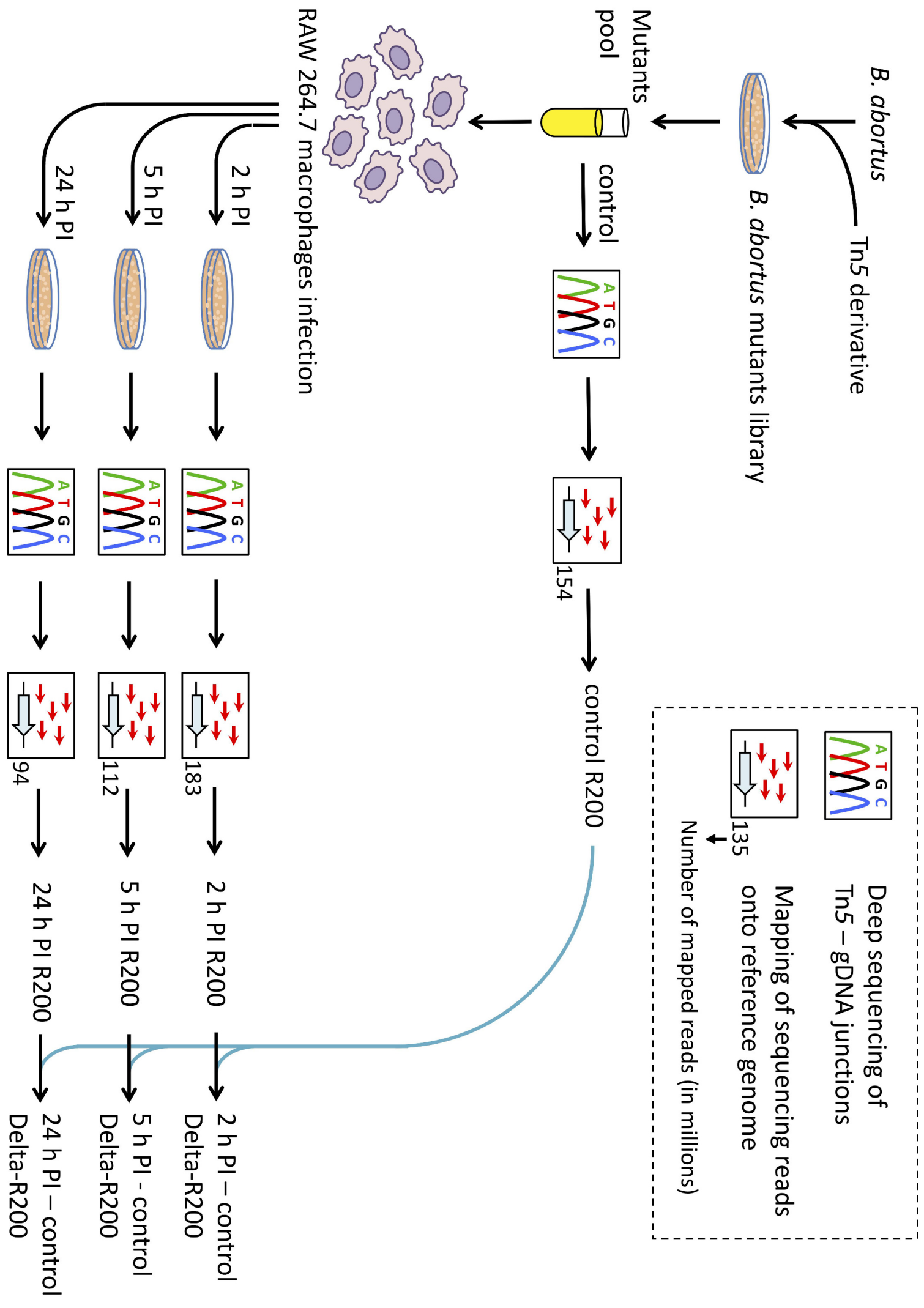
952 infection of RAW 264.7 macrophages with individual mutants in *omp2a*, *ftsK*-like, *wadB* and

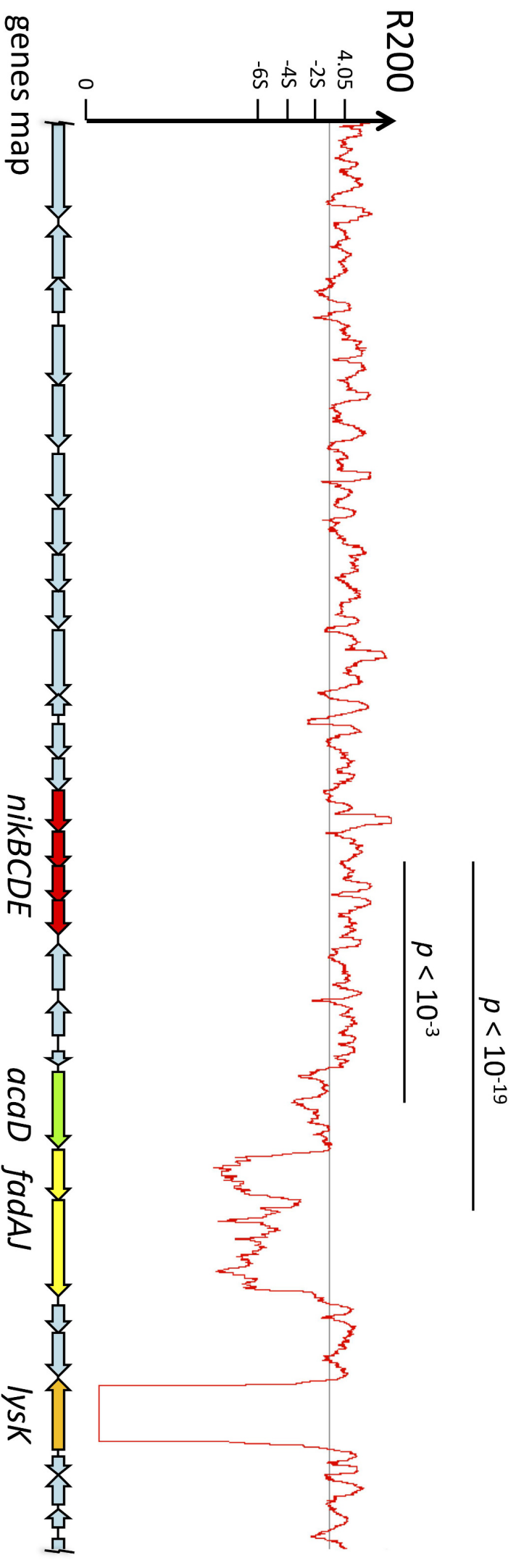
953 *pgk*. The Tn-seq data indicate that *omp2a* and *ftsK*-like mutants are fully virulent at 2 h PI

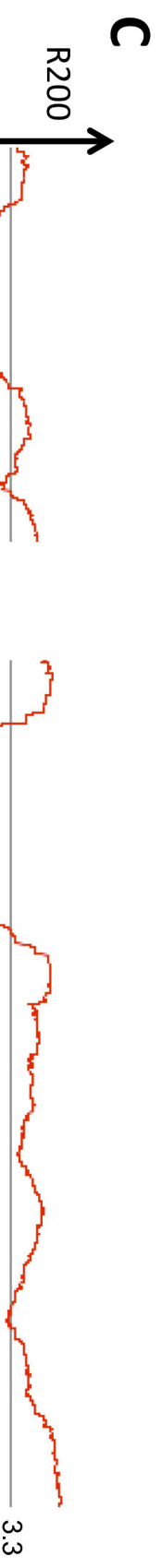
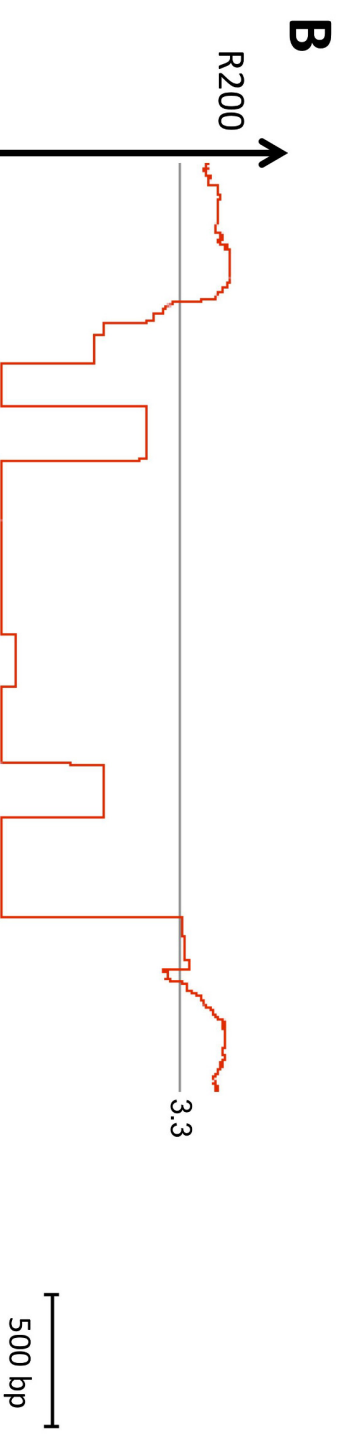
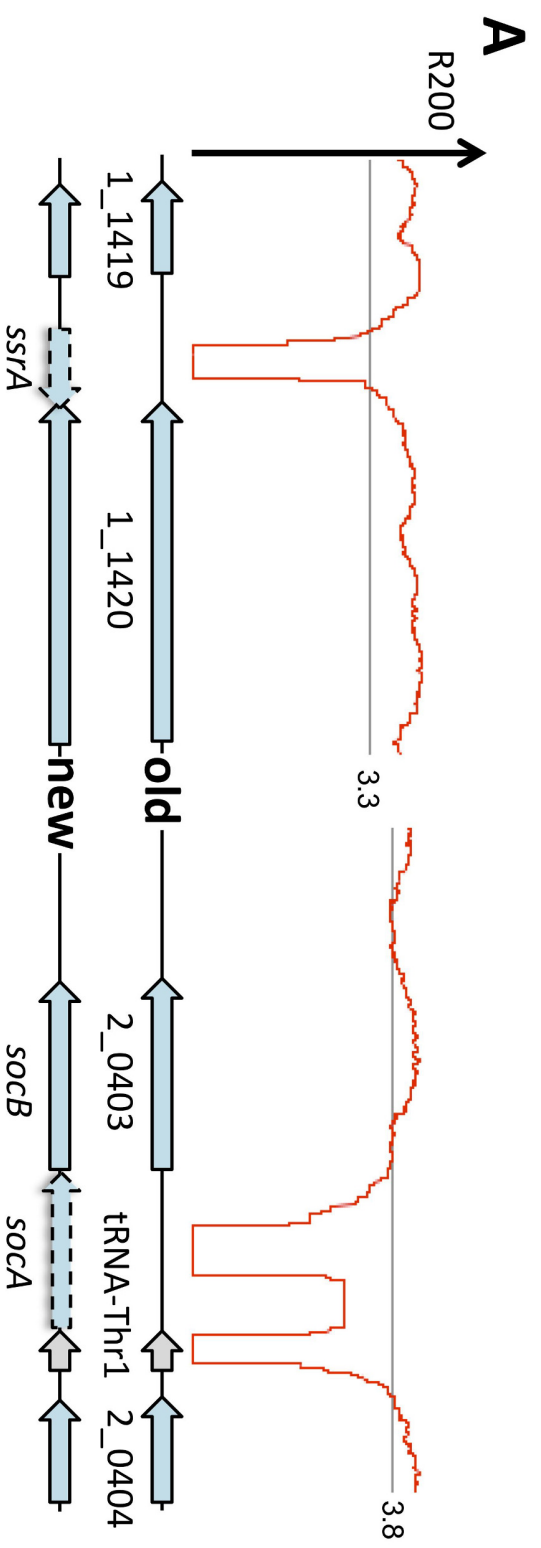
954 while the *wadB* and *pgk* mutants are attenuated. The wild type (wt) strain was used as a
955 virulent control. * = $p < 0.05$, *** = $p < 0.001$. (B) Comparison of the Tn-seq profiles of the
956 *wadB* and *pgk* mutants, highlighting the growth defect of the *pgk* mutant (below the -4S
957 threshold shown as a hatched line, i.e. 4 standard deviations under the average of the
958 theoretical distribution of R200 value, see supplementary Fig. S2). The grey lines correspond
959 to the average R200 or average Δ R200 for the whole chromosome. (C) Pictures of the wild
960 type strain, *wadB* mutant, and *pgk* mutant colonies on rich medium, supporting the hypothesis
961 of the *pgk* growth defect.

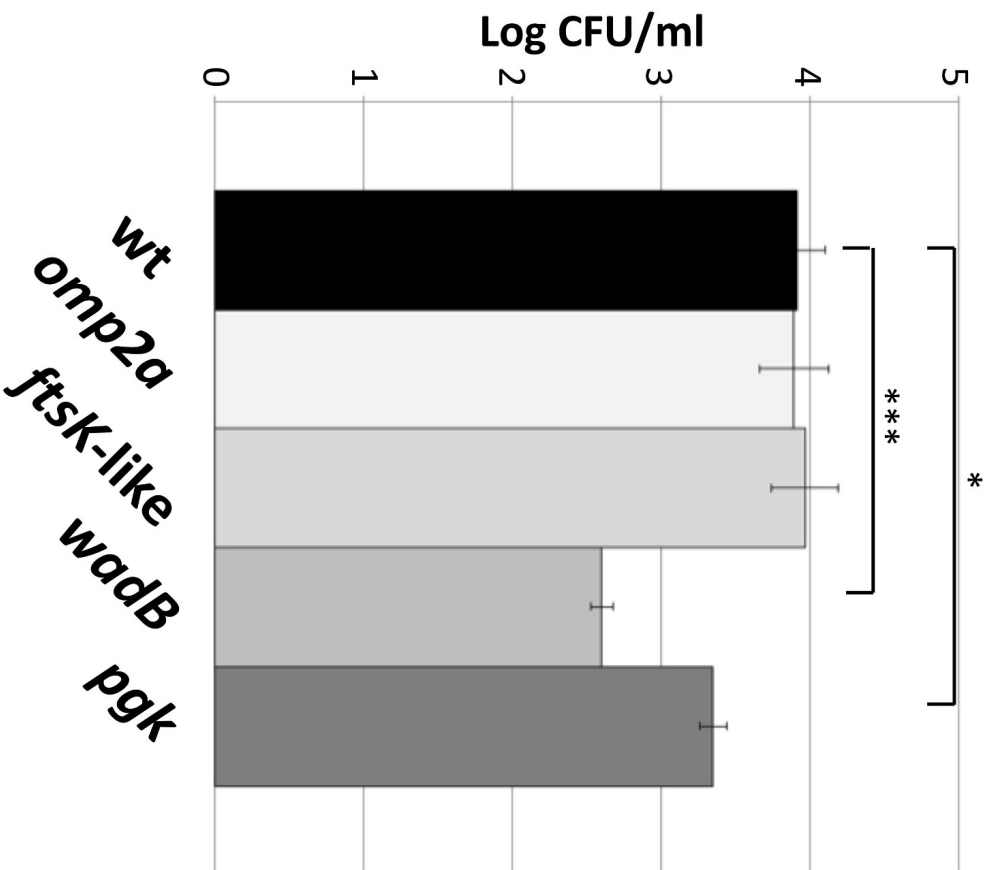
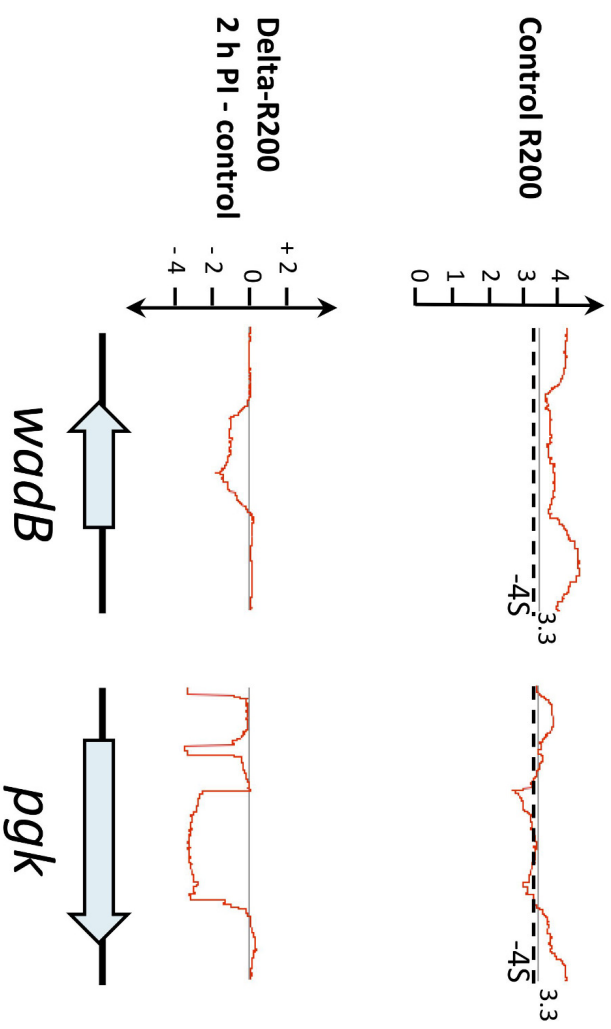
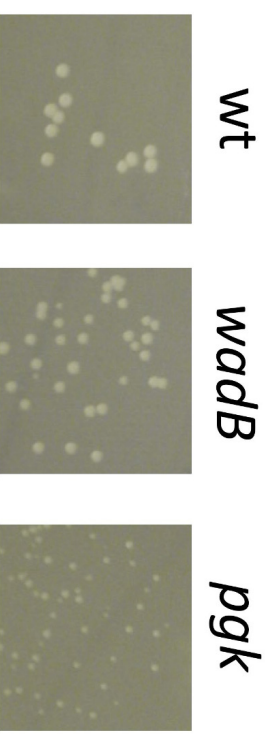
962

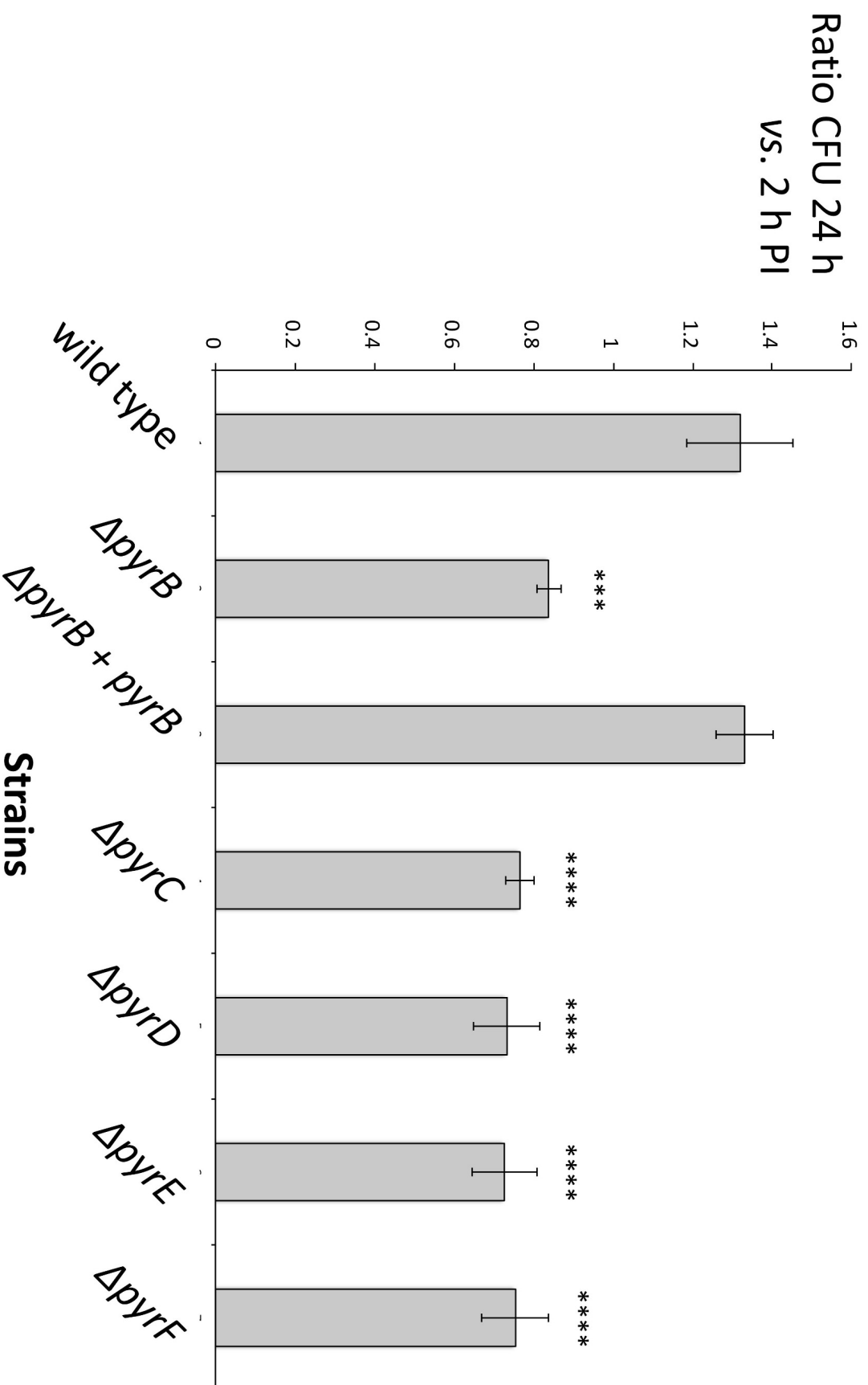
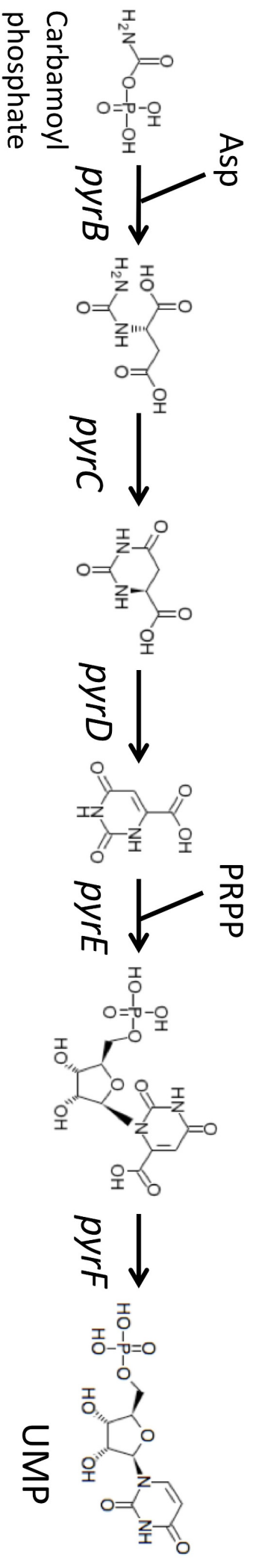
963 **FIG 5** Intracellular growth of *pyr* mutants. The pyrimidine biosynthesis pathway with the
964 corresponding genes for each step, with aspartate (Asp) and phosphoribosylpyrophosphate
965 (PRPP) involved in uridine monophosphate (UMP) synthesis. CFUs ratio for each *pyr* mutant
966 after infection of RAW 264.7 macrophages at 2 h PI and 24 h PI. For each strain, the
967 \log_{10} CFUs counting after a 24 h infection of RAW 264.7 macrophages was divided by the
968 corresponding \log_{10} CFUs counting after a 2 h infection, resulting in a ratio depicting the
969 evolution of the bacterial load from 2 h PI to 24 h PI. Accordingly, an increased load will give
970 a ratio > 1 . Each strain was compared to the wild type control using a Scheffé analysis
971 (Anova 1) and significant differences are indicated by *** ($p < 0.001$) or **** ($p < 0.0001$).







A**B****C**



Appendix 4

Learning from the master: Targets and functions of the CtrA response regulator in *Brucella abortus* and other alpha-proteobacteria

Katy Poncin, Sébastien Gillet and Xavier De Bolle¹

One sentence summary: Comparative analysis of α -proteobacteria reveals how the control of CtrA and its regulon have been adapted along evolution, and particularly in the *Brucella abortus* pathogen.

Keywords: CtrA; Brucella; cell cycle; alpha-proteobacteria; infection; regulation network evolution

Abstract

The α -proteobacteria are a fascinating group of free-living, symbiotic and pathogenic organisms, including the *Brucella* genus, which is responsible for a worldwide zoonosis. One common feature of α -proteobacteria is the presence of a conserved response regulator called CtrA, first described in the model bacterium *Caulobacter crescentus*, where it controls gene expression at different stages of the cell cycle. Here, we focus on *Brucella abortus* and other intracellular α -proteobacteria in order to better assess the potential role of CtrA in the infectious context. Comparative genomic analyses of the CtrA control pathway revealed the conservation of specific modules, as well as the acquisition of new factors during evolution. The comparison of CtrA regulons also suggests that specific clades of α -proteobacteria acquired distinct functions under its control, depending on the essentiality of the transcription factor. Other CtrA-controlled functions, for instance motility and DNA repair, are proposed to be more ancestral. Altogether, these analyses provide an interesting example of the plasticity of a regulation network, subject to the constraints of inherent imperatives such as cell division and the adaptations to diversified environmental niches.

¹ **Corresponding author:** Xavier De Bolle; University of Namur, Research Unit in Biology of Microorganisms, Rue de Bruxelles 61, 5000 Namur, Belgium; Tel: +32 (0)81/72.44.38; Fax : +32 (0)81/72.42.97; e-mail : xavier.debolle@unamur.be

Introduction

Brucella species are responsible for Brucellosis, a major and worldwide zoonosis. In animals, it occurs as a chronic infection that is characterized by epididymitis in males or placentitis and abortion in pregnant females (Carvalho Neta *et al.*, 2010). Humans are accidental hosts of *B. melitensis*, *B. abortus* and *B. suis*, in which they are responsible for a debilitating disease known as undulant fever or Malta fever (Moreno & Moriyon, 2006). Usually, human infections happen through the ingestion of contaminated dairy products or by exposure to infected animals. Another major way of infection is through the aerosol route, which is why *Brucella* strains are subjected to strict regulations in laboratories (Yagupsky & Baron, 2005). There are currently no vaccines available for humans and the only treatment is the use of a combination of antibiotics (Moreno & Moriyon, 2006).

This review aims at summarizing what is known about *B. abortus* infectious process in host cells, with a particular emphasis on its cell cycle regulation. Indeed, *B. abortus* has been reported to stall its cell cycle in the G1 phase, which corresponds to a non-replicating stage, for up to eight hours at the onset of infection of HeLa cells or RAW 264.7 macrophages (Deghelt *et al.*, 2014). This review therefore focuses on the master regulator CtrA, a transcription factor particularly well conserved in α -proteobacteria and known to regulate the *Caulobacter crescentus* cell cycle (Laub *et al.*, 2002; Brill *et al.*, 2010). Up to now, the only comparative studies about the CtrA regulons of different α -proteobacteria were mainly based on bioinformatics predictions (Hallez *et al.*, 2004; Brill *et al.*, 2010). As literature on CtrA has been dramatically increasing over the last years, it is now possible to compile experimental data. We thus give an overview of the conservation of specific modules in the CtrA regulon, as well as the acquisition of new factors that occurred during evolution, while focusing more particularly on intracellular bacteria.

Brucella inside host cells

***Brucella* intracellular trafficking**

A whole genome-based phylogeny study revealed that brucellosis probably appeared in wildlife populations in the past 86,000 to 296,000 years (Foster *et al.*, 2009). It thus happened before livestock domestication, even though this crucial step in history probably played a role in allowing the worldwide spreading of these pathogens (Foster *et al.*, 2009). Even though they can be cultivated on artificial media, it is established that *Brucella* need to enter inside their host cells in order to complete a successful infection process (Moreno & Moriyon, 2006). This is why they are now considered as facultatively extracellular intracellular parasites (Moreno & Moriyon, 2002).

The mechanism by which *Brucella* manage to invade their host organism is not very clear but they seem to cross the mucosal barrier, which could imply an interaction with epithelial cells (Roop *et al.*, 2009). The role of these cells has not been deciphered yet but epithelial HeLa cells have been effectively used as models for *Brucella* infection in non-professional phagocytes (Pizarro-Cerda *et al.*,

1998; Castaneda-Roldan *et al.*, 2004; Starr *et al.*, 2008). Once inside its host, *Brucella* could also get internalized by professional phagocytes such as macrophages or dendritic cells. There, the bacterium can survive and multiply before disseminating in the organism (Archambaud *et al.*, 2010). Surprisingly, *B. melitensis* has also been reported to be able to invade murine erythrocytes during infection, which suggests that other cellular and *in vivo* models of infection should be developed to fully understand *Brucella* pathogenesis (Vitry *et al.*, 2014).

The entry of *Brucella* into epithelial or phagocytic cells occurs within minutes after cell-to-cell contact (Pizarro-Cerda *et al.*, 1998). Once internalized, the bacterium stays in a membrane-bound *Brucella*-containing vacuole (BCV) that interacts with the endocytic pathway (therefore termed eBCV) (**Figure 1**). Early endosomal markers, such as Rab5, are rapidly followed by the acquisition of late endosomal markers, typically lysosomal membrane-associated protein-1 (LAMP1) (Pizarro-Cerda *et al.*, 1998). Transient interactions with lysosomes have also been reported (Starr *et al.*, 2008). This eventually leads to eBCV acidification, which is deleterious to many bacteria, but nonetheless necessary for *Brucella* to reach their replicative niche and survive in the long-term (Porte *et al.*, 1999; Boschioli *et al.*, 2002; Celli *et al.*, 2003; Starr *et al.*, 2008). Indeed, the acidic pH of the eBCV has been linked to the capacity of the pathogen to induce the expression of the *virB* operon (Boschioli *et al.*, 2002). These genes code for a type IV secretion system (T4SS) that is essential for the bacteria to reach their proliferation niche (Boschioli *et al.*, 2002).

The *Brucella* replicative niche (rBCV) has been known for years to derive from the endoplasmic reticulum (ER), in both HeLa cells and macrophages (Pizarro-Cerda *et al.*, 1998; Celli *et al.*, 2003). It is only recently that the rBCV was shown to actually be part of the endoplasmic reticulum (Sedzicki *et al.*, 2018) (**Figure 1**). The transition from eBCV to rBCV is not clearly understood yet, but it has been suggested that its maturation could occur at the ER exit sites (Celli *et al.*, 2005; Celli, 2015). Several ER-associated functions have been linked to *Brucella* infection, such as the unfolded protein response IRE1 \square signaling pathway (Qin *et al.*, 2008; Smith *et al.*, 2013; Taguchi *et al.*, 2015), some autophagy-associated factors such as ATG9 and WIPI (Taguchi *et al.*, 2015) and the early secretory trafficking depending on the Sar1/coat protein complex II (Celli *et al.*, 2005; Taguchi *et al.*, 2015). Since the T4SS is essential for *Brucella* to reach the rBCV, it is expected that the maturation of the BCV would be mediated by the delivery of bacterial effectors inside the host cell. One such effector is BspB, shown to target the Golgi apparatus by interacting with the oligomeric Golgi tethering complex (Miller *et al.*, 2017). This leads to the redirecting of Golgi-derived vesicles to the BCV by remodeling the ER-Golgi secretory trafficking (Miller *et al.*, 2017). It is important to note that there exist alternatives to the ER-derived replicative niche since opsonized *B. abortus* proliferate in a non-acidic LAMP1-positive compartment in the human monocytic cell line THP-1 (Bellaire *et al.*, 2005) and in endosomal inclusions in extravillous trophoblasts (Salcedo *et al.*, 2013).

Once the number of bacteria within a cell reaches a critical level, destruction of the host cell can be observed (Moreno & Moriyon, 2006). Another means for *Brucella* to spread from one cell to its neighbors has been shown by Starr *et al.* (2012). The formation of a compartment with autophagic features (aBCV) could be the key to this important step of the infection (**Figure 1**). Indeed, autophagy-deficient *Brucella* are not able to perform cell-to-cell spreading when cellular infections are prolonged for long periods, typically 72 h (Starr *et al.*, 2012). Interestingly, only the initiation complex of autophagy seems to be needed by *Brucella* to promote reinfection (Starr *et al.*, 2012). Indeed, markers of the elongation phase of autophagy such as ATG5 and LC3 were not found to be associated to the aBCV (Starr *et al.*, 2012). It should be noted that autophagy is particularly important at birth. At that time, the transplacental nutrient supply is no longer available, which suggests that autophagy is

strongly activated in the neonate in order to adapt to the early neonatal starvation period (Kuma *et al.*, 2004). The use of this process by the bacteria could therefore be relevant for their spreading inside newborn calves.

Growth and replication of *Brucella*

B. abortus possesses two distinct chromosomes (Chain *et al.*, 2005). Surprisingly, bacteria with multipartite genomes are not uncommon, at about 10% of the sequenced species (Val *et al.*, 2014). Contrarily to plasmids that are known to initiate replication several times during the bacterial cell cycle, chromids (also known as megaplasmids) code for essential genes and initiate their replication only once per cell cycle, like chromosomes (Pinto *et al.*, 2012; Val *et al.*, 2014). In *B. abortus*, the large and circular chromosome (I) is 2.1 Mb long and possesses a ParAB segregation system with three centromere-like *parS* sites, while the small chromosome (II) of 1.2 Mb is a chromid, with its replication being controlled by a RepABC system (see Pinto *et al.*, 2012 for a review on this segregation system). The *repABC* operon also contains two centromere-like sequences called *repS* (Livny *et al.*, 2007; Deghelt *et al.*, 2014). The chromosomal replication status of *B. abortus*, and thus the stage of its cell cycle, can be followed with fluorescent reporters of the segregation markers ParB and RepB, as well as with fluorescent reporters allowing the localization of the replication origins (*ori*) and terminators (*ter*). Both chromosomes are oriented along the cell length, with *oriI* and *terI* associated with the poles, whereas *oriII* and *terII* are usually found closer to the midcell (Deghelt *et al.*, 2014). This is in agreement with what has been found in *Sinorhizobium meliloti*, another α -proteobacterium. Indeed, this bacterium possesses a tripartite genome with one primary chromosome (3.65 Mb) and two chromids (1.35 Mb for pSymA and 1.68 Mb for pSymB) (Galibert *et al.*, 2001). Both chromids are segregated by a RepABC system and their *ori* are not anchored to the poles (Kahng & Shapiro, 2003; Frage *et al.*, 2016). *S. meliloti* is capable of colonizing the soil rhizosphere as a free-living bacterium, but also of invading the roots of leguminous plants as an intracellular symbiotic nitrogen-fixing bacterium, involving complex interactions between the bacterium and its host (Gibson *et al.*, 2006). Similarly to *C. crescentus* and *B. abortus*, free-living *S. meliloti* regulate their cell cycle so that replication of their genome occurs once-and-only-once per cell division (Mergaert *et al.*, 2006). In both *B. abortus* and *S. meliloti*, a temporal coordination of replication and segregation was found, as the initiation of replication of their chromids is always delayed compared to the main chromosome (Deghelt *et al.*, 2014; Frage *et al.*, 2016). In *Brucella*, the replication of *oriI* starts before *oriII* and both chromosomes would finish their replication at approximately the same time (Deghelt *et al.*, 2014). Note that the size of the chromids do not seem to be the determining factor for the temporal regulation of their replication initiation. Indeed, in *S. meliloti*, it has been proposed that the smaller pSymA initiates its replication when the *ori* of the main chromosome has reached the new pole and that it is followed by the bigger pSymB, which behaves in a similar manner after the pSymA *ori* has been replicated (Frage *et al.*, 2016).

Two main phases can be observed during HeLa cells infection by *B. abortus*. Indeed, when the bacterium is transiting within the eBCV, it is unable to proliferate, which reflects the fact that the number of colony forming unit (CFU) is stable during this non-proliferative stage (Comerci *et al.*, 2001; Starr *et al.*, 2008; Deghelt *et al.*, 2014). The second phase occurs when *Brucella* reaches its ER-derived proliferative niche, with the number of CFU increasing drastically (Pizarro-Cerda *et al.*, 1998; Celli *et al.*, 2003; Starr *et al.*, 2008). Thanks to fluorescent reporter systems that can track *ori*, it has been possible to follow the *B. abortus* cell cycle inside host cells. One interesting observation was that during the non-proliferative stage of the trafficking in HeLa cells and RAW 264.7 macrophages, the bacteria are blocked in G1 (only one focus of *oriI*), similarly to what happens in the carbon-starved

swarmer cells of *C. crescentus*, a free living α -proteobacterium (Lesley & Shapiro, 2008; Deghelt *et al.*, 2014). As *Brucella* exhibits asymmetric growth like other Rhizobiales (Brown *et al.*, 2012), it is also possible to use Texas Red Succinimidyl Ester – a fluorescent compound that covalently binds amine groups on the bacterial surface – as a mean to follow the bacterium unipolar growth (Brown *et al.*, 2012) inside host cells (Deghelt *et al.*, 2014). These techniques brought to light the fact that the bacteria found within the eBCV at early times after infection are predominantly non-growing newborn cell types. This term refers to bacteria that recently divided but did not yet initiate chromosome replication (Deghelt *et al.*, 2014). They stay in this state for up to eight hours before resuming their growth and chromosome replication when they still reside within an eBCV (Deghelt *et al.*, 2014).

Roles and regulation of CtrA

B. abortus* CtrA regulation is similar to that of *C. crescentus

Since the invasive *B. abortus* are mainly in the G1 phase of their cell cycle (Deghelt *et al.*, 2014), it is possible that transcription factors involved in cell cycle regulation could be also important for *Brucella* virulence. One such factor is CtrA. This transcription factor is very well conserved amongst α -proteobacteria (Brilli *et al.*, 2010) and has been best studied in the model organism *C. crescentus*. This remarkable bacterium possesses two distinct life forms. One is a sessile stalked form, which allows the bacterium to adhere to surfaces when it is in a nutrient-rich environment. The other form is a motile swarmer cell that is used for scouting and colonizing new favourable environments but that is not competent for replication (Ausmees & Jacobs-Wagner, 2003; Quardokus & Brun, 2003). Importantly, *C. crescentus* divides asymmetrically into its two phenotypically different daughter cells after each cell division. This is why this bacterium is considered as an excellent model for bacterial cell cycle studies. In this context, the transcription factor CtrA has been found to be of utmost importance as it is a master regulator of *C. crescentus* cell cycle (Quon *et al.*, 1996) (**Figure 2**). Indeed, one of CtrA many targets is the *ori*, thus preventing the DnaA protein from initiating the replication of *C. crescentus* chromosome as long as CtrA is present (Quon *et al.*, 1998; Siam & Marczyński, 2000). As CtrA needs to be phosphorylated to be active, a tight regulatory network based on two-component regulators is in charge of its synthesis, phosphorylation and degradation (Quon *et al.*, 1996; Domian *et al.*, 1997; Wu *et al.*, 1998; Biondi *et al.*, 2006; Tsokos *et al.*, 2011).

In *C. crescentus*, the dual CckA enzyme that possesses both kinase and phosphatase activities regulates the phosphorylation level of CtrA and CpdR, a response regulator stimulating CtrA proteolysis when dephosphorylated (Jenal & Fuchs, 1998; Jacobs *et al.*, 2003; Biondi *et al.*, 2006). CckA does so by interacting with the phosphotransferase ChpT (Biondi *et al.*, 2006). The kinase activity of CckA is inhibited by the phosphorylated form of the response regulator DivK, which is stabilized by the atypical histidine kinase DivL (Tsokos *et al.*, 2011; Childers *et al.*, 2014). DivK phosphorylation is itself regulated by the histidine kinase DivJ and by the phosphatase PleC (Wu *et al.*, 1998; Wheeler & Shapiro, 1999). PleC is also able to phosphorylate the diguanylate cyclase PleD, which in turn will synthesize cyclic di-GMP (Paul *et al.*, 2008). The binding of this secondary messenger to CckA will force CckA to switch from its kinase to its phosphatase mode, thus preventing

the phosphorylation of CtrA (Lori *et al.*, 2015). Cyclic di-GMP also binds to PopA, which interacts with RcdA, another protein involved in CtrA proteolysis at the stalked cell pole (Ozaki *et al.*, 2014; Smith *et al.*, 2014). Interestingly, several genes coding for proteins regulating CtrA are also part of its regulon, including *divK* (Laub *et al.*, 2000) and *divJ* (Fumeaux *et al.*, 2014) in *C. crescentus*.

At the transcription level, *ctrA* is regulated by two proteins in *C. crescentus*. One of them is CtrA itself (Domian *et al.*, 1999). The other one is GcrA, an unconventional transcription factor that binds to the housekeeping σ^{70} factor (Haakonsen *et al.*, 2015). Since *gcrA* transcription is repressed by CtrA and *ctrA* transcription is activated by GcrA, the two transcription factors are present temporally and spatially out-of-phase during the cell cycle of *C. crescentus* (Holtzendorff *et al.*, 2004). Of note, DnaA also participates to *gcrA* transcription (Collier, 2012).

The spatio-temporal regulation of CtrA is particularly well adapted to *C. crescentus* aquatic free-living lifestyle, but it appears to be surprisingly conserved in other α -proteobacteria with very different ways of life (Brilli *et al.*, 2010; Pini *et al.*, 2015; Schallies *et al.*, 2015; Willett *et al.*, 2015). In *B. abortus*, the core actors involved in the CtrA regulatory network, defined here as the PleC/DivJ/DivK and CckA/ChpT/CtrA two-component systems, are conserved (Hallez *et al.*, 2004; Brilli *et al.*, 2010)(**Figure 2**). Another gene, called *pdhS* for PleC/DivJ homologue sensor, has also been found to be part of this network (Hallez *et al.*, 2004). Both *pleC* and *divK* from *B. abortus* are able to heterocomplement the corresponding deletion mutants in *C. crescentus*, which suggests that their function is conserved between both organisms (Hallez *et al.*, 2007). In addition, in *B. abortus* DivK has been found by yeast two-hybrid experiment to bind to DivJ, PleC, DivL and PdhS (Hallez *et al.*, 2007). Nevertheless, the localization of PleC is different between *B. abortus* and *C. crescentus* and DivJ was not found to be crucially involved in DivK phosphorylation (Hallez *et al.*, 2007). Indeed, in a $\Delta divJ$ background, DivK did not lose its phosphorylation-dependent polar localization (Hallez *et al.*, 2007), while a loss-of-function of *pdhS* generates delocalization of DivK-YFP (Van der Henst *et al.*, 2012). As *pdhS* is an essential gene and depletion strains were not available at that time, its involvement in DivK phosphorylation could only be suggested through indirect experiments. PdhS was also shown to accumulate at the old pole of the large cells, which is the same localization as the phosphorylated form of DivK (Hallez *et al.*, 2007). Of note, this localization is similar to the one of DivJ in *C. crescentus*, which suggests a common function between *B. abortus* PdhS and *C. crescentus* DivJ (Hallez *et al.*, 2007). As PdhS is cytoplasmic in *B. abortus*, it is possible that its function is shared with DivJ depending on the time and/or space of DivK phosphorylation (Hallez *et al.*, 2007). The polar localization of PdhS is conserved at 48 hours post infection in bovine macrophages (Hallez *et al.*, 2007), but nothing is known about the role of DivJ in this context and at later times of the infection. As for the phosphorelay going from CckA to CtrA and CpdR via ChpT, it has been confirmed to be functional in *B. abortus* (Willett *et al.*, 2015). As was the case for *C. crescentus* (Laub *et al.*, 2000; Fumeaux *et al.*, 2014), several genes predicted to be involved in CtrA regulation have been found by CHIP-seq to be potentially part of CtrA regulon in *B. abortus*, including *ctrA* itself, *divK*, *divJ*, *divL*, *chpT*, *cpdR* and *rcdA* (Francis *et al.*, 2017). If all of these genes are indeed regulated by *B. abortus* CtrA, it would mean that the control of this transcription factor is more complex in this bacterium than in *C. crescentus* (**Figure 2**). One tempting hypothesis is that the regulation of *B. abortus* CtrA could reflect a need for the bacterium to precisely regulate its cell cycle depending on its intracellular environment.

***B. abortus* CtrA controls the expression of genes involved in envelope biogenesis**

The impact of *B. abortus* CtrA levels inside host cells could potentially be very important, as this transcription factor seems to be involved in both cell cycle regulation and bacterial envelope composition (Francis *et al.*, 2017). Actually, one striking feature of *B. abortus* CtrA regulon is the high number of genes involved in envelope biogenesis (Francis *et al.*, 2017). Indeed, in addition to revealing the direct interaction between CtrA and the promoters of genes involved in the regulation of LPS and peptidoglycan synthesis, a ChIP-seq experiment also showed that promoters of genes coding for abundant outer membrane proteins (OMP) are also bound by CtrA (Francis *et al.*, 2017). CtrA-dependent regulation of these genes was supported by western blots against Omp2b and Omp25, two major OMPs of *B. abortus* that were found at lower levels in a CtrA depletion strain (Francis *et al.*, 2017). In addition, Omp25 homogenous localization patterns are perturbed when CtrA is absent (Francis *et al.*, 2017). This modification of the envelope composition could potentially have an impact on the bacterial fitness inside its host cell (Cha *et al.*, 2012). Indeed, the levels of Omp2b have been shown to decrease after 20 to 40 hours during the course of macrophage infection by *B. abortus* (Lamontagne *et al.*, 2009). As for *omp25*, its disruption in *B. abortus* led to an increased sensitivity to Polymyxin B *in vitro* (Manterola *et al.*, 2007). In HeLa cells and murine macrophages, this strain was not shown to be involved in virulence, as its intracellular replication was similar to that of the WT (Manterola *et al.*, 2007). In BALB/C mice, however, results were different in two independent experiments. In the first, a *B. abortus omp25* mutant was injected intravenously at 5×10^4 CFU and led to an attenuation of virulence at 18 weeks post infection, when compared to the wild type strain (Edmonds *et al.*, 2002). In the second experiment, mice were infected via the intraperitoneal route with 10^5 CFU and behaved like the wild-type strain even after 24 weeks (Manterola *et al.*, 2007). This suggests that the route of infection could be an important factor to take into account when studying *B. abortus* infection. In this respect, it would be more appropriate to use a more physiological mode of infection in future research, such as the intranasal one (Hanot Mambres *et al.*, 2016). Note that the *omp25* mutant seems to have different phenotypes depending on the *Brucella* species in which it is studied. Indeed, in *B. suis*, the disruption of this gene had much more dramatic consequences, as it was already attenuated from 1 to 8 weeks post infection, before to be completely cleared from mice spleen (Edmonds *et al.*, 2002). The authors suggested that this might be due to the fact that the *B. suis* strain that they used is a naturally occurring rough strain, thus the loss of the structural Omp25 could be more damaging in this case (Edmonds *et al.*, 2002). Another difference between the two *Brucella* strains is that in *B. suis*, Omp25 is involved in the inhibition of the production of the pro-inflammatory TNF- α cytokine in human macrophages (Jubier-Maurin *et al.*, 2001; Luo *et al.*, 2017), whereas in *B. abortus*, it could be involved in the activation of the synthesis of TNF- α in human trophoblastic cells (Zhang *et al.*, 2017).

The regulation of genes involved in the structure of the bacterial envelope by CtrA is probably not exclusive to *B. abortus* as many other α -proteobacteria do seem to regulate such genes via CtrA (Laub *et al.*, 2000; Brilli *et al.*, 2010). Nevertheless, it could have a more important impact on intracellular bacteria, as their envelope will be presented at the interface with their host cell and could therefore impact the host immune response and the survival of the bacteria inside them. For instance, the obligate intracellular *Ehrlichia chaffeensis* is thought to regulate the expression of its *pal* gene, coding

for a major outer membrane stabilizing protein, through CtrA (Cheng *et al.*, 2011). This α -proteobacterium is the causative agent of the life-threatening human monocytic ehrlichiosis and has a developmental cycle comprising two forms in mammalian cells (Zhang *et al.*, 2007). The small dense-cored cells (with dense nucleoids) attach to and enter into the host cells, then differentiate into larger reticulate cells (defined by uniformly dispersed nucleoids) that can multiply for 48 h before transforming back into dense-cored cells at 72 h post infection in order to prepare for reinfection (Zhang *et al.*, 2007). Interestingly, both *pal* and *ctrA* gene expression were found to be highest when bacteria were in their dense-cored infectious form (Cheng *et al.*, 2011). Conversely, CtrA was found to be rapidly degraded, following a proline and glutamine uptake, after bacterial entry in host cells (Cheng *et al.*, 2014). Pal is known to be immunogenic in dogs infected with *E. chaffeensis* and bacteria treated with anti-Pal antibodies were shown to be less infectious *in vitro* (Cheng *et al.*, 2011). Note that *E. chaffeensis* has been reported to lack lipopolysaccharide (Lin & Rikihisa, 2003).

S. meliloti also interacts tightly with host cells during nodulation. Very interestingly, it appears that *B. abortus* and *S. meliloti* do share some similarities in their potential CtrA targets. Indeed, CtrA binds to the promoter of several genes coding for L,D-transpeptidases homologs in *B. abortus* (BAB1_0047, BAB1_0138, BAB1_0589, BAB1_0978, BAB1_1159 and BAB1_1867) and *S. meliloti* (SMc00150, SMc01200, SMc01575 and SMc01769). L,D-transpeptidases are required to cross-link peptides in the peptidoglycan, and appear to be localized at the specific growth sites in the Rhizobiale *Agrobacterium tumefaciens* (Cameron *et al.*, 2014), another Rhizobiale displaying a unipolar growth (Brown *et al.*, 2012). Still, *B. abortus* seems to have evolved to possess more complex regulation of envelope biogenesis than *S. meliloti*: All but one (BAB1_0785) L,D-transpeptidase gene promoters are bound by CtrA in *B. abortus* (Francis *et al.*, 2017), as opposed to four out of seven in the case of *S. meliloti* (the others being SMc02636, SMc02582 and SMc00039) (Pini *et al.*, 2015). These L,D-transpeptidases should be further investigated in order to understand how they are truly regulated, as well as their specific roles in peptidoglycan growth and homeostasis. To determine if the envelope biogenesis regulation can directly be linked to the lifestyle of the bacteria would of course require more experimental data from other intracellular bacteria.

The expression of *ctrA* is not crucial for *B. abortus* trafficking to the rBCV

The regulation of genes according to the stage of *B. abortus* cell cycle can be observed through the use of a fluorescent-based reporter system. Such genes are *ccrM* and the *repABC* operon, and both are probably regulated by CtrA as the activities of their promoters were abolished when their respective CtrA-binding boxes were mutated (Francis *et al.*, 2017). As the activity of the promoter of the *repABC* operon seems to be inverted compared to the one of *ctrA*, it is expected that CtrA acts as a negative regulator of chromosome II replication (Francis *et al.*, 2017). Knowing that *B. abortus* first has to go through a non-replicative phase inside the eBCV, one can expect that CtrA would be important during this specific stage of the infection. However, CtrA was not found to be essential for the ability of *B. abortus* to infect cells in the models of infection tested thus far. Indeed, a study performed with a thermo-sensitive allele of *B. abortus ctrA* concluded that the transcription factor is not required for the entry of the bacterium inside THP-1 macrophages (Willett *et al.*, 2015). Inside HeLa cells, the CtrA depletion phenotypes of *B. abortus* were also visible around or after 10 h post infection (Francis *et al.*, 2017). Furthermore, a *B. abortus* CtrA depletion strain was able to reach its rBCV replicative niche in

the same proportion as the wild type strain (Francis *et al.*, 2017). This supports the view that CtrA function is dispensable for *B. abortus* trafficking inside these host cells.

Nevertheless, at 48 h post infection, CtrA depletion strains underwent a clear drop of CFU in both cellular infection models (Willett *et al.*, 2015; Francis *et al.*, 2017). The defects leading to bacterial cell death are unclear but could be explored by the analysis of suppressor mutants. The fact that CtrA might only be necessary at late time points during *Brucella* infection does make sense, though, as its level needs to be regulated more particularly during late phases of other intracellular α -proteobacteria life cycle. For example, in the obligate intracellular pathogen *E. chaffeensis*, CtrA is important during the late stage of intracellular growth (Cheng *et al.*, 2011). It has been observed that the *ctrA* gene is up-regulated at 72 h post infection, which corresponds to the time when the bacteria differentiate back from large reticulate cells to small infectious dense-cored cells in order to prepare to spread from the present to the next host cells (Zhang *et al.*, 2007; Cheng *et al.*, 2011). Similarly, in *S. meliloti*, CtrA levels are high before infection, then a decrease of *ctrA* transcription coincides with bacteroid differentiation within the nodule (Roux *et al.*, 2014) and the CtrA protein is absent in mature bacteroids (Pini *et al.*, 2013).

It is possible that CtrA is only required when *Brucella* find themselves in a particular situation. For instance, *C. crescentus* is known to regulate CtrA levels in response to stresses affecting its envelope, and this in a CckA-dependent manner, but independently of DivK and cyclic-di-GMP (Heinrich *et al.*, 2016). In *E. chaffeensis*, *surE* has been proposed to code for a protein involved in bacterial growth under stress and it is thought to be part of CtrA regulon (Cheng *et al.*, 2011). It is therefore possible that the *in vitro* models of infection tested thus far for *B. abortus* CtrA function do not reflect the environment and the stresses that they would have to face inside a living animal. In this respect, an *in vivo* model of infection might prove to be much more relevant for deciphering the potential impact of CtrA depletion in *B. abortus*.

Hypotheses emerging from analyses of CtrA regulons

Regulation of the cell cycle in different α -proteobacteria

As several groups are now focusing on CtrA functions in other α -proteobacteria, more data about this transcription factor have become available over the last years. Despite their very diverse ways of life, α -proteobacteria do share some common traits, including the presence of a gene coding for CtrA (Brilli *et al.*, 2010). The comparison of the CtrA regulons in different bacteria, in light of their respective evolutionary lineage and lifestyle, might lead to interesting hypotheses regarding CtrA functions in *B. abortus* and other intracellular bacteria. Indeed, comparison of the direct CtrA regulons, when they are available, clearly indicate that CtrA binds to promoters of orthologous genes, suggesting that the control of these promoters by CtrA is a conserved feature. With that in mind, we compiled the experimental data that were available for this transcription factor in different α -proteobacteria. Data were collected in a hierarchical manner: (i) direct binding of CtrA to its target promoter, typically by ChIP-seq data, was considered first, (ii) when no such data were available,

mRNA-level studies (for example microarrays) were used, (iii) bioinformatics predictions were taken into account only if no experimental data were found. For the determination of the predicted targets, we used RSAT (van Helden, 2003). All data were compiled in **Figure 3**. It is important to keep in mind that the approaches based on protein binding, mRNA levels or bioinformatics only are not a direct proof of gene regulation and that they should be considered with reserve. This section is thus more prospective since meta-analyses usually generate working hypotheses that, if they lead to correlation, could indicate that similar processes are at play. Importantly, the absence of correlation does not necessarily mean the opposite. Hypotheses proposed here might therefore be challenged in the future.

In **Figure 3**, it appears at first sight that the bacteria reported in this table belong to three distinct categories. The first one comprises *A. tumefaciens*, *S. meliloti*, *B. abortus* and *C. crescentus*, *i.e.* Rhizobiales and Caulobacterales. These bacteria have the common characteristic that the gene coding for CtrA is essential (Barnett *et al.*, 2001; Christen *et al.*, 2011; Figueroa-Cuilan *et al.*, 2016; Francis *et al.*, 2017). Moreover, at the exception of *A. tumefaciens*, their cell cycle has been shown to be regulated by CtrA (Quon *et al.*, 1998; Reisenauer *et al.*, 1999; Laub *et al.*, 2002; Pinto *et al.*, 2012; Pini *et al.*, 2015; Francis *et al.*, 2017). Therefore, it is not surprising to see that CtrA binds promoters for many genes involved in chromosome replication and segregation, as well as cell division. It is interesting to note that these processes are achieved through different genes in different bacteria and that it reflects their evolutionary lineage. Indeed, both *A. tumefaciens* and *S. meliloti*, which are closely related, seem to directly regulate their main chromosomal origin partitioning genes (*parAB*) through CtrA, while *B. abortus* is proposed to regulate its chromosome I replication through *dnaA*. As for *C. crescentus*, CtrA is directly binding to the *ori* as discussed earlier. It also seems that when a bacterium in this clade possesses a secondary chromosome, CtrA regulates its partition via the *repABC* operon (Pinto *et al.*, 2012; Pini *et al.*, 2015; Francis *et al.*, 2017). One feature that is shared between Rhizobiales and *C. crescentus* is the predicted regulation of *ftsK* and *ftsQ* by CtrA, FtsK being involved in the segregation of the *ter* (Stouf *et al.*, 2013) and FtsQ in the Z ring formation and constriction (Carson *et al.*, 1991). The Z ring is composed of the tubulin-like FtsZ proteins, triggering the invagination of the cytoplasmic membrane, thus leading to septation and cytokinesis of the bacterium (Lutkenhaus & Addinall, 1997). Interestingly, the *ftsZ* gene seems to be a target of CtrA in the first group of bacteria in **Figure 3**. Note that in the case of *A. tumefaciens*, two copies of *ftsZ* exist and it is only the promoter region of the second one (Atu2086) that is predicted to possess an 8-mer CtrA binding site. There are also two *ftsZ* genes encoded in *S. meliloti* genome, and in this case, only the promoter of *ftsZ1* is predicted to have a *S. meliloti*-specific CtrA-binding box with a AACCAT motif (Ichida & Long, 2016), with one substitution (AGCCAT). However, neither of the two *ftsZ* promoters was found to be bound by ChIP-seq, so it was concluded that *S. meliloti* regulates its cell division through the control of *minC* and *minD* expression (Pini *et al.*, 2015). Indeed, MinC and MinD participate to the proper localization of the Z ring in *Escherichia coli* (de Boer *et al.*, 1989) and many other bacteria. Interestingly, CtrA seems to systematically bind the promoter the *minCDE* operon in Rhizobiales. Note that this operon is absent in *C. crescentus*, where it is replaced by *mipZ* (Thanbichler & Shapiro, 2006). Altogether, these analyses indicate that a number of crucial targets involved in different stages of the cell cycle were placed under the control of CtrA in the ancestors of Rhizobiales.

In *C. crescentus*, some genes that are regulated by CtrA need to be expressed at very specific times. The most recent model to explain how CtrA-dependent genes are regulated in a timely manner is based on two other transcription factors, SciP and MucR (Fumeaux *et al.*, 2014). Genes that need to be expressed only in G2 phase cells, such as the DNA methyltransferase *ccrM*, are repressed by SciP in G1 phase cells even when CtrA is present (Gora *et al.*, 2010). On the other hand, genes that need to be expressed only in G1 phase cells are repressed by MucR in predivisional bacteria (Fumeaux *et al.*, 2014). From **Figure 3** it is clear that *mucR* is not predicted to be regulated by CtrA, in contrast to *sciP*, which is potentially regulated in *S. meliloti*, *B. abortus* and *C. crescentus*. The absence of a conserved CtrA-binding box in *A. tumefaciens* is surprising but does not mean that the gene is not regulated by CtrA in this bacterium.

Another important player in *C. crescentus* gene expression regulation is the methyltransferase CcrM. As discussed above, *ccrM* temporal regulation by CtrA is important since it must only be present in late predivisional cells, where it methylates the newly synthesized DNA strands on GANTC sites precisely before cell division occurs (Stephens *et al.*, 1996; Reisenauer *et al.*, 1999). This means that, according to their chromosomal position away from the origin of replication, genes stay hemi-methylated for a different amount of time during the cell cycle (Marczynski, 1999). This could have an important impact on gene expression at the whole genome level (Kozdon *et al.*, 2013). In fact, the transcription of several genes of *C. crescentus* has been observed to change in response to the methylation state of their promoters (Collier & Shapiro, 2007; Gonzalez & Collier, 2013). Remarkably, the promoter of *ctrA* is one of those (Reisenauer & Shapiro, 2002). This is also supported by the fact that *ccrM* overexpression leads to abnormal chromosome content (Zweiger *et al.*, 1994). In the first group, *ccrM* appears to be uniquely regulated by CtrA. This suggests that DNA methylation could be important for cell-cycle regulation in these bacteria. Of note, the function of GcrA has been demonstrated to be sensitive to CcrM DNA methylation in *C. crescentus* (Fioravanti *et al.*, 2012). As mentioned earlier, GcrA controls *ctrA* expression in this bacterium and *vice versa* (Holtzendorff *et al.*, 2004; Haakonsen *et al.*, 2015). The regulation of *gcrA* by CtrA in *C. crescentus* was predicted by Brill *et al.* (2010) to be an exception in α -proteobacteria. Experimental data obtained since then seem to be in agreement with this prediction, as *gcrA* has not yet been found to be part of the direct CtrA regulon in *B. abortus* (Francis *et al.*, 2017), *S. meliloti* (Pini *et al.*, 2015) or *A. tumefaciens* (**Figure 3**).

The second group of bacteria in **Figure 3** ranges from *Sphingomonas melonis* to *Magnetospirillum magneticum*. In this group, CtrA is not essential and the cell cycle progression does not seem to be coupled to this transcription factor (Greene *et al.*, 2012). Nevertheless, it is notable that some bacteria in this category could be at an evolutionary crossroads between the first and third group, as *S. melonis* (Francez-Charlot *et al.*, 2015) and *Rhodospirillum centenum* are both predicted to regulate the cell cycle transcription factor SciP. Of note, CtrA levels are regulated by quorum sensing in *Dinoroseobacter shibae* (Wang *et al.*, 2014), *Rhodobacter capsulatus* (Mercer *et al.*, 2010) and *Ruegeria* (Zan *et al.*, 2013). Despite not being involved in the cell cycle regulation of these bacteria, the role of CtrA as a regulator of bacterial development, like in *C. crescentus*, seems to be conserved in this class. Indeed, cells of *ctrA* deletion strains are elongated (Wang *et al.*, 2014; Francez-Charlot *et al.*, 2015), which is reminiscent to the observation made with α -proteobacteria depletion strains when *ctrA* is essential (Reisenauer & Shapiro, 2002; Figueroa-Cuilan *et al.*, 2016; Francis *et al.*, 2017).

One can wonder how the cell cycle is regulated in α -proteobacteria that do not rely on CtrA for this function. Interestingly, bacteria from other clades developed similar strategies than *C. crescentus* to avoid replication over-initiation (Wolanski *et al.*, 2014). For example, the Gram-positive species *Streptomyces coelicolor* relies on AdpA to directly bind to its *ori* and inhibit binding of the replication machinery (Wolanski *et al.*, 2012), whereas the γ -proteobacterium-*Escherichia coli* uses SeqA for a similar purpose (Nievera *et al.*, 2006). It is thus possible that α -proteobacteria inherited a similar mechanism from a more distantly related ancestor. When the regulation of DNA replication was put under the control of CtrA (in bacteria of the first group in **Figure 3** for example), this ancestral system could have progressively become obsolete, whereas it kept its role in the other α -proteobacteria. Importantly, essential vital functions may be regulated by redundant mechanisms to ensure their precise control. In the case of chromosome replication, redundant mechanisms are indeed often at play, such as proteolytic degradation of DnaA, its titration, the modulation of its activity by other proteins or a tight control of the expression of the *dnaA* gene (Wolanski *et al.*, 2014). Only future studies will be able to reveal the real actors of cell cycle regulation in the second group of α -proteobacteria but GcrA could be a good candidate for this function. Indeed, in *C. crescentus*, the transcription factor GcrA is known to participate in cell cycle regulation by regulating CtrA expression but also, amongst others, by inhibiting the expression of *dnaA* when it is not necessary (Holtzendorff *et al.*, 2004). As a gene coding for GcrA is predicted to be present in all the α -proteobacteria of the second group, it is possible that GcrA still retains this particular function in these bacteria. Note that *M. magneticum* does not seem to possess a *gcrA* gene, but this particular bacterium is apparently an exception, as all other Rhodospirillales studied thus far do possess one (Brilli *et al.*, 2010). A gene predicted to code for CcrM was also found in the genome of all the bacteria of the second group (Brilli *et al.*, 2010). If the ability of GcrA to differentiate genes during the cell cycle according to their CcrM-dependent methylation status is conserved in these bacteria, the two proteins might be sufficient to adequately control expression of cell cycle-related genes.

The third group of bacteria in **Figure 3** is composed of the Rickettsiales *E. chaffeensis*, *Wolbachia wMel*, the endosymbiont of *Drosophila melanogaster*, and *Rickettsia prowazekii*. Not much is known about CtrA regulon and essentiality in these bacteria. However, the prediction that genes involved in cell division and chromosome replication are regulated by CtrA in these organisms is in agreement with the fact that the *ori* of *R. prowazekii* is bound by CtrA (Brassinga *et al.*, 2002) and that the promoter of the *E. chaffeensis pal* gene has been found as a target of the transcription factor (Cheng *et al.*, 2011). Moreover, eight strains of *Wolbachia*, in addition to other Rickettsiales, were found to possess DnaA binding sites and up to five CtrA consensus binding sites per *ori* (Ioannidis *et al.*, 2007). It is thus possible that *ctrA* regulates the cell cycle and is essential in this group of bacteria (**Figure 4**). If this is confirmed in the future, it could mean that CtrA gained the function of regulating the cell cycle twice during evolution: once before the emergence of Rickettsiales and once before the appearance of Caulobacterales and Rhizobiales (**Figure 4**). An alternative hypothesis would be that the regulation of the cell cycle was an ancestral function of CtrA that was lost early, but that seems less likely as it would imply the re-acquisition of this function in *C. crescentus* and Rhizobiales. Note that the third group in **Figure 3** is quite different from the first group, as they do not possess genes coding for the other cell cycle transcription factors such as SciP, MucR or GcrA. Nonetheless, they were found to possess a CckA/CtrA two-component system (Christensen & Serbus, 2015). Furthermore, all *Wolbachia* CckA proteins were found to share a common conserved PAS domain, which could suggest that this protein has a “sensor” capacity with a possibly conserved signal (Christensen & Serbus, 2015). This potentially intrinsic ability of CckA to detect environmental

signals has also been suggested to explain how *C. crescentus* is able to regulate CckA independently of the PleC/DivJ/DivK two-component system under stress (Heinrich *et al.*, 2016).

In light of what can be observed in these three groups of bacteria, a hypothesis can be proposed about why *B. abortus* CtrA was not found to be important for infecting cells (Willett *et al.*, 2015; Francis *et al.*, 2017). It is possible that *B. abortus* does not rely solely on CtrA to regulate its cell cycle. Maybe another transcription factor, such as GcrA, directs this important function during the first phase of the infection, when *B. abortus* are in their non-replicative stage. Since the function of *B. abortus* CtrA during later times post infection was not investigated, it would be interesting to test whether this transcription factor is required for reinfection, as in *E. chaffeensis* (Cheng *et al.*, 2011). It is also possible that CtrA is only necessary during infection, when CckA responds to specific environmental stressors, similar to its role in *C. crescentus* (Heinrich *et al.*, 2016). These hypotheses are of course speculative and will need to be tested in the future.

Could DNA repair regulation be an ancestral function of CtrA?

Elucidation of the targets of *M. magneticum* CtrA suggests that motility is an ancestral trait of α -proteobacteria (Greene *et al.*, 2012). The authors of that study also proposed that the transition to the intracellular lifestyle of *E. chaffeensis* and *R. prowazekii* led to the loss of flagellar and chemotaxis genes and thus the loss of this regulation function (Greene *et al.*, 2012). Alternatively, the regulation of motility could have occurred on an evolutionary branch that is further away from the Rickettsiales (**Figure 4**). *Brucella* is also a non-motile and non-flagellated intracellular bacterium but it retains flagellar genes that appear to be important during infection (Halling, 1998). Indeed, flagellin was shown to modulate the host response and bacterial proliferation in a mouse model of infection (Terwagne *et al.*, 2013). This is an interesting example of alteration of a given protein during evolution, from its initial function as a flagellin into a host protective factor (Shames & Finlay, 2010; Terwagne *et al.*, 2013). The flagella of *Bartonella bacilliformis*, a close phylogenetic relative of *Brucella*, were also found to be required for entry into host erythrocytes (Scherer *et al.*, 1993), illustrating that the function of these organelles diverged quickly during the course of evolution.

In a transcriptomic study focusing on the *M. magneticum* CtrA regulon, the promoters of genes coding for proteins involved in motility were not predicted to be enriched amongst CtrA targets, even though the regulation of such genes by CtrA is proposed to be ancestral in α -proteobacteria (Greene *et al.*, 2012). Another functional category that could have been underestimated is DNA repair. Indeed, all α -proteobacteria studied in the context of CtrA regulation have at least one DNA repair gene predicted or effectively shown to be part of CtrA regulon. In the first and third groups, one interesting observation is that promoters of genes coding for the Mismatch Repair (MR) system appear to be systematically targeted by CtrA. The MR system, composed of MutH, MutL and MutS proteins, is dependent on the Dam-related methylation status of *E. coli* DNA. Indeed, in this γ -proteobacterium, MutH is able to discern the parental DNA strand (that serves as template) from the newly synthesized one by recognizing the non-methylated state of the new DNA (Yamaguchi *et al.*, 1998; Kunkel & Erie, 2005). Thus, after MutS has detected the distortion in the helix caused by a base mismatch, MutL

is recruited to allow the interaction between MutS and MutH. After MutH has excised the base, an exonuclease degrades a portion of DNA on the mutated and non-methylated strand, which is later repaired by the DNA polymerase III and a ligase (Kunkel & Erie, 2005). In *B. abortus* and other α -proteobacteria, a homologous gene coding for MutH is missing (Martins-Pinheiro *et al.*, 2007; Guarne, 2012). However, it has been proposed that in such a case, MutL is able to also perform the MutH function (Kadyrov *et al.*, 2006; Pillon *et al.*, 2010).

In *C. crescentus*, *mutS* expression has been found to be cell cycle regulated (Laub *et al.*, 2000). Moreover, *mutS* was over-expressed in a CtrA depletion background, suggesting that it is under the control of CtrA (Laub *et al.*, 2000). As for *mutL*, it is not cell cycle regulated but its promoter has been found to be potentially linked to CtrA, based on a DNA microarray experiment (Laub *et al.*, 2002). It should be noted that in *C. crescentus*, another gene is oriented opposite of *mutL*, so it is possible that this gene is the one being regulated by CtrA. However, the promoter of either *mutL* or *mutS* is consistently predicted to be bound by CtrA in other α -proteobacteria where CtrA probably regulates their cell cycle (**Figure 3**, groups 1 and 3). One hypothesis would therefore be that the regulation of the MR system along the cell cycle would insure the correct timing for the utilization of this DNA repair mechanism. Indeed, the use of MR system is not always favourable, as it is known to result in enhanced mutagenesis in bacteria treated with e.g. alkylating agents (Nakano *et al.*, 2017). Note that in *C. crescentus*, CtrA directly activates the expression of the gene coding for S-adenosylmethionine (SAM) synthase, the enzyme responsible for the production of SAM (Laub *et al.*, 2002). SAM is a methyl-donor for CcrM but it is also known to be a weak aspecific endogenous alkylating agent (Rydberg & Lindahl, 1982). As for *B. abortus*, the promoter of *tagA*, which codes for a protein specifically involved in repairing alkylated DNA (Mielecki & Grzesiuk, 2014), is directly bound by CtrA (Francis *et al.*, 2017). Incidentally, it would be interesting to know if TagA is required during *B. abortus* cellular infection, as it would suggest that alkylating stress is met by the bacterium inside its host. Knowing that several other genes involved in DNA repair are cell cycle regulated in *C. crescentus*, including the gene coding for the SOS repressor LexA (Laub *et al.*, 2000), it would also be interesting to investigate whether bacteria are more prone to DNA damage during certain stages of their cell cycle or not.

In *C. crescentus*, both *mutL* and *mutS*, in addition to *ctrA*, are considered to be part of the GcrA regulon, as their promoters are all bound by GcrA in a ChIP-seq experiment and their expression changes in cells depleted in GcrA compared to wild-type cells (Haakonsen *et al.*, 2015). As GcrA is able to sense CcrM-dependent methylation on DNA (Fioravanti *et al.*, 2013) and since this specific type of methylation is cell cycle regulated in *C. crescentus* (Stephens *et al.*, 1996) and probably also in *B. abortus* (Francis *et al.*, 2017), an interesting hypothesis would be that the regulation of the MR system by CtrA is a way to prevent it from functioning after full methylation has occurred and thus to avoid the cleavage of the wrong strand. However, CcrM-dependent methylation has been shown to be dispensable for *C. crescentus* to perform proper MR, as suggested by the frequency of rifampicin resistant mutants (Gonzalez *et al.*, 2014). This either means that the MR system is independent of CcrM methylation in *C. crescentus* (Gonzalez *et al.*, 2014), or alternatively that there are redundant DNA repair systems that prevent mismatches from occurring in *C. crescentus*, such as a robust base excision repair system (Martins-Pinheiro *et al.*, 2007).

Two other genes that are supposedly involved in DNA repair could often be regulated by CtrA: *dprA*, also known as *smf*, and *radC* (**Figure 3**). Both *dprA* and *radC* code for proteins with enigmatic

functions. DprA interacts with RecA and is known to be essential for natural competence (Kidane *et al.*, 2012; Yadav *et al.*, 2013; Le *et al.*, 2017). However, the gene coding for this protein is conserved in many bacteria that are not naturally competent. In the α -proteobacterium *R. capsulatus*, DprA is involved in the regulation of Gene Transfer Agent (GTA) production in a CtrA-dependent manner (Brimacombe *et al.*, 2014). A GTA system is analogous to phage transduction but it is unable to fully self-propagate and contains random segments of the host DNA that spread from one cell to another (Lang *et al.*, 2012). As for RadC, and despite numerous efforts, its real function has remained elusive (Ogura *et al.*, 2002; Peterson *et al.*, 2004; Attaiech *et al.*, 2008). It is also known to be specifically expressed in naturally competent bacteria (Ogura *et al.*, 2002; Peterson *et al.*, 2004; Redfield *et al.*, 2005; Vickerman *et al.*, 2007). In the Rickettsial pathogen *Wolbachia*, there exist three homologues of *radC* and all of them are associated with a cluster of genes that are distantly related to phage repressors (Wu *et al.*, 2004). Therefore, one hypothesis would be that RadC and DprA are not involved in competence in these bacteria but rather in coping with phage-derived DNA integration.

Note also that each α -proteobacterium seems to possess its own specific CtrA-dependent DNA repair targets. For example, *D. shibae* CtrA could regulate *recA* expression (Wang *et al.*, 2014), while it seems to be *uvrB* in the case of *R. capsulatus* (Mercer *et al.*, 2010). As for *E. chaffeensis*, it has a perfect 8-mer CtrA binding box in the promoter of its *mfd* gene, which codes for the Transcription Repair Coupling Factor that affects nucleotide excision repair (Selby & Sancar, 1993). Thus, each bacterium probably optimized the different cellular functions regulated by CtrA through evolution according to its specific lifestyle.

The clade of α -proteobacteria is composed of organisms with very different phenotypes and lifestyles. As proposed by others (Greene *et al.*, 2012), it seems that motility is an ancestral trait of CtrA regulon in these organisms. In addition to this observation, our review has proposed that DNA repair could also be a common target of this transcription factor. More precisely, the CtrA regulon seems to have evolved to couple the MR system to cell cycle regulation in some bacteria and to modulate the levels of DprA and RadC in others. It also appears that each bacterium has selected the regulation of some specific DNA repair genes under the control of CtrA, which could reflect the kind of stresses that they meet in their respective environments. Yet, in *B. abortus* and most other α -proteobacteria, there is a gap in the literature on DNA repair. In the case of *B. abortus*, addressing this question would undoubtedly help to better understand what type of stresses are met by the bacterium inside its host cells and thus, to better understand the infectious process itself. In this regard, it would be very interesting to know if the blockage in G1 in HeLa cells and RAW 264.7 macrophages (Deghelt *et al.*, 2014) is linked to more resistance to DNA damage.

Concluding remarks

One surprising conclusion about CtrA is that it is neither involved in the ability of *B. abortus* to enter inside its host cells, nor in its capacity to reach its replicative niche (Willett *et al.*, 2015; Francis *et al.*, 2017). As the survival of a *B. abortus* CtrA depletion strain decreases after 48 h post infection (Willett *et al.*, 2015; Francis *et al.*, 2017), investigation of the impact of the protein at later times could lead to interesting discoveries and might provide answers to some open questions. For example, is the ability of CtrA to modify the bacterial envelope a way to modulate its pathogenicity? Is CtrA necessary for the cell-to-cell spreading of *B. abortus*, like in *E. chaffeensis* (Cheng *et al.*, 2011)?

The fact remains that *B. abortus* does need to tightly regulate its cell cycle at early times post infection, so that it is blocked in the G1 phase for up to eight hours after the entry inside HeLa cells and RAW 264.7 macrophages (Deghelt *et al.*, 2014). As this process is apparently independent of CtrA (Francis *et al.*, 2017), the question remains as to what is the molecular mechanism ensuring this G1 blockage. As *B. abortus* was suggested to face starvation while it is inside the eBCV, it is possible that the ppGpp-dependent starvation response is involved at that stage (Dozot *et al.*, 2006). In favour of this hypothesis, ppGpp has been found to regulate DnaA stability and initiation of DNA replication in carbon-starved *C. crescentus* (Lesley & Shapiro, 2008), as well as to modulate the cell cycle when *C. crescentus* is unable to synthesize fatty acids (Stott *et al.*, 2015) or when it senses a decrease in intracellular glutamine concentration (Ronneau *et al.*, 2016). Another transcription factor that is supposed to be involved in cell cycle regulation, such as GcrA, could also perform this function. Another important question to answer is to know whether this blockage occurs in all eukaryotic cell types, or if it is specific to infection of HeLa cells and RAW 264.7 macrophages.

Conversely, one could wonder why *B. abortus* has evolved to favour a delay in its cell cycle progression during infection. One hypothesis would be that avoiding DNA replication as long as the bacterium is in the endosomal pathway is a way to prevent the fixation of mutations. Indeed, the passage through the eBCV is thought to be very stressful for the bacterium, which could cause DNA damage (Roop *et al.*, 2009). In addition, at that stage, most proteins -including those for DNA repair - are very weakly produced (Lamontagne *et al.*, 2009). It would therefore be more advantageous for *B. abortus* to wait for the storm to pass and repair its DNA when it is safe to do so. Otherwise, there is a risk that replication forks would stall and eventually collapse, which would lead to cell death (Cox *et al.*, 2000). As for the absence of growth itself during the first hours of the infection, it could be a way for *B. abortus* to limit its pathogen associated molecular pattern production and thus limit its recognition by host cells. Not growing could also be a way for the bacterium to avoid using too many resources while it still resides in the eBCV, which is usually considered a nutrient-poor environment (Roop *et al.*, 2009).

The question of whether the G1 block is a common strategy to other intracellular pathogens also merits attention. Indeed, *Legionella*, *Salmonella*, *Chlamydia* and *Francisella* have also been reported to display a biphasic infection, with a relatively long non-proliferative period followed by a phase of massive proliferation (Salcedo & Holden, 2005). There is a crucial need to address these fundamental issues in the future, as only a good knowledge of bacterial biology and infectious processes will allow us to combat pathogens that are becoming more and more resistant to antibiotic treatments.

Acknowledgements

We thank J. Van Helden for uploading *Rhodospirillum centenum* genome on RSAT on request. We thank the members of the URBM for stimulating discussions and UNamur (<https://www.unamur.be/>) for financial and logistic support. The authors declare no conflict of interest.

References

- Archambaud C, Salcedo SP, Lelouard H, *et al.* (2010) Contrasting roles of macrophages and dendritic cells in controlling initial pulmonary Brucella infection. *European journal of immunology* **40**: 3458-3471.
- Attaiech L, Granadel C, Claverys JP, *et al.* (2008) RadC, a misleading name? *J Bacteriol* **190**: 5729-5732.
- Ausmees N & Jacobs-Wagner C (2003) Spatial and temporal control of differentiation and cell cycle progression in *Caulobacter crescentus*. *Annu Rev Microbiol* **57**: 225-247.
- Barnett MJ, Hung DY, Reisenauer A, *et al.* (2001) A homolog of the CtrA cell cycle regulator is present and essential in *Sinorhizobium meliloti*. *J Bacteriol* **183**: 3204-3210.
- Bellaire BH, Roop RM, 2nd & Cardelli JA (2005) Oposonized virulent *Brucella abortus* replicates within nonacidic, endoplasmic reticulum-negative, LAMP-1-positive phagosomes in human monocytes. *Infect Immun* **73**: 3702-3713.
- Biondi EG, Reisinger SJ, Skerker JM, *et al.* (2006) Regulation of the bacterial cell cycle by an integrated genetic circuit. *Nature* **444**: 899-904.
- Boschiroli ML, Ouahrani-Bettache S, Foulongne V, *et al.* (2002) The *Brucella suis virB* operon is induced intracellularly in macrophages. *Proc Natl Acad Sci U S A* **99**: 1544-1549.
- Boschiroli ML, Ouahrani-Bettache S, Foulongne V, *et al.* (2002) Type IV secretion and *Brucella* virulence. *Veterinary microbiology* **90**: 341-348.
- Brassinga AKC, Siam R, McSween W, *et al.* (2002) Conserved Response Regulator CtrA and IHF Binding Sites in the -Proteobacteria *Caulobacter crescentus* and *Rickettsia prowazekii* Chromosomal Replication Origins. *Journal of Bacteriology* **184**: 5789-5799.
- Brilli M, Fondi M, Fani R, *et al.* (2010) The diversity and evolution of cell cycle regulation in alpha-proteobacteria: a comparative genomic analysis. *BMC Syst Biol* **4**: 52.
- Brimacombe CA, Ding H & Beatty JT (2014) *Rhodobacter capsulatus* DprA is essential for RecA-mediated gene transfer agent (RcGTA) recipient capability regulated by quorum-sensing and the CtrA response regulator. *Mol Microbiol* **92**: 1260-1278.
- Brown PJ, de Pedro MA, Kysela DT, *et al.* (2012) Polar growth in the Alphaproteobacterial order Rhizobiales. *Proc Natl Acad Sci U S A* **109**: 1697-1701.
- Cameron TA, Anderson-Furgeson J, Zupan JR, *et al.* (2014) Peptidoglycan synthesis machinery in *Agrobacterium tumefaciens* during unipolar growth and cell division. *mBio* **5**: e01219-01214.

- Carson MJ, Barondess J & Beckwith J (1991) The FtsQ protein of *Escherichia coli*: membrane topology, abundance, and cell division phenotypes due to overproduction and insertion mutations. *J Bacteriol* **173**: 2187-2195.
- Carvalho Neta AV, Mol JP, Xavier MN, *et al.* (2010) Pathogenesis of bovine brucellosis. *Veterinary journal (London, England : 1997)* **184**: 146-155.
- Castaneda-Roldan EI, Avelino-Flores F, Dall'Agnol M, *et al.* (2004) Adherence of *Brucella* to human epithelial cells and macrophages is mediated by sialic acid residues. *Cell Microbiol* **6**: 435-445.
- Celli J (2015) The changing nature of the *Brucella*-containing vacuole. *Cell Microbiol* **17**: 951-958.
- Celli J, Salcedo SP & Gorvel JP (2005) *Brucella* coopts the small GTPase Sar1 for intracellular replication. *Proc Natl Acad Sci U S A* **102**: 1673-1678.
- Celli J, de Chastellier C, Franchini DM, *et al.* (2003) *Brucella* evades macrophage killing via VirB-dependent sustained interactions with the endoplasmic reticulum. *J Exp Med* **198**: 545-556.
- Cha SB, Rayamajhi N, Lee WJ, *et al.* (2012) Generation and envelope protein analysis of internalization defective *Brucella abortus* mutants in professional phagocytes, RAW 264.7. *FEMS Immunol Med Microbiol* **64**: 244-254.
- Chain PS, Comerci DJ, Tolmasky ME, *et al.* (2005) Whole-genome analyses of speciation events in pathogenic *Brucellae*. *Infect Immun* **73**: 8353-8361.
- Cheng Z, Lin M & Rikihisa Y (2014) *Ehrlichia chaffeensis* proliferation begins with NtrY/NtrX and PutA/GlnA upregulation and CtrA degradation induced by proline and glutamine uptake. *mBio* **5**: e02141.
- Cheng Z, Miura K, Popov VL, *et al.* (2011) Insights into the CtrA regulon in development of stress resistance in obligatory intracellular pathogen *Ehrlichia chaffeensis*. *Mol Microbiol* **82**: 1217-1234.
- Childers WS, Xu Q, Mann TH, *et al.* (2014) Cell fate regulation governed by a repurposed bacterial histidine kinase. *PLoS Biol* **12**: e1001979.
- Christen B, Abeliuk E, Collier JM, *et al.* (2011) The essential genome of a bacterium. *Mol Syst Biol* **7**: 528.
- Christensen S & Serbus LR (2015) Comparative analysis of *wolbachia* genomes reveals streamlining and divergence of minimalist two-component systems. *G3 (Bethesda)* **5**: 983-996.
- Collier J (2012) Regulation of chromosomal replication in *Caulobacter crescentus*. *Plasmid* **67**: 76-87.
- Collier J & Shapiro L (2007) Spatial complexity and control of a bacterial cell cycle. *Curr Opin Biotechnol* **18**: 333-340.
- Comerci DJ, Martinez-Lorenzo MJ, Sieira R, *et al.* (2001) Essential role of the VirB machinery in the maturation of the *Brucella abortus*-containing vacuole. *Cell Microbiol* **3**: 159-168.

- Cox M, Goodman M, Kreuzer K, *et al.* (2000) The importance of repairing stalled replication forks. *Nature* **404**: 37-41.
- de Boer PA, Crossley RE & Rothfield LI (1989) A division inhibitor and a topological specificity factor coded for by the minicell locus determine proper placement of the division septum in *E. coli*. *Cell* **56**: 641-649.
- Deghelt M, Mullier C, Sternon JF, *et al.* (2014) The newborn *Brucella abortus* blocked at the G1 stage of its cell cycle is the major infectious bacterial subpopulation. *Nature Communications* **5**: 4366.
- Domian IJ, Quon KC & Shapiro L (1997) Cell type-specific phosphorylation and proteolysis of a transcriptional regulator controls the G1-to-S transition in a bacterial cell cycle. *Cell* **90**: 415-424.
- Domian IJ, Reisenauer A & Shapiro L (1999) Feedback control of a master bacterial cell-cycle regulator. *Proc Natl Acad Sci U S A* **96**: 6648-6653.
- Dozot M, Boigegrain RA, Delrue RM, *et al.* (2006) The stringent response mediator Rsh is required for *Brucella melitensis* and *Brucella suis* virulence, and for expression of the type IV secretion system virB. *Cell Microbiol* **8**: 1791-1802.
- Edmonds MD, Cloeckaert A & Elzer PH (2002) *Brucella* species lacking the major outer membrane protein Omp25 are attenuated in mice and protect against *Brucella melitensis* and *Brucella ovis*. *Veterinary microbiology* **88**: 205-221.
- Figueroa-Cuilan W, Daniel JJ, Howell M, *et al.* (2016) Mini-Tn7 Insertion in an Artificial attTn7 Site Enables Depletion of the Essential Master Regulator CtrA in the Phytopathogen *Agrobacterium tumefaciens*. *Appl Environ Microbiol* **82**: 5015-5025.
- Fioravanti A, Clantin B, Dewitte F, *et al.* (2012) Structural insights into ChpT, an essential dimeric histidine phosphotransferase regulating the cell cycle in *Caulobacter crescentus*. *Acta Crystallogr Sect F Struct Biol Cryst Commun* **68**: 1025-1029.
- Fioravanti A, Fumeaux C, Mohapatra SS, *et al.* (2013) DNA binding of the cell cycle transcriptional regulator GcrA depends on N6-adenosine methylation in *Caulobacter crescentus* and other Alphaproteobacteria. *PLoS Genet* **9**: e1003541.
- Foster JT, Beckstrom-Sternberg SM, Pearson T, *et al.* (2009) Whole-genome-based phylogeny and divergence of the genus *Brucella*. *J Bacteriol* **191**: 2864-2870.
- Frage B, Dohlemann J, Robledo M, *et al.* (2016) Spatiotemporal choreography of chromosome and megaplasmids in the *Sinorhizobium meliloti* cell cycle. *Mol Microbiol* **100**: 808-823.
- Francez-Charlot A, Kaczmarczyk A & Vorholt JA (2015) The branched CcsA/CckA-ChpT-CtrA phosphorelay of *Sphingomonas melonis* controls motility and biofilm formation. *Mol Microbiol* **97**: 47-63.
- Francis N, Poncin K, Fioravanti A, *et al.* (2017) CtrA controls cell division and outer membrane composition of the pathogen *Brucella abortus*. *Mol Microbiol* **103**: 780-797.

Fumeaux C, Radhakrishnan SK, Ardisson S, *et al.* (2014) Cell cycle transition from S-phase to G1 in *Caulobacter* is mediated by ancestral virulence regulators. *Nat Commun* **5**: 4081.

Galibert F, Finan TM, Long SR, *et al.* (2001) The composite genome of the legume symbiont *Sinorhizobium meliloti*. *Science* **293**: 668-672.

Gibson KE, Campbell GR, Lloret J, *et al.* (2006) CbrA is a stationary-phase regulator of cell surface physiology and legume symbiosis in *Sinorhizobium meliloti*. *J Bacteriol* **188**: 4508-4521.

Gonzalez D & Collier J (2013) DNA methylation by CcrM activates the transcription of two genes required for the division of *Caulobacter crescentus*. *Mol Microbiol* **88**: 203-218.

Gonzalez D, Kozdon JB, McAdams HH, *et al.* (2014) The functions of DNA methylation by CcrM in *Caulobacter crescentus*: a global approach. *Nucleic Acids Res* **42**: 3720-3735.

Gora KG, Tsokos CG, Chen YE, *et al.* (2010) A cell-type-specific protein-protein interaction modulates transcriptional activity of a master regulator in *Caulobacter crescentus*. *Molecular cell* **39**: 455-467.

Greene SE, Brill M, Biondi EG, *et al.* (2012) Analysis of the CtrA pathway in *Magnetospirillum* reveals an ancestral role in motility in alphaproteobacteria. *J Bacteriol* **194**: 2973-2986.

Guarne A (2012) The functions of MutL in mismatch repair: the power of multitasking. *Prog Mol Biol Transl Sci* **110**: 41-70.

Guindon S & Gascuel O (2003) A simple, fast, and accurate algorithm to estimate large phylogenies by maximum likelihood. *Systematic biology* **52**: 696-704.

Haakonsen DL, Yuan AH & Laub MT (2015) The bacterial cell cycle regulator GcrA is a sigma70 cofactor that drives gene expression from a subset of methylated promoters. *Genes & development* **29**: 2272-2286.

Hallez R, Bellefontaine AF, Letesson JJ, *et al.* (2004) Morphological and functional asymmetry in alpha-proteobacteria. *Trends Microbiol* **12**: 361-365.

Hallez R, Mignolet J, Van Mullem V, *et al.* (2007) The asymmetric distribution of the essential histidine kinase PdhS indicates a differentiation event in *Brucella abortus*. *EMBO J* **26**: 1444-1455.

Halling SM (1998) On the presence and organization of open reading frames of the nonmotile pathogen *Brucella abortus* similar to class II, III, and IV flagellar genes and to LcrD virulence superfamily. *Microbial & comparative genomics* **3**: 21-29.

Hanot Mambres D, Machelart A, Potemberg G, *et al.* (2016) Identification of Immune Effectors Essential to the Control of Primary and Secondary Intranasal Infection with *Brucella melitensis* in Mice. *Journal of immunology (Baltimore, Md : 1950)* **196**: 3780-3793.

Heinrich K, Sobetzko P & Jonas K (2016) A Kinase-Phosphatase Switch Transduces Environmental Information into a Bacterial Cell Cycle Circuit. *PLoS Genet* **12**: e1006522.

Holtzendorff J, Hung D, Brende P, *et al.* (2004) Oscillating global regulators control the genetic circuit driving a bacterial cell cycle. *Science* **304**: 983-987.

- Ichida H & Long SR (2016) LDSS-P: an advanced algorithm to extract functional short motifs associated with coordinated gene expression. *Nucleic Acids Res* **44**: 5045-5053.
- Ioannidis P, Dunning Hotopp JC, Sapountzis P, *et al.* (2007) New criteria for selecting the origin of DNA replication in Wolbachia and closely related bacteria. *BMC Genomics* **8**: 182.
- Jacobs C, Ausmees N, Cordwell SJ, *et al.* (2003) Functions of the CckA histidine kinase in Caulobacter cell cycle control. *Mol Microbiol* **47**: 1279-1290.
- Jenal U & Fuchs T (1998) An essential protease involved in bacterial cell-cycle control. *Embo j* **17**: 5658-5669.
- Jubier-Maurin V, Boigegrain RA, Cloeckeaert A, *et al.* (2001) Major outer membrane protein Omp25 of Brucella suis is involved in inhibition of tumor necrosis factor alpha production during infection of human macrophages. *Infect Immun* **69**: 4823-4830.
- Kadyrov FA, Dzantiev L, Constantin N, *et al.* (2006) Endonucleolytic function of MutLalpha in human mismatch repair. *Cell* **126**: 297-308.
- Kahng LS & Shapiro L (2003) Polar localization of replicon origins in the multipartite genomes of *Agrobacterium tumefaciens* and *Sinorhizobium meliloti*. *J Bacteriol* **185**: 3384-3391.
- Kidane D, Ayora S, Sweasy JB, *et al.* (2012) The cell pole: the site of cross talk between the DNA uptake and genetic recombination machinery. *Crit Rev Biochem Mol Biol* **47**: 531-555.
- Kozdon JB, Melfi MD, Luong K, *et al.* (2013) Global methylation state at base-pair resolution of the Caulobacter genome throughout the cell cycle. *Proc Natl Acad Sci U S A* **110**: E4658-4667.
- Kuma A, Hatano M, Matsui M, *et al.* (2004) The role of autophagy during the early neonatal starvation period. *Nature* **432**: 1032-1036.
- Kunkel TA & Erie DA (2005) DNA mismatch repair. *Annual review of biochemistry* **74**: 681-710.
- Lamontagne J, Forest A, Marazzo E, *et al.* (2009) Intracellular adaptation of *Brucella abortus*. *J Proteome Res* **8**: 1594-1609.
- Lang AS, Zhaxybayeva O & Beatty JT (2012) Gene transfer agents: phage-like elements of genetic exchange. *Nat Rev Microbiol* **10**: 472-482.
- Laub M, Chen S & McAdams LSH (2002) Genes directly controlled by CtrA, a master regulator of the Caulobacter cell cycle. *Proc Natl Acad Sci U S A* **99**: 4632-4637.
- Laub M, McAdams H, Feldblyum T, *et al.* (2000) Global analysis of the genetic network controlling a bacterial cell cycle. *Science* **290**: 2144-2148.
- Le S, Serrano E, Kawamura R, *et al.* (2017) Bacillus subtilis RecA with DprA-SsbA antagonizes RecX function during natural transformation. *Nucleic Acids Res* **45**: 8873-8885.
- Lesley JA & Shapiro L (2008) SpoT regulates DnaA stability and initiation of DNA replication in carbon-starved *Caulobacter crescentus*. *J Bacteriol* **190**: 6867-6880.

- Leung MM, Brimacombe CA & Beatty JT (2013) Transcriptional regulation of the *Rhodobacter capsulatus* response regulator CtrA. *Microbiology* **159**: 96-106.
- Lin M & Rikihisa Y (2003) *Ehrlichia chaffeensis* and *Anaplasma phagocytophilum* lack genes for lipid A biosynthesis and incorporate cholesterol for their survival. *Infect Immun* **71**: 5324-5331.
- Livny J, Yamaichi Y & Waldor MK (2007) Distribution of centromere-like *parS* sites in bacteria: insights from comparative genomics. *J Bacteriol* **189**: 8693-8703.
- Lori C, Ozaki S, Steiner S, *et al.* (2015) Cyclic di-GMP acts as a cell cycle oscillator to drive chromosome replication. *Nature* **523**: 236-239.
- Luo X, Zhang X, Wu X, *et al.* (2017) *Brucella* Downregulates Tumor Necrosis Factor-alpha to Promote Intracellular Survival via Omp25 Regulation of Different MicroRNAs in Porcine and Murine Macrophages. *Frontiers in immunology* **8**: 2013.
- Lutkenhaus J & Addinall SG (1997) Bacterial cell division and the Z ring. *Annual review of biochemistry* **66**: 93-116.
- Manterola L, Guzman-Verri C, Chaves-Olarte E, *et al.* (2007) BvrR/BvrS-controlled outer membrane proteins Omp3a and Omp3b are not essential for *Brucella abortus* virulence. *Infect Immun* **75**: 4867-4874.
- Marczynski G (1999) Chromosome methylation and measurement of faithful, once and only once per cell cycle chromosome replication in *Caulobacter crescentus*. *J Bacteriol* **181**: 1984-1993.
- Marczynski G & Shapiro L (1992) Cell-cycle control of a cloned chromosomal origin of replication from *Caulobacter crescentus*. *J Mol Biol* **226**: 959-977.
- Martins-Pinheiro M, Marques RC & Menck CF (2007) Genome analysis of DNA repair genes in the alpha proteobacterium *Caulobacter crescentus*. *BMC Microbiol* **7**: 17.
- Mercer RG, Callister SJ, Lipton MS, *et al.* (2010) Loss of the response regulator CtrA causes pleiotropic effects on gene expression but does not affect growth phase regulation in *Rhodobacter capsulatus*. *J Bacteriol* **192**: 2701-2710.
- Mergaert P, Uchiumi T, Alunni B, *et al.* (2006) Eukaryotic control on bacterial cell cycle and differentiation in the *Rhizobium*-legume symbiosis. *Proc Natl Acad Sci U S A* **103**: 5230-5235.
- Mielecki D & Grzesiuk E (2014) Ada response - a strategy for repair of alkylated DNA in bacteria. *FEMS Microbiol Lett* **355**: 1-11.
- Miller CN, Smith EP, Cundiff JA, *et al.* (2017) A *Brucella* Type IV Effector Targets the COG Tethering Complex to Remodel Host Secretory Traffic and Promote Intracellular Replication. *Cell Host Microbe* **22**: 317-329 e317.
- Moreno E & Moriyon I (2002) *Brucella melitensis*: a nasty bug with hidden credentials for virulence. *Proc Natl Acad Sci U S A* **99**: 1-3.
- Moreno E & Moriyon I (2006) The Genus *Brucella*. *Prokaryotes* **5**: 315-456.

- Nakano K, Yamada Y, Takahashi E, *et al.* (2017) E. coli mismatch repair enhances AT-to-GC mutagenesis caused by alkylating agents. *Mutat Res* **815**: 22-27.
- Nievera C, Torgue JJ, Grimwade JE, *et al.* (2006) SeqA blocking of DnaA-oriC interactions ensures staged assembly of the E. coli pre-RC. *Molecular cell* **24**: 581-592.
- Ogura M, Yamaguchi H, Kobayashi K, *et al.* (2002) Whole-Genome Analysis of Genes Regulated by the Bacillus subtilis Competence Transcription Factor ComK. *Journal of Bacteriology* **184**: 2344-2351.
- Ozaki S, Schalch-Moser A, Zumthor L, *et al.* (2014) Activation and polar sequestration of PopA, a c-di-GMP effector protein involved in Caulobacter crescentus cell cycle control. *Mol Microbiol* **94**: 580-594.
- Paul R, Jaeger T, Abel S, *et al.* (2008) Allosteric regulation of histidine kinases by their cognate response regulator determines cell fate. *Cell* **133**: 452-461.
- Peterson SN, Sung CK, Cline R, *et al.* (2004) Identification of competence pheromone responsive genes in Streptococcus pneumoniae by use of DNA microarrays. *Molecular Microbiology* **51**: 1051-1070.
- Pillon MC, Lorenowicz JJ, Uckelmann M, *et al.* (2010) Structure of the endonuclease domain of MutL: unlicensed to cut. *Molecular cell* **39**: 145-151.
- Pini F, De Nisco NJ, Ferri L, *et al.* (2015) Cell Cycle Control by the Master Regulator CtrA in Sinorhizobium meliloti. *PLoS Genet* **11**: e1005232.
- Pini F, Frage B, Ferri L, *et al.* (2013) The DivJ, CbrA and PleC system controls DivK phosphorylation and symbiosis in Sinorhizobium meliloti. *Mol Microbiol* **90**: 54-71.
- Pinto UM, Pappas KM & Winans SC (2012) The ABCs of plasmid replication and segregation. *Nat Rev Microbiol* **10**: 755-765.
- Pizarro-Cerda J, Meresse S, Parton RG, *et al.* (1998) Brucella abortus transits through the autophagic pathway and replicates in the endoplasmic reticulum of nonprofessional phagocytes. *Infect Immun* **66**: 5711-5724.
- Porte F, Liautard JP & Kohler S (1999) Early acidification of phagosomes containing Brucella suis is essential for intracellular survival in murine macrophages. *Infect Immun* **67**: 4041-4047.
- Qin QM, Pei J, Ancona V, *et al.* (2008) RNAi screen of endoplasmic reticulum-associated host factors reveals a role for IRE1alpha in supporting Brucella replication. *PLoS Pathog* **4**: e1000110.
- Quardokus EM & Brun YV (2003) Cell cycle timing and developmental checkpoints in Caulobacter crescentus. *Curr Opin Microbiol* **6**: 541-549.
- Quon K, Yang B, Domian I, *et al.* (1998) Negative control of bacterial DNA replication by a cell cycle regulatory protein that binds at the chromosome origin. *Proc Natl Acad Sci U S A* **95**: 120-125.
- Quon KC, Marczyński GT & Shapiro L (1996) Cell cycle control by an essential bacterial two-component signal transduction protein. *Cell* **84**: 83-93.

- Redfield RJ, Cameron AD, Qian Q, *et al.* (2005) A novel CRP-dependent regulon controls expression of competence genes in *Haemophilus influenzae*. *J Mol Biol* **347**: 735-747.
- Reisenauer A & Shapiro L (2002) DNA methylation affects the cell cycle transcription of the CtrA global regulator in *Caulobacter*. *EMBO J* **21**: 4969-4977.
- Reisenauer A, Quon K & Shapiro L (1999) The CtrA response regulator mediates temporal control of gene expression during the *Caulobacter* cell cycle. *J Bacteriol* **181**: 2430-2439.
- Ronneau S, Petit K, De Bolle X, *et al.* (2016) Phosphotransferase-dependent accumulation of (p)ppGpp in response to glutamine deprivation in *Caulobacter crescentus*. *Nat Commun* **7**: 11423.
- Roop RM, 2nd, Gaines JM, Anderson ES, *et al.* (2009) Survival of the fittest: how *Brucella* strains adapt to their intracellular niche in the host. *Med Microbiol Immunol* **198**: 221-238.
- Roux B, Rodde N, Jardinaud MF, *et al.* (2014) An integrated analysis of plant and bacterial gene expression in symbiotic root nodules using laser-capture microdissection coupled to RNA sequencing. *Plant J* **77**: 817-837.
- Rydberg B & Lindahl T (1982) Nonenzymatic methylation of DNA by the intracellular methyl group donor S-adenosyl-L-methionine is a potentially mutagenic reaction. *Embo j* **1**: 211-216.
- Salcedo SP & Holden DW (2005) Bacterial interactions with the eukaryotic secretory pathway. *Curr Opin Microbiol* **8**: 92-98.
- Salcedo SP, Chevrier N, Lacerda TL, *et al.* (2013) Pathogenic *brucellae* replicate in human trophoblasts. *The Journal of infectious diseases* **207**: 1075-1083.
- Schallies KB, Sadowski C, Meng J, *et al.* (2015) *Sinorhizobium meliloti* CtrA Stability Is Regulated in a CbrA-Dependent Manner That Is Influenced by CpdR1. *J Bacteriol* **197**: 2139-2149.
- Scherer DC, DeBuron-Connors I & Minnick MF (1993) Characterization of *Bartonella bacilliformis* flagella and effect of anti-flagellin antibodies on invasion of human erythrocytes. *Infect Immun* **61**: 4962-4971.
- Sedzicki J, Tschon T, Low SH, *et al.* (2018) 3D correlative electron microscopy reveals continuity of *Brucella*-containing vacuoles with the endoplasmic reticulum. *Journal of cell science*.
- Selby CP & Sancar A (1993) Molecular mechanism of transcription-repair coupling. *Science* **260**: 53-58.
- Shames SR & Finlay BB (2010) Breaking the stereotype: virulence factor-mediated protection of host cells in bacterial pathogenesis. *PLoS Pathog* **6**: e1001057.
- Siam R & Marczyński GT (2000) Cell cycle regulator phosphorylation stimulates two distinct modes of binding at a chromosome replication origin. *Embo j* **19**: 1138-1147.
- Smith JA, Khan M, Magnani DD, *et al.* (2013) *Brucella* induces an unfolded protein response via TcpB that supports intracellular replication in macrophages. *PLoS Pathog* **9**: e1003785.

- Smith SC, Joshi KK, Zik JJ, *et al.* (2014) Cell cycle-dependent adaptor complex for ClpXP-mediated proteolysis directly integrates phosphorylation and second messenger signals. *Proc Natl Acad Sci U S A* **111**: 14229-14234.
- Starr T, Ng TW, Wehrly TD, *et al.* (2008) *Brucella* intracellular replication requires trafficking through the late endosomal/lysosomal compartment. *Traffic* **9**: 678-694.
- Starr T, Child R, Wehrly TD, *et al.* (2012) Selective subversion of autophagy complexes facilitates completion of the *Brucella* intracellular cycle. *Cell Host Microbe* **11**: 33-45.
- Stephens C, Reisenauer A, Wright R, *et al.* (1996) A cell cycle-regulated bacterial DNA methyltransferase is essential for viability. *Proc Natl Acad Sci U S A* **93**: 1210-1214.
- Stott KV, Wood SM, Blair JA, *et al.* (2015) (p)ppGpp modulates cell size and the initiation of DNA replication in *Caulobacter crescentus* in response to a block in lipid biosynthesis. *Microbiology* **161**: 553-564.
- Stouf M, Meile J & Cornet F (2013) FtsK actively segregates sister chromosomes in *Escherichia coli*. *Proc Natl Acad Sci U S A* **110**: 11157-11162.
- Taguchi Y, Imaoka K, Kataoka M, *et al.* (2015) Yip1A, a novel host factor for the activation of the IRE1 pathway of the unfolded protein response during *Brucella* infection. *PLoS Pathog* **11**: e1004747.
- Terwagne M, Ferooz J, Rolan HG, *et al.* (2013) Innate immune recognition of flagellin limits systemic persistence of *Brucella*. *Cell Microbiol* **15**: 942-960.
- Thanbichler M & Shapiro L (2006) MipZ, a spatial regulator coordinating chromosome segregation with cell division in *Caulobacter*. *Cell* **126**: 147-162.
- Tsokos CG, Perchuk BS & Laub MT (2011) A dynamic complex of signaling proteins uses polar localization to regulate cell-fate asymmetry in *Caulobacter crescentus*. *Dev Cell* **20**: 329-341.
- Val ME, Soler-Bistue A, Bland MJ, *et al.* (2014) Management of multipartite genomes: the *Vibrio cholerae* model. *Curr Opin Microbiol* **22**: 120-126.
- Van der Henst C, Beaufay F, Mignolet J, *et al.* (2012) The histidine kinase PdhS controls cell cycle progression of the pathogenic alphaproteobacterium *Brucella abortus*. *J Bacteriol* **194**: 5305-5314.
- van Helden J (2003) Regulatory Sequence Analysis Tools. *Nucleic Acids Research* **31**: 3593-3596.
- Vickerman MM, Iobst S, Jesionowski AM, *et al.* (2007) Genome-wide transcriptional changes in *Streptococcus gordonii* in response to competence signaling peptide. *J Bacteriol* **189**: 7799-7807.
- Vitry MA, Hanot Mambres D, Deghelt M, *et al.* (2014) *Brucella melitensis* invades murine erythrocytes during infection. *Infect Immun* **82**: 3927-3938.

Wang H, Ziesche L, Frank O, *et al.* (2014) The CtrA phosphorelay integrates differentiation and communication in the marine alphaproteobacterium *Dinoroseobacter shibae*. *BMC Genomics* **15**: 130.

Wheeler RT & Shapiro L (1999) Differential localization of two histidine kinases controlling bacterial cell differentiation. *Molecular cell* **4**: 683-694.

Willett JW, Herrou J, Briegel A, *et al.* (2015) Structural asymmetry in a conserved signaling system that regulates division, replication, and virulence of an intracellular pathogen. *Proc Natl Acad Sci U S A* **112**: E3709-3718.

Williams KP, Sobral BW & Dickerman AW (2007) A robust species tree for the alphaproteobacteria. *J Bacteriol* **189**: 4578-4586.

Wolanski M, Jakimowicz D & Zakrzewska-Czerwinska J (2012) AdpA, key regulator for morphological differentiation regulates bacterial chromosome replication. *Open biology* **2**: 120097.

Wolanski M, Jakimowicz D & Zakrzewska-Czerwinska J (2014) Fifty years after the replicon hypothesis: cell-specific master regulators as new players in chromosome replication control. *J Bacteriol* **196**: 2901-2911.

Wu J, Ohta N & Newton A (1998) An essential, multicomponent signal transduction pathway required for cell cycle regulation in *Caulobacter*. *Proc Natl Acad Sci U S A* **95**: 1443-1448.

Wu M, Sun LV, Vamathevan J, *et al.* (2004) Phylogenomics of the reproductive parasite *Wolbachia pipientis* wMel: a streamlined genome overrun by mobile genetic elements. *PLoS Biol* **2**: E69.

Yadav T, Carrasco B, Hejna J, *et al.* (2013) *Bacillus subtilis* DprA recruits RecA onto single-stranded DNA and mediates annealing of complementary strands coated by SsbB and SsbA. *J Biol Chem* **288**: 22437-22450.

Yagupsky P & Baron EJ (2005) Laboratory exposures to brucellae and implications for bioterrorism. *Emerging infectious diseases* **11**: 1180-1185.

Yamaguchi M, Dao V & Modrich P (1998) MutS and MutL activate DNA helicase II in a mismatch-dependent manner. *J Biol Chem* **273**: 9197-9201.

Zan J, Heindl JE, Liu Y, *et al.* (2013) The CckA-ChpT-CtrA phosphorelay system is regulated by quorum sensing and controls flagellar motility in the marine sponge symbiont *Ruegeria* sp. KLH11. *PLoS One* **8**: e66346.

Zhang J, Zhang Y, Li Z, *et al.* (2017) Outer Membrane Protein 25 of *Brucella* Activates Mitogen-Activated Protein Kinase Signal Pathway in Human Trophoblast Cells. *Front Vet Sci* **4**: 197.

Zhang JZ, Popov VL, Gao S, *et al.* (2007) The developmental cycle of *Ehrlichia chaffeensis* in vertebrate cells. *Cell Microbiol* **9**: 610-618.

Zweiger G, Marczyński G & Shapiro L (1994) A *Caulobacter* DNA methyltransferase that functions only in the predivisional cell. *J Mol Biol* **235**: 472-485.

Figure 1

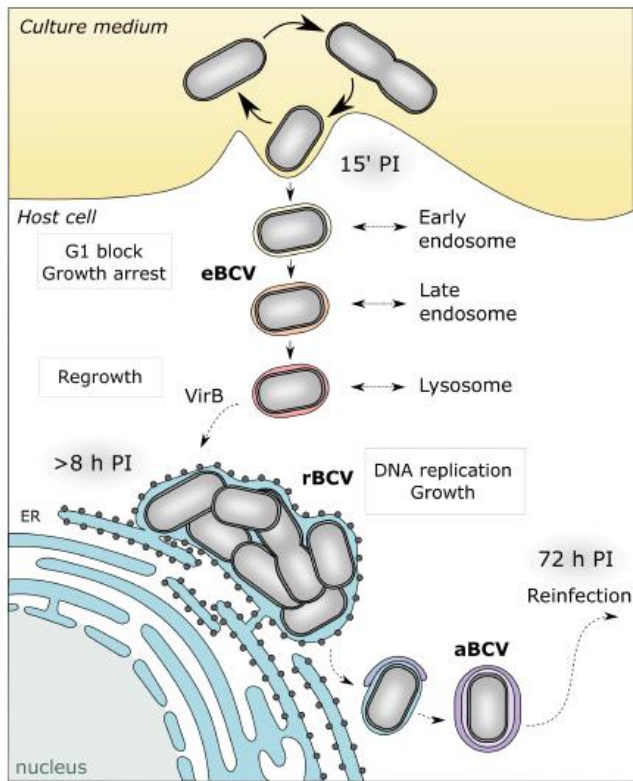


Figure 1. Schematic representation of *B. abortus* trafficking inside host cells. Once inside its host cell, *B. abortus* extensively interacts with the endocytic pathway. The compartment in which it resides at that stage can be referred to as the endocytic *Brucella*-containing vacuole (eBCV). In HeLa cells and RAW 264.7, during this first step of the infection, the bacterium is blocked in G1 and its growth is arrested. After a transient interaction with the lysosomes and thanks to its type IV secretion system VirB, the bacterium reaches its replicative niche (rBCV), which is part of the endoplasmic reticulum (ER) in most cell types. Later on, bacteria are found in autophagy-dependent vacuoles (aBCV) and are proposed to reinfect neighbor cells.

Figure 2

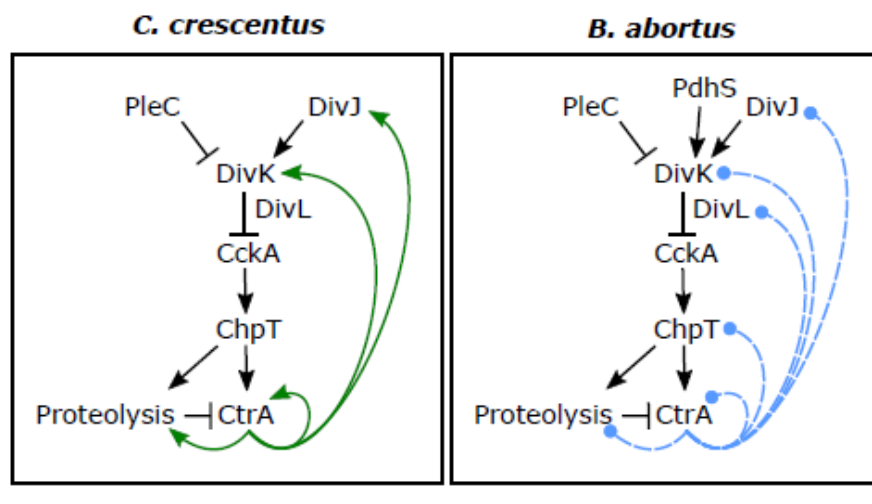


Figure 2. Models for CtrA regulation in two α -proteobacteria. The schemes represented here are mainly based on *C. crescentus* CtrA regulation (Laub *et al.*, 2000; Laub *et al.*, 2002; Fumeaux *et al.*, 2014), therefore it is important to take into consideration the fact that the phosphorylation cascade events might not happen exactly as depicted. In the case of *B. abortus*, data were obtained from Willet *et al.* (2015) and Francis *et al.* (2017). Green arrows correspond to confirmed CtrA targets that are positively regulated by the transcription factor. Blue rounded arrows correspond to targets that are bound by CtrA on their promoter, but for which the effect of this binding still remains unknown.

Figure 3

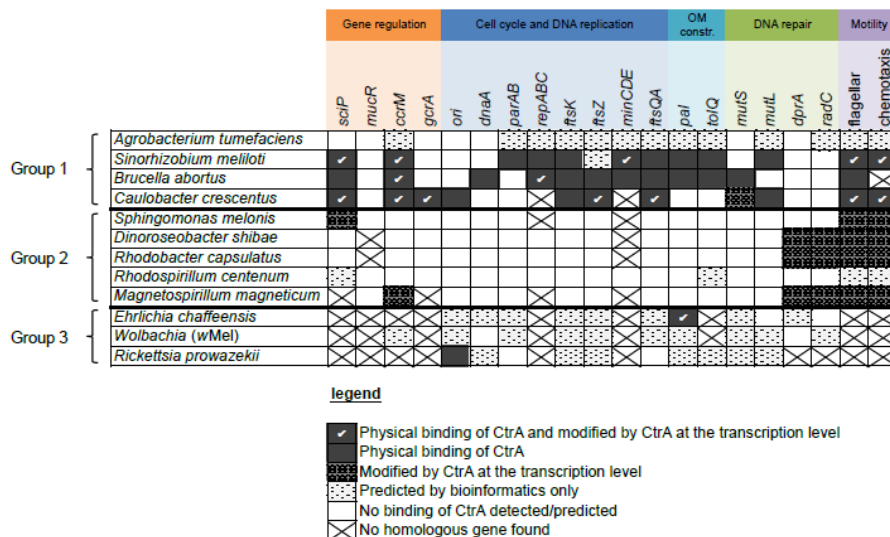


Figure 3. Comparison between CtrA targets in different α -proteobacteria. Data were collected in a hierarchical manner. Information about the direct binding of CtrA were found for *C. crescentus* (Laub *et al.*, 2000; Laub *et al.*, 2002; Fumeaux *et al.*, 2014), *B. abortus* (Francis *et al.*, 2017), *S. meliloti* (Pini *et al.*, 2015; Ichida & Long, 2016), *E. chaffeensis* (Cheng *et al.*, 2011) and *R. prowazekii* (Brassinga *et al.*, 2002). Data concerning the mRNA-level of potential CtrA targets were then collected for *S. melonis* (Francez-Charlot *et al.*, 2015), *D. shibae* (Wang *et al.*, 2014), *R. capsulatus*

(Mercer *et al.*, 2010; Leung *et al.*, 2013) and *M. magneticum* (Greene *et al.*, 2012). Finally, when no experimental data were available, we considered bioinformatics predictions. In the case of Rickettsiales and *A. tumefaciens*, some were already available (Hallez *et al.*, 2004; Ioannidis *et al.*, 2007; Pinto *et al.*, 2012). For *S. meliloti*, prediction on *ftsZ1* promoter was based on Ichida and Long (2016), with one substitution allowed. To complete these data, we also predicted CtrA targets for *A. tumefaciens*, *E. chaffeensis*, *Wolbachia* wMel and *R. prowazekii*. To do so, we used RSAT (van Helden, 2003) and considered genes based on the presence in their promoter of either a 9-mer (TTAAN₇TTAAC) or a 8-mer (TTAACCAT) CtrA-binding box (Marczynski & Shapiro, 1992; Laub *et al.*, 2002) with one substitution allowed. Note that we considered that *ftsZ* was potentially regulated by CtrA when it was the case for the *ddl* gene, as *ftsZ* is probably in operon with this gene in *S. meliloti*, *B. abortus* and *A. tumefaciens*. In *C. crescentus*, CtrA was found to bind upstream the *ruvCAB* operon, itself located upstream the *tolQRAB* operon. We considered that the spacing between these two operons did not allow the prediction of a CtrA control on the *tolQRAB* operon. The ORF of each gene analyzed here are available in supplementary data. See the text for a detailed discussion about this figure. “OM constr.” stands for outer membrane constriction.

Figure 4

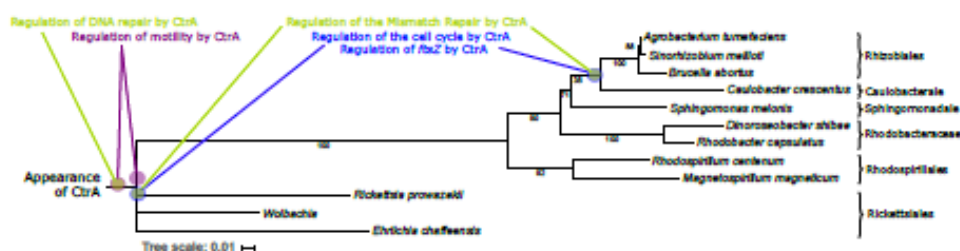


Figure 4. Phylogenetic tree of α -proteobacteria based on CtrA. The tree was constructed with CtrA sequences from the genome of *A. tumefaciens* C58, *S. meliloti* 1021, *B. abortus* 2308, *C. crescentus* CB15, *S. melonis* TY, *R. capsulatus* SB 1003, *D. shibae* DFL 12, *M. magneticum* AMB-1, *R. centenum* SW ATCC 51521, *R. prowazekii* Rp22, *Wolbachia* wMel and *E. chaffeensis* Arkansas (<https://biocyc.org/>). Sequences were aligned with Clustal Omega (version 1.2.4; <http://www.clustal.org/omega/>) and curated manually with Jalview (<http://www.jalview.org/download>). The tree was created with PhyML (Guindon & Gascuel, 2003) with the following settings: Starting tree = BioNJ; Tree Topology = SPR Move; Bootstrap = 100 replicates; Substitution model = WAG. The final figure was formatted on iTol (<https://itol.embl.de/>), then on Inkscape. This tree is in agreement with previously published results (Williams *et al.*, 2007; Greene *et al.*, 2012). Numbers correspond to bootstrap values. The units of branch length are nucleotide substitutions per site (the number of changes divided by the length of the sequence). This

figure suggests a possible timing, along evolution, of major events concerning genes that were taken under the control of CtrA. Note that cell cycle regulation seems to always coincide with a regulation of *ftsZ* and mismatch repair genes.

Supplementary data

	<i>A. tumefaciens</i> C58	<i>S. meliloti</i> 1021	<i>B. abortus</i> 2308	<i>C. crescentus</i> CB15	<i>S. melonis</i> TY	<i>D. shibae</i> DFL 12	<i>R. capsulatus</i> SB 1003	<i>R. centenum</i> SW	<i>M. magneticum</i> AMB-1	<i>Wolbachia</i> wMel	<i>E. chaffeensis</i> Arkansas	<i>R. prowazekii</i> Rp22
<i>ctrA</i>	Atu2434	SMc00654	BAB1_1614	CC_3035	BJP26_06220	Dshi_1508	RCAP_rcc01663	RC1_1752	amb0629	WD0732	ECH_1012	rpr22_CDS069
<i>sciP</i>	Atu8136	SMc00657	BAB1_1609	CC_0903	BJP26_13545	Dshi_1507	RCAP_rcc01662	RC1_1399	-	-	-	-
<i>mucR</i>	Atu0916	SMc00058 SMa0748 SMa1705	BAB1_0594	CC_0933 CC_0949	BJP26_04725 BJP26_14535 BJP26_18250	-	-	RC1_2608 RC1_1344	amb2337 amb4459 amb0993 amb2080 amb3183 amb3297 amb1206 amb0924	-	-	-
<i>ccrM</i>	Atu8136	SMc00021	BAB1_0516	CC_0378	BJP26_01315	Dshi_0024	RCAP_rcc00201	RC1_3173	amb3988	WD0263 WD0594	-	-
<i>gcrA</i>	Atu0426	SMc02139	BAB1_0329	CC_2245	BJP26_05815	Dshi_2616	RCAP_rcc03144	RC1_0907	-	-	-	-
<i>dnaA</i>	Atu0324	SMc01167	BAB1_0001	CC_0008	BJP26_18250	Dshi_3373	RCAP_rcc00001	RC1_3057	amb0636	WD0001	ECH_0809	rpr22_CDS577
<i>parA</i>	Atu2136	SMc02800	BAB1_2060	CC_3753	BJP26_03085	Dshi_3457	RCAP_rcc00061	RC1_1628	amb0004	WD1217	ECH_1156	rpr22_CDS056
<i>repA</i>	Atu3924 Atu5000 Atu6043	SMb20046 SMa2395 SMb20598	BAB2_1163	-	-	Dshi_4023 Dshi_4104	RCAP_rcp00114	RC1_3742	-	-	-	-
<i>ftsK</i>	Atu3210 Atu2759	SMc03808 SMb20595	BAB1_1895	CC_3704	BJP26_03230	Dshi_0059	RCAP_rcc03328	RC1_2785	amb0016	WD0120	ECH_0890	rpr22_CDS803
<i>ftsZ</i>	Atu2086 Atu4673	SMc01874 SMc04296	BAB1_1444	CC_2540	BJP26_12215	Dshi_2416	RCAP_rcc00826	RC1_0606	amb3854 amb1015	WD0723	ECH_1153	rpr22_CDS643
<i>minC</i>	Atu3249	SMb21524	BAB2_0884	-	-	-	-	RC1_3503	-	-	-	-
<i>ftsQ</i>	Atu2088	SMc01872	BAB1_1446	CC_2542	BJP26_12225	Dshi_2418	RCAP_rcc00824	RC1_0608	amb3852	WD0096	ECH_0337	rpr22_CDS244
<i>pal</i>	Atu3713	SMc02942	BAB1_1707	CC_3229	BJP26_03845	Dshi_1112	RCAP_rcc03195	RC1_1799	amb3210 amb3209	WD1255	ECH_0462*	rpr22_CDS753
<i>toiQ</i>	Atu3717	SMc03958	BAB1_1712	CC_3233	BJP26_03825	Dshi_1108	RCAP_rcc03199	RC1_1803	amb3214	-	-	rpr22_CDS303
<i>mutS</i>	Atu0345	SMc01125	BAB1_0146	CC_0012	BJP26_12770	Dshi_3466	RCAP_rcc03495	RC1_2903	amb0287	WD0190 WD0952	ECH_0824	rpr22_CDS292
<i>mutL</i>	Atu0699	SMc00932	BAB2_0212	CC_0695	BJP26_09470	Dshi_0363	RCAP_rcc00266	RC1_3601	amb4416	WD1306 WD0509	ECH_0884	rpr22_CDS858
<i>dprA</i>	Atu1305	SMc01363	BAB2_0638	CC_2447	BJP26_04460	Dshi_1138	RCAP_rcc03098	RC1_1527	amb0681	WD0092	ECH_0883	-
<i>radC</i>	Atu1607	SMc00299	BAB1_1301	CC_2680	BJP26_00830	Dshi_3569	RCAP_rcc00222	RC1_3389	RS10505	WD0357 WD0625 WD0257	ECH_0363	-

*The similarity of this ORF with the *pal* gene is rather low. In addition, the "*pal*" gene is not accompanied by a complete Tol system. Nevertheless, Cheng et al (2011) reported the existence of a *pal/ompA* gene in *E. Chaffeensis*, so we decided to include this locus as such.

